Nanosized Polymer Carriers for Metallocene Catalysts in Heterogeneous Olefin Polymerization

Dissertation

Zur Erlangung des Grades
„Doktor der Naturwissenschaften“

am Fachbereich Chemie und Pharmazie der
Johannes-Gutenberg-Universität zu Mainz
vorgelegt von

Yong-Jun Jang
geboren in Kwangju, Süd-Korea

Mainz 2005

Dekan: Herr Prof. Dr. R. Zentel

1. Berichterstatter: Herr Prof. Dr. K. Müllen

2. Berichterstatter: Herr Prof. Dr. R. Zentel

Tag der mündlichen Prüfung:

Die vorliegende Arbeit wurde in der Zeit von Juli 2001 bis Juli 2004 im Max-Planck-Institut für Polymerforschung in Mainz unter Anleitung von Herrn Prof. Dr. K. Müllen ausgeführt.

Herrn Professor Dr. K. Müllen danke ich für seine wissenschaftliche und persönliche Unterstützung sowie für zahlreiche motivierende Diskussionsbereitschaft.

Dedicated to my wife and family

Table of Contents:

Chapter 1. Introduction

1.1. Polyolefin and olefin polymerization

Polyolefins are the most important modern commodity among commercial polymers and the major tonnage plastic materials worldwide. The polyolefin world market share was around 20% of the total thermoplastics sales in the sixties, while it is reaching almost 65 % of polypropylene (PP) and 40 % of polyethylene (PE) in the year of 2005 [1].

Polyolefins are commercially produced using free radical initiators, Ziegler-Natta catalysts or more recently metallocene catalysts. At first, polyethylene was produced commercially by using free radical polymerization at high temperatures (~ 250 ^{o}C) and high pressures (~ 2700 bar) [2]. The ethylene polymers produced via free-radical polymerization are known as high-pressure low-density polyethylene (HP-LDPE) having short and long chain branches which make the density of the polyethylene products decrease and affect important rheological and mechanical properties. HP-LDPE is used for making films because of its toughness and transparency.

To realize the development of more polyolefin products, the Ziegler–Natta catalysis has been a fundamental factor and is still playing a key role for the industrial field [3]. Ziegler-Natta catalysts have evolved considerably since their discovery by K. Ziegler and G. Natta in the early fifties [4]. These catalysts have been used in homogeneous, heterogeneous and colloidal forms to synthesize various types of polymers and copolymers [5]. This catalyst is composed of a transition metal salt of metals from groups IV to VIII as the catalyst and a metal alkyl of a base metal from groups I to III as the co-catalyst or activator. However, not all combinations of them are equally efficient nor can all monomer types be used. The most important polyolefins by Ziegler-Natta catalysts are the synthesis of linear high-density polyethylene (HDPE), the copolymerization of ethylene and α-olefins to produce linear low-density polyethylene (LLDPE), and the production of highly isotactic and syndiotactic polypropylene.

Recently, many sophisticated new catalysts have opened the wide range of application. The most important breakthrough is the discovery of the metallocene catalysts and methylalumoxane (MAO) cocatalyst [6]. The general formula of metallocene catalysts is Cp_2MX_2. Figure 1-1 shows the typical chemical structure of a metallocene catalyst. The typical chemical structure of a metallocene catalyst characterized by a constrained metal site

consists of a transition metal atom that is strically hindered. In that, it is sandwiched between π-carbocyclic ligands such as cyclopentadienide, fluorenide, indenide or their substituted derivatives [7].

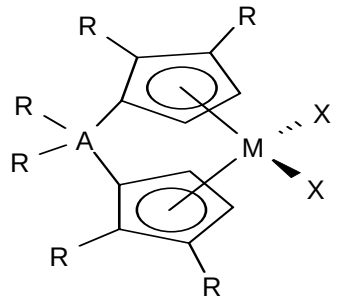

Figure 1-1. Typical chemical structure of a metallocene catalyst

Two cyclopentadienide ligands in Figure 1-1 coordinate to a transition metal (M) and the transition metal is typically titanium, zirconium or hafnium [8 and 9]. R can be substituted by alkyl, alkenyl, aryl and alkylaryl groups, with fused aromatic or aliphatic rings and The X ligands derive either from halogen atoms (typically chlorine) or from hydrocarbons (e.g. methyl or n-butyl groups). A is an optional bridging atom usually Si or C atom.

MAO is an oligomer with a degree of oligomerization varying between 5 – 28 and the repeat unit is -[-Al(CH_3)-O-]-. MAO is the product of a controlled reaction between trimethylaluminum and H_2O. The water source is generally a hydrated inorganic salt, as $Al_2SO_4 \cdot 16H_2O$, $CuSO_4 \cdot 5H_2O$, $FeSO_4 \cdot 7H_2O$ [10]. Sinn and Kaminsky combined the metallocenes with a new co-catalyst, methylalumoxane (MAO), obtaining with very high catalytic activity, polyethylene and low molecular mass atactic polypropylene [11]. The system of metallocene / MAO catalyst is using in the homogeneous and heterogeneous polymerization [12 and 13].

1.2. Heterogeneous olefin polymerization and supports used for the immobilization of catalyst

The immobilization of metallocene catalysts on a carrier is the way to apply in industrial polymerization system and control the morphology of the obtained polymers [14]. The immobilization of the catalyst on several different carriers such as SiO_2, Al_2O_3, and polymers was reported by many scientific papers [15, 16, 17 and 18].

Figure 1-2 shows the polyethylene products from homogeneous ethylene polymerization

(A) and heterogeneous ethylene polymerization (B) respectively. In the case of homogeneous polymerization, the polyethylene products are fluffy as a sponge and so the handling of polymer products is difficult. Also the reactor fouling on the reactor wall and stirrer occurs during each polymerization. On the other hand, the polyethylene products from heterogeneous polymerization are spherical particle with good morphology. After each polymerization in this case, there is no fouling and the handling product is easy.

(A) (B)

Figure 1-2. The products of polyethylene by homogeneous ethylene polymerization (A) and by heterogeneous olefin polymerization (B)

1.2.1. Inorganic support in heterogeneous olefin polymerization

A number of studies have been published concerning the immobilization of metallocene catalysts on several types of inorganic carriers such as silica, alumina, zeolite and so on [19]. The most commonly employed inorganic supports for metallocene catalysts are silica (SiO_2) [20 and 21]. Some other materials have been investigated such as alumina (Al_2O_3), zeolites, MgO, MgF_2, CaF_2, AlF_3, etc [22]. The functional groups on the reactive surface of a support are Brønsted acidic OH and Lewis basic oxide groups. In the system of the heterogenous olefin polymerization, the control of the number of Brønsted acidic OH group is very important because the Brønsted acidic OH group could deactivate the metallocene catalyst [23 and 24].

Silica with its surface area, porosity and pore volume is one of the most commercial carriers [25]. Silica gel has a maximum number of 8 Brønsted acidic OH groups per nm^2 (4

mmol OH / g for silica with an approximately 300 m^2 / g surface area) (Figure 1-3). Heat treatment (calcinations) of the silica at 200 ^oC gave partially dehydroxylated silica with 2.3 mmol OH / g. Half of them are geminal hydroxy pairs and the other half are vicinal pairs. The number of hydroxy groups decreases steadily upon heating at higher decomposition temperature (Td). Above 600 ^oC, a material referred to as dehydroxylated silica is obtained. It contains only 0.7 mmol OH / g. The number of Lewis basic oxide groups is 4, 3.5 and 3.7 / nm^2 for silica gel partially dehydroxylated silica and dehydroxylated silica respectively.

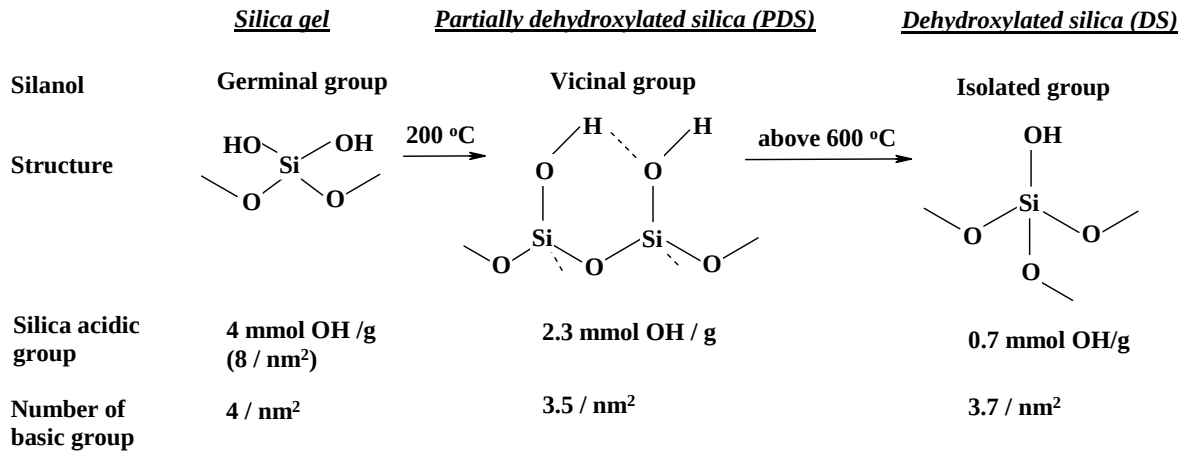

Figure 1-3. The procedure of calcinations of silica gel depending on the calcinations temperature

In the case of alumina, the surface chemistry of γ-alumina has been studied [26, 27, 28, 29 and 30]. Dehydroxylated alumina has ~ 0.12 / nm^2 Brønsted acidic OH groups, ~ 5.5 / nm^2 Lewis acidic Al_3^+ centers, and 5.5 / nm^2 Lewis basic oxide groups [31]. Clearly, even if the reaction condition is the same as olefin polymerization, the catalyst activity and the properties of polyolefins will be different depending on the kinds of these carriers.

1.2.2. Organic supports in heterogeneous olefin polymerization

Since the middle of the 1990's, there have been a number of papers concerning the use of polymers as carriers for metallocene catalysts in heterogeneous olefin polymerization [32, 33, 34 and 35]. One of the most important organic supports are Merrifield resins made by copolymerization of styrene derivatives [36, 37 and 38]. Merrifield resins have been proved to be one of the alternative catalyst carriers in olefin polymerization since 1995 [39, 40 and 41].

Soga and coworker reported that linear polystyrene (PS) supports were prepared by copolymerization of styrene derivatives having a Cs symmetrical ligand moiety and used as carrier for the synthesis of supported-type zirconocene catalysts (support 1). Propylene polymerization was conducted using the resulting catalyst together with MAO, which gave syndiotactic polypropylene with 86 rrrr (%) [42].

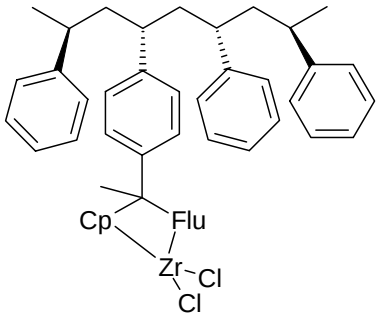

support 1

Also they have prepared four different supported zirconocenes bearing indenide (C_9H_7, Ind) groups on the polystyrene beads crosslinked with 2 % divinylbenzene [43]. The supported complexes have been used in polymerization of ethylene and propylene (support 2, 3, 4, 5). They describe that there is no leaching of catalyst from the support and that the supported catalysts were stable even at high temperature polymerization.

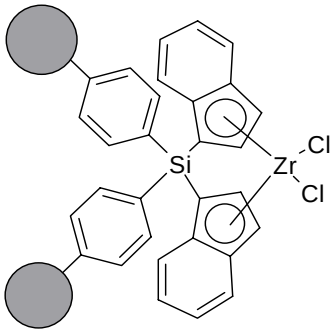

support 2

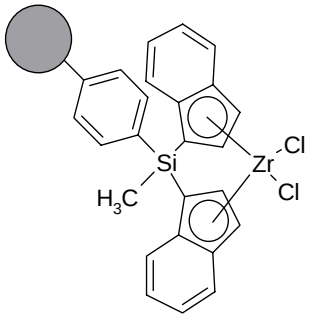

support 3

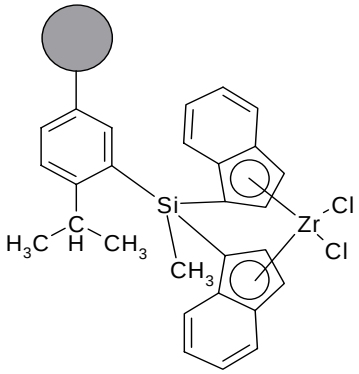

support 4

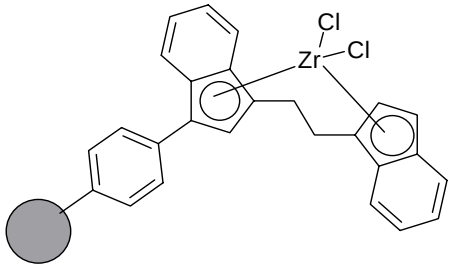

support 5

As another catalyst carrier, they have prepared supported catalysts with zirconocene and diindenide ligand complex on polystyrene (PS) beads (support 6) and investigated the mechanism of polyethylene particle growth by scanning electron microscopy (SEM) and electron prove microanalysis (EPMA) [44 and 45]. Also a spacer-modified polystyrene support with peralkylated titanocene was prepared (support 7). The polystyrene support has about 100 micrometer size and is crosslinked by 2 % divinylbenzene. They described that the supported catalysts have problems of metallocene catalyst diffusion within the PS beads [46].

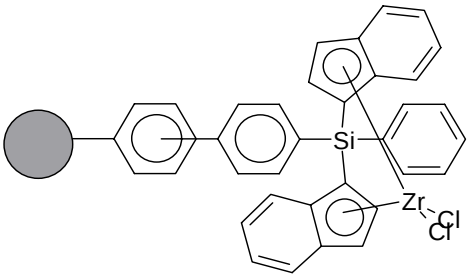

support 6

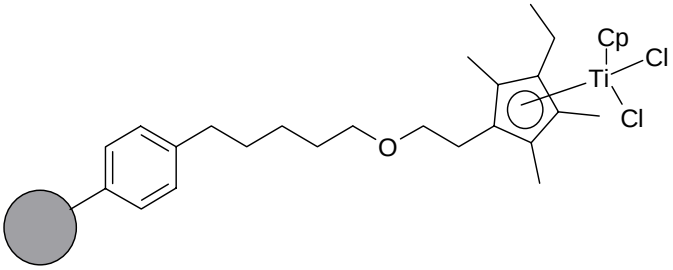

support 7

As well as immobilizing metallocenes on the PS support by direct covalent bonding, there have been reports of other methods of catalyst attachment on the support. Fréchet and co-workers [47] have immobilized metal cyclopentadienide complexes on a noninteracting polystyrene support. The metal complex is bound to the support through a weakly coordinating interaction between the activated Hf by the borane cocatalyst and the N of the supported amine (support 8).

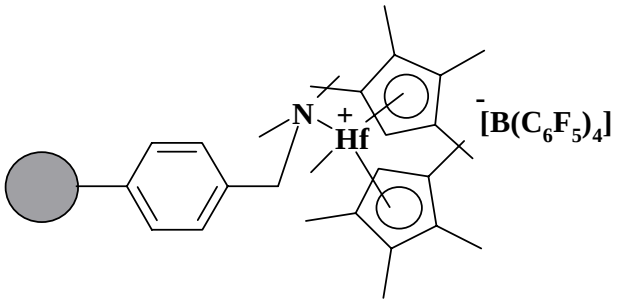

support 8

Uozumi and co-workers [48] have used a similar methodology to prepare the supported metallocene catalyst by using bis(cyclopentadienide) zirconocene dimethyl combined with

triphenylcarbenium tetrakis(pentafluorophenyl) borate on pyridine-derivatized PS support. They have attached the cationic zirconocene complex by treating the support with a mixture of Cp_2ZrMe_2 and $[PhNMe_2H]^+[B(C_6F_5)_4]^-$ (support 9). In case of the morphology of the polyethylene (PE) products, the size distribution and shape of PE was not uniform due to the PS support with non-uniform shape.

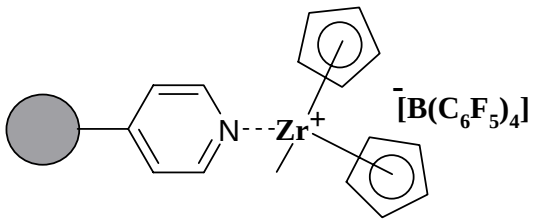

support 9

Another novel polymer-supported metallocene catalyst with a crosslinked poly(styrene-co-acrylamide) (PSAm) as a support (support 10) has been prepared and characterized by the group of Liu [49]. Through the infrared spectra of PSAm and the supported catalyst, they substantiate that amide groups in the support coordinates with MAO.

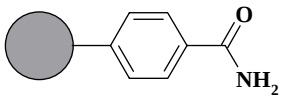

support 10

Hong, Kristen, and Reif [50] have immobilized metallocene catalysts in mere polystyrene by very simple methodology that is a swelling-shrinking characteristics of polystyrene (PS) beads in organic solvent. They prepared the supported metallocence catalyst by simple swelling and shrinking of polystyrene supports in organic solvent. The polystyrene beads were swelled in a metallocene and methylaluminoxane (MAO) solution of toluene. The solvent was then removed from the mixture to leave dry beads with the metal encapsulated. They described that the encapsulated metallocene in the PS support proved to be air and moisture stable.

Nonfunctionalized polyorganosiloxane microgels were applied as support materials for methylalumoxane (MAO)-type compounds (support 11) [51].

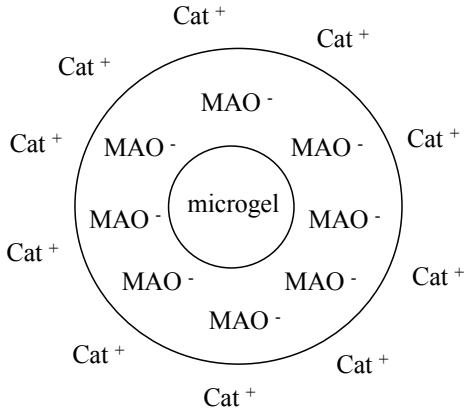

support 11

The functionalization of the microgels has a strong influence on the properties of the catalysts and the produced polyethylene. Microgels are introduced as suitable support materials for cocatalysts on the basis of methylalumoxane (MAO).

Two kinds of fluorenide containing zirconocene catalysts supported on polymethyl-siloxane micro gels and on silica were prepared (support 12 and support 13) and applied for ethylene polymerizations using methylalumoxane (MAO) as cocatalyst.

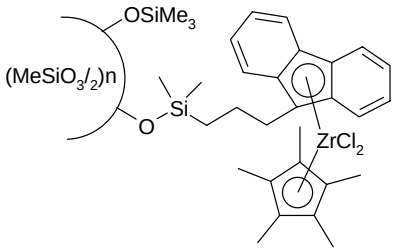

support 12

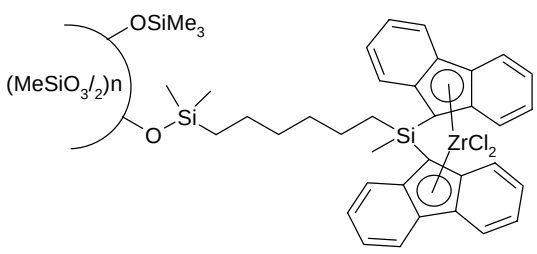

support 13

The observed activities were comparable to those of the corresponding silica supported catalysts. The average molecular weights of the obtained polymers differ from those of the corresponding homogeneous catalysts and from those of the silica-supported systems [52].

Macroporous functionalized polymer beads of poly(4-vinylpyridine-co-1,4-divinyl benzene) [P(VPy-co-DVB)] were prepared by a multistep polymerization [53]. The polymerization included a polystyrene (PS) template by emulsifier-free emulsion polymerization, linear PS seeds by staged template suspension polymerization, and macroporous functionalized polymer beads of P(VPy-co-DVB) by multistep seeded

polymerization. The polymer beads, having a cellular texture, were made of many small, spherical particles. The bead size was 10 - 50 micrometer, and the pore size was 0.1 - 1.5 micrometer. The polymer beads were used as supports for zirconocene catalysts in ethylene polymerization and acted very differently from traditional polymer supports. Thus, the polymer beads could be exfoliated to yield many spherical particles dispersed in the resulting polyethylene particles during ethylene polymerization.

By the condensation reaction of bisindenyldichlorosilane and p-dilithiobenzene or p-dilithiobiphenyl, new polymeric $[Ind_2Si(C_6H_4)]_n$ and $[Ind_2Si(C_6H_4)_2]_m$ compounds were synthesized [54]. The supported-type zirconocene catalysts were prepared by reacting them with zirconium tetrachloride (support 14 and support 15). The active species are markedly stabilized probably due to the rigid backbones of the carriers even at high temperatures.

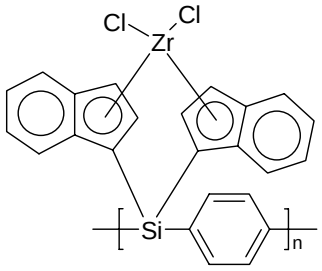

support 14

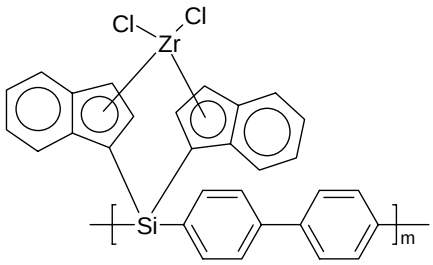

support 15

In our group new complex polystyrene supports have been prepared in order to improve the polymer-supported catalysts. The initial polystyrene support contained a simple metallocene complex directly synthesized and then covalently immobilized on the surface of the polystyrene [55]. The difference of this supported catalyst from the polymer supports mentioned above is the reversible crosslinking due to the Diels-Alder reaction between cyclopentadiene functional groups. This crosslinking is reversible in the olefin polymerization condition under high pressure and high temperature improving in this way the catalyst fragmentation and allowing polymerization on all active centers [56 and 57]. Even if the reversible polystyrene support crosslinked by Diels-Alder reaction have several advantages such as high catalyst activity, the drawback of this supported catalyst systems is the limited number of metallocene that can be synthesized on the support surface and the low bulk density of polyethylene obtained.

A different immobilization system was established by using the properties of MAO / metallocene active sites and the nucleophilic character of the methoxy groups [58]. It was

appropriate to immobilize the metallocene and MAO noncovalently on the methoxy functionalized polystyrene due to the cationic character of these complexes. In comparison with the silica supported catalyst system, there is no treatment with extra MAO to avoid possible deactivation of the catalyst. By using this support, propylene polymerization was carried out for the control of polypropylene (PP) tacticity. The characteristics of PP obtained by the catalyst supported polystyrene (PS) functionalized with methoxy groups were close to those of polypropylene (PP) prepared by homogeneous polymerization. There was no dust-like product and the particle morphology was good.

Another catalyst carrier prepared in our group was polyethyleneoxide functionalized polystyrene (PS) [59]. Due to the increased number of oxygen groups, the polyethyleneoxide (PEO) chains can coordinate and immobilize the metallocene / MAO complexes making the process completely heterogeneous and giving excellent polyolefin properties. The oxygen atoms of the polyethyleneoxide (PEO) can bind the active complexes of the catalyst and establish a network due to the many nucleophilic ether groups which act as anchors. The strong non-covalent immobilization of the ionic complexes of the catalyst was additionally strengthened by reversible crosslinking of the carrier through Diels-Alder reactions of cyclopentadiene functional groups. This crosslinking process helped in immobilization of the active species and controlled the catalyst fragmentation allowing polymerization at all active centers.

In the next approach to improve the catalyst carrier, nanosized polystyrene beads were introduced [60]. Nanosized PS as catalyst carrier can fragment to a high degree within the olefin polymer particles. Also the polystyrene (PS) support has a similar nature to that of the produced polyolefins which means that polystyrene support has no influence on the quality of the material obtained. The heterogeneous polymerization using nanosized PS supported metallocene catalyst can be regarded as a very promising approach in this area.

1.2.3. Fragmentation of the supported catalyst in olefin polymerization

During polymerization, the supported catalyst should be broken down which is called catalyst fragmentation. The fragmentation of supported catalyst is very important to understand the mechanism of olefin polymerization and the properties of polyolefin products. The fragmentation of the supported catalyst and the growth of the polymer particles on the supported catalysts have aroused much interest worldwide. [61]

The fragmentation process depends on the supported catalyst properties such as pore morphology and the polymerization conditions [62]. The porosity is a very important factor in the fragmentation process. The polymer produced during olefin polymerization could fill the inside of the pores of the catalyst support and induce stresses within the support particle. By the stress, the support can be fragmented to smaller particles. The fragments of the support are still connected by the polymer phase. Through the process of catalyst fragmentation during the polymerization, monomer gas can reach active catalyst centers located within the pores of the support. The final polyolefin product has 0.5 to 1mm particle size and contains a small fraction of catalyst residues. The catalyst supports can not be differentiated in the polymer particles [63]. Fragmentation of supported catalysts is known to affect both the properties of the final product and the characteristics of the polymerization process [64]. The properties of the polyolefin produced depend not only on the molecular architecture of the material but also on the morphology of the polymer particles such as particle size, shape and distribution of the catalyst support in the polymer phase.

In spite of the importance of catalyst fragmentation, the phenomenon has not yet been described properly because an experimental investigation of the catalyst fragmentation is very difficult [65]. The reason for the difficulty of the experimental study is that the fragmentation phenomena take place on a submicroscopic scale and may occur in fractions of the supported catalyst at a very early stage. For this reason, mathematical models were used to simulate the olefin polymerization process. Many mathematical models are available in the literature for heterogeneous catalytic polymerization. There are essentially three types of physical models found in the literature; the solid core model [66], the polymer flow model [67] and the multigrain model [68]. The solid core model does not assume the break-up of catalyst particle. The polymer is considered to grow around a solid catalyst core with all active sites located on its surfaces. The polymer flow model assumes that the growing polymer chains and the supported catalysts fragment in the form of a continuum [69, 70 and 71]. The polymer flow model does not consider the presence of microparticles and so it is applicable only to homogeneous polymer particles. The multigrain model gives a more detailed description of phenomena taking place during polymerization with supported catalysts [72 and 73]. Instead of using the homogeneous approximation of the polymer flow model, the multigrain model takes into account the heterogeneous nature of the resulting polymer particle [74]. The multigrain model was derived for conventional Ziegler-Natta catalysts and only a completely fragmented particle is considered. Bonini et al. showed that

the MGM cannot fit experimental data involving gradual particle fragmentation and developed a 'particle growth model' for silica supported metallocene catalysts [75]. Fink et al. proposed a more general approach directly derived from the Bonini model and proposed a gradual particle fragmentation for silica supported metallocene catalysts [76].

However, the supported catalysts in heterogeneous olefin polymerization break up during the early stages of the polymerization. Most models available in the literature are not useful to simulate the very early stages of heterogeneous olefin polymerizations and therefore cannot be used for analysis and design of pre-polymerizations. To visualize the catalyst fragmentation directly, many methods are available in industrial and academic research. The representative instruments are scanning electron microscopy (SEM), transmission electron microscopy (TEM), atomic forth microscopy (AFM), X-ray microscopy and synchrotron micro-tomography techniques [77, 78, 79 and 80]

Electron microscopy is a very popular technique to study catalyst fragmentation. By using the scanning electron microscopic technique (SEM), Mackie and co-workers observed that the nascent polymer particles produced by the supported catalysts replicate the original catalyst morphology [81]. Hock also visualized the internal structure of the nascent polymer particles by electron microscopy and explained the agglomerates of many thousands of fine polymer globules. [82] From their results, it was accepted that the nascent polymer particle replicates not only the external structure of the original catalyst particle but also its internal structure. Kakugo and co-workers observed by scanning electron microscopy (SEM) that the size of the primary polymer particles is in good agreement with that predicted from the polymer yield and the size of the original catalyst crystallites [83]. In spite of such extensive efforts, however, the relationship between the primary polymer particle and the primary catalyst crystallite is still not completely elucidated due to the lack of a suitable observation method.

Kakugo and co-workers observed the internal structure of nascent polypropylene particles using transmission electron microscopy (TEM) in a two-step staining method employing 1,7-octadiene and osmiumtetraoxide (OsO_4). He described in his paper that the PP particles are agglomerates of many primary polymer particles with diameters of 0.2 - 0.35 micrometer. It was shown that scanning electron microscopy (SEM) is not pertinent to this purpose because of the inherent disadvantage that the catalyst crystallite embedded within the polymer particles cannot be observed. On the other hand, transmission electron microscopy (TEM) is obviously a powerful method for this purpose [84]. Kakugo and co-workers also investigated

the nascent polypropylene particles prepared with 6-$TiC1_3$ catalyst systems by small-angle X-ray scattering, wide-angle X-ray diffraction, and electron microscopy [85]. They explained that the catalyst crystallites which disperse at the initial stage of polymerization uniformly within the polymer particles, retain their initial size during the course of polymerization. As the polymerization proceeds, the primary polymer particles become visible under an electron microscope, and their size increases in proportion to the cube root of the polymer yield.

More recently, Fink and co-workers studied the fragmentation process [86]. They studied how and by which parameters polymerization kinetics, polymer growth, polymer morphology, and particle fragmentation are influenced [80]. They have contributed to a great extent to the understanding of the polymerization behavior of SiO_2 supported metallocene catalysts at low temperature, low catalyst concentration, low monomer concentration as the polymerization conditions that facilitated a time-resolved representation of the polymerization and its various stages. By using detailed electron-microscopic and kinetic studies, the polymerization process was interpreted and a model for olefin polymerization was developed (Figure 1-4). It appeared that the particle growth starts only after an induction period and then proceeds continually as the polymerization activity increases. The onset of fragmentation of the support is a prerequisite for the particle growth and the simultaneous morphology conservation.

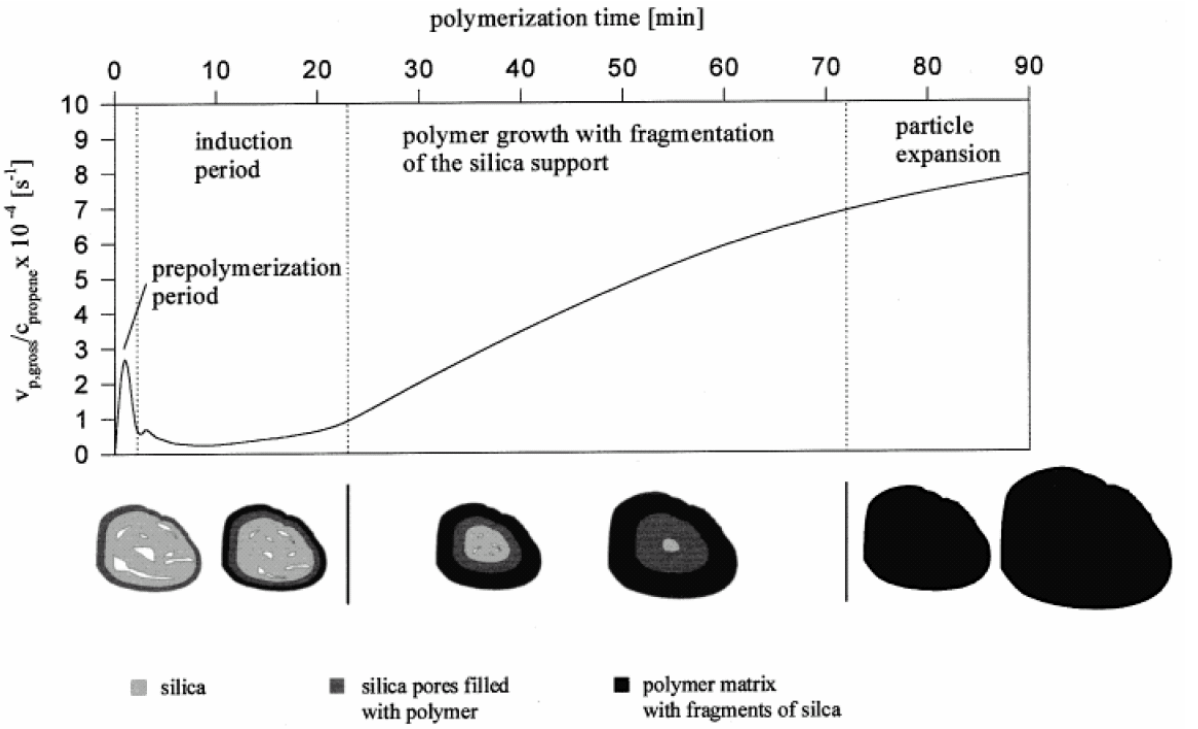

Figure 1-4. Schematic particle growth model for the propylene polymerization of a silica-supported metallocene / MAO catalyst [62]

However, SEM and TEM techniques suffer from many drawbacks due to the requirement of a conductive coating to the particle that may influence the topography of the particles. As another instrument to study the catalyst fragmentation, atomic force microscopy (AFM) was used to study the fragmentation of the supported catalyst in olefin polymerization [87]. Normally AFM is widely used to image the surface of solid materials [88]. It works by scanning a very sharp tip across a sample surface and measuring the forces of interaction between the tip and the substrate. In the use of AFM for the study of the catalyst fragmentation in heterogeneous polymerization system, AFM avoids the prerequisite for a conducting coating and provides topographical information. The breakup of the silica supported catalyst during olefin polymerization has been followed by contact mode, tapping mode and phase-image AFM. AFM detected the supported catalyst undergoing continuous breakup during the formation of polymer with the larger fragments being pushed out toward the surface where they undergo further fragmentation.

Also models of the micro-tomography have been proposed to study the catalyst fragmentation and the distribution of the fragments within the growing particle. [89 and 90] Especially Conner and co-workers investigated the heterogeneous polymer products by computed micro-tomography. [91] They used X-ray microscopy and computed micro-tomography to study polyethylene polymerization particles with varying low amounts of polymer and containing significant residual catalyst. The images of X-ray tomography allow definition of catalyst fragment and void size as well as spatial distribution within a single polymer particle. They also proved the utility of a new imaging technology that will aid in the understanding and design of improved polymerization catalysts. Also Conner and co-workers found a bimodal distribution of pores developed during activation for the most active catalysts and speculated that the mesoporosity found in these catalysts were the primary pathways for fragmentation. They studied the changes in the pore structure as polymer was formed and concluded that the fragmentation was progressive, beginning with the larger mesopores (10 - 30 nm) [92, 93 and 94]. Calorimetry is an integral method describing the whole polymerization process such as catalyst activity and productivity [95]. However, it does not allow visualization of particle growth and the fragmentation of a single catalyst particle. From these several measurements, mathematical models have been developed. But the theoretical investigation and description of such a fragmentation process is very time-consuming and demanding [96]. Therefore there is still need for new techniques allowing on one hand the investigation of single particles and on the other hand being fast and easily

applicable enough to study a larger number of particles within a short time.

For the need of new instruments to study the particle growth, a first progress was made with the use of video microscopy in olefin polymerization as presented by the Reichert group [97]. By combining a small mini-reactor for gas-phase polymerization and a video microscope with attached camera the particle growth during olefin polymerization was visualized depending on the reaction temperature and pressure. They showed that individual catalyst particles start to grow single polymer particles during polymerization. Recently, in a more extensive work Fink et al. demonstrated that this method could be applied to study the polymerization process by measuring the growth of single particles and to develop a kinetic model [98].

1. P. Galli and G. Vecellio, *Prog. Polym. Sci*., **2001**, 26, 1287.

2. R.P. Goldstein and N.R. Amundson, *Chem. Eng. Sci*., **1965**, 20, 195.

3. K. Ziegler, E. Holzkamp, H. Breil and H. Martin, *Angew. Chem*., **1955**, 57, 541.

4. Z. Natta, *Angew. Chem*., **1956**, 68, 393.

5. J. Huang and G. L. Rempel, *Prog. Polym. Sci*., **1995**, 20, 459.

6. H. Sinn and W. Kaminsky, *Adv. Organomet. Chem*. 18, 99, 1980.

7. O. Olabist, M. Atiqullah and W. Kaminsky, *Rev. Macromol. Chem. Phys*., **1997**, 37, 519.

8. H. Lang, S. Blau, A. Muth, K. Weiss and U. Neugebauer *J. Organomet. Chem*., **1995**, 490, 32.

9. K. Weiss, U. Neugebauer, S. Blau and H. Lang, *J. Organomet. Chem*., **1996**, 520, 171,.

10. E. Giannetti, G. Nicoletti and R. Mazzocchi, *J. Polym. Sci., Polym. Chem. Ed*., **1985**, 23, 2117.

11. H. Sinn, W. Kaminsky, H.J. Vollmer and R. Woldt, *Angew. Chem*., **1980**, 92, 396.

12. J.J. Eisch, S.I. Bombrick and G.X. Zheng, *Organometallics*, **1993**, 12, 3856.

13. R.F. Jordan, W.E. Dasher and S.F. Echols, *J. Am. Chem. Soc*., **1986**, 108, 1718.

14. F. Ciardelli, A. Altomare and M. Michelotti, *Catal. Today*, **1998**, 41, 149.

15. J.C.W. Chien and D. He, *J. Polym. Sci. Part A: Polym. Chem*., **1991**, 29, 1603.

16. K. Soga and M. Kaminaka, *Makromol. Chem*., **1993**, 194, 1745.

17. W. Kaminsky and F. Renner, *Makromol. Chem. Rapid Commun*., **1993**, 14, 239.

18. Y.X. Chen, M.D. Rausch and J.C. Chien, *J. Polym. Sci. Part A: Polym. Chem*. **1995**, 33, 2093.

19. S. Collins, W.M. Kelly and D.A. Holden, *Macromolecules*, **1992**, 25**,** 1780; W. Kaminsky and F. Renner, *Makromol. Chem., Rapid Commun*., **1993**, 14**,** 239; K. Soga and M. Kaminaka, *Makromol. Chem.,* **1993**, 194**,** 1745; J.C.W. Chien and D. He, *J. Polym. Sci., Part A,* **1991**, 29**,** 1603; K. Soga, R. Koide and T. Uozumi, *Makromol. Chem. Rapid Commun*. **1993**, 14, 511; J. Klinowski, *Chem. Rev*. **1991**, 91, 1459.

20. J. Tian, S. Wang, Y. Feng, J. Li and S. Collins, *J. Mol. Catal A: Chem*., **1999**, 144, 137.

21. F. Silveira, S.R. Loureiro, G.B. Galland, F.C. Stedile, J.H.Z. dos Santos and T. Teranishi, *J. Mol. Catal. A: Chem*. **2003**, 206, 389.

22. S.I. Woo, Y.S. Ko and T.K. Han, *Macromol. Rapid Commun*. **1995**, 16, 489; Y.S. Ko, T.K. Han, J.W. Park and S.I. Woo, *Macromol. Chem. Rapid Commun*. **1996**, 17, 749; Y.S. Ko and S.I. Woo, *Macromol. Chem. Phys*. **2001**, 202, 739; A. C. A. Casagrande, T. T. da R.

Tavares , M. C. A. Kuhn , O. L. Casagrande, Jr. , J. H. Z. dos Santos and T. Teranishi, *J. Mol. Catal. A: Chem*. **2004**, 212, 267.

23. G.G. Hlatky, *Chem. Rev*., **2000**, 100, 1347.

24. G.A. Ozin and C. Gil, *Chem. Rev*., **1989**, 89, 1749.

25. G. G. Hlatky, *Chem. Rev*., **2000**, 100, 1347.

26. H. Knozinger and P. Ratnasamy, *Catal. Rev. Sci. Eng*., **1978**, 17, 31.

27. H.A. Benesi and B.H.C. Winquist, *Adv. Catal*., **1978**, 27, 97.

28. J. Kijenski and A. Baiker, *Catal. Today,* **1989**, 5, 1.

29. D. Harrison, I. M. Coulter, S. Wang, S. Nistala, B. A. Kuntz, M. Pigeon, J. Tian and S. Collins, *J. Mol. Catal. A: Chem*., **1998**, 128, 65.

30. J. Tian, S. Wang, Y. Feng, J. Li and S. Collins, *J Mol. Catal. A: Chem*. **1999**, 144, 137.

31. T.J. Marks, *Acc. Chem. Res.*, **1992**, 25, 57.

32. D. Lee and K. Yoon,*Macromol Rapid Commun.,* **1994**, 15, 841.

33. L. Sun, A. Shariati, J. C. Hsu and D. W. Bacon, *Stud. Surf. Sci. Catal.,* **1994**, 89, 81.

34. L. Sun, C.C. Hsu and D.W. Bacon, *J. Polym. Sci. Part A: Polym. Chem.,* **1994**, 32, 2127.

35. G. Yu, H. Chen, X. Zhang, Z. Jiang, B and Huang, *J. Polym. Sci. Part A: Polym. Chem.,* **1996**, 34, 2237.

36. G.G. Hlatky, *Chem. Rev.,* **2000**, 100, 1347.

37. K. Soga, T. Arai, B. T. Hoang and T. Uozumi, *Macromol. Rapid. Commun.,* **1995**, 16, 905.

38. S.B. Metza, C.C. Hsu and D. W. Bacon, *J Polym Sci Part A: Polym Chem* **1996**, 34, 1693.

39. H. Mori, K. Ohnishi, M. Terano, *Macromol Rapid Commun* **1996**, 17, 25.

40. T. Arai, B.T. Hoang, T. Uozumi and K. Soga, *Macromol Chem Phys* **1997**, 198, 229.

41. P. Galli, G. Collina, P. Sgarzi, G. Baruzzi and E. Marchetti, *J. Appl. Polym. Sci.,* **1997**, 66, 1831.

42. T. Kitagawa, T. Uozumi and K. Soga and T. Takata, *Polymer* **1997**, 38, 615.

43. H. Nishida, T. Uozumi, T. Arai and K. Soga, *Macromol. Rapid Commun*., **1995**, 16, 821.

44. S. C. Hong, T. Teranishi, and K. Soga, *Polymer,* **1998**, 39, 7153.

45. T. Kitagawa, T. Uozumi, K. Soga and T. Takata, *Polymer,* **1997**, 38, 615.

46. A. G. M. Barrett and Y. R. de *Miguel, Chem. Commun*., **1998**, 2079.

47. S. B. Roscoe, J. M. J. Fréchet, J. F. Walzer and A. J. Dias, *Science,* **1998**, 280, 270.

48. K. Musikabhumma, T. Uozumi, T. Sano and K. Soga, *Macromol. Rapid. Commun*., **2000**, 21, 675.

49. S. Liu, F. Meng, G. Yu, B. Huang *J. App. Polym. Sci*., **1999**, 71, 2253.

50. S. C. Hong, U. Rief and M. O. Kristen, *Macromol. Rapid. Commun*., **2001**, 22, 1447.

51. R. Schmidt, H. G. ALT and J. Ebenhoch, *J App. Polym. Sci*., **2001**, 80, 281.

52. H. G. Alt, P. Schertl, A. Koppl, *J Organometal. Chem*., **1998**, 568, 263.

53. C. Liu, T. Tang, B. Huang *J Polym. Sci. Part A: Polym. Chem*., **2003**, 41, 873.

54. H.T. Ban, T. Uozumi, T. Sano, K. Soga, *Macromol. Chem. Phys*., **1999**, 200, 1897.

55. M. Stork, M. Koch, M. Klapper and K. Mullen, *Macromol. Rapid. Commun*., **1999**, 20, 210.

56. M. Klapper, M. Koch, M. Stork, N. Nenov and K. Mullen, *Organometallic Catalysts and Olefin Polymerisation: Catalyst for a New Millenium,* **2001**, 387.

57. M. Koch, M. Klapper and K. Mullen *Organometallic Catalysts and Olefin Polymerisation: Catalyst for a New Millenium*., **2001**, 396.

58. M. Koch, M. Stork, M. Klapper and K. Müllen *Macromolecules*, **2000**, 33, 7713.

59. N. Nenov, M. Koch, M. Klapper and K. Müllen *Polym. Bull*., **2002**, 47, 391.

60. M. Koch, A. Falcou, N. Nenov, M. Klapper and K. Müllen *Macromol. Rapid. Commun*., **2001**, 22, 1455.

61. V. W. Buls,; T. L. Higgins, *J. Polym. Sci. Polym. Chem. Ed*., **1970**, 8, 1037; L. A. M. Rodriguez and J. A. Gabant, *J. Polym. Sci.,* **1963**, 4, 125; P. Blais, R. St. John Manley, *J. Polym. Sci., Polym. Chem. Ed*., **1966**, 4, 1971; J. Y. Guttman and J. E. Guillet, *Macromolecules* **1968**, 1, 461; A. Keller,; F. M. Willmouth, *Makromol. Chem*., **1969**, 121, 42; H. D. Chanzy, R. H. Marchessault, *Macromolecules,* **1969**, 2, 108; R. T. K. Baker, P. S. Harris, R. J. Waite and A. N. Roper, *J. Polym. Sci. Polym. Lett. Ed*., **1973**, 11, 45; R. J. L. Graff, G. Koitleve, C. G. Vonk, *J. Polym. Sci., Polym. Lett. Ed*., **1970**, 8, 735; J. J. Wristers, *Polym. Sci., Polym. Phys. Ed.,* **1973**, 11,1601; R. Hoseman, M. Hentschel, E. Ferracini, A. Ferrero, s. Martelli, F. Riva and M. Vittori Antisari, *Polymer,* **1982**, 23, 979.

62. G. Fink, B. Steinmetz, J. Zechlin, C. Przybyla, and B. Tesche, *Chem. Rev*., **2000**, 100, 1377.

63. Z. Grof, *AIChE J.,* **2003**, 49, 1002.

64. M. A. Ferrero, R. Sommer, P. Spanne, K.W. Jones and W. C. Conner, *J of Polym. Sci. Part A Polym. Chem*., **1993**, 31, 2507.

65. D. M. Merquior, E. L. Lima and J. C. Pinto; *Polym. React. Eng*., **2003**, 11, 133.

66 J. W. Begley, *J. Polym. Sci. A*, **1966**, 4, 319.

67 L. Bohm, *Chem. Ing. Tech*., **1984**, 56, 674.

68 E. J. Nagel, V. A. Kirillov,W. Harmon Ray, *Ind. Eng. Chem. Prod. Res. Dev*., **1980**, 19, 372.

69. D. Singh, and R.R. Merrill, *Macromolecules,* **1971**, 4, 599.

70. W.R. Schmeal and J.R. Street, *AIChE Journal,* **1971**, 17, 1188.

71. R. Galvan, and M. Tirrell, *Comp. Chem. Eng*., **1986**, 10, 77.

72. S. Floyd, T. Heiskanen, T.W. Taylor, G.E. Mann and W.H. Ray, *J App. Polym. Sci*., **1987**, 33, 1021.

73. R.A. Hutchinson, C.M. Chen and W.H. Ray, *J. of App. Polym. Sci*. **1992**, 44, 1389.

74. J. B. P. Soares, *Chem. Engin. Sci*. **2001**, 56, 3931.

75 F. Bonini, V. Fraaije, G. Fink, *J. Polym. Sci. A*, **1995**, 33, 2393.

76 A. Alexiadis, C. Andes, D. Ferrari, F. Korber, K. Hauschild, M. Bochmann, G. Fink, *Macromol. Mater. Eng*., **2004**, 457, 289.

77. W. D. Niegisch, S. T. Crisafulli, T. S. Nagel and W. D. Wagner, *Macromolecules*, **1992**, 25, 3910.

78. J. A. Szymura, P. A. Zielinski, I. G. Dalla Lana, *Catal. Lett*., **1992**, 15, 145.

79. S. W. Webb, E. L. Weist, M. G. Chivetta, R. L. Laurence, and W. C. Conner, *Can. J. Chem. Eng*., **1990**, 69, 665.

80. W. C. Conner, S. W. Webb, P. Spanne, and K. W. Jones, *Macromolecules*, **1990**, 23, 4742.

81. P. Mackie, M. N. Berger, B. M. Grieveson and D. J. Lawson, *Polym. Sci., Polym. Lett. Ed*., **1967**, 5, 493.

82. C. W. Hock*, J. Polym. Sci., Polym. Chem. Ed*., **1966**, 4, 55.

83. M. Kakugo, H. Sadatoshi, M. Yokoyama, and K. Kojima *Macromolecules,* **1989**, 22, 547.

84. M. Kakugo, H. Sadatoshi, M. J. Yokoyama, *Polym. Sci., Polym. Lett. Ed*., **1986**, 24, 171.

85. M. Kakugo, H. Sadatoshi, J. Sakai and M. Yokoyama, *Macromolecules,* **1989**, 22, 3172.

86. G. Fink, B. Steinmetz, J. Zechlin, C. Przybyla and B. Tesche, *Chem. Rev*., **2000**, 100, 1377; A. Alexiadis, C. Andes, D. Ferrari, F. Korber, K. Hauschild, M. Bochmann, G. Fink, *Macromol. Mat. Eng*., **2004**, 289, 457; S. Knoke, F. Korber, G. Fink, B. Tesche, *Macromol. Chem. Phy*., **2003**, 204, 607; Bonini, V. Fraaije, G. Fink, *J. Polym. Sci. Part A*, **1995**, 33,

2393.

87. V. J. Ruddick and J. P. S. Badyal, *J. Phys. Chem. B.*, **1997**, 101, 1791.

88. G. Binnig, C. F. Quate and C. Gerber, *Phys. Rev. Lett*., **1986**, 56, 930.

89. K.W. Jones, P. Spanne, S. W. Webb, W. C. Conner, R. A. Beyerlein, W. J. Reagan and F.M. Dautzengerg, *Nuclear Instruments and Methods in Physics Research Section B: Beam Interactions with Materials and Atoms*, **1991**, 56, 427.

90. Jones K.W., Spanne P., Lindquist W. B., Conner W. C., and Ferrero M. A., *Nucl. Instr. and Meth. B*, **1992**, 68, 105.

91. W. C. Conner, S. W. Webb, P. Spanne, and K. W. Jones, *Macromolecules*, **1990**, 23, 4742.

92. E. L. Weist, A. H. Ali, and W. C. Conner, *Macromolecules*, **1987**, 20, 689.

93. E. L. Weist, A. H. Ali, B. G. Naik, and W. C. Conner, *Macromolecules*, **1989**, 22, 3244.

94. S. W. Webb, E. L. Weist, M. G. Chivetta, R. L. Laurence, and W. C. Conner, Can. *J. Chem. Eng*., **1991**, 69, 665.

95. R. Goretzki, G. Fink, B. Tesche, B. Steinmetz, R. Rieger, W. Uzick, *J. Polym. Sci. Part A,* **1999**, 37, 677.

96. G. Weickert, G. B. Meier, J. T. M. Pater and K. R. Westerterp, *Chem. Eng. Sci*., **1999**, 54, 3291.

97. M. Abboud, K. Kallio, K.H. Reichert, *Chem. Eng. Tec*., **2004**, 27, 694.

98. S. Knoke, D. Ferrari, B. Tesche and G. Fink, *Angew. Chem. Int. Ed*., **2003**, 42, 5090.

Chapter 2. Motivation and Objectives

The heterogenization of metallocene catalysts on the support (carrier) is necessary in order to produce high bulk density polyolefin product with good morphology and prevent a reactor fouling after each olefin polymerization [1]. This heterogeneous catalyst system is the important requirement for an industrial system [2]. As a catalyst carrier in heterogeneous polymerization, SiO_2, Al_2O_3, zeolites, montmorillonite and polymer beads have been used [3, 4, 5 and 6].

The advantages of the polymer beads over the inorganic carrier in heterogeneous polymerization is (1) easy support handling, (2) better fragmentation of support within the polyolefin products, (3) better incorporation into the polyolefin products, (4) absence of inorganic impurities in the polyolefin products and (5) highly transparent film formed [7].

For the immobilization of metallocene catalysts on this carrier, the supports should satisfy some requirements as a proper catalyst carrier in heterogeneous polymerization. Firstly, the support should have high surface area for anchoring enough metallocene catalyst (Figure 2-1). The amount of catalyst immobilized on the support surface determines the catalyst activity, productivity and the product morphology.

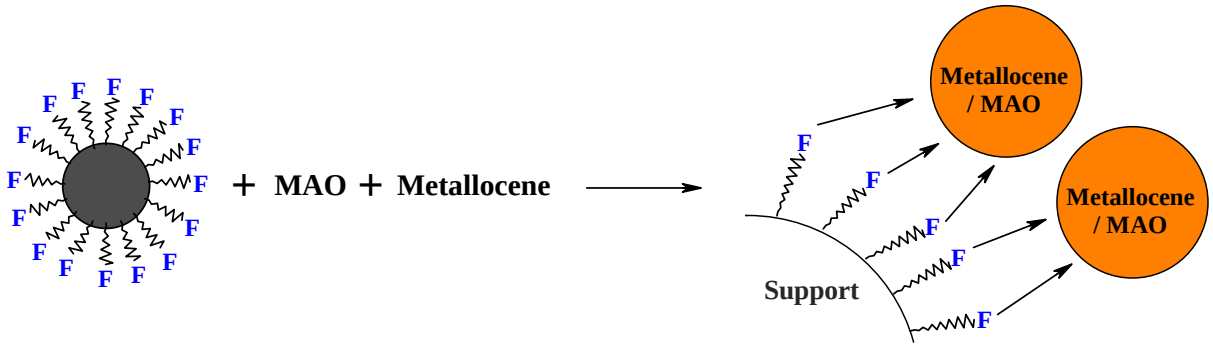

Figure 2-1. Scheme of supporting metallocene catalyst activated by methylalumoxane cocatalyst

Secondly, the support should have enough mechanical strength during olefin polymerization. This mechanical strength within the supports (secondary particle) is to tighten the primary particles and to keep the particle shape of support (Figure 2-2). This property of the support is related to the replication of the support shape and polyolefin product.

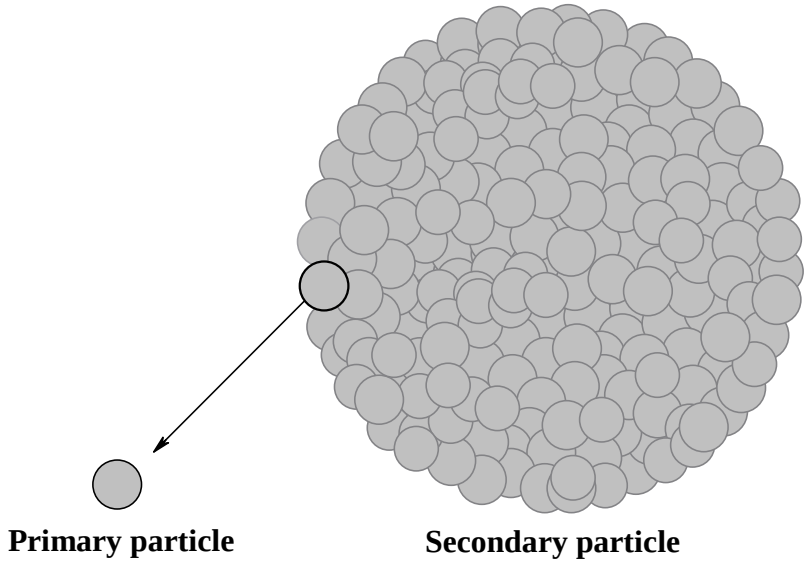

Figure 2-2. Primary and secondary particle as a support

If the supports (secondary particles) have low mechanical strength, they can not keep the shape during polymerization and the polyolefin products are fluffy. Figure 2-3 shows the scheme of polymerization with a perfect replica of the supported catalyst. The spherical particles within the support in this figure grow bigger and bigger with keeping the shape during polymerization.

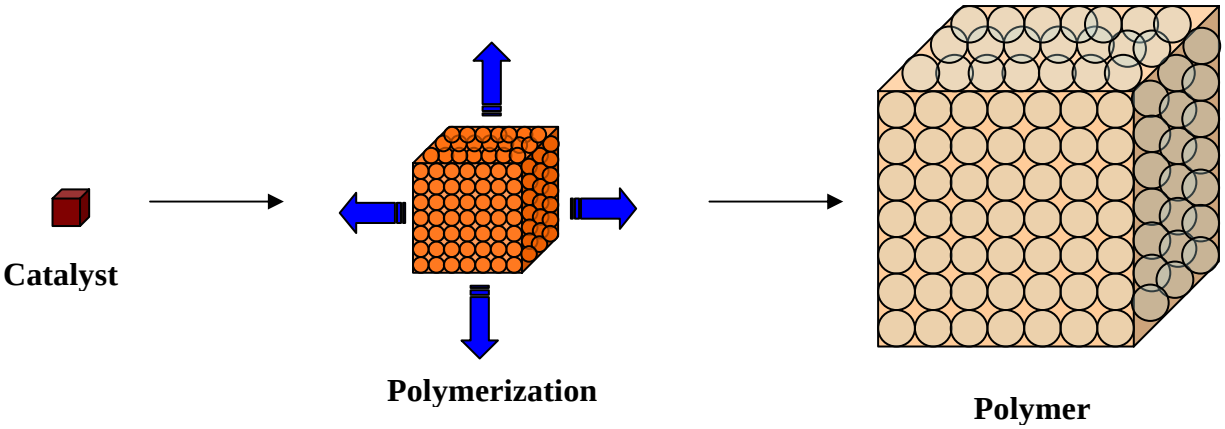

Figure 2-3. Scheme of polymerization with a perfect replica of the supported catalyst

Thirdly, the support should be broken down into microscopic particles during polymerization for the homogeneous distribution of active sites within the polyolefin products. The particles distributed homogeneously should provide ready access of monomer gas to the active catalyst. That is called as 'the fragmentation of support' within the

polyolefin products.

One of the aims of the present work is to develop new supports to satisfy these requirements for the heterogeneous olefin polymerization. For these objectives;

→ The new polymer support should be developed by simple synthetic method and cheap starting materials having well-defined morphology which suggests the use of polystyrene materials.

→ The new polymer support should be well-defined, spherical and nanosized particle beads. The metallocene catalyst should distribute homogeneously on the carrier and the supported catalyst should fragment homogeneously within the polyolefin products.

→ The new support should immobilize the catalyst strongly enough in order not to leach the metallocene catalyst from carriers. If the immobilization is not strong to anchor the metallocene, the polyolefin products have bad morphology and are fluffy. Furthermore, the support should not deactivate the metallocene catalyst. Functionalization with strong nucleophilic PEO or PPO chains on the polymer beads is suitable for the non-covalent bonding of the active species with the support.

→ The new support should be tested in different polymerization condition such as different pressure and temperature to investigate the stability under the different condition. Also it should be tested in different polymerizations such as ethylene polymerization, copolymerization of ethylene with α-olefin monomers and propylene polymerization. Especially for propylene polymerization, the influence of the support on the properties of polypropylene such as tacticity, melting point and mechanical properties should be studied.

The other key aim in the present work is to develop a new method to study the fragmentation of the supported catalyst on the different carriers. So far, for the study of catalyst fragmentation within the polyolefin products, X-ray tomography, atomic force microscopy (AFM), scanning electron microscopy (SEM) and transmission electron microscopy (TEM) have been used [8, 9, 10 and 11]]. However these methods need special instrument often for section polyolefin particle and visualization of the supported catalyst fragmented within the polyolefin products. The requirement of our optical is to study the internal structure of polyolefin products and the fragmentation behavior of the supported catalyst during olefin polymerization.

For the above investigations, the working program is as follows;

(1) Synthesis of the new support material,

(2) Grafting of the MAO cocatalyst onto the carrier,

(3) Metallocene impregnation on the carrier treated with MAO,

(4) Olefin polymerization of the olefin monomer,

(5) Characterization of olefin polymer and fragmentation study of the supported catalyst in heterogeneous olefin polymerization.

1. F. Ciardelli, A. Altomare and M. Michelotti, *Catalysis Today*, **1998**, 41, 149,.

2. J. H. Z. dos Santos, H. T. Ban, T. Teranishi, T. Uozumi, T. Sano and K. Soga, *J. Mol. Cat. A: Chem.*, **2000**, 158, 541,.

3. M. Kaminaka, K. Soga, *Macromol. Rapid Commun.*, **1991**, 12, 367,.

4. L.K. Van Looveren, D. E. De Vos, K. A. Vercruysse, D. F. Geysen, B. Janssen, P. A. Jacobs, *Catal. Lett.*, **1998**, 56, 53,.

5. S. I. Woo, Y. S. Ko, T. K. Han, *Macromol. Rapid Commun.*, **1995**, 16, 489,.

6. J. S. Bergman, H. Chen, E. P. Giannelis, M. G. Thomas, G. W. Coates, *Chem. Commun.*, **1999**, 2179.

7. Nikolay Nenov, Dissertation, Johannes Gutenberg Universitat, Mainz, **2003**.

8. W. D. Niegisch, S. T. Crisafulli, T. S. Nagel and W. D. Wagner, *Macromolecules*, **1992**, 25, 3910.

9. J. A. Szymura, P. A. Zielinski, I. G. Dalla Lana, *Catal. Lett.*, **1992**, 15, 145,.

10. S. W. Webb, E. L. Weist, M. G. Chivetta, R. L. Laurence, and W. C. Conner, *Can. J. Chem. Eng.*, **1990**, 69, 665.

11. W. C. Conner, S. W. Webb, P. Spanne, and K. W. Jones, *Macromolecules*, **1990**, 23, 4742,.

Chapter 3. Nanosized polystyrene (PS) beads as a support in heterogeneous ethylene polymerization

One of the successful approaches for the preparation of nanosized polymer beads involves the use of amphiphilic block copolymers having reactive functional groups. Polyethylene oxide-block-polystyrene (PEO-b-PS) was used to prepare core shell nanospheres [1]. The polystyrene part of the polyethyleneoxide-block-polystyrene tends to become entangled in the core of polystyrene crosslinked by divinylbenzene and the polyethyleneoxide part tends to form a shell on the surface of PS beads. The polyethyleneoxide (PEO) functionalized supports have been proven to immobilize the MAO / metallocene complex [1].

In this chapter, the influence of the PEO concentration of the nanosized PS beads on the catalyst activity in heterogeneous ethylene polymerization and the morphology of polyethylene products is studied. The concentration of functional groups on the support is considered as an important factor to influence the supported catalyst behavior in heterogeneous polymerization. This is similar to the silica-supported catalyst system where the concentration of hydroxyl groups on the silica surface is a very important factor [2].

3.1. Nanosized PS beads functionalized with polyethyleneoxide (PEO) as support in heterogeneous ethylene polymerization

- prepared by PS-PEO block copolymer

3.1.1. Preparation of nanosized PS beads functionalized with polyethyleneoxide (PEO) and the supported catalyst

Nanosized polystyrene (PS) beads functionalized with polyethyleneoxide (PEO) were prepared by miniemulsion polymerization. Miniemulsion polymerization has been a useful method to prepare nanosized polymer lattices [3, 4 and 5]. The term miniemulsion is related to the sub-micron monomer droplets containing a co-emulsifier. Miniemulsion polymerization using an effective emulsifier / coemulsifier system produces very small polymer particles with a uniform copolymer composition and narrow particle size distribution which is advantageous in comparison with the products obtained from conventional emulsion polymerization [6].

Several nanosized PS beads functionalized with different concentrations of PEO were

prepared by varying the amount of surfactant (0.1 mol% to 10 mol% of PS-PEO block copolymer). The monomers used are styrene, divinylbenzene as crosslinker and PEO-b-PS (polyethyleneoxide-block-polystyrene) copolymer as surfactant (Scheme 3-1). The procedure used was as follows: styrene, divinylbenzene as crosslinker and hexadecane were stirred for 5 min. The PEO-PS block copolymer was dispersed in water homogeneously at 80 ^{o}C and then cooled down to room temperature. The homogeneous block copolymer dispersed in water was mixed with the styrene oil phases and stirred at the highest power of the magnetic stirrer for 1 hr to form a microemulsion. The microemulsion was ultrasonicated for 5 min with a Branson Sonifier 450 W and 70 % power under ice cooling to form a miniemulsion. The miniemulsion was heated in an oil bath at 72 °C and then the initiator $K_2S_2O_8$ was dissolved in a small quantity of distilled water and added to the miniemulsion reactor. After 12 hr, the PS product was filtered by a stirred Ultrafiltration Millipore model 8050 with polyethersulfone membrane and dried in vacuum.

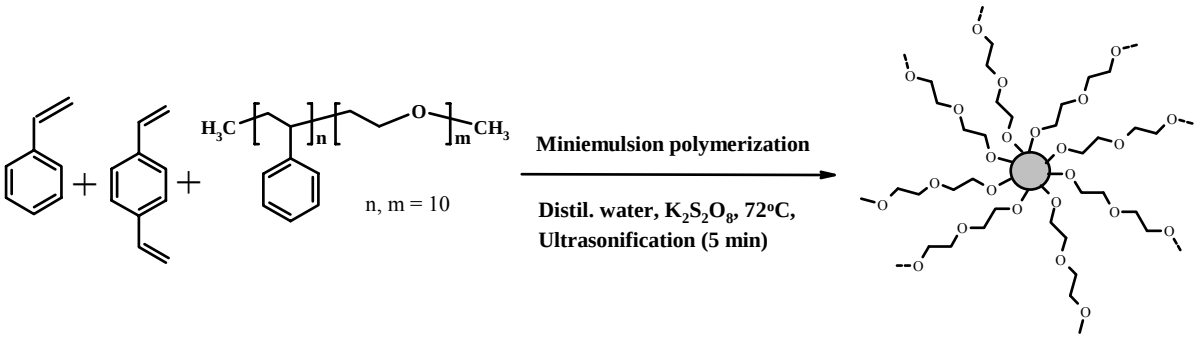

Scheme 3-1. The preparation of nanosized PS beads functionalized with polyethyleneoxide (PEO)

The SEM image and particle size distribution of the nanosized PS beads show a spherical shape with a particle size of about 50 nm (Figure 3-1). The PS particles appear to form aggregates in the SEM image which must have occurred during the drying process of the beads produced. The result of particle size analyzed by a Zetasizer shows that the PS beads have about 54 nm up to 185 nm in diameter suspended in water depending on the different concentration of PEO-PS block copolymer (Table 3-1). The size of PS beads prepared by miniemulsion polymerization is smaller than those made by conventional emulsion polymerization. According to the results of Dr. Nikolay Nenov [7], the particle size of PS beads functionalized with PEO prepared by conventional emulsion polymerization was about

300 - 1000 nm.

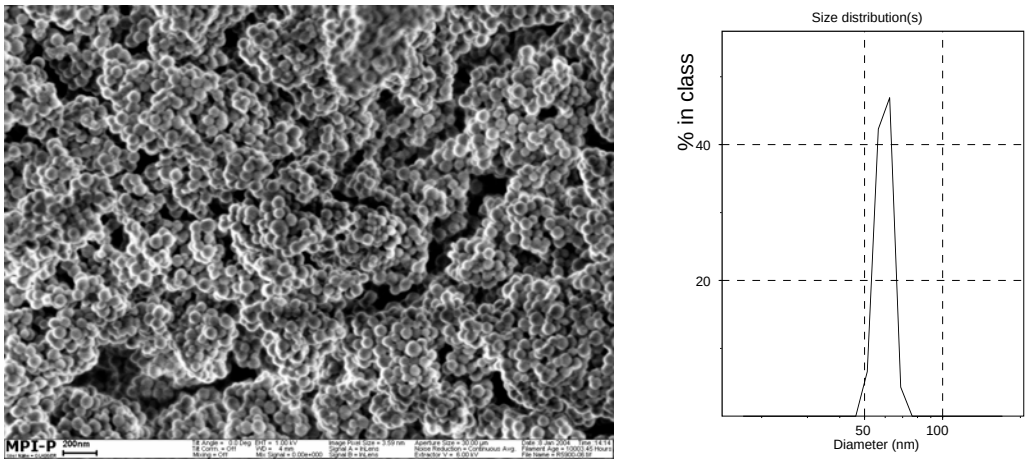

(A) (B)

Figure 3-1. (A) SEM image (scale bar – 200 nm) and (B) particle size distribution of nanosized PS beads (NPS1-1 in Table 3-1) functionalized with PEO groups

Table 3-1. Different molar ratios of monomers and particle size of PS beads

Support	Styrene (mol %)	Divinylbenzene (mol %)	PS-co-PEO (mol %)	Particle size [a] (nm)
NPS1-1	89.9	10	0.1	54
NPS1-2	89.5	10	0.5	88
NPS1-3	89	10	1	165
NPS1-4	85	10	5	170
NPS1-5	80	10	10	185

[a] measured by Zetasizer

For immobilizing the metallocene catalyst on the nanosized PS beads functionalized with PEO (Scheme 3-2), the PS beads were first mixed with a solution of methylalumoxane (MAO) in toluene to remove traces of water. Independently, the metallocene and MAO were mixed in toluene and stirred until completely dissolved. From this preformed metallocene / MAO complex, the calculated amount needed for the support immobilization was added to the suspension of the nanosized PS beads and MAO in toluene. Additional stirring for half an hour was needed for complete binding of the catalyst to the support. After stirring the mixture for 1 hr, it was washed with dry toluene / hexane (50 / 50 Vol %) mixture and the extra, i.e. non-supported metallocene / MAO solution was removed from the supported

catalyst via a *cannula*. The supported catalyst was washed two more times and then the remaining solid was dried in vacuum.

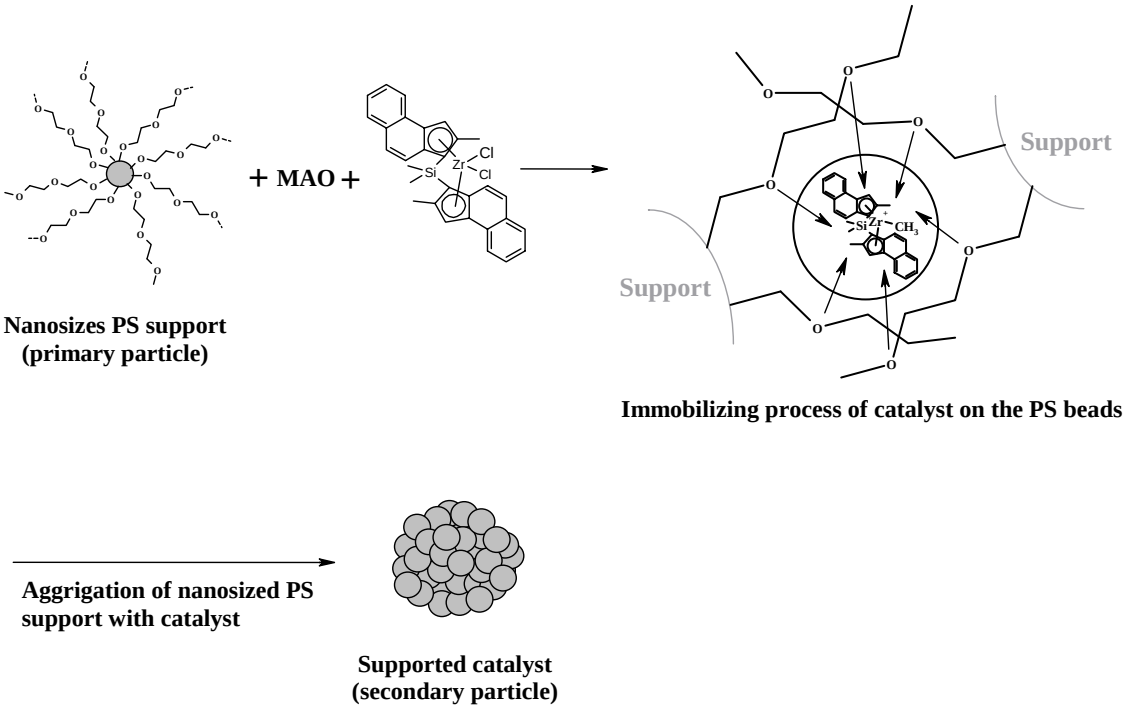

Scheme 3-2. Preparation of catalyst supported on the nanosized PS beads functionalized with PEO

In all experiments performed, $Me_2Si(2MeBenzInd)_2ZrCl_2$ was used as metallocene. As the PEO shell of the nanosized particles consists of very nucleophilic ether groups, the immobilization via a non-covalent bonding of the MAO / metallocene complexes can be achieved and the aggregation of the nanosized PS beads takes place. SEM pictures presented in Figure 3-2 show the morphology of the supported catalyst on the nanosized PS beads (NPS1-5). The supported catalyst particles obtained by the interaction between MAO / metallocene and the nanosized particles are normally spherical in shape. The particle size of the supported catalyst is about 50 - 100 micrometer which is about 1000 times larger than that of the nanosized PS beads due to the aggregation of the PS beads induced by the interaction between PEO chains on PS beads and the active metal sites. The SEM image of the supported catalyst particle in Figure 3-2 (B) and (C) show exactly the formation of the conglomerates of the nanosized PS beads (primary particles) through the interaction between PEO chains of the nanosized PS beads and MAO / zirconocene complexes in Scheme 3-2.

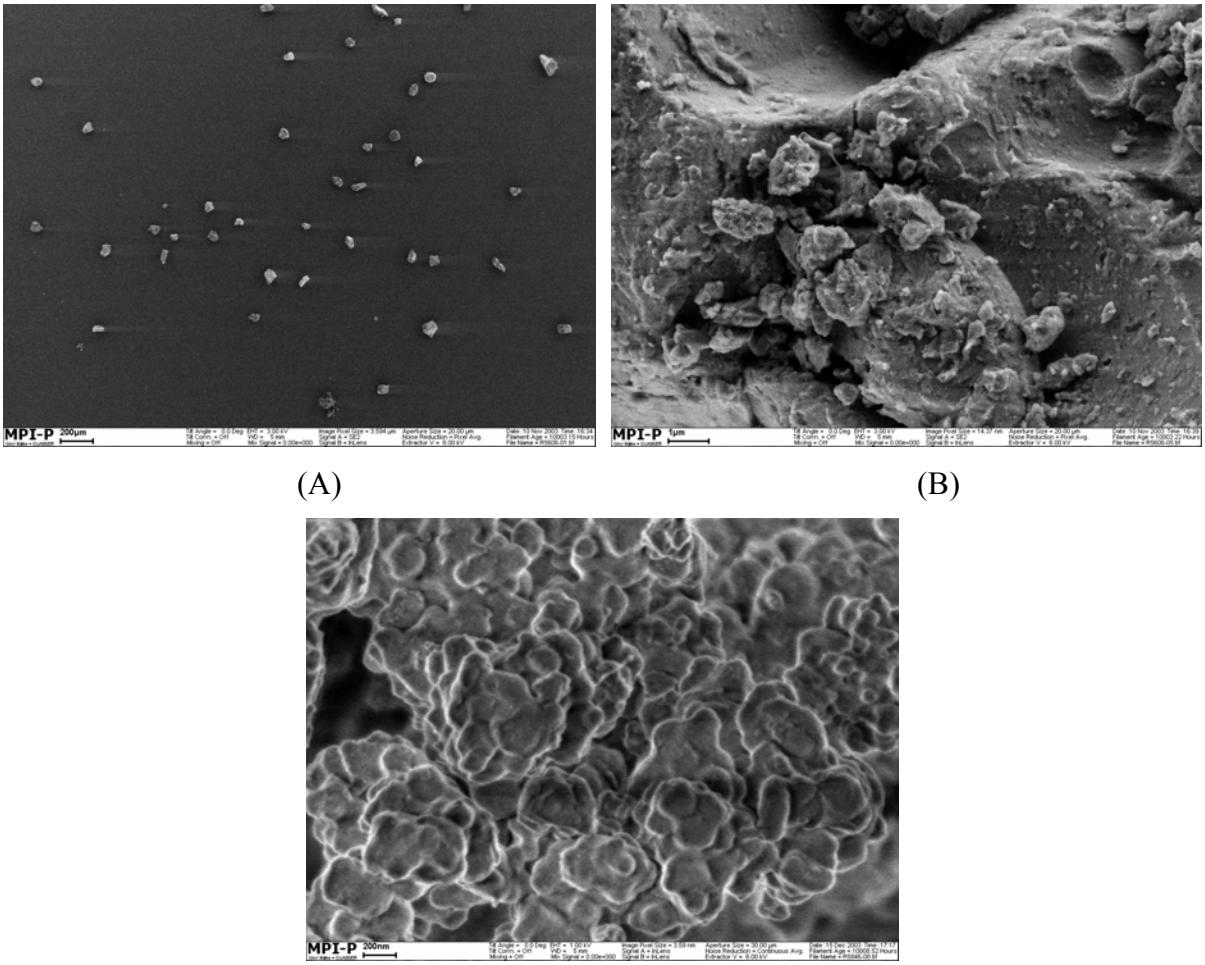

(A) (B)

(C)

Figure 3-2. SEM images of the supported catalyst on the nanosized PS beads (NPS1-5) functionalized with PEO: scale bar – (A) 200 µm, (B) 1 µm and (C) 200 nm

3.1.2. Ethylene polymerization and characteristics of the PE products

To study the influence of the concentration of PEO on the nanosized PS beads on the catalytic performance, several nanosized PS beads functionalized with polyethyleneoxide (PEO) and varying concentration of PS-co-PEO were used as support in heterogeneous ethylene polymerization. By using these nanosized PS beads, different supported catalysts were prepared and ethylene polymerizations were carried out at 70 ^{o}C polymerization temperature and 40 bar ethylene pressure in 400 ml isobutane as solvent. In this heterogeneous ethylene polymerization, 40 µmol / g metallocence activation and 350 MAO / Zr mol ratio were used. Based on the results of ethylene polymerizations, the trends of catalyst activity and bulk density of polyethylene (PE) obtained in heterogeneous polymerization can be deduced.

The supported catalyst prepared by the different concentration of PEO on the PS beads exhibits different activity and productivity (Table 3-2). With increasing the concentration of polyethyleneoxide (PEO) on the PS beads, the activity of the supported catalyst decreases but the bulk density of the polyethylene increases. The catalyst supported on the 0.1 mol% PEO functionalized PS beads exhibits an activity of about 2540 (kg PE / mol Zr hr bar) in Run PE-1 and the bulk density of polyethylene (PE-1) is 250 (g / l) which is a very low value and not suitable for industrial uses. The catalyst supported on the 1 mol% PEO functionalized PS beads has an activity of 1780 (kg PE / mol Zr hr bar) in Run PE-3. However, the bulk density of PE is increased up to 320 (g / l) in comparison to that produced by the supported catalyst on the PS beads functionalized 0.1 mol% PEO. When the PEO concentration increases up to 10 mol% on the PS beads, the bulk density of PE (PE-5) is 390 (g / l). On the other hand, the catalyst activity is decreased to nearly 1000 (kg PE / mol Zr hr bar) in Run PE-5. Thus the different concentrations of PEO on the PS beads influence the catalyst activity in olefin polymerization and the property of polyethylene such as bulk density of PE.

Table 3-2. Ethylene Polymerization[a] depending on the concentration of PEO on the nanosized PS beads

Run	PS-PEO (mol %)	Zr/cat (μmol/g)	MAO/Zr	Activity [b]	Productivity [c]	BD [d]
PE-1	0.1	40	350	2545	3460	250
PE-2	0.5	40	350	2205	3000	270
PE-3	1	40	350	1780	2420	320
PE-4	5	40	350	1330	1810	380
PE-5	10	40	350	1030	1400	390

[a] Reaction condition: 1 L autoclave, isobutane 400 ml, ethylene pressure 40 bar, 70 °C, 1 hr, amount of catalyst: 23 – 24 mg. [b] kg PE / mol Zr hr bar. [c] g PE / g cat hr. [d] BD: bulk density (g / l).

This dependence of catalyst activity upon the concentration of PEO on the PS beads can easily be explained by the interaction of primary particle and metallocene / MAO complex. At high PEO concentrations on the PS beads, the interaction between PS beads and metallocene / MAO complex is stronger than that at low PEO concentration on PS beads. This strong interaction results in a denser network of each primary PS bead which limits the

mobility of the primary particle and the fragmentation of the secondary catalyst particle. On the other hand at high PEO concentration on the PS beads, the reversible weak interaction between PEO chains and metallocene / MAO complex can result in a high fragmentation of the catalyst and a more homogeneous polymerization which produces low bulk density of polyethylene products.

The different concentrations of functional group on the PE beads also influence the morphology and the particle size of polyethylene product depending on the supported catalyst prepared by the different concentration on the support.

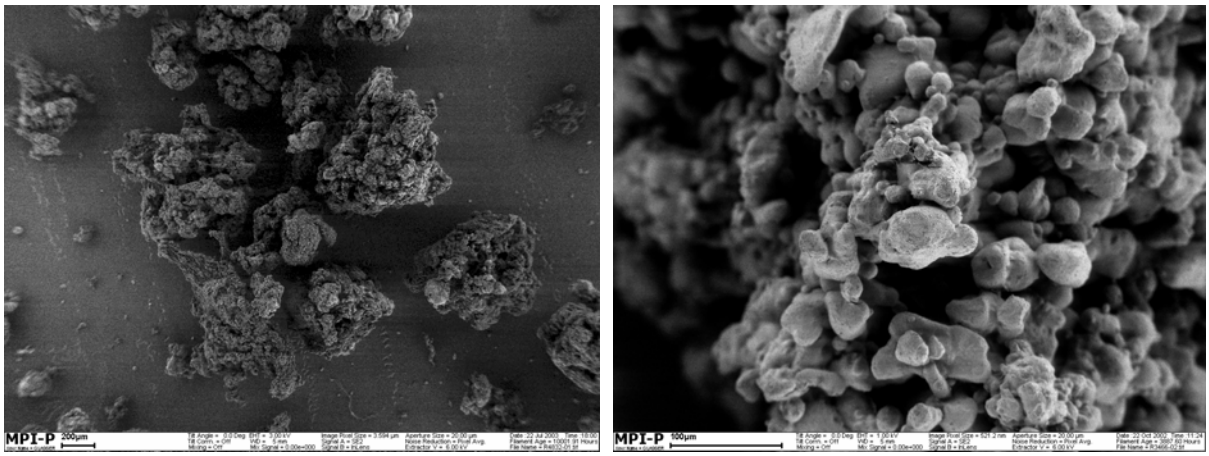

(A) (B)

Figure 3-3. SEM images of PE (PE-3) produced by the catalyst supported on the 1 mol % PEO functionalized nanosized PS beads: scale bar – (A) 200 μm and (B) 100 μm

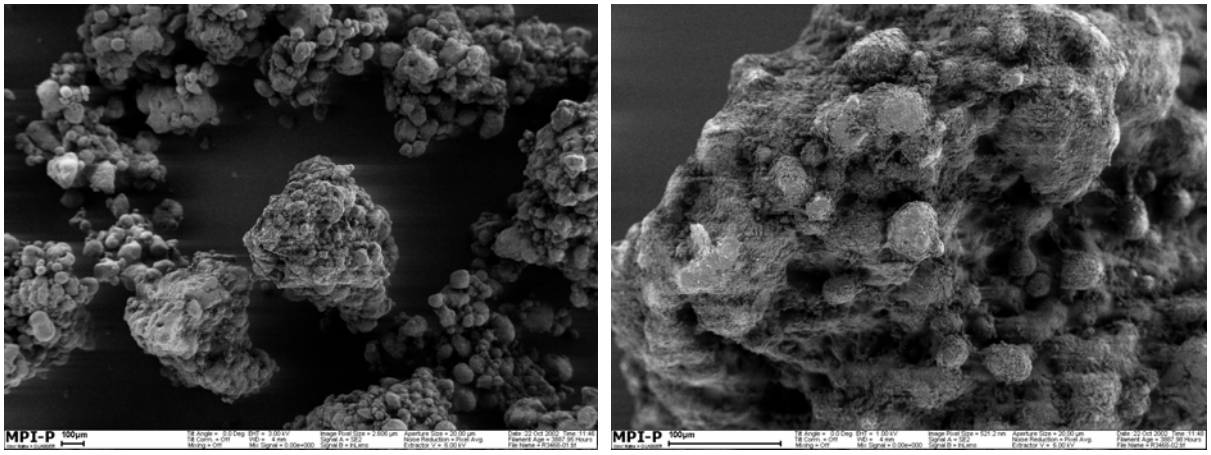

(A) (B)

Figure 3-4. SEM images of PE (PE-5) produced by catalyst supported on the 10 mol % PEO functionalized nanosized PS beads: scale bar – 100 μm

The polyethylene (PE-3) produced by the catalyst supported on the 1 mol % PEO functionalized PS beads is fluffy (Figure 3-3). On the other hand, the polyethylene (PE-5) produced by the catalyst supported on the 10 mol % PEO functionalized PS beads has normally hard and spherical particles (Figure 3-4). The particle size distribution of PE-5 is narrower than that (PE-3) produced by the supported catalyst on the PS beads functionalized with 1 mol % PEO. The PE products consist of many small spherical particles held tightly together. The characteristics of the polyethylene (PE) products are presented in Table 3-3. The melting points (Tm) and the crystallinity (Xc) of polyethylene measured by DSC are about 134.7 ^{o}C and 48.8 % respectively. For comparison with the crystallinity of each polyethylene (PE), every PE sample was measured by DSC with about 9.5 mg of PE sample and calculated by comparison with 100 % crystalline polyethylene (290 J / g) [8]. The PE products exhibit high molecular weights and low polymer dispersities. The molecular weights (Mw) are about 1,150,000 - 1,310,000 and the polydispersity index is about 2.3 - 2.6.

Table 3-3. Characteristics of polyethylene [a]: molecular weight, melting point and crystallinity of polyethylene products

Run	Mn [b] (g / mol)	Mw [b] (g / mol)	PDI	Tm [c] (^{o}C)	Xc [d] (%)
PE-1	519,000	1,204,000	2.32	134.7	48.8
PE-2	497,000	1,317,000	2.65	133.8	48.9
PE-3	499,000	1,212,000	2.43	133.5	48.8
PE-4	520,000	1,268,000	2.44	134.1	48.5
PE-5	514,000	1,156,000	2.25	133.7	48.7

[a] Reaction condition: in a 1 L autoclave, isobutane 400 ml, ethylene pressure 40 bar, 70 °C, 1 hr, catalyst activation: 40 Zr / cat (μmol / g), 350 MAO / Zr molar ratio, amount of catalyst 23 - 24 mg. [b] by gel permeation chromatography (GPC). [c] by differential scanning calorimetry (DSC). [d] Xc (%): Crystallinity = 100 (ΔH_m / ΔH_m^*); ΔH_m^* = 290 J / g [8].

3.2. Nanosized PS beads functionalized with polyethyleneoxide (PEO) as support in heterogeneous ethylene polymerization

- prepared by PEO functionalized with styrene

The use of nanosized PS beads functionalized with polyethyleneoxide (PEO) chains as catalyst carrier was investigated in heterogeneous ethylene polymerization in chapter 3.1. The nanosized PS beads were prepared with PS-PEO block copolymer. However, one can be worried about the leaching of the PEO-PS block copolymer physically crosslinked on the PS beads. Leaching out of PS-PEO block copolymer would influence the bulk density and the morphology of the PE products.

In this chapter, other nanosized PS beads functionalized with polyethyleneoxide (PEO) are introduced. Polyethyleneoxide (PEO) is thereby covalently bonded to the polystyrene core by copolymerization of styrene functionalized with PEO and styrene monomers.

3.2.1. Preparation of nanosized PS beads and the supported catalyst

4-Vinylphenyloxyundecanyl-oligo(ethylene oxide) as surfactant was synthesized by Tanja Nemnich at the MPIP and then this styrene compound was copolymerized with styrene and divinylbenzene by miniemulsion polymerization (Scheme 3-3).

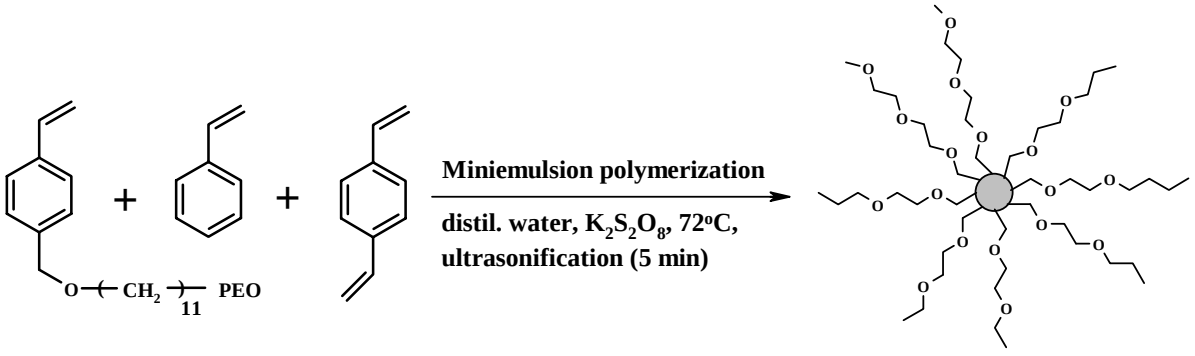

Scheme 3-3. Preparation of nanosized PS beads functionalized with polyethyleneoxide (PEO)

These nanosized PS beads were prepared according to the following procedure. The emulsifier [4-Vinylphenyloxyundecanyl-oligo(ethylene oxide)] was dissolved in dimethylformamide (DMF) in a concentration of about 1 mol% (regarding the total amount of the monomers) and then distilled water was added to the solution of the emulsifier in DMF.

The mixture was evaporated until the DMF was completely removed as its azeotropic mixture with water. To basify the reaction medium (necessary condition for the emulsion polymerization), 1N KOH (1.5 ml per 50 ml residual distilled water) was added. Styrene, divinylbenzene as crosslinker and hexadecane were stirred for 5 min and mixed with the solution of emulsifier / KOH. The mixture was stirred at the highest power of the magnetic stirrer for 1 hr to form a microemulsion. The microemulsion was ultrasonicated for 5 min with a Branson Sonifier 450 W AND 70 % power under ice cooling to form a miniemulsion. The miniemulsion was heated in an oil bath at 72 °C and then the initiator $K_2S_2O_8$ was dissolved in a small quantity of distilled water and added to the miniemulsion reactor. After 12 hr, the PS product was filtered by a stirred Ultrafiltration Millipore model 8050 with polyethersulfone membrane and dried in vacuum.

Table 3-4. Preparation of nanosized PS beads functionalized with polyethyleneoxide (PEO)

Support	PEO (units)	Surfactant (mol %)	Styrene (mmol)	DVB (mol %)	Particle size [a] (nm)
NPS2-1	10	1	90	9	70
NPS2-2	45	1	90	9	72

[a] measured by Zetasizer

Depending on the polyethyleneoxide (PEO) chain length, two kinds of nanosized PS beads as support were prepared (Table 3-4). One (NPS2-1) has 10 ethyleneoxide (EO) repeat units and the other (NPS2-2) has 45 ethyleneoxide (EO) repeat units on the polystyrene beads. The polystyrene beads functionalized with 10 ethyleneoxide (EO) units (NPS2-1) exhibit an average particle size of 70 nm and the other polystyrene beads functionalized with 45 ethyleneoxide (EO) units (NPS2-2) have an average particle size of 72 nm measured by the Zetasizer.

For immobilizing the metallocene catalyst on the PS beads functionalized with PEO (Scheme 3-4), the PEO-functionalized lattices were mixed with a solution of MAO in toluene to remove traces of water. The amount of MAO depends on the desired activation. After 12 hr, the solution of metallocene and MAO as cocatalyst was added to the MAO / support suspension. After stirring the mixture for 1 hr, it was washed with dry toluene / hexane (50 / 50 Vol %) mixture and the extra metallocene / MAO solution was removed from the supported catalyst via a cannula. After the procedure was repeated 3 times, the remaining

solid was dried in vacuum.

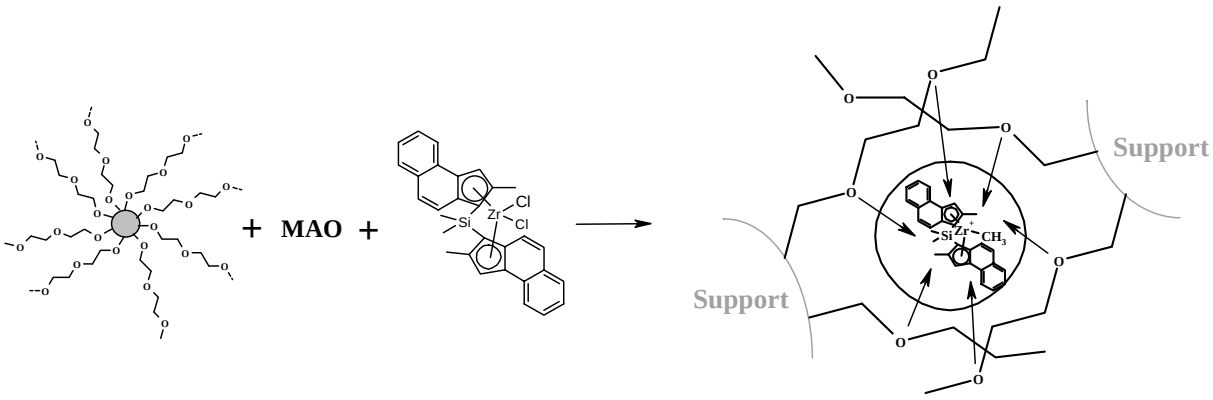

Scheme 3-4. Preparation of catalyst supported on the nanosized PS beads functionalized with PEO

SEM pictures (Figure 3-5) show the morphology of the supported catalyst. As can be seen in the first image (Figure 3-5, A), there is no complete control of the size of the secondary catalyst particles that are the crosslinked carrier activated with metallocene / MAO complexes. The size of the particles can be controlled only by the speed of stirring during the drying of the catalyst in vacuum. However, a reasonable size distribution was achieved by this simple immobilization method. These SEM images are similar to the images of the Figure 3-2 in chapter 3.1.

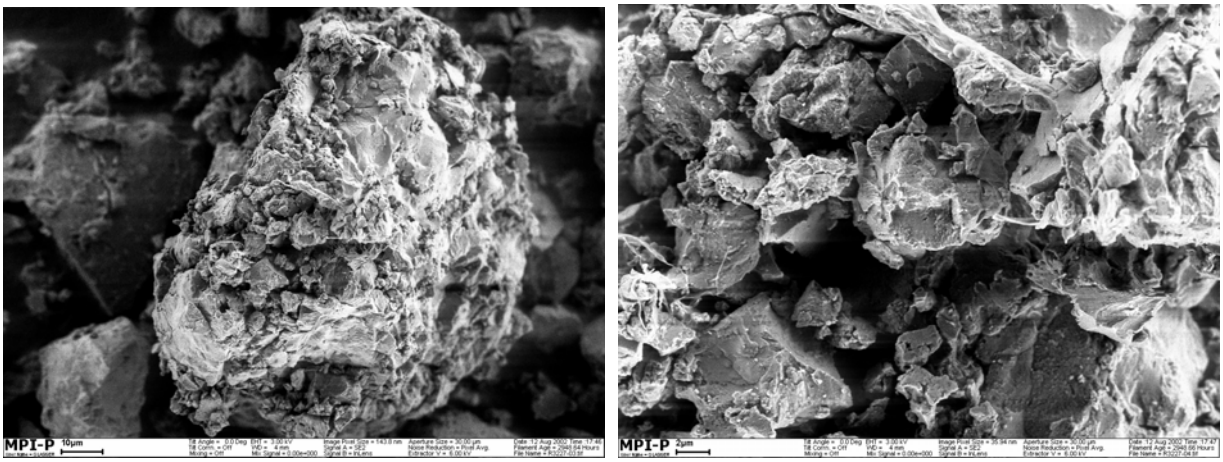

(A) (B)

Figure 3-5. SEM images of the supported catalyst on the nanosized PS beads (NPS2-2) functionalized with PEO: scale bar – (A) 10 µm and (B) 2 µm

3.2.2. Ethylene polymerization and characteristics of the PE products

Under a polymerization temperature of 70 ^{o}C and 40 bar ethylene pressure, ethylene polymerization was carried out in 400 ml isobutane as solvent. Two kinds of experimental conditions were tried for ethylene polymerization to study the influence of the different supported catalyst on the catalyst activities: first experimental condition was implied a catalyst activation of 30 μmol / g and 300 MAO / Zr molar ratio and the second one a catalyst activation of 40 μmol / g and 350 MAO / Zr molar ratio.

Table 3-5. Ethylene polymerization depending on the concentration of PEO on the nanosized PS beads [a]

Run	Support	Zr / cat (μmol / g)	MAO / Zr	Activity [b]	Productivity [c]	BD [d]
PE-6	NPS2-1	30	300	1260	1720	350
PE-7	NPS2-2	30	300	1510	2050	340
PE-8	NPS2-1	40	350	1710	1980	300
PE-9	NPS2-2	40	350	2140	2470	290

[a] Reaction condition: in a 1L autoclave, isobutane 400 ml, ethylene pressure 40 bar, 70 °C, 1 hr. amount of catalyst: 23 - 24 mg. [b] kg PE / mol Zr hr bar. [c] g PE / g cat hr. [d] BD: bulk density (g / l)

In the first case of 30 catalyst activation (μmol / g) and 300 MAO / Zr molar ratio, the catalyst supported on 10 units of PEO functionalized PS beads exhibits an activity of 1260 (kg PE / mol Zr hr bar) in Run PE-6 and the catalyst supported on the 45 units of PEO functionalized PS beads has an activity of 1510 kg PE/mol Zr hr bar in Run PE-7 (Table 3-5). The supported catalyst on PS beads with long PEO chains (NPS2-2) is thus more active than the supported catalyst on PS beads with the short PEO chains (NPS2-1). In the second case [40 catalyst activation (μmol / g) and 350 MAO / Zr molar ratio], the catalyst activity is higher than that of the first experimental condition due to the increase of the MAO / Zr molar ratio and catalyst activation. The bulk densities of PE produced with the different supported catalyst are also different. Support system (NPS2-1) exhibits an activity of 1710 kg PE / mol Zr hr bar in Run PE-8, while support system (NPS2-2) exhibited an activity of 2140 kg PE / mol Zr hr bar in Run PE-9. As shown in chapter 3.1, the catalyst activity is influenced by the concentration of the ethyleneoxide unit on PS beads. The supported catalyst on the long PEO chains is more active than the supported catalyst on the short PEO chains. These results are

comparable to those of Dr. Nicolay Nenov [13]. He prepared latex particles by using different length of PS-PEO block copolymers as emulsifiers: one (RS 2) was 30 chain units of PEO and 30 chain units of PS. The other (RS 5) was 10 chain units of PEO and 30 chain units of PS. At 36 μmol / g metallocence activation and 300 MAO / Zr mol ratio, the activity of the supported catalyst on RS 2 has higher than that of the supported catalyst on RS 5. The result was the same for 25 μmol / g metallocence activation and 400 MAO / Zr mol ratio. Clearly, the different chain lengths of PEO on PS beads influenced the catalyst behavior in the heterogeneous ethylene polymerization. This can be rationalized by taking into account the differences in flexibility and mobility of polyethyleneoxide chains on PS beads. As the chain length of PEO increases, a higher degree of freedom for segmental motion of PEO is expected [9]. At a polymerization temperature of 70 ^{o}C, the longer chain of polyethyleneoxide on PS beads possesses even more flexibility and mobility which makes monomer gas diffusion into the catalyst particle and subsequent fragmentation of catalyst particle rather easy.

From scanning electron microscopy (SEM) images of the supported catalyst and the corresponding polyethylene beads, it can be seen that the shape of the catalyst particles is reproduced in the product bead and is several orders of magnitude bigger (Figure 3-6).

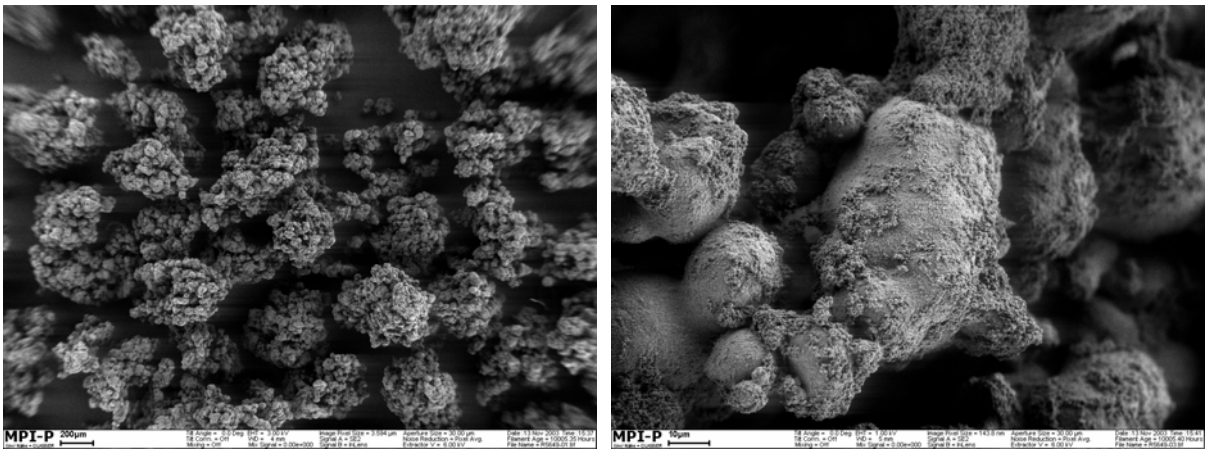

(A) (B)

Figure 3-6. SEM images of PE (PE-8) produced by catalyst supported on the nanosized PS beads (NPS2-2) functionalized with PEO: scale bar – (A) 200 μm and (B) 10 μm

The bulk density and morphology of polyethylene (PE-8) products is similar to that (PE-3) produced by the supported catalyst on the nanosized PS beads prepared by PS-PEO block copolymer in the chapter 3.1. There is thus no leaching of PS-PEO block copolymer from the

crosslinked polystyrene core in chapter 3.1.

Concerning the characteristics of the polymers obtained, the melting points are similar to those of the polymers produced with catalysts on the different support (Table 3-6). Using the catalysts with higher zirconocene concentration, the polyethylene parameters are almost equal and no significant influence upon the polymer characteristics is observed. The melting points (Tm) of all polyethylene measured by second heating of DSC are about 134 ^{o}C. The obtained PE possesses molecular weight (Mw) of about 1,100,000 – 1,300,000 and the polydispersity index is between about 2.1 – 2.8.

Table 3-6. Characteristics of polyethylene [a] - melting points, molecular weights and weight distributions of polyethylene

Run	Tm [b] (^{o}C)	Mn [c] (g / mol)	Mw [c] (g / mol)	PDI
PE-6	133.8	525,000	1,107,000	2.11
PE-7	134.4	476,000	1,323,000	2.78
PE-8	134.2	474,000	1,275,000	2.69
PE-9	134.4	531,000	1,077,000	2.03

[a] Reaction condition: in a 1 L autoclave, isobutane 400 ml, ethylene pressure 40 bar, 70 °C, 1 hr, amount of catalyst: 23 - 24 mg. [b] by differential scanning calorimetry (DSC). [c] by gel permeation chromatography (GPC)..

3.2.3. Summary

In this chapter 3.1 and 3.2, nanosized polystyrene (PS) beads functionalized with polyethyleneoxide (PEO) were prepared by miniemulsion polymerization. The miniemulsion polymerization was a very useful method to produce well-defined nanosized PS beads having diameters of around 100 nm. As a functional group, polyethyleneoxide (PEO) having nucleophilic ether groups immobilized MAO / metallocene complexes via a non-covalent bonding. Several nanosized PS beads functionalized with different concentrations of PEO group on the PS beads were prepared to study the influence of this concentration of PEO on the catalyst behavior. The supported catalysts on these PS beads were used for ethylene polymerization at the 70 ^{o}C and 40 bar. The different concentrations of PEO on the PS beads influenced the catalyst activity in ethylene polymerization and the property of polyethylene.

With increasing the concentration of polyethyleneoxide (PEO) on the surface of PS beads, the catalyst activity decreased but the bulk density of the polyethylene increased.

To confirm the results mentioned above and test the leaching of PEO-PS block copolymer from the PS core in chapter 3.1, other nanosized PS beads functionalized with polyethyleneoxide (PEO) were prepared. The polyethyleneoxide (PEO) part was covalently bonded to the polystyrene core by copolymerization with styrene monomers. Two kinds of nanosized PS beads as support were prepared depending on the polyethyleneoxide (PEO) chain length. One nanosized PS bead had 10 PEO repeat units and the other nanosized PS beads had 45 PEO repeat units. The supported catalyst on PS beads with long PEO chains was more active than the supported catalyst on PS beads with the short PEO chains. This finding was explained by the interaction and mobility of nanosized PS beads (primary particles) with metallocene / MAO complex. Based on these results, we concluded that the nature of the support surface influenced the catalyst activity. In the next chapter, the relation of the monomer diffusion and the supported catalyst will be discussed based on more results. The bulk density and morphology of PE products revealed that there was no leaching of the PS-PEO block copolymer from the core of PE beads shown in chapter 3.1.

3.3. Nanosized polystyrene (PS) beads functionalized with polypropyleneoxide (PPO) as support in olefin polymerizations

- *Ethylene polymerization, propylene polymerization and copolymerization of ethylene with α-olefin monomers)*

In chapter 3.1 and 3.2, nanosized PS beads functionalized with polyethyleneoxide (PEO) have been used for immobilizing the metallocene catalyst by non-covalent bonding between the nucleophilic ether groups on the support and the methylalumoxane / metallocene complexes. In this chapter, new nanosized polystyrene (PS) beads functionalized with polypropyleneoxide (4-Vinylphenyloxy-polypropyleneoxide) are introduced and olefin polymerizations (ethylene polymerization, propylene polymerization and copolymerization of ethylene with α-olefin monomers) are carried out by using the resulting supported catalyst. The polyethyleneoxide (PEO) group has hydrophilic properties that can absorb and retain moisture easily. These properties can cause the deactivation of the metallocene catalysts during catalyst preparation because matallocene catalysts are very moisture sensitive. Polypropyleneoxide (PPO) on the nanosized PS beads is less hydrophilic than polyethyleneoxide (PEO) but still possesses the nucleophilic ether groups for the immobilization of the metallocene complexes [10].

3.3.1. Nanosized PS beads functionalized with polypropyleneoxide (PPO) as support in heterogeneous ethylene polymerization

3.3.1.1. Preparation of nanosized polystyrene (PS) beads functionalized with polypropyeneoxide (PPO) and the supported catalyst

To prepare novel nanosized polymer beads, 4-Vinylphenyloxy-polypropyleneoxide was used as a surfmer in the miniemulsion process (Scheme 3-5). This compound was prepared by etherification of chloromethyl styrene with the sodium salt of monohydroxy functionalized PPO (15 repeat units). The desired latices were obtained by miniemulsion polymerization of styrene, divinylbenzene and styrene functionalized with PPO. The miniemulsion polymerization was shown to be useful to prepare nanosized PS beads in the chapter 3.1. The procedure to make nanosized PS beads functionalized with polypropyleneoxide (PPO) was as follows: Styrene, divinylbenzene as a crosslinker and hexadecane were stirred for 5 min.

Sodiumdodecyl sulfate (SDS) was dissolved in distilled water and this solution was mixed with 4-Vinylphenyloxy-polypropyleneoxide (10 mol %).

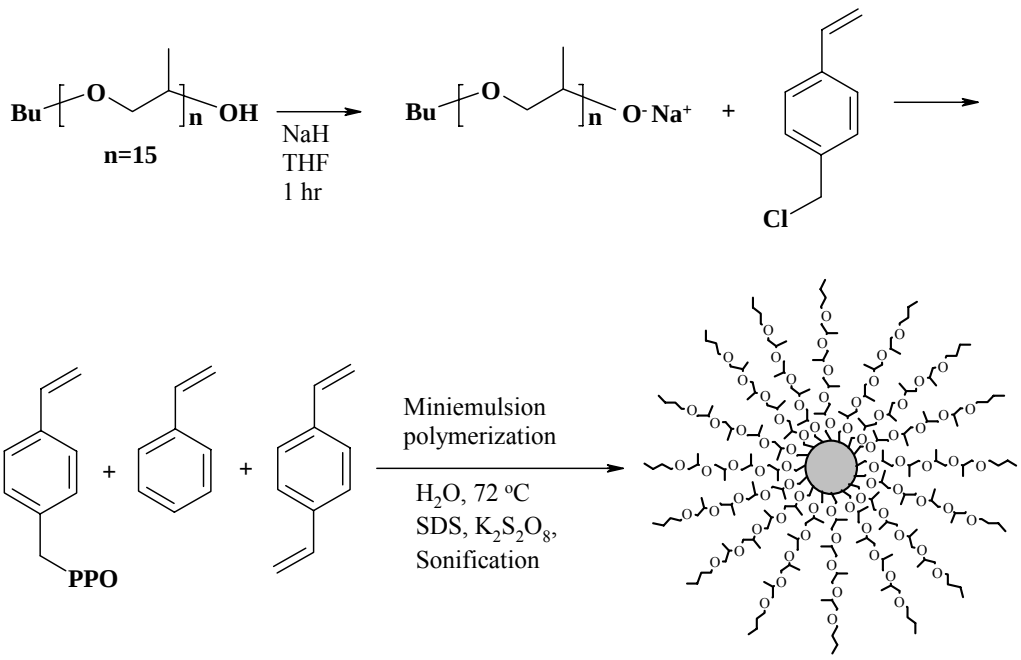

Scheme 3-5. Preparation of 4-Vinylphenyloxy-polypropyleneoxide and PS beads as support for metallocene catalyst

Then the mixed solution was added to the oil phases of styrene monomers and stirred at the highest power of the magnetic stirrer for 1 h to form a microemulsion. The microemulsion was carried out under ultrasonication for 5 min with a Branson Sonifier 450 W and 70 % power under ice cooling to form a miniemulsion. The miniemulsion was heated in an oil bath at 72 °C. Initiator $K_2S_2O_8$ dissolved in a small quantity of distilled water was added to the miniemulsion reactor. After polymerization for 12 hr, the product was filtrated by a stirred Ultrafiltration Millipore model 8050 with polyethersulfone membrane and dried in vacuum.

In Figure 3-7 (A), scanning electron microscopy (SEM) shows the nanosized PS beads prepared by miniemusion polymerization. Well-defined and spherical nanosized particles are observed. The average diameter of nanosized PS beads prepared using this procedure is about 60 nm and the shape of particles is spherical. The particle diameters measured by a Zetasizer (Figure 3-7, B) have a similar result to that obtained from the SEM image.

The immobilizing procedure of the metallocene catalyst [$Me_2Si(2MeBenzInd)_2ZrCl_2$] on the PS beads functionalized with PPO groups was same to that in chapter 3.2.1 (Scheme 3-6). As the polypropyleneoxide (PPO) shell of the nanosized PS beads consists of nucleophilic

ether groups, the immobilization of catalyst is achieved via a non-covalent bonding of the MAO / metallocene complexes and PPO functionalized PS beads.

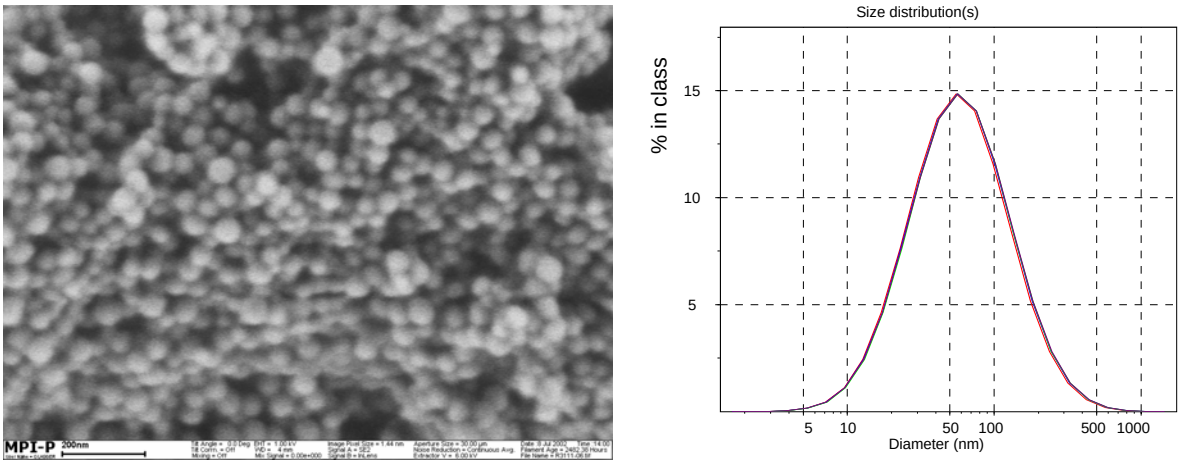

(A) (B)

Figure 3-7. (A) SEM image of nanosized PS beads and (B) particle size distribution of nanosized PS beads suspended in water (Average Mean: 60 nm)

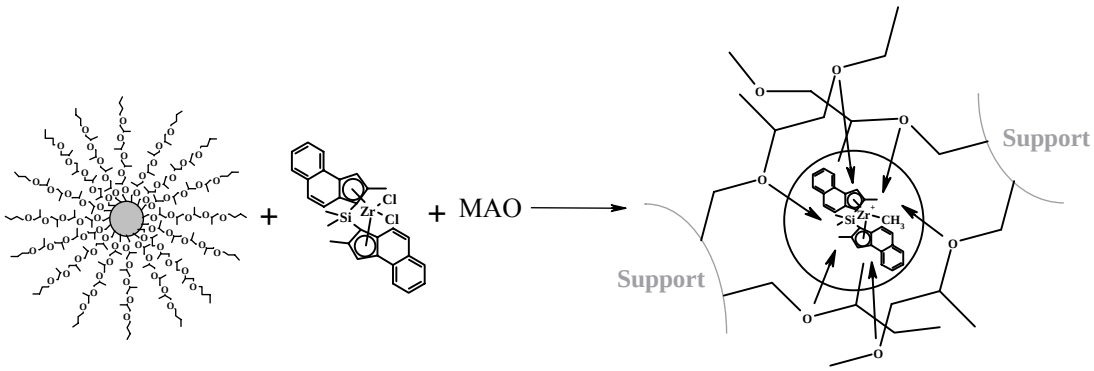

Scheme 3-6. Preparation of the supported catalyst on the PS beads functionalized with polypropyleneoxide (PPO)

SEM images in Figure 3-8 show the morphology of the supported catalyst. The particle size of the supported catalyst obtained by the mixing of MAO / metallocene with the nanosized PS beads is non-uniform (50 – 100 micrometer). The size of the supported catalyst is about 1000 times larger than that of the nanosized beads due to aggregation induced by the interaction between PPO chains on the PS beads and the MAO / metallocene complexes. The supported catalyst shows a spherical or rectangular shape with a rough surface. There are a few cracks on the surface of the supported catalyst.

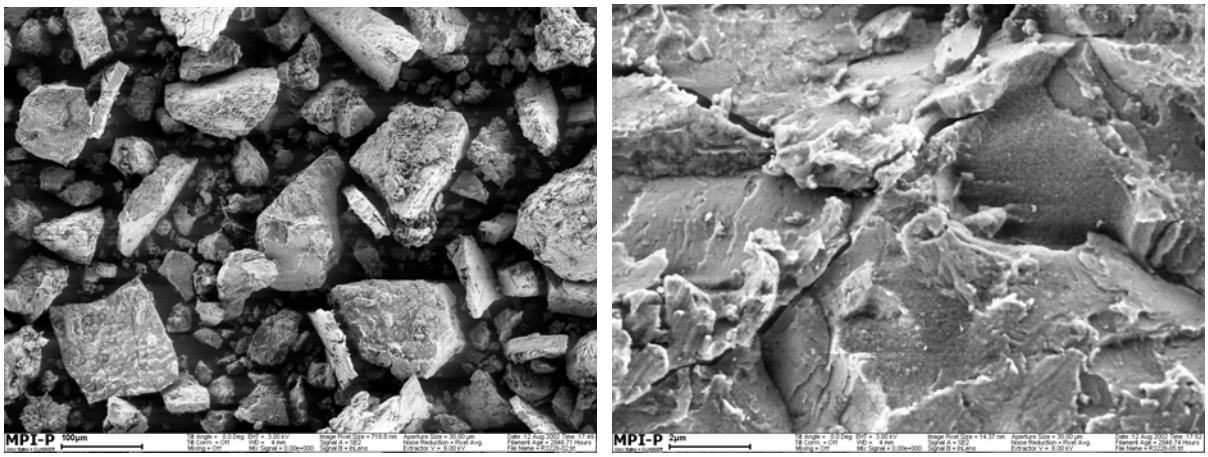

(A) (B)

Figure 3-8. SEM images of the supported catalyst on the nanosized PS beads functionalized with polypropyleneoxide (PPO): scale bar – (A) 100 µm and (B) 2 µm

3.3.1.2. Ethylene polymerization

Ethylene polymerizations were performed at 70 °C and 40 bar with 400 ml isobutane as solvent using the catalyst system of nanosized PS beads functionalized with PPO / $Me_2Si(2MeBenzInd)_2ZrCl_2$ / MAO. The zirconocene concentrations as well as MAO / Zr molar ratios were varied in order to investigate the influence on the activities and productivities of the catalyst and the morphology of the polyethylene products obtained. The results of the ethylene polymerization are summarized in Table 3-7. The supported catalysts on the nanosized PS beads functionalized with PPO show excellent activities in heterogeneous ethylene polymerization up to 2050 (kg PE / mol Zr hr bar). The polyethylene products are obtained as well-defined spherical particles with high bulk densities of polyethylene (PE). No dust-like products or reactor fouling was observed. In the catalyst activation of 24 - 25 Zr / cat (µmol / g), the supported catalyst has an activity of 2050 (kg PE / mol Zr hr bar) at the MAO / Zr molar ratio 600 (Run PE-10) but the catalyst activity decreases to 1550 (kg PE / mol Zr hr bar) at the MAO / Zr molar ratio 400 (Run PE-12). At the similar catalyst activation, the catalyst activity is decreased with decreasing the MAO / Zr molar ratio. On the other hand, in the MAO / Zr molar ratio of 350 - 370, the catalyst activity exhibits 1350 (kg PE / mol Zr hr bar) at the catalyst activation of 31 Zr / cat (µmol / g) (Run PE-13) and the catalyst activity is 1250 (kg PE / mol Zr hr bar) at the catalyst activation of 41 Zr / cat (µmol / g) (Run PE-15). For a similar MAO / Zr molar ratio the catalyst activity is similar even if increasing the catalyst activation. It appears that the activities of the catalyst

systems used depend more strongly on the MAO / Zr molar ratio than on the zirconocene concentration. According to Run PE-15 and Run PE-17, the activity of the supported catalyst washed by toluene is lower than that of the supported catalyst washed by hexane / toluene mixture in the procedure of the supported catalyst preparation.

Table 3-7. Ethylene polymerizations[a] (catalyst: $Me_2Si(2MeBenzInd)_2ZrCl_2$ / MAO supported on nanosized PS beads functionalized with PPO)

Run	Zr/cat (μmol/g)	MAO/Zr	Time (min)	Activity (kg PE/mol Zr hr bar)	Productivity (g PE/g cat hr)
PE-10	24	600	60	2050	1660
PE-11	24	600	120	1800	1460
PE-12	25	400	60	1550	1300
PE-13	31	370	60	1350	1400
PE-14	31	370	120	1300	1360
PE-15	41	350	60	1250	1750
PE-16	41	350	120	950	1300
PE-17 [b]	41	350	60	550	700
PE-18	45	300	60	650	1000
PE-19	45	300	120	750	1100

[a] Reaction condition: 1 L autoclave, isobutane 400 ml, ethylene pressure 40 bar, 70 °C, amount of catalyst: 22 - 24mg. [b] catalyst washed by just toluene instead of hexane/toluene mixture.

This decrease of the catalyst activity is attributed to the higher solubility of zirconocene / MAO complexes supported on the nanosized PS beads in toluene than in hexane / toluene mixture. In this way part of the zirconocene / MAO complexes is washed away from the supported catalyst which produces the lower activities and productivities. When two supported catalysts were prepared under the same amount of metallocene / MAO and washed with the same amount of solvent, the weight of the supported catalyst washed by hexane / toluene mixture was higher than that washed by just toluene. Accordingly, the loading of the metallocene / MAO complexes on the support washed by hexane / toluene mixture is higher than that on the support washed by just toluene. With increasing the polymerization time at

constant catalyst activation, the catalyst systems exhibit similar values of the activities and productivities to that of shorter time [(Run PE-10 and PE-11), (Run PE-13 and PE-14)] or (Run PE-15 and PE-16)] or slightly increases (Run PE-18 and PE-19). This result indicates that the catalyst remain stable during the polymerization as its activity is not influenced by longer reaction time, which is an important factor when considering a potential technical application.

3.3.1.3. Characterization of polyethylene products

Polyethylene (PE) products were obtained as hard spherical beads with diameters of about 0.5 - 1 mm. At MAO / Zr molar ratios between 300 and 370 (Run PE-13 to Run PE-19), all polyethylene products show well defined particles and good bulk densities of 390 - 420 (g / l) (Table 3-8).

Table 3-8. Characteristics of polyethylene [a] (catalyst: $Me_2Si(2MeBenzInd)_2ZrCl_2$ / MAO supported on nanosized PS beads functionalized with PPO)

Run	BD [b]	Tm [c] (^oC)	Mn [d] (g / mol)	Mw [d] (g / mol)	PDI
PE-10	300	134.5	495,000	1,262,000	2.55
PE-11	360	133.1	501,000	1,167,000	2.33
PE-12	340	133.3	459,000	1,147,000	2.50
PE-13	380	134.2	511,000	1,374,000	2.69
PE-14	400	134.7	523,000	1,286,000	2.46
PE-15	420	133.1	478,000	1,123,000	2.35
PE-16	430	134.2	531,000	1,189,000	2.24
PE-17[b]	370	134.1	472,000	1,184,000	2.51
PE-18	380	134.5	520,000	1,362,000	2.62
PE-19	420	133.8	509,000	1,247,000	2.45

[a] Reaction condition: in a 1 L autoclave, isobutane 400 ml, ethylene pressure 40 bar, 70 °C, amount of catalyst: 22 - 24 mg. [b] BD: bulk density (g / l), [c] by differential scanning calorimetry (DSC). [d] by gel permeation chromatography (GPC).

When the MAO / Zr molar ratios are increased up to 400 – 600 (Run PE-10 to Run PE-12), however, the bulk density of the polyethylene products obtained decreases to the range of 300 – 360 (g / l). This can be explained by a faster fragmentation of the supported catalyst due to higher activity and the more exothermic reaction inside the supported catalyst. All polyethylene products exhibit high molecular weights, low polymer dispersities and high melting points. The molecular weights are in the range of 1,100,000 - 1,300,000, the polydispersity index is between 2.3 - 2.6 and the melting point of PE is about 135 ^{o}C. Using the catalysts with different zirconocene concentration and molar ratio, the polyethylene parameters are almost equal and there is no significant influence of the catalyst activation.

Scanning electron microscopy (SEM) pictures (Figure 3-9) of the polyethylene (PE-15) products suggest that the particles of PE have the similar shape to that of the supported catalyst beads. The product particles appear as an assembly of small spherical beads. This aggregation of small spherical beads is typical for polyolefin particles obtained from silica-supported catalysts due to the polymer growth on the nanosized primary particles [11].

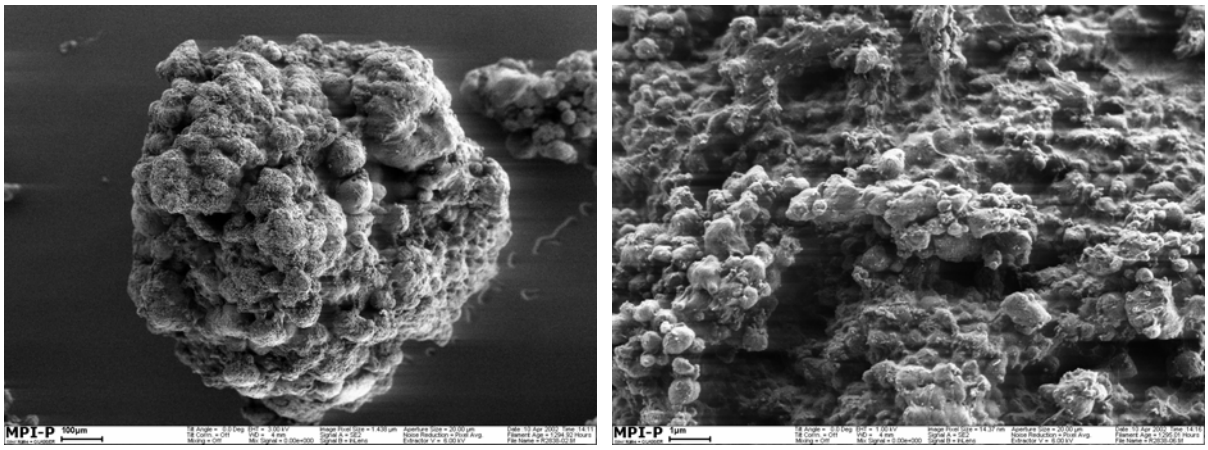

(A) (B)

Figure 3-9. SEM images of PE particle (PE-15) and the PE surface: scale bar – (A) 100 µm and (B) 1 µm

3.3.1.4. Summary

In chapter 3.1 and 3.2 we introduced the nanosized PS beads functionalized with polyethyleneoxide (PEO). The influence of different concentration of the functional group on the catalyst activity and the bulk density of polyethylene (PE) was investigated. In the present chapter, new nanosized polystyrene (PS) beads functionalized with

polypropyleneoxide (PPO) were introduced. The immobilization of metallocene catalyst on the nanosized polystyrene beads functionalized with polypropyleneoxide (PPO) was sufficient for use in ethylene polymerization. The supported catalyst on the nanosized PS beads functinalized with polypropyleneoxide (PPO) showed different activities depending on the molar ratio of MAO / metallocene and the amount of MAO. The polyethylene products had high bulk density and were obtained with spherical particle with good morphology without reactor fouling after ethylene polymerization.

3.3.2. Influence of the PPO concentration of the nanosized PS beads on the catalyst activity in ethylene polymerization

The influence of the concentration of polyethyleneoxide (PEO) was studied in chapter 3.1 and 3.2. The concentration of polyethyleneoxide (PEO) influenced the catalyst activity and the bulk density of PE products obtained in heterogeneous ethylene polymerization. To confirm the behavior of the catalyst supported on the nanosized PS beads, other nanosized PS beads functionalized with polypropyleneoxide (PPO) were prepared and the influence of the concentration of polypropyleneoxide (PPO) on the nanosized polystyrene (PS) on ethylene polymerizations was investigated.

3.3.2.1. Preparation of nanosized polystyrene (PS) beads functionalized with polypropyeneoxide (PPO) and the supported catalyst

Several nanosized PS beads functionalized with different concentration of PPO were obtained by miniemulsion polymerization (Scheme 3-7). By varying the amount of surfmer (0.5 mol % to 20 mol % of PPO functionalized styrene), nanosized PS beads containing different amounts of PPO chains on the surface were prepared. Depending on the concentration of polypropyleneoxide (PPO) chain on the PS bead, the particle size of PS beads ranged from 40 to 220 nm (Table 3-9). Upon use of 0.5 mol % and 10 mol % of styrene functionalized with 15 repeat units of polypropyleneoxide (NPS3-1 and NPS3-4 respectively), the average particle size of nanosized PS beads was about 60 nm and 70 nm respectively. On the other hand, the average particle size of PS beads increased up to 170 nm – 220 nm in the use of 1 mol %, 5 mol % and 20 mol % of styrene functionalized with polypropyleneoxide (NPS3-2, NPS3-3 and NPS3-5).

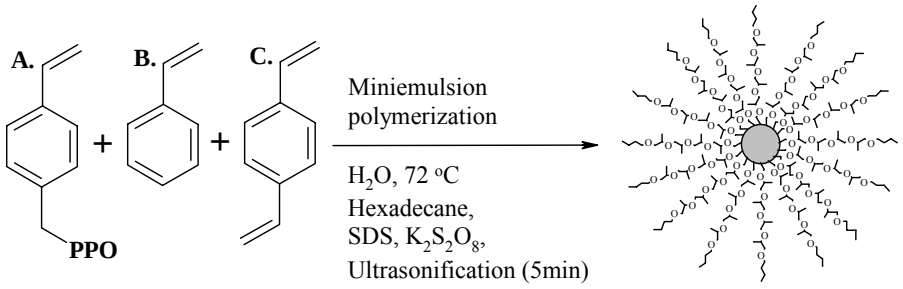

Scheme 3-7. The preparation of polypropyleneoxide functionalized nanosized PS bead

Table 3-9. Preparation of nanosized PS beads functionalized with polypropyleneoxide

Support	Repeat unit (n)	Styrene- PPO (mol %)	Styrene (mol %)	Divinylbenzene (mol %)	Particle size [a] (nm)
NPS3-1	15	0.5	89.5	10	74
NPS3-2	15	1	89	10	167
NPS3-3	15	5	85	10	220
NPS3-4	15	10	80	10	60
NPS3-5	15	20	70	10	187

[a] measured by Zetasizer

The supporting procedure of the metallocene catalyst on the PS beads functionalized with PPO groups was similar to that in chapter 3.2.1. In this heterogeneous ethylene polymerization, 40 μmol / g metallocence activation and 350 MAO / Zr mol ratio was used. Figure 3-10 shows the SEM images for the supported catalyst particles (NPS3-5). The particle shape of the supported catalyst obtained by the mixing of MAO / metallocene with the nanosized PS beads is non-uniform.

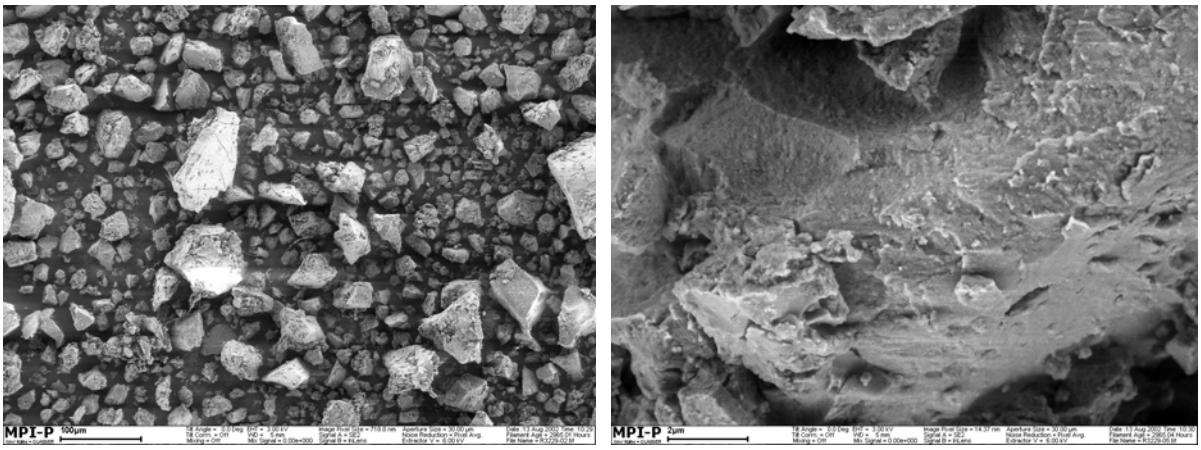

(A) (B)

Figure 3-10. SEM images of the supported catalysts (NPS3-5) on the nanosized PS beads functionalized with polypropyleneoxide (PPO): scale bar – (A) 100 μm and (B) 2 μm

3.3.2.2. Ethylene polymerization

Ethylene polymerizations were performed at 70 °C and 40 bar with 400 ml isobutane as solvent using nanosized PS beads functionalized with PPO / Me_2Si $(2MeBenzInd)_2ZrCl_2$ /

MAO (Table 3-10). In the case of 0.5 mol % PPO functionalized PS beads, the supported catalyst has an activity of 2950 (kg PE / mol Zr hr bar) in Run PE-20 and the bulk density of PE is 250 (g / l). In the case of 10 mol % PPO functionalized PS beads, the catalyst exhibits an activity of 1250 (kg PE / mol Zr hr bar) in Run PE-23 and the bulk density of PE is increased up to 420 (g / l). As the concentration of PPO chains on the nanosized PS beads increases, the activity of the supported catalyst decreases from 2950 to 1200. However, the bulk density of polyethylene obtained is greatly improved from 260 (g / l) up to 490 (g / l). Consequently, the concentration of functional groups on the support influences the catalyst activity and the behavior of the supported catalyst during ethylene polymerization as shown in chapter 3.1 and 3.2.

Table 3-10. Ethylene polymerization [a] (catalyst: $Me_2Si(2MeBenzInd)_2ZrCl_2$ supported on the nanosized PS beads functionalized with PPO).

Run	Amount of PPO (mol %)	Activity [b]	Productivity [c]	BD [d]
PE-20	0.5	2950	4100	260
PE-21	1	1800	2400	310
PE-22	5	1350	2000	360
PE-23	10	1250	1750	420
PE-24	20	1200	1700	490

[a] Reaction condition: 1L autoclave, isobutane 400ml, ethylene pressure 40bar, 70°C, 1 hr, catalyst activation: 40 Zr / cat (μmol / g), 350 MAO / Zr molar ratio, amount of catalyst: 23 – 24 mg. [b] kg PE / mol Zr hr bar. [c] g PE / g cat hr. [d] BD: bulk density (g / l) of PE.

To explain these results, several effects have to be considered. On one hand at low PPO concentration, the interaction between PPO and the MAO / metallocene complex is weak and immobilization might be limited which results in a more homogeneous polymerization and therefore in higher activities of the catalyst. The product has lower bulk densities of PE products. Furthermore, one has to consider not only the interaction between the metallocene / MAO complex and the support but also the interaction of different PS beads particles (primary particles). PS particles are reversibly crosslinked via an interaction between metallocene / MAO complexes and PPO chains. This interaction should be strengthened drastically by increasing the amount of PPO on the particles resulting in a more stable

network. Such a denser network can limit on one hand the diffusion of monomer into the active sites of the catalyst (Figure 3-11) and on the other hand the fragmentation of the supported catalyst. A low catalyst fragmentation permits access only to the outer active centers, so initially the inner centers are not able to contribute to the polymerization process.

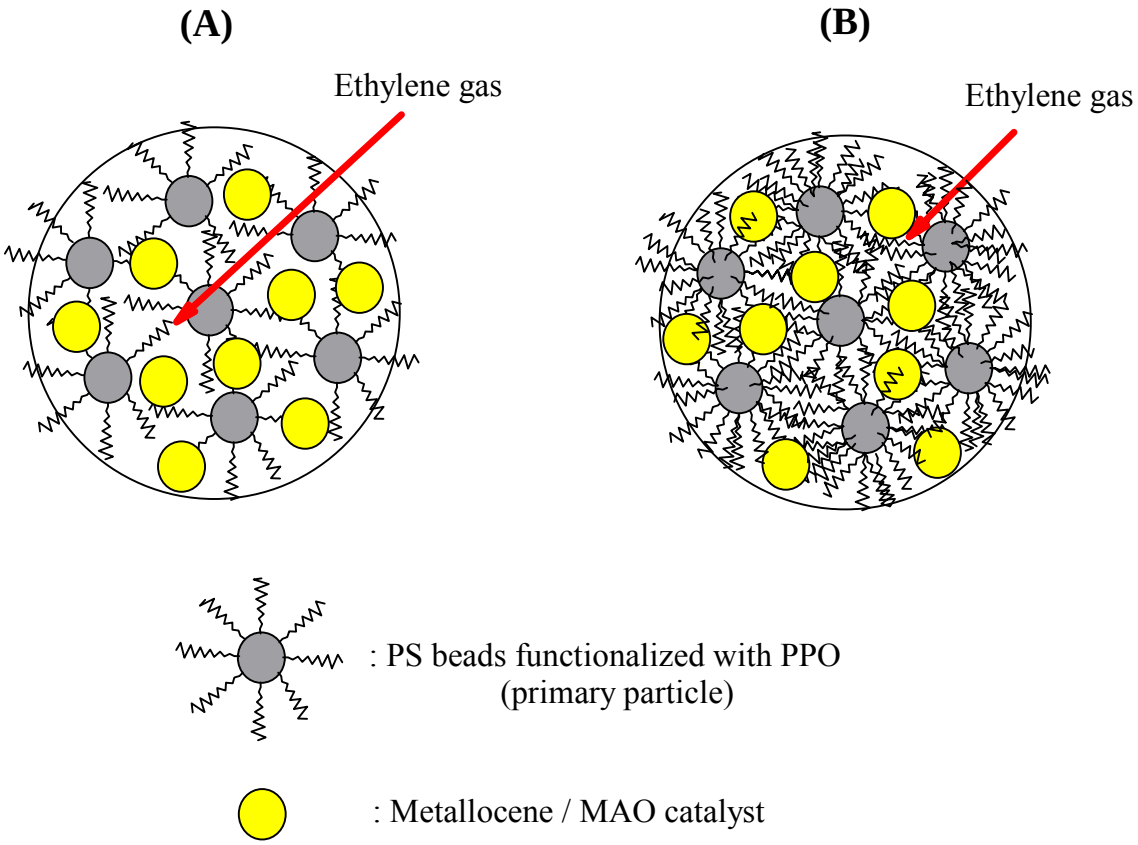

Figure 3-11. Influence of the PPO concentration of the surface of PS beads on the diffusion of monomer gas into the secondary particle: (A) low concentration of PPO on the PS beads and (B) high concentration of PPO on the PS beads.

Finally, one can conclude that there is an optimum of surface functionalization for obtaining catalysts exhibiting good activity and productivity as well as giving products with high bulk density. If the surface functionalization is too low, only low bulk density polyolefin products are obtained, however the catalyst activity is higher. On the other hand to get high bulk density which is essential for an industrial application, a decreased activity and productivity has to be accepted as a drawback.

3.3.2.3. Characterization of polyethylene products

The PE products are characterized by high molecular weights, low polydispersity and high melting points (Table 3-11). The molecular weights are about 1,200,000 with polydispersity of about 2.4 and the melting point of PE is 135 ^{o}C. Even if the catalyst activity differs depending on the concentration of functional groups on the nanosized PS beads, the characteristics of PE obtained have similar values.

Table 3-11. Characteristics of polyethylene [a]: Melting points and molecular weights of polyethylene

Run	Tm [b] (^{o}C)	Mn [c] (g / mol)	Mw [c] (g / mol)	PDI
PE-20	133.5	515,000	1,266,000	2.46
PE-21	134.2	491,000	1,009,000	2.57
PE-22	134.1	462,000	1,145,000	2.48
PE-23	133.7	481,000	1,221,000	2.54
PE-24	133.5	512,000	1,361,000	2.66

[a] Reaction condition: in a 1 L autoclave, isobutane 400 ml, ethylene pressure 40 bar, 70 °C, 1 hr, catalyst activation: 40 Zr / cat (μmol / g), 350 MAO / Zr molar ratio, amount of catalyst: 23 - 24 mg. [b] by differential scanning calorimetry (DSC). [c] by gel permeation chromatography (GPC).

Polyethylene (PE) products were obtained as spherical beads with diameters of about 0.2 - 1 mm depending on the concentration of PPO chains on the nanosized PS beads. Also the morphology of the PE product depends on the concentration of functional group on the nanosized PS support. Figure 3-12 shows the PE product from the catalyst supported on the 0.5 mol % PPO functionalized PS beads. The particle size distribution of PE is very wide, and there are many small particles with much lower bulk density (~ 260 g / l), so it is difficult to determine the average particle size of the PE. Figure 3-13 shows the PE product from the catalyst supported on the 10 mol % PPO functionalized PS beads. Normally the PE produced by the catalyst supported on the PS beads functionalized with 10 mol% PPO appears to be hard and spherical particles and the particle size distribution of PE is narrower than that in the case of 0.5 mol % PPO functionalized PS beads. A detailed investigation of the product beads in Figure 3-13 (B) shows that they consist of many small spherical particles held tightly together by the polyethylene beads.

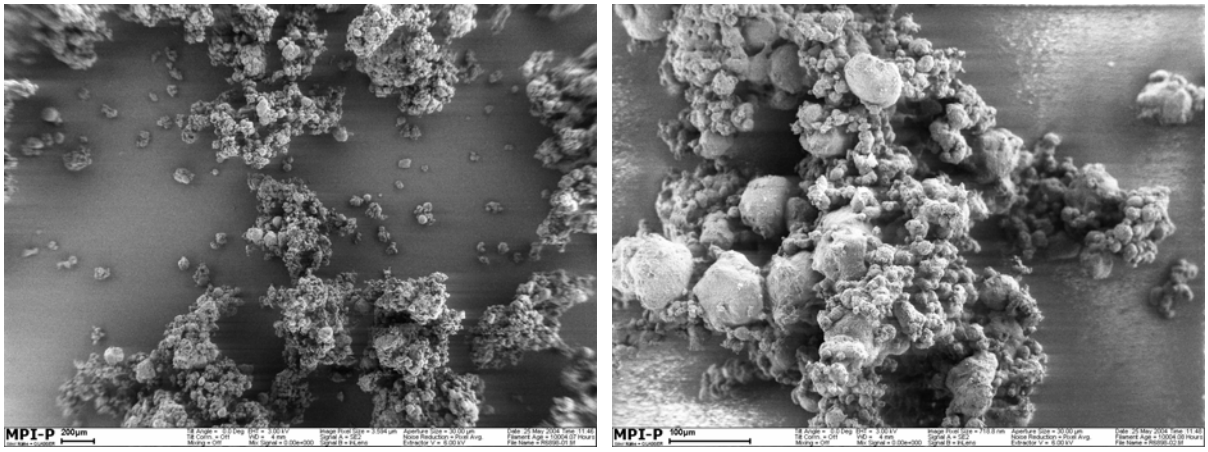

(A) (B)

Figure 3-12. SEM images of polyethylene (PE-20) by the supported catalyst on the 0.5 mol % PPO functionalized PS beads: scale bar – (A) 200 μm and (B) 100 μm

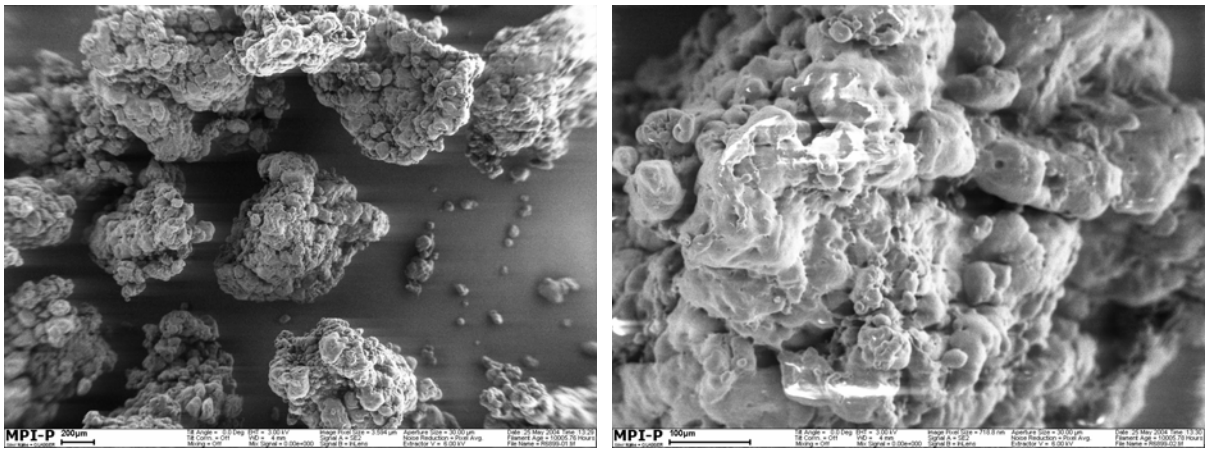

(A) (B)

Figure 3-13. SEM images of polyethylene (PE-23) by the catalyst supported on the 10 mol % functionalized PS beads: scale bar – (A) 200 μm and (B) 100 μm

3.3.2.4. Kinetic study of ethylene polymerization by the supported catalyst with the different concentrations of PPO on the PS beads

A key requirement for designing commercial processes in olefin polymerization is the study of kinetic mechanisms. In the current work, the kinetic study was carried together with the group of Prof. Fink at the Max-Planck Institute for Carbon Research in Mülheim (Germany).

Two kinds of nanosized PS beads with different concentration of polypropyleneoxide (0.5 mol % PPO and 10 mol % PPO on the PS beads) were used for this kinetic study. In this

heterogeneous ethylene polymerization, 40 μmol / g metallocence activation and 350 MAO / Zr mol ratio was used. The polymerization temperature was the same as the one used generally in our experiments, however, the ethylene pressure was 20 times lower.

The experiments by using these two catalysts supported on 0.5 mol % PPO and 10 mol % PPO on the PS beads at 2 bar ethylene pressure and 70 ^{o}C polymerization temperature exhibit a similar trend of catalyst activity to the results under 40 bar ethylene pressure and 70 ^{o}C polymerization temperature in 40 μmol / g metallocence activation and 350 MAO / Zr mol ratio (Table 3-12).

Table 3-12. Ethylene polymerization with the supported catalyst system: PPO functionalized PS beads / $Me_2Si(2MeBenzInd)_2ZrCl_2$ / MAO [a].

Run	Amount of PPO (mol %)	Catalyst (mg)	Yield (g)	Activity[b]	Productivity[c]
PE-25	0.5	20	3.21	3230	260
PE-26	10	19	0.95	1280	100

[a] Reaction condition: 1L autoclave, isobutane 400 ml, ethylene pressure 2 bar, 70 °C. catalyst activation: 40 Zr / cat (μmol/g), 350 MAO / Zr molar ratio, amount of catalyst: 23 - 24 mg. [b] kg PE / mol Zr hr bar. [c] g PE / g cat hr.

Under 2 bar ethylene pressure and 70 ^{o}C polymerization temperature, the catalyst supported on the 0.5 mol % PPO functionalized PS beads exhibits an activity of 3230 [kg PE / mol Zr hr bar] in Run PE-25 and the one on the 10 mol % PPO functionalized PS beads has an activity of 1280 [kg PE / mol Zr hr bar] in Run PE-26. With regard to the PE yield, the former catalyst with 20 mg produced 3.21 g of PE (PE-25), while the latter catalyst with 19 mg produced 0.95 g of PE (PE-25). Figure 3-14 shows the ethylene gas flow in ethylene polymerization by two different supported catalyst systems (0.5 mol % PPO functionalized PS beads and 10 mol % of PPO functionalized PS beads). The gas flow of the supported catalyst prepared with 0.5 mol % PPO functionalized PS beads shows a highest peak after 1 - 2 min polymerization and then the ethylene gas flow is reduced very quickly, while, the ethylene gas flow increases steadily and then reduces also steadily in the case of the catalyst prepared with 10 mol% PPO functionalized PS beads. These different curves of ethylene gas flow could explain the results from the previous experiment in chapter 3.3.2.2.

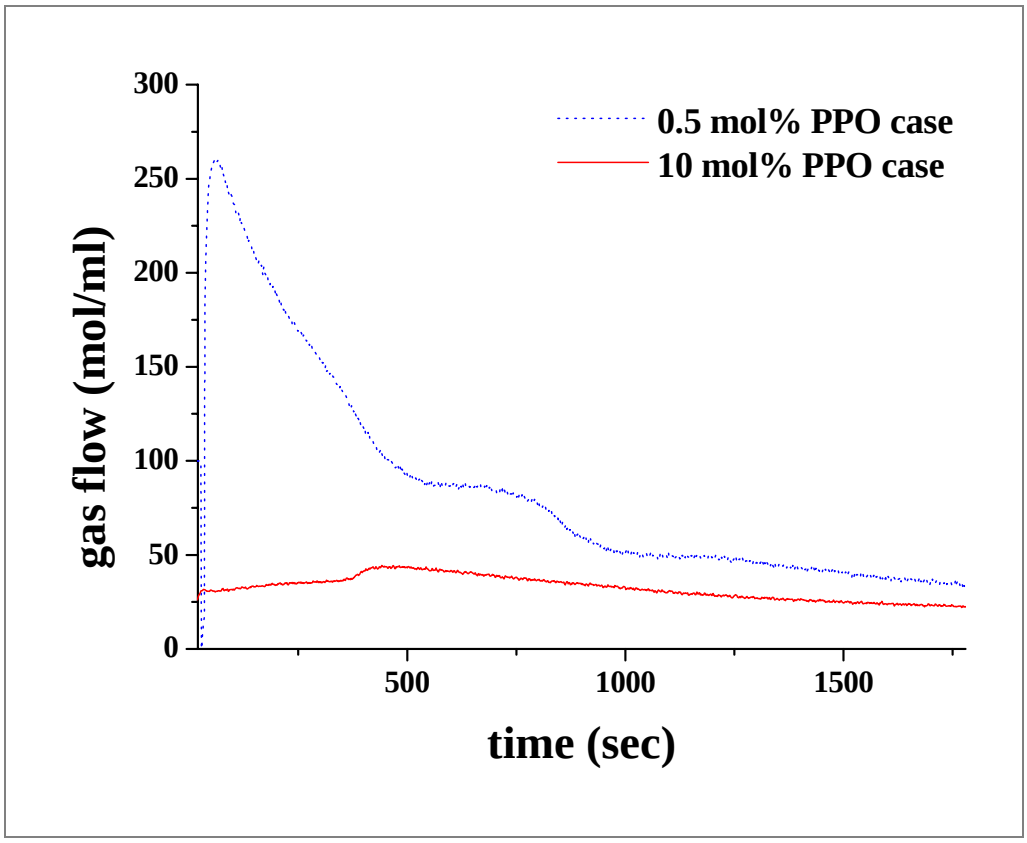

Figure 3-14. Ethylene gas flow in ethylene polymerization with the supported catalyst on two different concentrations (0.5 mol % and 10 mol % of PPO functionalized nanosized PS beads)

In the case of the catalyst produced by 0.5 mol % PPO functionalized PS beads, the interaction between each supported catalyst is weak due to the low concentration of PPO chains, that means, the reversible crosslinking is weak as well. This weak crosslinking facilitates the diffusion of monomer gas through the voids between each supported catalyst. The easy diffusion of monomer gas into the supported catalyst can make the catalyst fragmentation rapid and the fast fragmentation induces the high catalyst activity. However the catalyst activity can be deactivated rapidly as in homogeneous olefin polymerization. In the case of 10 mol % PPO functionalized PS beads, monomer gas can go inside the supported catalyst and the catalyst fragmentation can progress steadily because each supported catalyst is packed and networked densely. This dense network influences the diffusion of monomer into the active sites of the supported catalyst and the fragmentation of the supported catalyst. This result is similar to that of the catalyst systems prepared by Dr. Nicolay Nenov in our group using polyethyleneoxide functionalized PS supports [12]. Two kinds of catalysts immobilized on different supports were investigated. One support (NN2) was

polyethyleneoxide (PEO) functionalized linear PS crosslinked by cyclopentadiene groups that can be broken reversibly under high pressure and high temperature. The other support (NN4) was polyethyleneoxide (PEO) funtionalized PS beads without chemical crosslinking. The catalyst supported on the former one (NN2) showed a constant activity during 30 min of polymerization. The former result is similar to the catalyst supported on the 10 mol % functionalized PS beads. On the other hand, the catalyst supported on the PS beads (NN4) showed high activity at first and then the catalyst activity decreased rapidly. The catalyst supported on the latter one (NN4) has similar behavior to that from the catalyst supported on the 0.5 mol % PPO functionalized PS beads. Through the integration of ethylene gas flow (ml) curve (Figure 3-15), the consumption of ethylene gas was detected indirectly in each case.

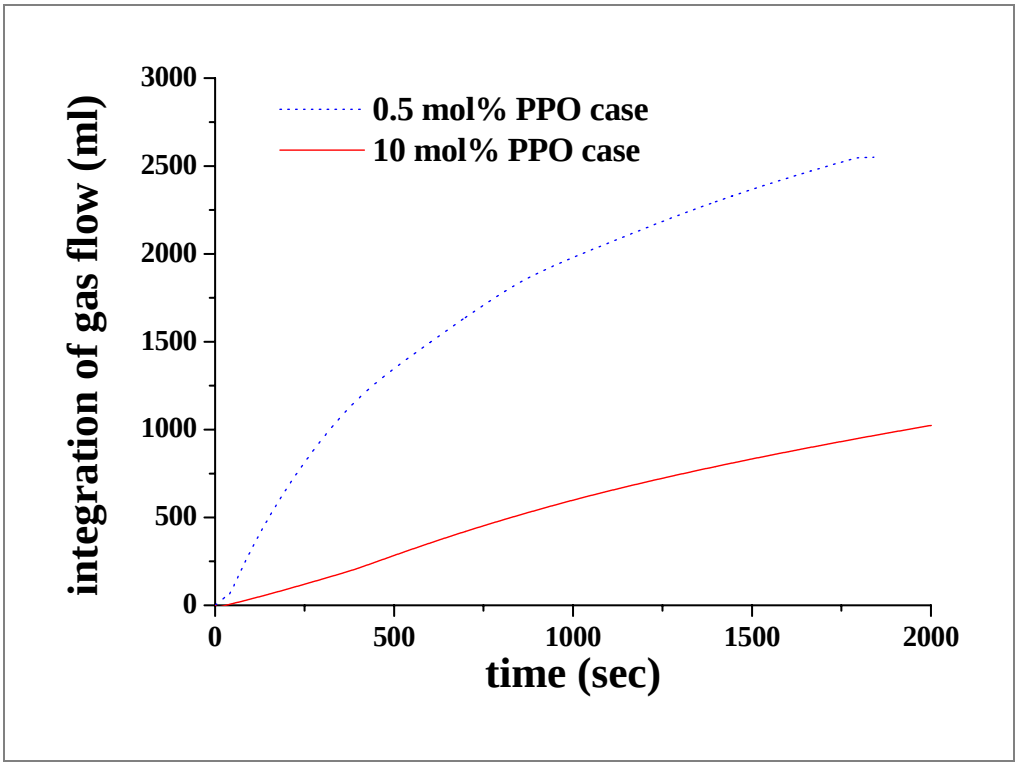

Figure 3-15. Integration of gas flow in ethylene polymerization with the supported catalyst system: two different concentrations (0.5 mol % and 10 mol %) of PPO functionalized on the nanosized PS beads.

The integration of monomer gas flow for the catalyst supported on the 0.5 mol% PPO functionalized nanosized PS beads increases very fast at first and then keeps steady, while the integration of gas flow increases steadily and continuously in the case of the supported

catalyst on the 10 mol % PPO functionalized nanosized PS.

Figure 3-16 and 3-17 shows the morphology of PE produced by the catalyst supported on 0.5 mol % PPO functionalized nanosized PS beads and 10 mol % PPO functionalized nanosized PS beads. The PE product beads from the catalyst supported on 10 mol % PPO (Figure 3-17) appear to be larger than those from catalyst supported on 0.5 mol % PPO (Figure 3-16). However both surfaces of PE have very similar structure. These PE products produced under 2 bar and 70 ^{o}C display a different morphology from the PE products obtained at 40 bar and 70 ^{o}C. The PE particles produced under 2 bar and 70 ^{o}C are smaller and less uniform than the PE products from 40 bar and 70 ^{o}C.

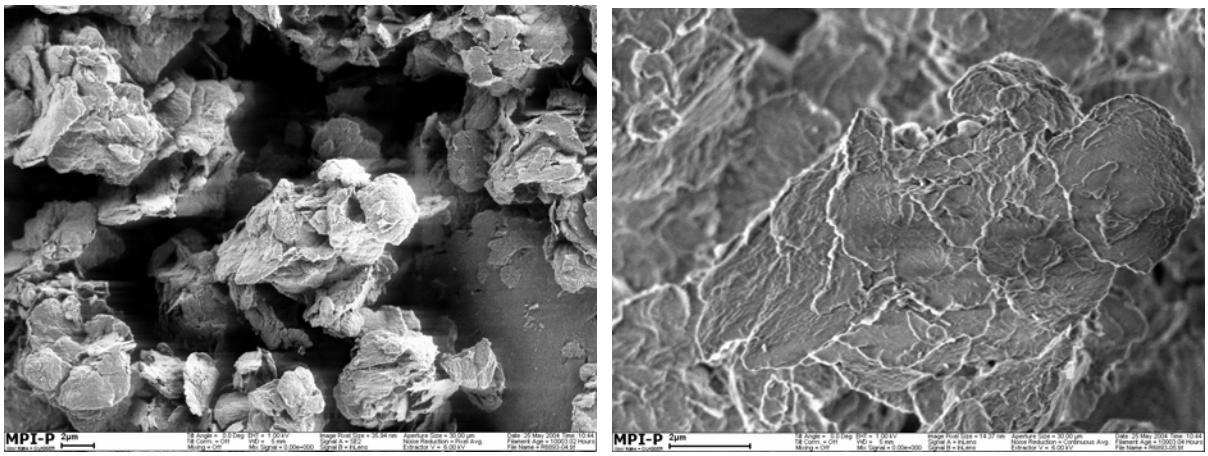

Figure 3-16. SEM images of polyethylene (PE-25) by catalyst supported on the 0.5 mol % PPO functionalized PS: scale bar – 2 μm

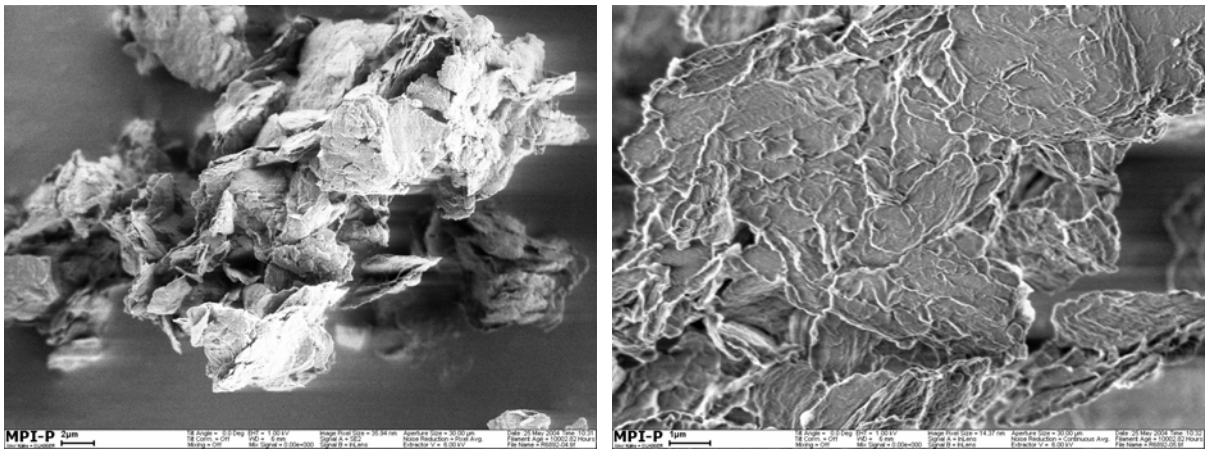

(A) (B)

Figure 3-17. SEM images of polyethylene (PE-26) by catalyst supported on the 10 mol % PPO functionalized PS: scale bar – (A) 2 μm and (B) 1 μm

3.3.2.5. Summary

In this chapter, the influence of the different concentrations of polypropyleneoxide (PPO) on the catalyst activity in heterogeneous ethylene polymerizations and the bulk density of PE product was investigated by using new nanosized PS beads. Upon increasing the concentrations of polypropyleneoxide (PPO) chains on the PS beads, the catalyst activity of ethylene polymerization decreased at the polymerization conditions of 70 ^{o}C and 40 bar. However, the bulk density of polyethylene obtained was greatly enhanced. These results were explained by the interaction between PPO chains and the metallocene complex and the different fragmentation behavior of the supported catalyst on the PS beads. To confirm the above interpretation of the polymerization results at 40 bar and 70 ^{o}C, the ethylene polymerizations were carried out under different polymerization conditions (2 bar and 70 ^{o}C). The experimental results at 2 bar and 70 ^{o}C showed a similar trend. Based on these findings, we concluded that the different concentrations of functional groups on the support significantly influence the catalyst behavior during polymerization. The melting points and molecular weights of polyethylene produced were 134.7 ^{o}C and 1,200,000 respectively. These results were not influenced by the different concentration of the functional group on the support surface.

3.3.3. Influence of the different preparation method of the supported catalyst on the ethylene polymerization and the PE product

The techniques used for supporting the metallocene catalyst as well as the nature of the catalyst carrier have a crucial influence on the results of the catalyst behavior during olefin polymerization and the properties of the olefin polymers obtained [13]. As already mentioned, the preparation routes presented in the literature for metallocene immobilization on the support can be classified according to three methods. The first method involves direct impregnation of metallocene on the support [14]. The second method involves immobilization of MAO on the support followed by reaction with the metallocene compound [15]. The third method involves immobilization of aryl ligands on the support followed by addition of metal salt such as zirconium halide [16]. In our group, the second method was used for immobilizing the metallocene on the nanosized PS beads in heterogeneous polymerization.

In this chapter, two methods for catalyst preparation are introduced. One is an ultrasonication method during the catalyst preparation and the other is a sieving method for separating the uniform catalyst particles as the ultimate supported catalyst. In the first case, ultrasonication of support / metallocene catalyst in toluene or support / MAO in toluene is used for improving the homogeneous distribution of metallocene catalyst within the support. In the second one, the sieving method is used for improving the particle size distribution of the supported catalyst and finally the polyethylene products.

3.3.3.1. The influence of the ultrasonication of the supported catalyst system on the ethylene polymerization and the PE product

3.3.3.1.1. Preparation of the supported catalyst

Nanosized PS beads functionalized with polypropyleneoxide (10 mol% of PPO) were also used as catalyst carrier in heterogeneous ethylene polymerizations. The two preparation methods of the supported catalysts were performed as follows (Figure 3-18).

Method 1: The dry nanosized PS beads were mixed with MAO solution in toluene and then stirred for 12 hr. Metallocene / MAO solution in toluene was added to the suspension of PS beads and MAO in toluene and stirred for 1 hr. The supported catalyst was washed with dry

hexane / toluene mixture several times and then dried under vacuum.

Method 2: The dry nanosized PS beads were mixed with dry toluene and then stirred for 10 min. The methylalumoxane (MAO) was added to the suspension of PS beads in toluene and stirred again for 10 min. The suspension of nanosized PS beads and MAO in toluene was put in an ultrasonication bath for 20 min and then stirred again for 30 min. Metallocene and MAO solution in toluene was added to the suspension. The supported catalyst was washed several times with dry hexane / toluene mixture and then dried.

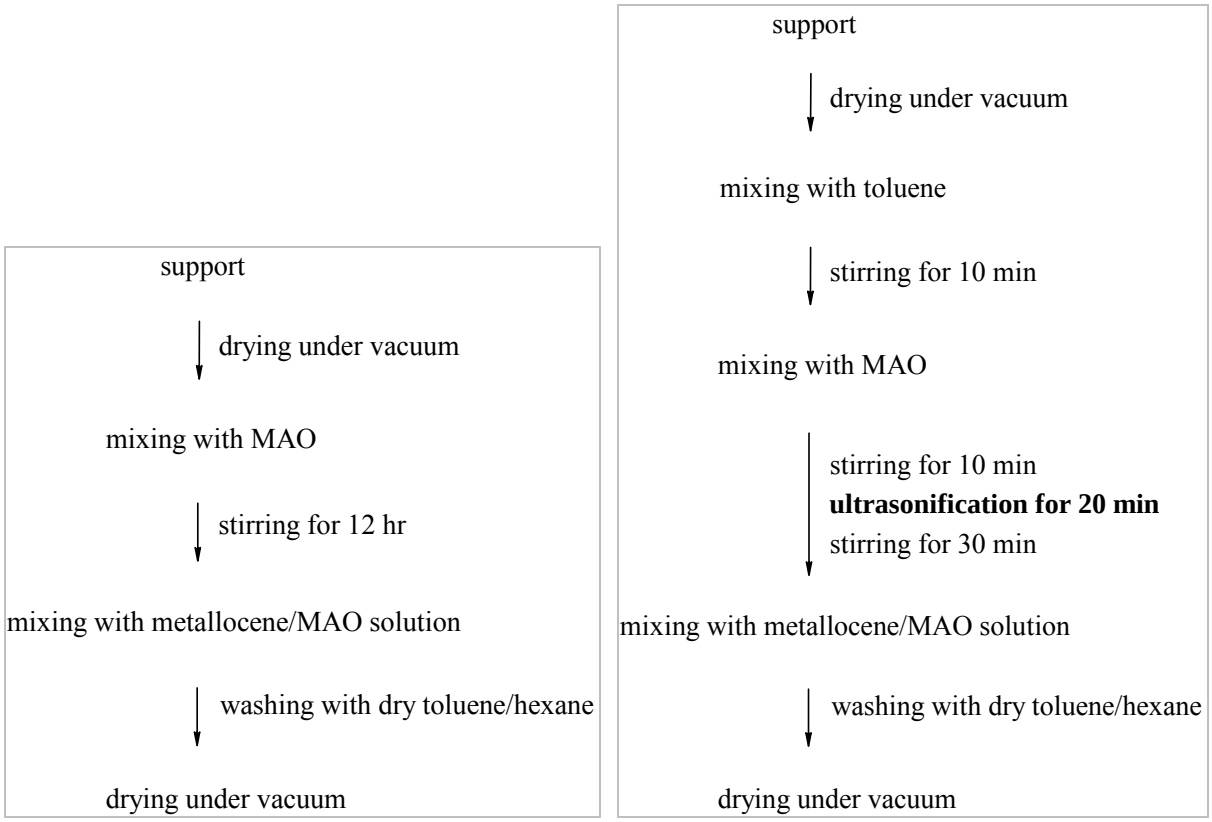

(A) Method 1 (B) Method 2

Figure 3-18. The preparation methods of the supported catalyst: (A) method 1 – the existing procedure and (B) method 2 – the new method using ultrasonication.

As shown in Scheme 3-8, the reason for using ultrasonication during the preparation of the supported catalyst is to obtain a uniform distribution of metallocene catalyst on the support. SEM images of the supported catalyst on nanosized PS beads without or with the ultrasonication process show no considerable difference of morphology in each case (Figure 3-19). It follows that this method doesn't affect the morphology and the particle size of the supported catalyst.

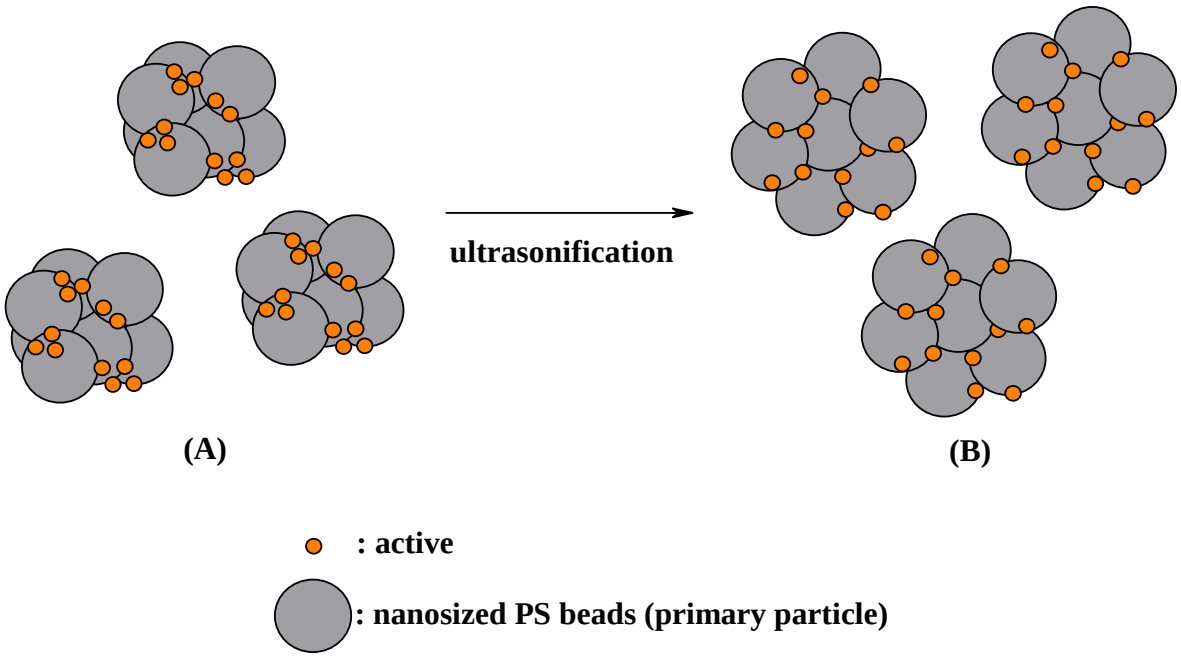

Scheme 3-8. Schematic preparation of catalyst: (A) without ultrasonication and (B) with ultrasonication in preparation of the supported catalyst

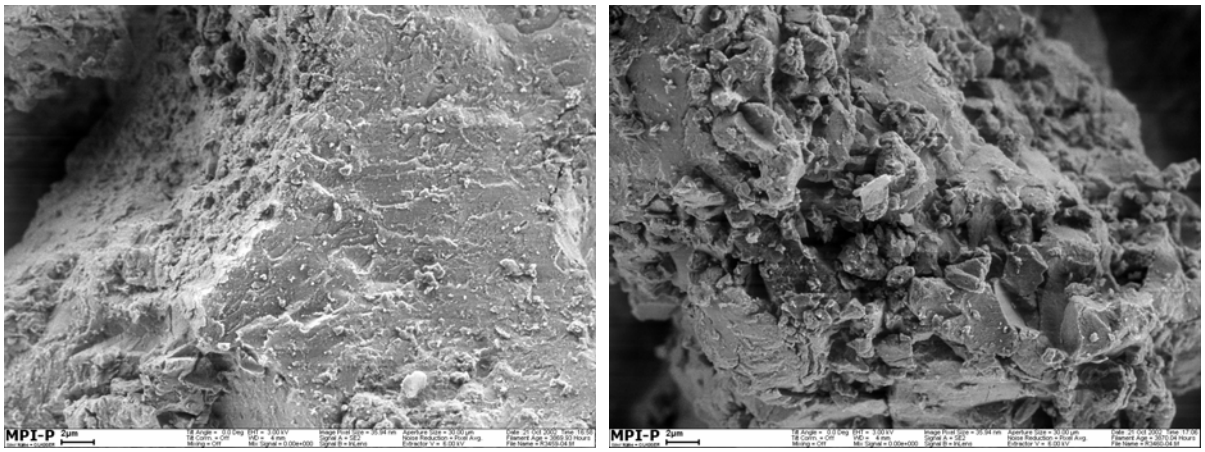

(A) (B)

Figure 3-19. SEM images of the supported catalyst produced without ultrasonication in preparation (A, method 1) and with ultrasonication in preparation (B, method 2): scale bar – 2 μm

3.3.3.1.2. Ethylene polymerization and characteristics of the PE products

Ethylene polymerizations were carried out using the supported catalysts prepared by method 1 and method 2 at 70 ^{o}C polymerization temperature and 40 bar ethylene monomer pressure. In this heterogeneous ethylene polymerization, 30 μmol / g metallocence activation

and 300 MAO / Zr mol ratio was used. Table 3-13 presents the result of ethylene polymerizations including the catalyst activity, the catalyst productivity and the bulk density of PE obtained. Even if the morphologies of the supported catalysts look very similar, the catalyst activities are quite different. Two kinds of nanosized PS beads are used for this experiment. One is 1 mol% PPO functionalized PS beads and the other is 10 mol% PPO functionalized PS beads. The concentration of functional group on the PS beads results in the different catalyst activity under the same condition.

Table 3-13. Polymerization of ethylene (catalyst: $Me_2Si(2MeBenzInd)_2ZrCl_2$ /MAO[a] supported on nanosized PS beads functionalized with PPO)

Run	Amount of PPO (mol %)	Method	Activity [b]	Productivity [c]
PE-27	1	1	1800	1860
PE-28	1	2	2020	2060
PE-29	10	1	1350	1400
PE-30	10	2	2450	2500

[a] Reaction condition: 1 L autoclave, isobutane 400 ml, ethylene pressure 40 bar, 70 °C, 1 hr, catalyst activation: 30 Zr / cat (μmol / g), 300 MAO / Zr molar ratio, amount of catalyst: 23 – 24 mg. [b] kg PE / mol Zr hr bar. [c] g PE / g cat hr.

In the case of 1 mol % PPO on the nanosized PS beads, the supported catalyst prepared without ultrasonication (method 1) exhibits an activity of 1800 [kg PE / mol Zr hr bar] and productivity of 1860 [g PE / g cat hr] in Run PE-27. However the catalyst prepared with ultrasonication (method 2) has an activity of 2020 [kg PE / mol Zr hr bar] and productivity of 2060 [g PE / g cat hr] in Run PE-2. Even though the latter catalyst activity and productivity in Run PE-27 are higher than the former ones in Run PE-28, the difference is not considerable. On the other hand, in the case of 10 mol % PPO on the nanosized PS support, the influence of ultrasonication on the catalyst activity and productivity is much higher than that in the case of 1 mol % PPO functionalized PS beads. The supported catalyst prepared without ultrasonication (method 1) exhibits an activity of 1350 [kg PE / mol Zr hr bar] and productivity of 1400 [g PE / g cat hr] in Run PE-29. However the catalyst prepared with ultrasonication (method 2) has an activity of 2450 [kg PE / mol Zr hr bar] and productivity of 2500 [g PE / g cat hr] in Run PE-30. The catalyst activity in Run PE-33 is increased by more than 50 % in Run PE-30. These results suggested that the dispersion of the metallocene

catalysts in the case of high amounts of functional groups on the PS support are more influenced by ultrasonication than that for low amounts of functional groups on the PS beads. The nanosized PS beads are reversibly crosslinked via an interaction between metallocene / MAO complexes and PPO chains during the supporting procedure. At low PPO concentration on the PS support, the metallocene catalyst can disperse freely and uniformly on the PS supports because the crosslinking of metallocene / MAO complexes and PPO chains is lower. On the other hand, at high PPO concentration on the PS support, the interaction between metallocene / MAO complexes and PPO chains can be strengthened by increasing the amount of PPO on the particles resulting in a more stable network. The dispersion of the metallocene catalyst on the PS beads is thus limited. The ultrasonication can make the metallocene catalysts disperse more homogeneously on the PS support than that without the process which influence the catalyst activity.

Even if the catalyst activity is changed by the ultrasonication process under the same reaction conditions, other characteristics and the morphology of the PE products are similar in both cases (Figure 3-20 and Table 3-14). They are characterized by high molecular weights, high melting points and reasonable dispersities. The melting points of polyethylene measured by DSC are about 134.7 ^{o}C. The molecular weights are about 1,330,000 - 1,500,000 and the polydispersity is 2.5 - 2.8. Many small aggregated particles are observed on the surface of the PE particles.

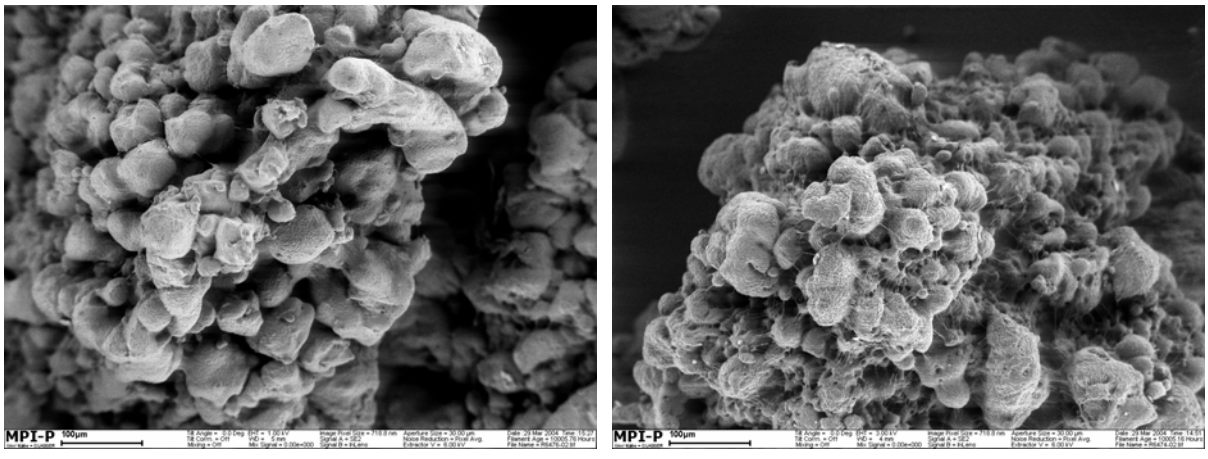

(A) (B)

Figure 3-20. SEM images of (A) polyethylene (PE-27) produced by the supported catalyst without ultrasonication and (B) polyethylene (PE-29) produced by the supported catalyst with ultrasonication: scale bar – 100 μm

Table 3-14. Characteristics of polyethylene [a]: melting point (Tm) and molecular weight (Mw) of polyethylene

Run	Tm [b] (°C)	Mn [c] (GPC)	Mw [c] (GPC)	PDI
PE-27	134.2	565,000	1,479,000	2.6
PE-28	134.4	562,000	1,494,000	2.6
PE-29	134.1	518,000	1,501,000	2.8
PE-30	134.2	534,000	1,335,000	2.5

[a] Reaction condition: in a 1 L autoclave, isobutane 400 ml, ethylene pressure 40 bar, 70 °C, 1 hr, catalyst activation: 30 Zr / cat (μmol/g), 300 MAO / Zr molar ratio, amount of catalyst 23 - 24 mg. [b] by differential scanning calorimetry (DSC). [c] by gel permeation chromatography (GPC).

3.3.3.2. The influence of sieving method in the supported catalyst system on the ethylene polymerization and the PE product

As mentioned above, the disadvantage of the supported catalyst system based on the nanosized polystyrene (PS) beads is the wide distribution of the catalyst particle size. That influenced the distribution of the polyolefin particles obtained. To overcome this problem of wide distribution of the catalyst particle size, a sieving of the supported catalyst for obtaining uniform catalyst particle size is introduced. This process is intended to improve the particle size distribution of the final olefin polymer because the shape and size of the supported catalyst is expected to influence the particle size distribution and morphology of the final polyolefin product.

3.3.3.2.1. Preparation of the supported catalyst

In this work, nanosized PS beads functionalized with PPO were used for supporting the metallocene catalyst. The supporting procedure was same as the previous one in chapter 3.3.2. After the preparation of the supported catalyst, the dried catalyst was separated by using sieves with uniform pore size. SEM images of the supported catalyst in Figure 3-21 and 3-22 show the different particle size distribution before sieving process and after one. The supported catalyst particles (Catalyst 1) before sieving in Figure 3-21 have a variety of large

and small sizes, while Figure 4-16 shows catalyst particles (Catalyst 2) after sieving with uniform size.

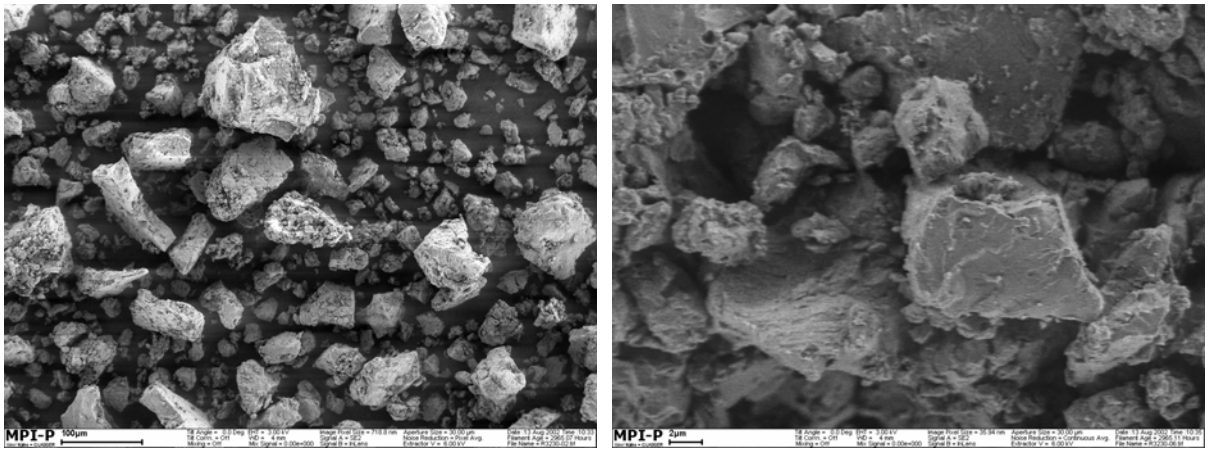

(A) (B)

Figure 3-21. SEM images of the supported catalyst (Catalyst 1) before sieving: scale bar – (A) 100 µm and (B) 2 µm

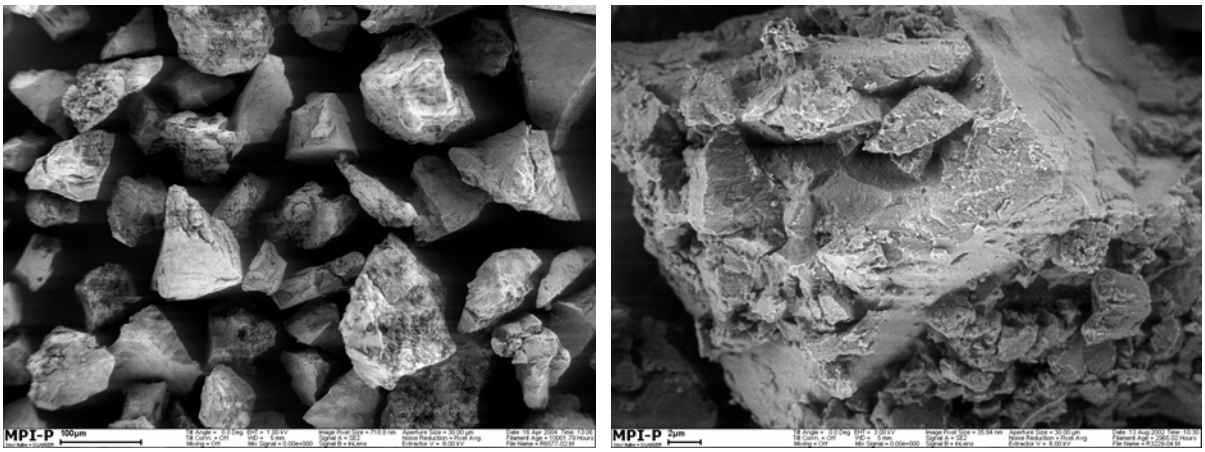

(A) (B)

Figure 3-22. SEM images of the supported catalyst (Catalyst 2) after sieving: scale bar – (A) 100 µm and (B) 2 µm

3.3.3.2.2. Ethylene polymerization and characteristics of the PE products

At 70 ^{o}C and 40 bar, ethylene polymerizations were carried out using catalyst 1 of Figure 3-21 and catalyst 2 of Figure 3-22. In this heterogeneous ethylene polymerization, 40 µmol / g metallocence activation and 350 MAO / Zr mol ratio was used. The results of ethylene polymerizations are presented in Table 3-15. The catalyst activity in the cases of sieved and

non-sieved supported catalyst is about 1200 (kg PE / mol Zr hr bar). Also the bulk density of the PE is similar in each run. The bulk density of PE is about 380 (g / l) which is good for industrial uses. The only difference is the particle size distribution of PE obtained by the supported catalyst before sieving and after sieving.

Table 3-15. Polymerization of ethylene [a] (catalyst: $Me_2Si(2MeBenzInd)_2ZrCl_2$ / MAO supported on PPO functionalized nanoparticles)

Run	Catalyst	Activity (kg PE / mol Zr hr bar)	Productivity (g PE / g cat hr)	BD [b] (g / l)
PE-31	1	1200	1635	370
PE-32	1	1230	1670	380
PE-33	2	1170	1600	390
PE-34	2	1260	1710	370

[a] Reaction condition: 1 L autoclave, isobutane 400 ml, ethylene pressure 40 bar, 70 °C, 1 hr, catalyst activation: 40 Zr / cat (μmol / g), 350 MAO / Zr molar ratio, amount of catalyst 23 - 24 mg. [b] BD: bulk density (g / l).

Figure 3-23 shows the particle size distribution of PE obtained by the sieved and non-sieved supported catalyst. The particle size distribution of polyethylene (PE-31) obtained by using the non-sieved catalyst particles are very wide with 300 micrometer diameter (Figure 3-23, A).

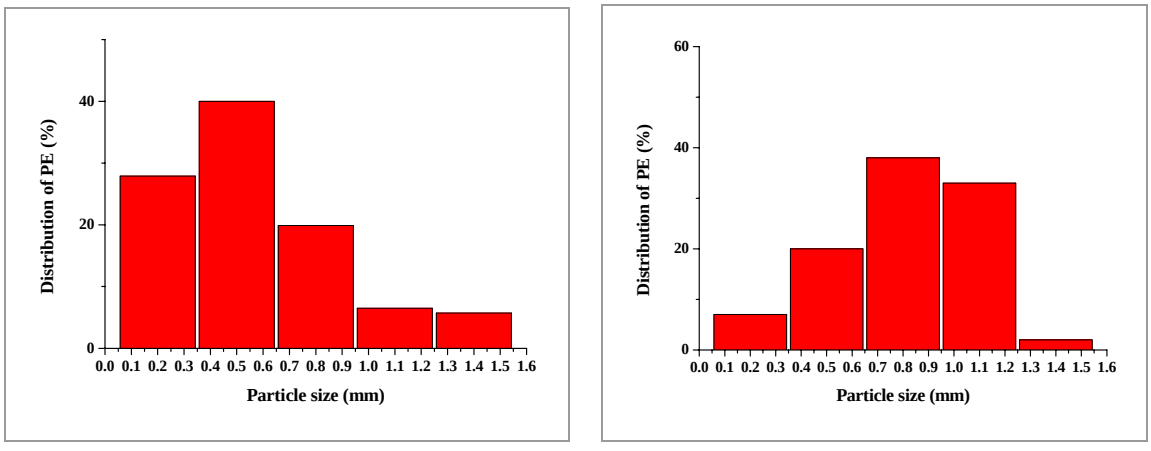

(A) before sieving (B) after sieving

Figure 3-23. Particle size distribution of (A) PE-31 from the supported catalyst before the sieving and (B) PE-33 from the supported catalyst after the sieving

Using the sieved catalyst particles, the particle size distribution of polyethylene (PE-33) obtained becomes most narrow (Figure 3-23, B). Figure 3-24 displays the SEM images of PE particles produced by the supported catalyst before sieving and after sieving respectively. Figure 3-24 (A) shows that there are very small and large particles of PE, on the other hand the SEM image of PE particles produced by the supported catalyst after sieving in Figure 3-24 (B) displays a uniform particle size of PE.

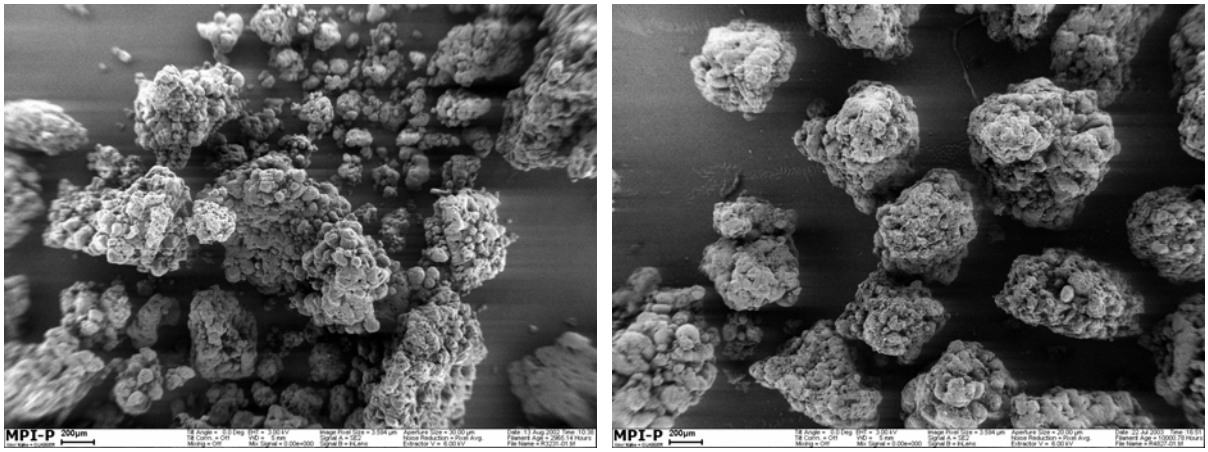

(A) (B)

Figure 3-24. SEM images of (A) polyethylene (PE-35) obtained by the supported catalyst before sieving and (B) polyethylene (PE-37) obtained by the supported catalyst after sieving: scale bar - 200 µm

Table 3-16. Characteristics of polyethylene [a]: melting point (Tm) and molecular weight (Mw) of polyethylene

Run	Tm [b] (^{o}C)	Mn [c] (g / mol)	Mw [c] (g / mol)	PDI
PE-31	134.2	596,000	1,370,000	2.3
PE-32	134.4	518,000	1,295,000	2.5
PE-33	134.7	584,000	1,402,000	2.4
PE-34	134.2	552,000	1,436,000	2.6

[a] Reaction condition: in a 1 L autoclave, isobutane 400 ml, ethylene pressure 40 bar, 70 °C, 1 hr, catalyst activation: 41 Zr / cat (µmol / g), 350 MAO / Zr molar ratio, amount of catalyst 23 - 24 mg. [b] by differential scanning calorimetry (DSC). [c] by gel permeation chromatography (GPC). [c]

Concerning the characteristics of the polymers obtained, the melting points of PE are similar to those of the polymers produced with the supported catalysts obtained by different procedures (Table 3-16). They exhibit high molecular weights, low polymer dispersities and high melting points. The molecular weights are in the range of 1,200,000 - 1,400,000 and the polydispersity index is between 2.3 - 2.6. The melting point of PE is about 134 ^{o}C.

3.3.3.3. Summary

In this chapter, two different processes were used to improve the particle size distribution of polyethylene by a sieving method and the homogeneous distribution of metallocene catalyst on the support by an ultrasonication method. By using sieving, uniform catalyst particles were obtained and used in the ethylene polymerization. The particle size distribution of the obtained PE was much improved over that of the non-sieved catalyst. The catalyst activity in the both cases of sieved and non-sieved supported catalysts was similar and also the bulk density of the PE product was similar in each run. The ultrasonication was expected to homogeneously disperse the metallocene catalyst on the support. After using ultrasonication, the catalyst activities were increased by up to 40 – 50 %. However, the morphologies of the supported catalysts and polyethylene products remained unaffected.

3.3.4. Nanosized PS beads functionalized with polypropyleneoxide (PPO) as support in heterogeneous copolymerizations of ethylene with α-olefin monomers

Ethylene polymerizations were studied under various conditions by using supported catalysts on nanosized PS beads functionalized with PEO and PPO as catalyst carrier. Polyethylene (PE) is a partially amorphous and partially crystalline polymer. In controlling the degree of crystallinity, side chain branching is the key factor [17 and 18]. If the side chain branching is controlled, the polymer properties are changed. Copolymerization of ethylene with higher α-olefins can create polyethylene with branched side chains. This can change the properties of the polymers such as the mechanical properties and incorporate other desirable properties such as fire retardancy, dyeability, solvent and chemical resistance [19, 20 and 21]. Such copolymers have considerable industrial potential. They exhibit lower melting points, lower molecular weights and lower crystallinity than the homo-polymers which makes them suitable candidates for various industrial applications.

To investigate the applicability of our system (nanosized PS beads / $Me_2Si(2MeBenzInd)_2$ $ZrCl_2$ / MAO) in heterogeneous olefin polymerization, co-polymerizations of ethylene with several co-monomers (1-hexene, 1-octene, 1-decene or norbornene) were performed.

3.3.4.1. Preparation of nanosized polystyrene (PS) beads functionalized with polypropyeneoxide (PPO) and the supported catalyst

The nanosized PS beads functionalized with polypropyleneoxide (10 mol %) were used as support in heterogeneous copolymerization of ethylene with several co-monomers. In all experiments performed, the immobilization procedure of metallocene and MAO was used according to chapter 3.3.1.1

3.3.4.2. Copolymerization of ethylene with α-olefin monomers

The copolymerization conditions were kept the same as in the case of ethylene homo-polymerization. The catalyst activation was selected as Zr concentration of 40 μmol / g and MAO / Zr molar ratio of 350 for comparison with the result of ethylene homo-polymerization, while varying the co-monomer concentration in the reactor.

The activities and productivities of the supported catalyst are much higher than those of

ethylene homo-polymerization when 1-hexene co-monomers were used (Table 3-17). In the case of ethylene homo-polymerization (Run PE-23), the catalyst exhibits an activity of 1250 (kg PE / mol Zr hr bar) and a productivity of 1750 (g PE / g cat hr). On the other hand, when 1-hexene of 0.2 (mol / l) as co-monomer is used (Table 3-17), the catalyst has an activity and productivity of 2700 (kg PE / mol Zr hr bar) and 2950 (g PE / g cat hr) respectively in Run PEHe-1. When the 1-hexene amount is increased, the catalyst activity and productivity are up to 5-fold higher than that of ethylene homo-polymerization. Also co-polymerizations of ethylene with 1-octene or 1-decene are carried out under the same polymerization condition while varying the co-monomer concentration in the reactor.

Table 3-17. Co-polymerization [a] of ethylene and 1-hexene by the supported catalyst on the nanosized PS beads functionalized with PPO / $Me_2Si(2MeBenzInd)_2ZrCl_2$ / MAO

Run	Co-monomer	Amount of co-monomer (mol/l)	Activity [b]	Productivity [c]
PE-23	0	0	1250	1750
PEHe-1	1-hexene	0.20	2700	2950
PEHe-2	1-hexene	0.40	3000	3400
PEHe-3	1-hexene	1.60	6100	6800

[a] Reaction condition: in a 1L autoclave, isobutane 400 ml, ethylene pressure 40 bar, 70 °C, catalyst activation: 40 Zr / cat (μmol / g), 350 MAO / Zr molar ratio, amount of catalyst: 23 - 24 mg, [b] kg PE / mol Zr hr bar, [c] g PE / g cat hr.

Table 3-18 shows that the activities and productivities of the supported catalyst also in copolymerization with 1-octene are much higher than those of ethylene homo-polymerization. When 1-octene of 0.15 (mol / l) as co-monomer is used, the catalyst exhibits an activity and productivity of 2950 (kg PE / mol Zr hr bar) and 3650 (g PE / g cat hr) respectively in Run PEOc-1. When 1-decene of 1.30 (mol / l) as co-monomer is used, the catalyst has an activity and productivity of 3350 (kg PE / mol Zr hr bar) and 3700 (g PE / g cat hr) respectively in Run PEOc-2. The increase of the catalyst activity when increasing the amount of comonomer can readily be explained by the well-known comonomer effect [22, 23, 24 and 25]. This effect is the enhancement of the catalyst activity due to better copolymer solubility with the incorporation of comonomer.

Table 3-18. Co-polymerization [a] of ethylene and 1-octene or 1-decene by the supported catalyst on the PS beads functionalized with PPO / $Me_2Si(2MeBenzInd)_2ZrCl_2$ / MAO

Run	Co-monomer	Amount of co-monomer (mol/l)	Activity [b]	Productivity [c]
PEOc-1	1-octene	0.15	2950	3650
PEOc-2	1-octene	0.34	3300	3700
PEOc-3	1-octene	0.63	4400	4900
PEOc-4	1-decene	1.30	3350	3700

[a] Reaction condition: in a 1L autoclave, isobutane 400 ml, ethylene pressure 40 bar, 70 °C, catalyst activation: 40 Zr / cat (μmol / g), 350 MAO / Zr molar ratio, amount of catalyst: 23 - 24 mg, [b] kg PE / mol Zr hr bar, [c] g PE / g cat hr.

In comparison to the catalyst activities of the copolymerization of ethylene with aliphatic olefin co-monomers (1-hexene, 1-octene and 1-decene), those of norbornene copolymers are increased slightly upon varying the co-monomer concentration between 0.13 mol / l and 0.53 mol / l of norbornene but decrease when the concentration is above 1.10mol / l (Table 3-19). The activities and productivities of norbornene are lower than those for copolymerization of aliphatic olefin co-monomers which is obviously due to the bulkiness of the norbornene molecule [26].

Table 3-19. Copolymerization [a] of ethylene and norbornene by the supported catalyst on the PS beads functionalized with PPO / $Me_2Si(2MeBenz\ Ind)_2ZrCl_2$ / MAO

Run	Co-monomer	Amount of co-monomer (mol/l)	Activity [b]	Productivity [c]
PENo-1	norbornene	0.13	1150	1550
PENo-2	norbornene	0.28	1300	1750
PENo-3	norbornene	0.53	2000	2480
PENo-4	norbornene	1.10	500	550

[a] Reaction condition: in a 1L autoclave, isobutene 400 ml, ethylene pressure 40 bar, 70 °C, catalyst activation: 40 Zr / cat (μmol / g), 350 MAO / Zr molar ratio, amount of catalyst: 23 - 24 mg, [b] kg PE / mol Zr hr bar, [c] g PE / g cat hr.

3.3.4.3. Characterization of copolymers

The influence of the co-monomer concentration on the degree of crystallinity (Xc) and the melting temperature (Tm) of the copolymer products of ethylene with α-olefin monomers is investigated (Table 3-20). As the co-monomer content increases, there is a decrease of the degree of crystallinity (Xc) and the melting temperature (Tm) for the ethylene / α-olefin copolymers. The degree of crystallinity influences the thermal property of ethylene copolymer due to increasing amorphous character. Copolymers of ethylene and cyclic olefins like norbornene are known to be amorphous resins [27, 28 and 29]. Their stiffness, low creep tendency and water resistance make them useful in optical storage media, capacitor films and medical applications [30].

Table 3-20. Characterization of copolymers [a] of ethylene with α-olefin comonomers (1-hexene, 1-octene, 1-decene or norbornene)

Run	Comonomer	Amount of Comonomer (mol/l)	Tm [b] (°C)	Xc [c] (%)
PE-23	0	0	134.8	48.8
PEHe-1	1-hexene	0.20	123.3	36.7
PEHe-2	1-hexene	0.40	111.6	29.2
PEHe-3	1-hexene	1.60	93.6	20.7
PEOc-1	1-octene	0.15	123.5	40.9
PEOc-2	1-octene	0.34	115.3	32.9
PEOc-3	1-octene	0.63	100.8	22.9
PEOc-4	1-decene	1.30	128.8	42.8
PENo-1	norbornene	0.13	128.8	34.3
PENo-2	norbornene	0.28	122.3	30.3
PENo-3	norbornene	0.53	116.5	27.6
PENo-4	norbornene	1.10	- [d]	-

[a] Reaction condition: in a 1L autoclave, isobutane 400 ml, ethylene pressure 40 bar, 70 °C, catalyst activation: 40 Zr / cat (μmol / g), 350 MAO / Zr molar ratio, amount of catalyst: 23 - 24 mg, [b] by differential scanning calorimetry (DSC). [c] Xc (%): Crystallinity = 100 (ΔH_m / ΔH_m^*); ΔH_m^* = 290 J / g, [d] no melting point

Figure 3-25 shows the DSC thermograms of polyethylene and copolymers of ethylene with α-olefin monomers (1-hexene, 1-octene, 1-decene or norbornene). As already mentioned, the melting point of the copolymers is lower than that of the ethylene homo-polymer. This result is related to the incorporation of 1-hexene, 1-octene or 1-decene molecules into the polymer chain modifying the polymer crystallinity and therefore lowering the melting temperature. Besides, the copolymer DSC curve is broader than the homo-polymer one. This is characteristic for materials with crystallites of different sizes. The copolymers from the copolymerization of ethylene with aliphatic monomer (1-hexene, 1-octene and 1-decene) are obtained as spherical beads.

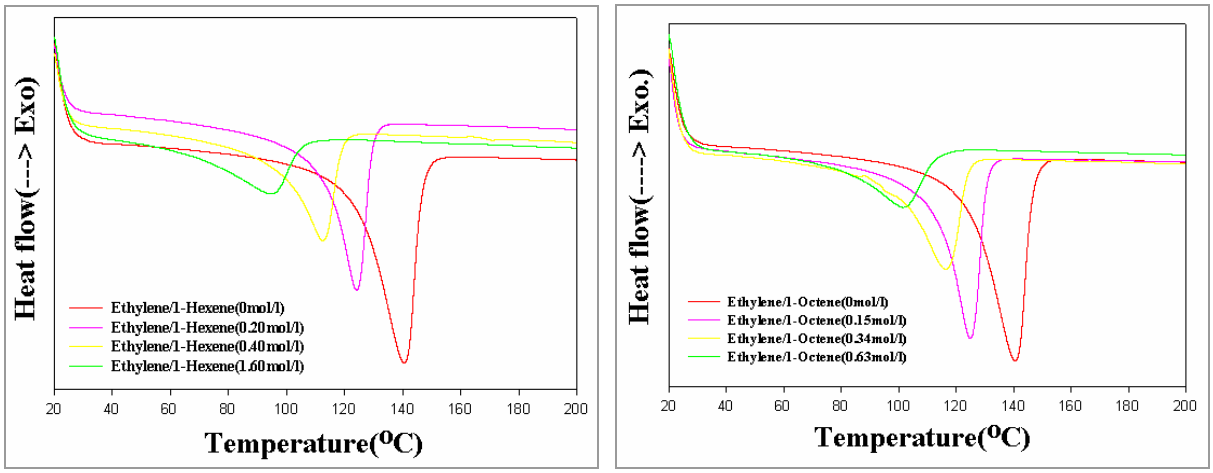

(A) (B)

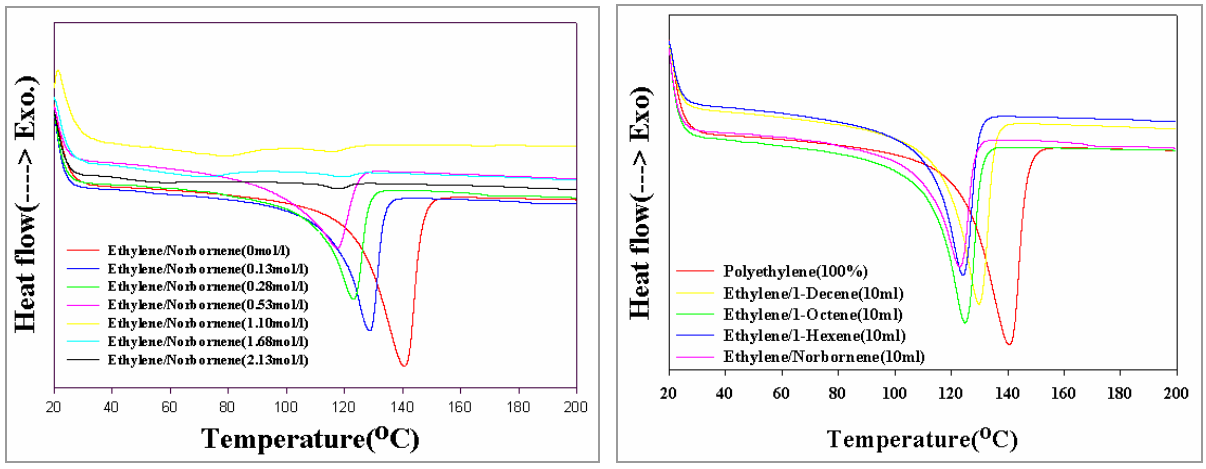

(C) (D)

Figure 3-25. DSC thermograms of copolymers: (A) copolymers of ethylene with 1-hexene, (B) copolymers of ethylene with 1-octene, (C) copolymers of ethylene with norbornene and (D) copolymers of ethylene with co-monomers

The SEM images of copolymers of ethylene with 1-hexene or 1-octene show that the copolymer particles are spherical with good morphology (Figure 3-26 and 3-27). On the other hand, the copolymers from the copolymerization of ethylene with norbornene are rubber-like materials.

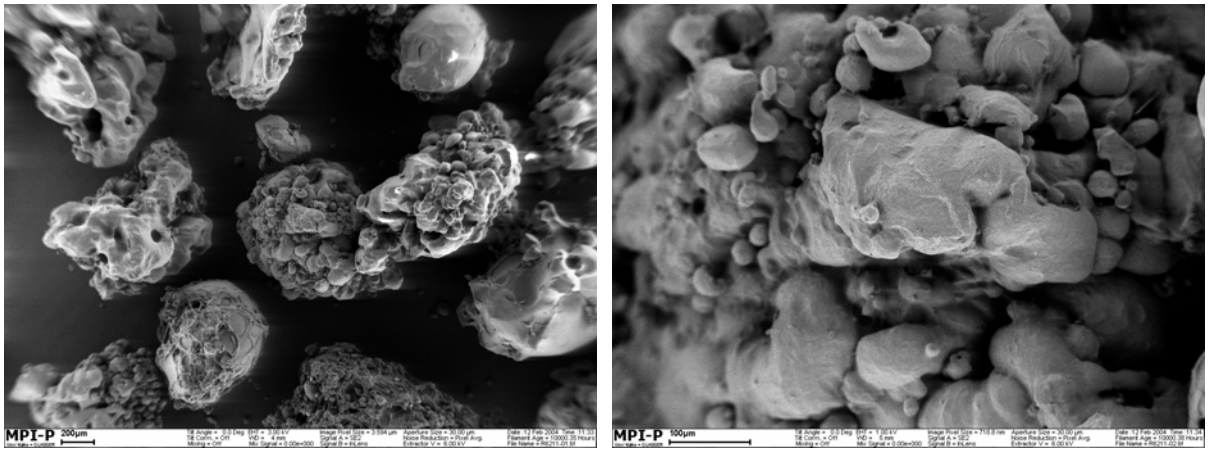

Figure 3-26. SEM images of copolymer (PEHe-1) of ethylene with 1-hexene (0.20 mol / l): scale bar – (A) 200 µm and (B) 100 µm

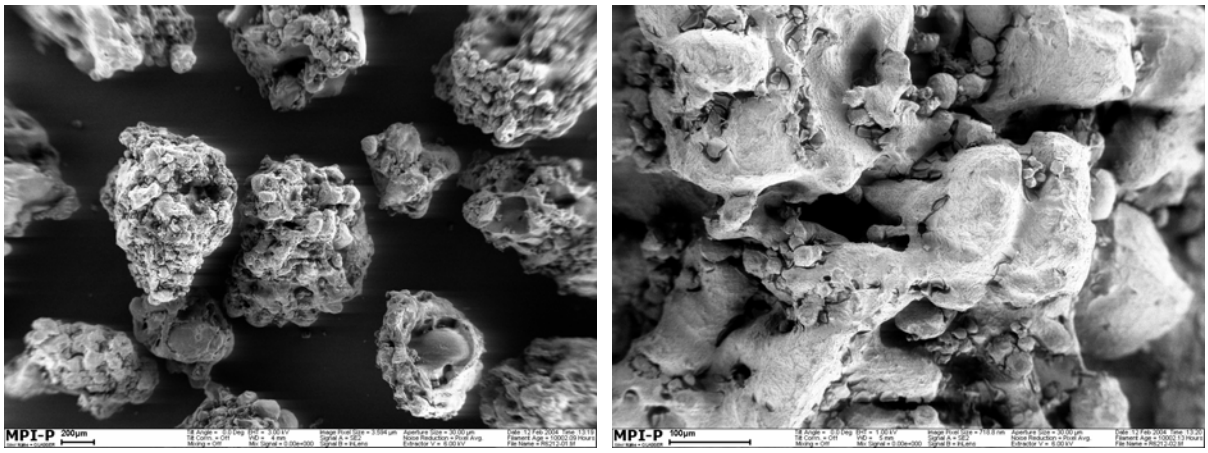

Figure 3-27. SEM images of copolymer (PEOc-1) of ethylene with 1-octene (0.15 mol / l): scale bar – (A) 200 µm and (B) 100 µm

3.3.4.4. Summary

In this chapter, copolymerizations of ethylene with several comonomers (1-hexene, 1-octene, 1-decene or norbornene) were carried out to investigate the applicability of the system (nanosized PS beads / $Me_2Si(2MeBenzInd)_2ZrCl_2$ / MAO) in heterogeneous olefin polymerization. The activities of the supported catalyst in copolymerization of ethylene with

1-hexene, 1-octene or 1-decene were much higher than those of ethylene homopolymerization due to the well-known comonomer effect. However, the activities of the supported catalyst in the copolymerization of ethylene with norbornene were lower than those for copolymerization of aliphatic olefin comonomers due to the bulkiness of the norbornene molecule. As the comonomer content increased, there was a decrease of the melting temperature (Tm) and the degree of crystallinity (Xc) due to the decrease of the crystallite size. The copolymers from copolymerization of ethylene with aliphatic monomers were obtained as spherical beads. On the other hand, the copolymers from copolymerization of ethylene with norbornene monomer were rubber-like materials even if using the supported catalyst.

3.3.5. Nanosized PS beads functionalized with polypropyleneoxide (PPO) as support in heterogeneous propylene polymerization

3.3.5.1. Introduction

Propylene polymerization has been of a great interest due to a number of practical applications of polypropylene (PP). Polypropylene (PP) is the commodity polymer with the fastest growing market [31]. Major markets for the polypropylene (PP) are filaments, fibers, automotive, house-wares, packaging containers, furniture, toys depending on the properties of polypropylene (PP). The mechanical and physical characteristics of polypropylene are dependent on the microstructure of the polymer as well as on the molecular weight and the molecular weight distribution of the polymer product [32]. The wide field of applications of polypropylene (PP) results from the fact that the polymer microstructure can be controlled by the catalyst symmetry and also has a major influence on the bulk properties of the polymer.

There are three kinds of polypropylene (PP) based on the polymer microstructure: isotactic, syndiotactic and atactic polypropylene [26]. Highly isotactic polypropylene [33, 34 and 35], for example, is a crystalline, thermoplastic material with a melting point around 165 ^{o}C, which is used as a constructive material. Highly syndiotactic polypropylene [36 and 37] is also a crystalline thermoplastic material with a high melting point. The differences between isotactic and syndiotactic polypropylene (PP) can be found in the elastic modulus, impact strength, opacity and crystallization behavior. Atactic polypropylene [38, 39 and 40], however, is amorphous with an appearance ranging from oil to a soft and waxy material used in cosmetics or as fuel additives. In each system of polymerization for isotactic PP, syndiotactic PP and atactic PP, the propylene monomer offers two faces for the coordination to a metal center. The steric environment at the active center, formed by the coordinated ligands and the growing polymer chain, determines the orientation of the incoming new monomer in the polymer chain and metallocene [41].

In C_2-symmetric catalysts, the two polymerization sites are identical and therefore possess equal selectivity for the coordination of the propylene monomer [42, 43 and 44]. All coordinations lead to identical stereoselectivity insertions and an isotactic polypropylene chain is produced. Complexes with Cs-symmetry catalyst bear an internal mirror plane [45, 46 and 47]. The two coordination sites formed after activation are mirror images and show opposite selectivity for the coordination and insertion of the propylene monomer. This means

that the preferred face for coordination changes after every insertion step which affords a syndiotactic polypropylene microstructure. The approach towards the preparation of elastomeric polypropylene was to use an unbridged bis(indenyl) zirconium dichloride bearing bulky phenyl substitutes in 2-position of the indenyl moiety [48, 49, 50, 51 and 52]. The proposed mechanism for the formation of an isotactic-atactic block copolymer involves isomerization between an isospecific, C_2-symmetric form and aspecific geometry, which interconvert during the course of the polymerization. In elastomeric polypropylenes, the statistic arrangement of the methyl groups prevents crystallization of the polymer material. Elastomeric polypropylenes are therefore amorphous materials. In isotactic-atactic block-like copolymers, the isotactic sequences crystallize to form microphase separated crystalline domains incorporated in an amorphous matrix of atactic polypropylene, where the crystalline domains act as physical cross-links.

3.3.5.2. Preparation of the support and the supported catalyst

The nanosized PS functionalized with polypropyleneoxide (10 mol %) was used as catalyst carrier. In all experiments performed, the immobilization procedure of each metallocene catalyst was used as the previous one in chapter 3.3.1.1

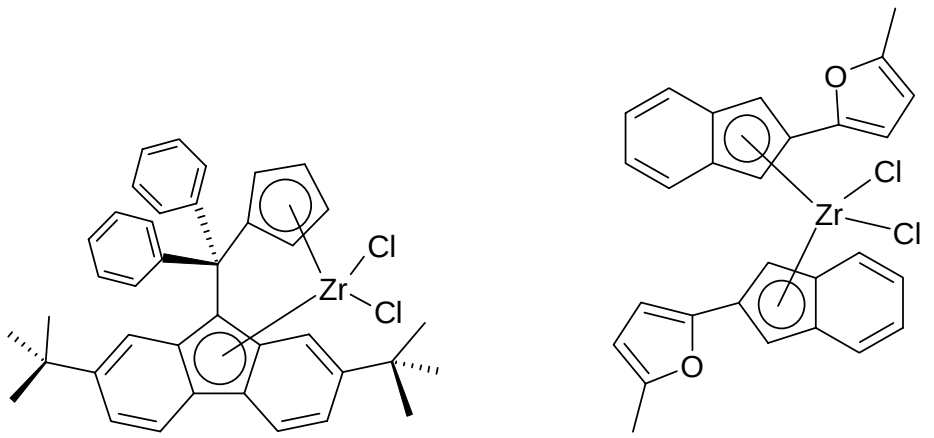

(A) (B)

Figure 3-28. Metallocene catalysts used: (A) $Ph_2C(2,7\text{-}Bu_2Flu)(Cp)ZrCl_2$ and (B) bis[η^5-1-(5-methyl-2-furyl)indenyl]$ZrCl_2$.

Figure 3-28 shows the different metallocene catalysts which were used in homogeneous or heterogeneous polymerization: (A) $Ph_2C(2,7\text{-}Bu_2Flu)(Cp)$ $ZrCl_2$ donated by Prof.

Kaminsky's group in Hamburg University for syndiotactic polypropylene and (B) bis[η^5-1-(5-methyl-2-furyl)indenyl]$ZrCl_2$ donated by Prof. Erker's group in Münster University for elastomeric polypropylene.

Figure 3-29 shows the SEM images of the supported catalyst ($Ph_2C(2,7\text{-}Bu_2Flu)(Cp)ZrCl_2$ / MAO / nanosized PS). Like the result of the supported catalyst on nanoszied PS beads functionalized with PPO for ethylene polymerization, the particle size is non-uniform and small particles are aggregated on the surface of the supported catalyst.

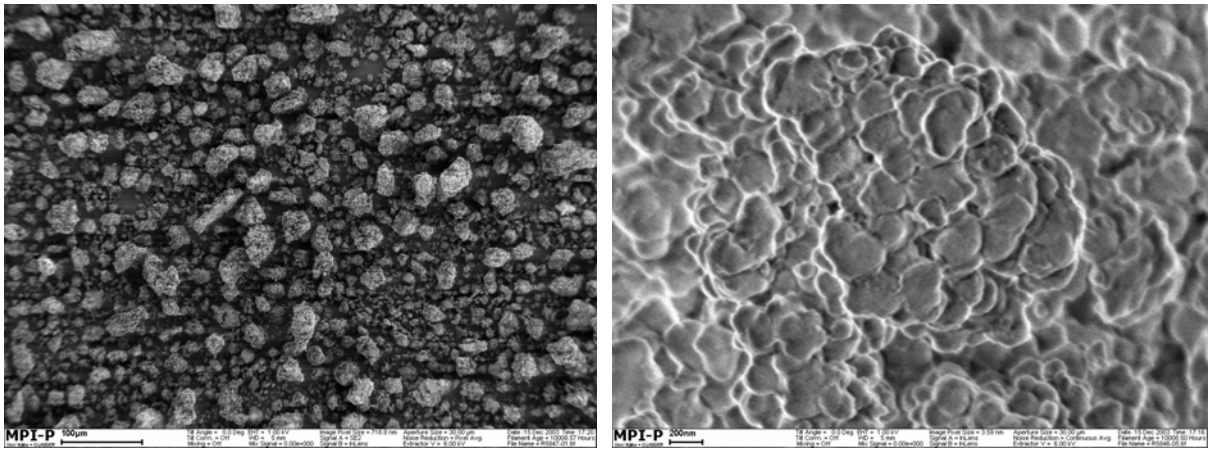

(A) (B)

Figure 3-29. SEM images of the supported catalyst ($Ph_2C(2,7\text{-}Bu_2Flu)(Cp)ZrCl_2$ catalyst / MAO / nanosized PS beads) for propylene polymerization: scale bar – (A) 100 μm and (B) 200 nm

3.3.5.3. Polymerization of propylene

Two polymerization systems such as homogeneous and heterogeneous polymerization were used and the results of propylene polymerization and the properties of each polypropylene (PP) obtained were compared. The polymerizations using each supported catalyst were performed two or three times under the same reaction condition in order to ensure reproducibility of the observations made. The polymerization using a homogeneous and heterogeneous catalyst system was polymerized as follows.

Homogeneous polymerization: all homogeneous polymerizations were carried out in a 1 L glass autoclave charged with 400 ml toluene and 20 ml MAO (10 weight % solution in toluene). The stirred (100 rpm) mixture was saturated for 1hr with propylene gas at 2.5 bar. The catalyst solution in toluene (5 ml) was injected by applying argon gas pressure to the

reactor and the propylene gas was charged up to 4 bar. After polymerization at a permanent propylene pressure of 4 bar, the reaction mixture was terminated with 5 ml MeOH, treated with HCl / MeOH solution for overnight and then the PP product was washed by MeOH, filtrated and dried in vacuum.

Heterogeneous polymerization: All heterogeneous polymerizations were carried out in a 1 L glass autoclave charged with 400 ml toluene and 10 ml MAO (10 weight % solution in toluene). The stirred (100 rpm) mixture was saturated for 1hr with propylene gas at 2.5 bar. The supported catalyst (100 – 120 mg) suspended in TIBA 5 ml (in hexane) was injected by using argon gas pressure to the reactor and the propylene gas was charged up to 4 bar. After polymerization at a permanent propylene pressure of 4 bar, the reaction mixture was terminated with 5 ml MeOH, treated HCl / MeOH solution for overnight and the filtrated PP product dried in a vacuum oven.

3.3.5.3.1. Syndiotactic polypropylene

Under 50 ^{o}C polymerization temperature and 4 bar propylene pressure in a slurry phase, heterogeneous and homogeneous propylene polymerizations were carried out several times. Table 3-21 presents the results of propylene polymerization. The catalyst activity in homogeneous polymerization ($Ph_2C(2,7\text{-}Bu_2Flu)(Cp)ZrCl_2$ / MAO system) is higher than that in the heterogeneous polymerization.

Table 3-21. Propylene polymerization [a] and melting temperature of syndiotactic polypropylene produced by heterogeneous and homogeneous polymerization

Run	Zr / cat (μmol / g)	MAO / Zr	Activity (kg PE / mol Zr hr bar)	Tm [b] (^{o}C)
PP-1 [c]	18	600	1580	145.4
PP-2 [c]	18	600	1420	145.5
PP-3	Homogeneous polymerization [d]		17200	140.4
PP-4	Homogeneous polymerization [d]		16400	140.2

[a] medium: toluene 400 ml and 4 bar propylene pressure, [b] by differential scanning calorimetry (second heat), [c] heterogeneous polymerization, [d] [Zr]: 20 μmol and 1500 MAO / Zr molar ratio.

In the case of heterogeneous polymerization, the catalyst exhibits an activity of about 1500 (kg PE / mol Zr hr bar) in Run PP-1 and PP-2. On the other hand, in the case of homogeneous polymerization, the catalyst has an activity of about 17000 (kg PE / mol Zr hr bar) in Run PP-3 and PP-4. The polypropylene (PP-1 and PP-2) obtained in heterogeneous polymerization has a melting point of about 145 ^{o}C, on the other hand polypropylene (PP-3 and PP-4) from homogeneous polymerization has a melting point of about 140 ^{o}C. The properties of polypropylene obtained in homogeneous polymerization are similar to the result of Kaminsky who produced this catalyst [$Ph_2C(2,7\text{-}Bu_2Flu)(Cp)ZrCl_2$] and polymerized polypropylene (PP) under different conditions [53]. In his case of homogeneous polymerization, the melting points of polypropylene were 129 ^{o}C – 148 ^{o}C depending on the polymerization temperature. At a polymerization temperature of 30 ^{o}C in homogeneous polymerization, the melting temperature of the PP obtained was 141 ^{o}C and at 45 ^{o}C reaction temperature, it was 139 ^{o}C. At an even higher reaction temperature (60 ^{o}C), the melting temperature of the PP was reduced to 129 ^{o}C compared to that of the PP produced at 30 – 45 ^{o}C polymerization temperature. Normally in the case of Cs symmetric ansa-metallocene, the melting point of polypropylene (PP) produced from heterogeneous polymerization is higher than that from homogeneous polymerization [54]. Figure 3-30 shows SEM images of polypropylene (PP-1) produced by heterogeneous polymerization. The morphology of polypropylene particles produced by heterogeneous polymerization is very good and well defined.

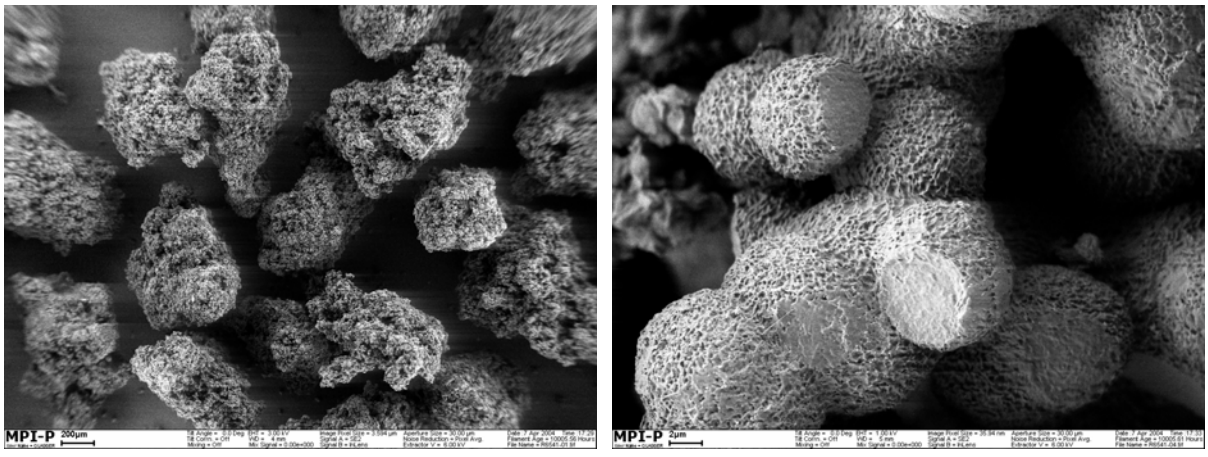

(A) (B)

Figure 3-30. SEM images of polypropylene (PP-1): scale bar – (A) 200 µm and (B) 2 µm

There are many small particles aggregated on the surface of the polypropylene particle

obtained by heterogeneous system. The small spherical particles look like the primary nanosized PS beads. The tacticity of polypropylene (PP) is calculated by using ^{13}C NMR spectroscopy at 135 ^{o}C in o-dichlorobenzene. The structure and properties of polypropylene (PP) such as chain configurations, crystal structure and mechanical strength are profoundly dependent on the tacticity or the stereoregularity of the polymeric chains [55]. Table 3-22 shows the methyl pentad distribution of syndiotactic polypropyene and presents the percentage of pentads (rrrr). All polypropylenes from homogeneous and heterogeneous polymerization show high syndiotactic and the supported catalyst system slightly influences the stereoregularity of the obtained PP. In the case of homogeneous polymerization system [Ph_2C(2,7-Bu_2Flu) (Cp)$ZrCl_2$ / MAO in toluene], the percentage of pentads (rrrr) of PP-3 and PP-4 ranges from 93.9 to 94.1 %. This percentage of rrrr pentads is similar to that produced by Kaminsky's group [52]. On the other hand, in the case of a heterogeneous polymerization system (Ph_2C(2,7-Bu_2Flu)(Cp)$ZrCl_2$ / MAO / nanosized PS beads functionalized with PPO), the percentage of pentads (rrrr) of PP-1 reaches up to 95.8 %. By supporting the metallocene catalyst, the bonding energies in the transition state of the active sites are increased. This means that in most cases the activity goes down [56]. On the other hand, the steric hindrance and the rigidity increases which can change the tacticity of the polypropylene produced.

Table 3-22. Methyl pentad distribution [a] of syndiotactic polypropylene produced by heterogeneous and homogeneous polymerization

Run	Polymerization	mmmm (%)	rmmr (%)	mmrr (%)	rrmr (%)	rrrr (%)
PP-1	Heterogeneous (Nanosized PS)	0.4	0.7	1.9	1.2	95.8
PP-2	Heterogeneous (Nanosized PS)	0.3	0.9	1.8	1.4	95.6
PP-3	Homogeneous	0.6	0.9	2.1	2.3	94.1
PP-4	Homogeneous	0.8	0.6	2.2	2.5	93.9

[a] determined by ^{13}C NMR at 135 ^{o}C in O-dichlorobenzene.

3.3.5.3.2. Elastomeric polypropylene

The unbriged metallocene catalysts produced polypropylene (PP) with different properties from the catalysts in chapter 3.3.5.3.1. In the case of an unbridged metallocene, the aromatic rings with bulky substituents can rotate freely even at very low temperatures which gives rise to an equilibrium between two rotational isomers: one with *quasi*-C_2-symmetry (*rac*-like form) and the other with *quasi*-C_s-symmetry (*meso*-like form). This behavior has been called as oscillating. By this unbridged metallocene catalyst, polypropylene (PP) was obtained with both isotactic and atactic sequences. In this catalyst system (bis[η^5-1-(5-methyl-2-furyl)indenyl] $ZrCl_2$ / MAO / nanosized PS beads functionalized with PPO) (Table 3-24), the catalyst activity is different with the catalyst results in chapter 3.3.5.3.1. As increasing the polymerization temperature, normally the catalyst activity is increased in the case of the catalyst systems (Ph_2C(2,7-Bu_2Flu)(Cp)$ZrCl_2$ / MAO / nanosized PS beads functionalized with PPO) [57, 58 and 59]. However, in the bis[η^5-1-(5-methyl-2-furyl)indenyl]$ZrCl_2$ / MAO / nanosized PS beads functionalized with the PPO system, the catalyst activity is increased with decreasing polymerization temperature. This phenomenon has been explained by Prof. Alt in Hamburg University as follow: '*with increasing reaction temperature the catalyst activity and productivity is expected to increase. However, in the most cases investigated the decrease with rising polymerization temperature, this behavior could be rather due to the partial decomposition of the catalyst at elevated temperatures and not to different kinetics*' [60]. At 40 ^oC and 20 ^oC in Run PP-9 to PP-12, the catalyst activity is very low and so not enough polypropylene is obtained for NMR, DSC etc analysis. At 10 ^oC in Run 13 to PP-16, PP product is obtained by heterogeneous and homogeneous polymerization (Table 3-23). The elastomeric polypropylene (Run PP-9) produced by heterogeneous polymerization has a melting point of 143 ^oC and the elastomeric PP (Run PP-11) produced by homogeneous polymerization has a melting point of 141 ^oC.

The polypropylene produced by homogeneous polymerization was soluble in the reaction medium – a sticky elastomeric polymer. When the polypropylene solution was poured into HCl / MeOH solution, the polypropylene aggregated to form a large sphere. However, the polypropylene produced by heterogeneous polymerization precipitated in HCl / MeOH many separate particles shown in Figure 3-31. On the surface of the polypropylene particle obtained by the heterogeneous system, there are many small particles aggregated due to the sticky polypropylene. The tacticity of polypropylene was calculated by using ^{13}C NMR.

Table 3-23. Propylene polymerization [a] of elastomeric polypropylene

Run	Cat act. [μmol/g]	MAO/Zr	Temp (°C)	Time (hr)	Activity [b] (Kg PP/mol [Zr] h bar)	Tm [c] (°C)
PP-5	20	600	40	3	-	-
PP-6	20	600	40	6	-	-
PP-7	20	600	20	3	1.3	[c]
PP-8	20	600	20	6	1.1	[c]
PP-9	20	600	10	3	5.2	143.6
PP-10	20	600	10	6	5.6	143.8
PP-11	Homogeneous polymerization [d]		10	3	220	141.2
PP-12	Homogeneous polymerization		10	6	206	141.1

[a] medium: toluene 400 ml and 4 bar propylene gas pressure, [b] Activity [Kg PP / mol Zr h bar], [c] not enough material for investigation, [d] [Zr]: 20μmol and 1500 MAO / Zr mole ratio. [c] by differential scanning calorimetry (DSC).

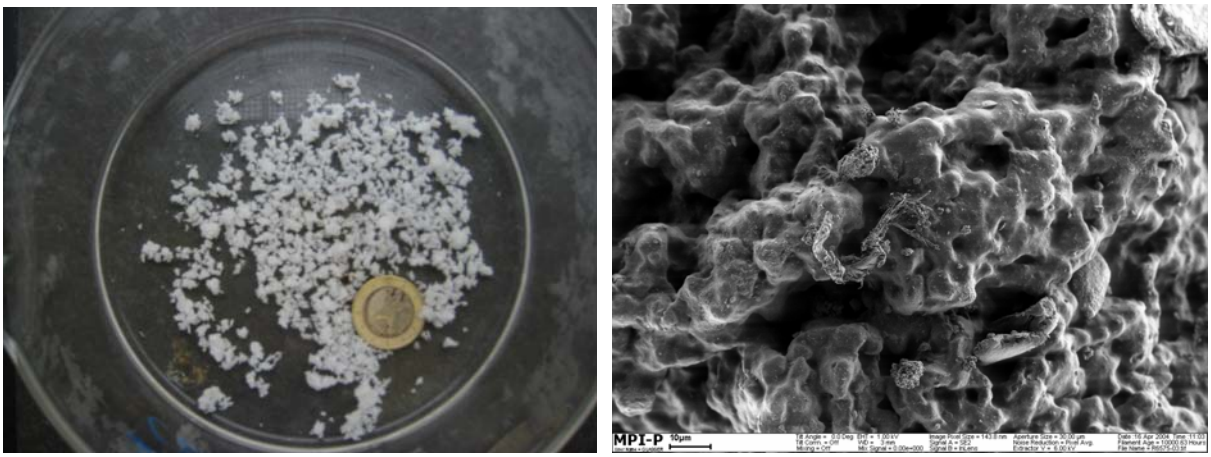

(A) (B)

Figure 3-31. (A) Polypropylene (PP-9) particles produced by heterogeneous polymerization in MeOH and (B) SEM image of PP-9 product: scale bar – 10 μm

As mentioned already, the structure and properties of polypropylene are profoundly dependent on the tacticity or the stereoregularity of the polymeric chains. Elastomeric polypropylene, alternatively, has the chiral carbon atoms of a random chirality. Carbon atoms

in the main backbone of isotactic polypropylene have the same chirality and therefore give rise to a block polymeric structure. Elastomeric polypropylene, however, is a tacky and gum-like material of no obvious mechanical integrity [61 and 62]. On the other hand, isotactic polypropylene is expected to have a well-defined crystal structure with high stiffness, mechanical strength and chemical resistance. The structure of the polypropylene obtained from this experiment was elastomeric. It was observed that the isotactic pentads (mmmm) are much more abundant than the syndiotactic pentads (rrrr) (Table 3-24). The percentages of pentads (mmmm) were different in each polypropylene sample produced by heterogeneous or homogeneous catalyst system. The methyl pentad analysis gave information on the tacticity of the polymeric chains yielding about 40 % of mmmm and 1.5 % rrrr pentads of polypropylene (PP-13) produced in heterogeneous polymerization. In the case of homogeneous polymerization, the tacticity of polypropylene (PP-11) corresponded to about 30 % mmmm and 1.6 % rrrr pentads.

Table 3-24. Methyl pentad distribution [a] of elastomeric polypropylene

Run	mmmm (%)	mmmr (%)	rmmr (%)	mmrr (%)	rrmr (%)	mrmr (%)	rrrr (%)	rrrm (%)
PP-9	42.2	15.6	3.3	9.6	15.7	6.3	0.9	3.1
PP-11	31.0	16.2	4.4	9.4	19.2	9.2	1.6	4.7

[a] determined by ^{13}C NMR at 135 ^{o}C in O-dichlorobenzene.

Two elastomeric polypropylenes produced by homogeneous and heterogeneous polymerization show the different result of hysteresis curves measured by Prof. Erker's group at Münster University. The hysteresis curves of both samples produced by homogeneous (Run PP-11) and heterogeneous (Run PP-9) polymerization are shown in Figure 3-32 and 3-33 respectively. All the strain is almost recovered upon removing the load, however the unloading curves show the different path as the loading curve. In the case of PP-11 produced from homogeneous polymerization, 1.7 MPa stress makes an elongation of the PP sample of about 400 % (Figure 3-32). On the other hand in the case of PP-9 produced from heterogeneous polymerization, 3.4 MPa stress loads to an elongation of about 400 % (Figure 3-33). The elastomers obtained from the heterogeneous catalyst system yielded more to the applied strain than those obtained from the homogeneous catalyst system

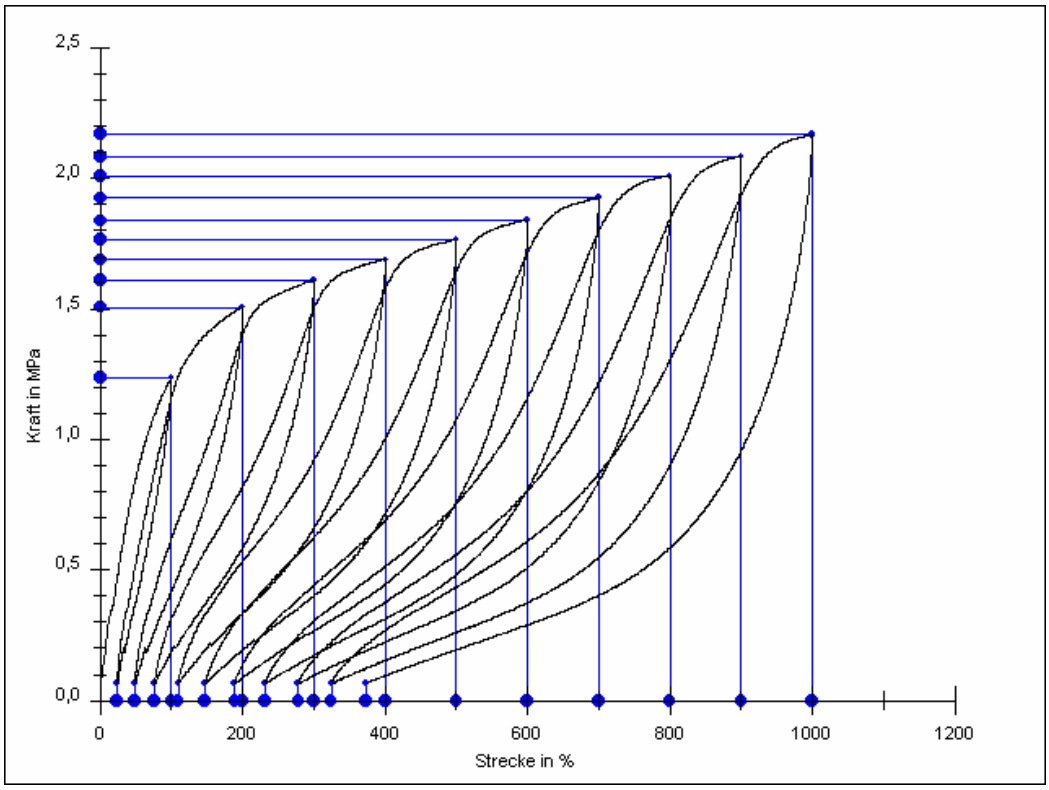

Figure 3-32. The hysteresis curves of elastomeric PP produced by homogeneous polymerization (Run PP-11)

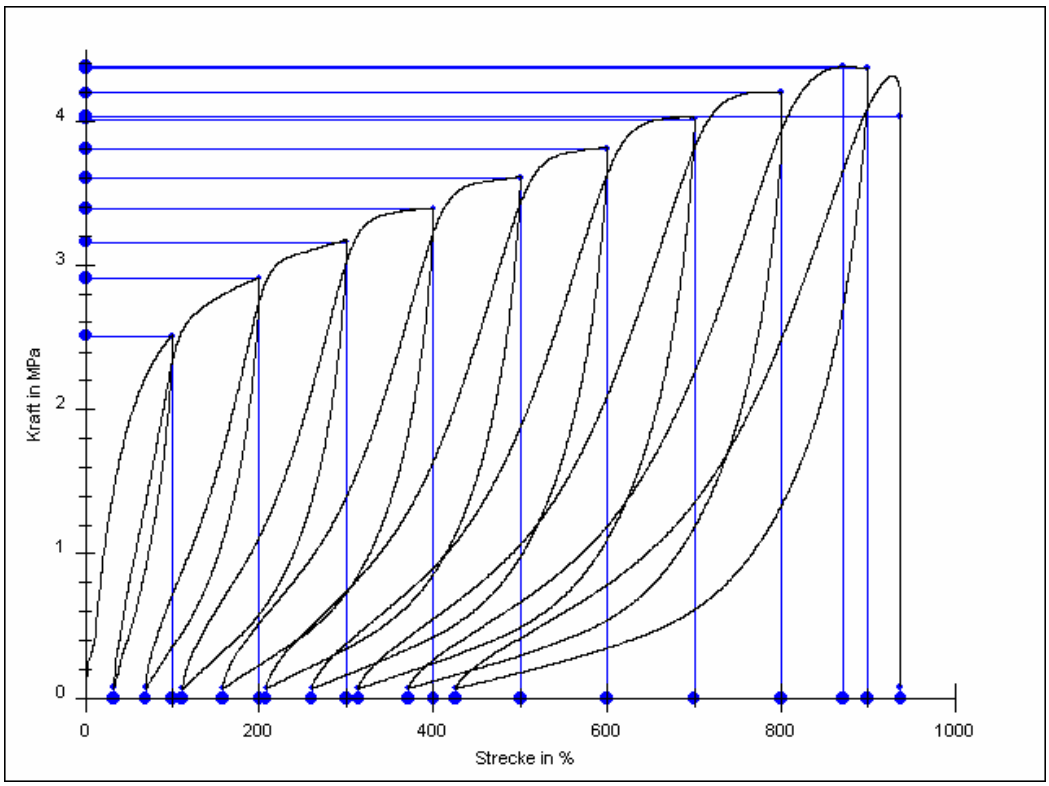

Figure 3-33. The hysteresis curves of elastomeric PP produced by heterogeneous polymerization (Run PP-9)

Also, when each curve in Figure 3-32 and 3-33 is compared, the area in the case of PP-9 is wider than that in the case of the PP-11. Each integral area between two curves making one cycle serves as a criterion to compare the elastomeric properties because the integral area corresponds to the energy dissipated within the cycle. Conclusively the more highly isotactic polypropylenes obtained from the heterogeneous catalyst system (Run PP-9) had lower elastomeric properties compared to those made by the homogeneous catalyst system (Run PP-11).

3.3.5.4. Summary

Propylene was polymerized by using two metallocene catalysts $Ph_2C(2,7\text{-}Bu_2Flu)(Cp)ZrCl_2$ and bis[η^5-1-(5-methyl-2-furyl)indenyl]$ZrCl_2$) in a homogeneous and heterogeneous polymerization system. For the $Ph_2C(2,7\text{-}Bu_2Flu)(Cp)ZrCl_2$ system, all of the polypropylene products had high syndiotacticity. On the other hand, unbriged metallocene catalysts (bis[η^5-1-(5-methyl-2-furyl)indenyl]$ZrCl_2$) produced elastomeric polypropylenes consisting of isotactic and atactic blocks. The catalyst activity in the heterogeneous polymerization system was much lower than that in the homogeneous system. However, the tacticity and morphology of the polypropylene produced in the heterogeneous case was better than that made under homogeneous conditions. By supporting the metallocene catalyst, the bonding energies in the transition state of the active sites are increased. This means that in most cases the activity goes down [56]. On the other hand, the steric hindrance and the rigidity increase which can change the tacticity of the produced polypropylene. The elastomeric property of the polypropylenes from the homogeneous catalyst system in the elongation experiments appears to be slightly better than those made using the heterogeneous catalyst system. However, the elastomers obtained from the heterogeneous catalyst yielded more to the applied strain than those obtained from the homogeneous catalyst due to the higher isotacticity.

1. M. Koch, A. Falcou, N. Nenov, M. Klapper and K. Müllen, *Macromol. Rapid. Commun*., **2001**, 22, 1455.

2. J.L. Atwood, W.E. Hunter, D.C. Hrncir, E. Samuel, H. Alt and M. Rausch, *Inorg. Chem*., **1975**, 14, 1757.

3 K. Landfester, *Macromol. Rapid. Commun*., **2001**, 22, 896.

4 I. Capek and C.S. Chern, *Adv. Polym. Sci*., **2001**, 155, 41.

5 J.M. Asua, *Prog. Polym. Sci*., **2002**, 7, 1283.

6 I. Capek and C. S. Chern, *Adv. Polym. Sci*., **2001**, 155, 101.

7 Nikolay Nenov, Dissertation, Johannes Gutenberg Universitat, Mainz, **2003**.

8 S. Bensason, J. Minick, A. Moet, S. Chum, A. Hiltmer, E. Baer, *J. Polym. Sci. Polym. Phys. Ed*., **1996**, 34, 1301.

9 F Yuan, H-Z Chen, H-Y Yang, H-Y Li and M Wang, *Mat. Chem. Phy*., **2005**, 89, 390.

10 L. Pei, K. Kurumada, M. Tanigaki, M. Hiro and K. Susa, *J. Colloid Interface Sci*., **2005**, 284, 222.

11. E. Lindner, S. Brugger, S. Steinbrecher, E. Plies, M. Seiler, H. Bertagnolli, P. Wegner and H. A. Mayer, *Inorg. Chim. Acta*, **2002**, 327, 54.

12. Nikolay Nenov, Dissertation, Johannes Gutenberg Universitat, Mainz, **2003**.

13. E. Ochoteco, M. Vecino, M. Montes and J. C. de la Cal, *Chem. Eng. Sci*., **2001**, 56, 4169.

14. C. Alonso, A. Antiñolo, F. Carrillo-Hermosilla, P. Carrión, A. Otero, J. Sancho and E. Villaseñor, *J. Mol. Catal. A, Chem*., **2004**, 220, 286.

15. K. Soga, T. Ari, B.H. Hoang and T. Uozumi. *Macromol. Rapid Commun*., **1995**. 16, 905.

16. B.L. Moroz, N.V. Semikolenova, A.V. Nosov, V.A. Zakharov, S. Nagy and N.J. O'Reilly, J. *Mol. Catal. A: Chem*., **1998**, 130, 121.

17. D. Rana, H. L. Kim, H.J. Kwag and S.J. Choe, *Polymer*, **2000**, 41, 7067.

18. K. Nomura, K. Oya and Y. Imanishi, *Polymer*, **2000**, 41, 2755.

19. V.B.F. Mathot, R.L. Scherrenberg and T.F.J. Pijpers, *Polymer*, **1998**, 39, 4541.

20. A.G. Simanke, G.B. Galland, L. Freitas, J. Alziro, H. Da Jornada, R. Quijada and R.S. Mauler, *Polymer,* **1999**, 40, 5489.

21. M. L. Britto, G. B. Galland, J. H. Z. dos Santos and M. C. Forte, *Polymer*, **2001**, 42, 6355.

22. W. Kaminsky and C. Piel, *J. Mol. Catal. A: Chem*., **2004**, 213, 15.

23. G. B. Galland, J. H. Z. dos Santos, F. C. Stedile, P. P. Greco and A. D. Campani, J. *Mol. Catal. A: Chem*., **2004**, 210, 149.

24. P. Kumkaew, L. Wu, P. Praserthdam and S. E. Wanke, *Polymer*, **2003**, 44, 4791.

25. H. S. Cho and W. Y. Lee, *J. Mol. Catal. A: Chem.*, **2003**, 191, 155.

26. C. T. Zhao, M. R. Ribeiro, M. F. Portela, *J Mol. Catal. A: Chem.*, **2002**, 185, 81.

27. W. Kaminsky, A. Bark and M. Arndt. *Makromol. Chem. Macromol. Symp*., **1991**, 47, 8.

28. H. Cherdron, M. J. Brekner and F. Osan, *Angew. Makromol. Chem*., **1994**, 223, 121.

29. D. Ruchatz and G. Fink, *Macromolecules*, **1998**, 31, 4669.

30. H.T. Land, F. Osan and T. Wehrmeister, *Polym. Mater. Sci. Eng*., **1997**, 76, 22.

31 V. Busico and R. Cipullo, *Prog. in Polym. Sci.,* **2001**, 26, 443.

32 V. Busico and R. Cipullo, *Prog. Polym. Sci*., **2001**, 26, 443.

33. W. Kaminsky, K. Kulper, H.H. Brintzinger and F.R.W.P. Wild, *Angew. Chem*., **1985**, 97, 507.

34. J.A. Ewen, *J. Am. Chem. Soc*., **1984**, 106, 6355.

35. W. Kaminsky, K. Kulper, H.H. Brintzinger and F.R.W.P. Wild, *Angew. Chem. Int. Ed. Engl*., **1985**, 24, 507.

36. J.A. Ewen, R.L. Jones, A. Razavi and J.D. Ferrara, *J. Am. Chem. Soc*., **1988**, 110, 6255.

37. J.A. Ewen, M.J. Elder, R.L. Jones, L. Haspeslagh, J.L. Atwood, S.G. Bott and K. Robinson, *Makromol. Chem. Macromol. Symp*., **1991**, 49, 253.

38. G.W. Coates and R.M. Waymouth, *Science,* **1995**, 267, 217.

39. J.C.W. Chien, G.H. Llinas, M.D. Rausch, G.-Y. Lin and H.H. Winter, *J. Am. Chem. Soc*., **1991**, 113, 8569.

40. J.W. Collette, C.W. Tullock, R.N. MacDonald, W.H. Buck, A.C.L. Su, J.R. Harrell, R. Mulhaupt and B.C. Anderson, *Macromolecules,* **1989**, 22, 3851.

41 L. Resconi, L. Cavallo, A. Fait and F. Piemontesi, *Chem. Rev.,* **2000**, 100**,** 1253.

42. H.H. Brintzinger, D. Fischer, R. Mülhaupt, B. Rieger and R.M. Waymouth, *Angew. Chem. Int. Ed. Engl*., **1995**, 31, 1143.

43. W. Spaleck, F. Kuber, A. Winter, J. Rohrmann, B. Bachmann, M. Antberg, V. Dolle and E.F. Paulus, *Organometallics,* **1994**, 13, 954.

44. N. Schneider, M.E. Huttenloch, U. Stehling, R. Kristen, F. Schaper and H.H. Brintzinger, *Organometallics,* **1993**, 12, 1283.

45. A. Razavi and J. Ferrara, *J. Organomet. Chem*., **1992**, 435, 299.

46. J.A. Ewen and M.J. Elder, *Makromol. Chem. Macromol. Symp*., **1993**, 66, 179.

47. L. Resconi, L. Cavallo, A. Fait and F. Piemontesi, *Chem. Rev*., **2000**, 100, 1253.

48. (a) J.W. Collette, D.W. Ovenall, W.H. Buck and R.C. Ferguson, *Macromolecules,* **1989**, 22, 3858.

49. G. Erker, M. Aulbach, M. Knickmeier, D. Wingbermuhle, C. Kruger, M. Nolte and S. Werner, *J. Am. Chem. Soc*., **1993**, 115, 4590.

50. W.J. Gauthier and S. Collins, *Macromolecules,* **1995**, 28, 3779.

51. W.J. Gauthier, J.F. Corrigan, N.J. Taylor and S. Collins, *Macromolecules,* **1995**, 28, 3771.

52. G.H. Llinas, S.-H. Dong, D.T. Mallin, M.D. Rausch, Y.-G. Lin, H.H. Winter and J.C.W. Chien, *Macromolecules,* **1992**, 25, 1242.

53. A. Hopf and W. Kaminsky, *Catal. Comm*., **2002**, 3, 459.

54. P. Longo, A. Grassi, C. Pellecchia and A. Zambelli, *Macromolecules*, **1987**, 20, 1015.

55. T. Hatanaka, H. Mori and M. Terano, *Polym. Degrad. Stab*., **1999**, 64, 313.

56. W. Kaminsky and H. Winkelbach, *Topics in Catalysis*, **1999**, 7, 61.

57. T. Dreier, K. Bergander, E. Wegelius, R. Fröhlich, and G. Erker; *Organometallics*, **2001**, 20, 5067.

58. T. Dreier, R. Fröhlich, G. Erker, *J. Organometal. Chem*., **2001**, 621, 197.

59. T. Dreier, G. Unger, G. Erker, B. Wibbeling, R. Fröhlich1, *J. Organometal. Chem*., **2001**, 622, 143.

60. H.H. Alt, *J. organometal. Chem*., **2001**, 621, 304.

61. T.M. Madkour and J.E. Mark, *J. Polym. Sci. Polym. Phys. Ed*., **1997**, 35, 2757.

62. G. Natta. *J. Polym. Sci*., **1959**, 34, 531.

Chapter 4. Influence of the different supports on heterogeneous ethylene polymerization

4.1. Introduction

The influence of different supports on the catalyst behavior in ethylene polymerization and the properties of the polyethylene obtained are investigated. Studies of supported metallocene catalysts have indicated that the nature of the support plays an important role not only in the catalytic activity but also in the final properties of the polymers such as morphology [1, 2 and 3]. Furthermore, morphology studies of polymers obtained with metallocenes anchored on different supports have indicated a direct relation between the polymer and support morphology [4, 5 and 6]. Four kinds of supports were used for this investigation. The first carrier type was microsized PS beads functionalized with hydroxyl groups. Such microsized PS beads are one of the catalyst carriers used in academic research and the typical particle size is 100 micrometer [7]. The advantage of these microsized PS beads as a support is the replication of the support particle and easy immobilization of metallocene catalyst on the surface of the support [8]. The second carrier type was nanosized PS beads functionalized with hydroxyl groups having about 60 nm particle size. Ethylene polymerization using a catalyst supported on nanosized PS beads functionalized with hydroxyl group is compared with the results from using microsized PS beads functionalized with the hydroxyl group. One can study the influence of the primary particle size of the supported catalyst on the catalyst activity in heterogeneous ethylene polymerization and the polymer properties by using the PS beads having the same chemical structure (hydroxyl group functionalized with polystyrene beads) but different primary particle size (60 nm PS beads and 100 µm PS beads). The third catalyst carrier was silica gel. Silica gel is the most widely used catalyst carrier for heterogeneous olefin polymerizations. Its most important properties as a catalyst carrier are the wide surface area with functional groups for catalyst immobilization (silanol and ether group) and the easy fragmentation of the supported catalyst during olefin polymerization [9]. The fourth support type was a dendrimer support having a very well defined and nanosized structure. The dendrimer support is functionalized with polyethyleneoxide for immobilization of the metallocene catalyst in heterogeneous polymerization like the previously described nanosized PS support functionalized with PEO in chapter 3.2. and 3.3.

Figure 4-1 shows SEM images of the first three catalyst carriers and the structure of the

dendrimer. The primary particle size of these supports ranges from 60 nm to 100 μm. One expects that these different particle sizes will strongly influence the catalyst fragmentation and behavior in heterogeneous polymerization. Fragmentation means the distribution of the catalyst within the formed polymer during olefin polymerization down to the size of the primary particles of the support. The fragmentation process of the catalyst system and the catalyst distribution within the polyolefin products are the main factors that determine the quality of the materials obtained [10].

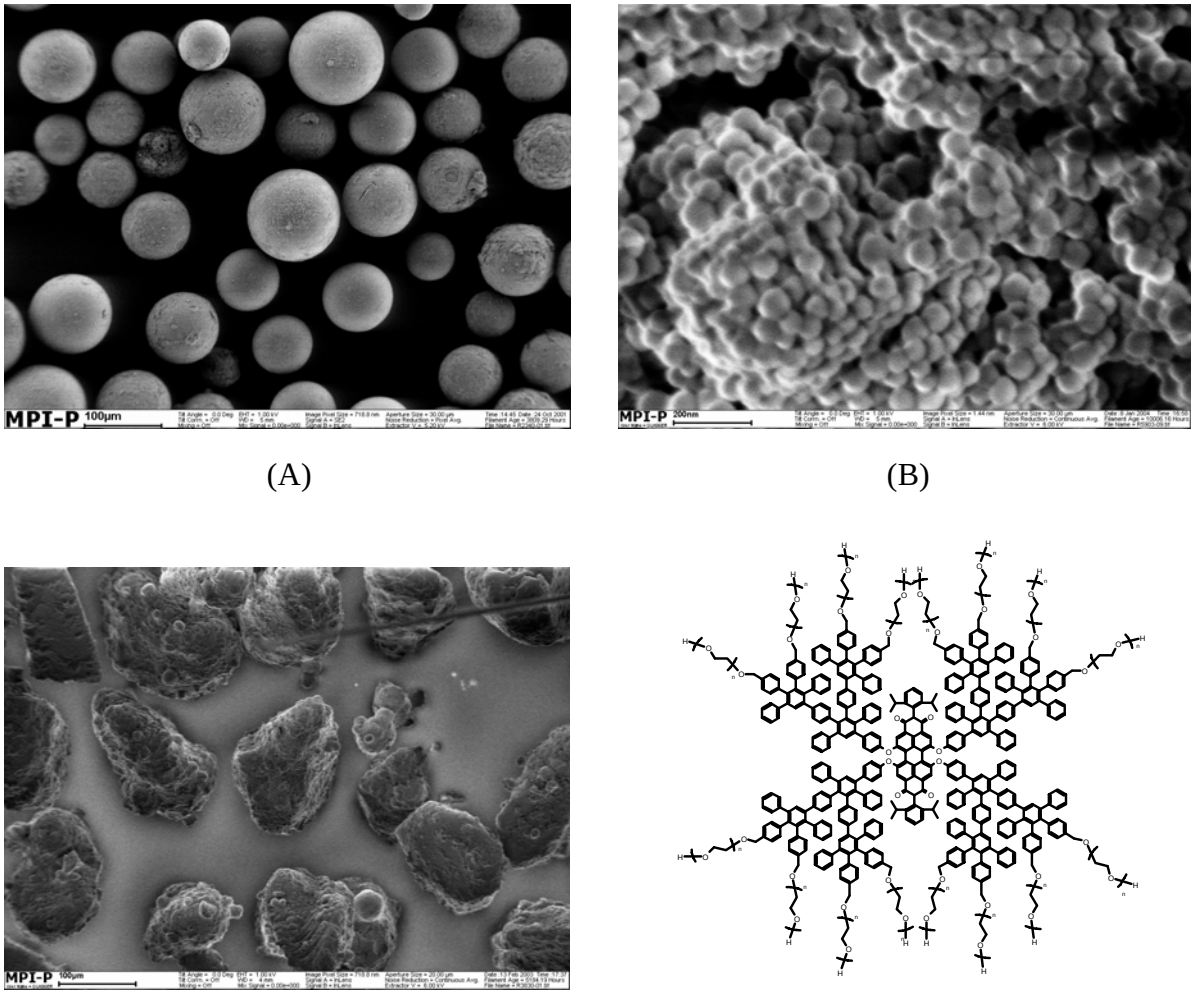

(A) (B)

(C) (D)

Figure 4-1. Four different supports: (A) microsized PS beads, (B) nanosized PS beads, (C) silica gel (Davison 952) and (D) dendrimer [$PDIG_2(PEO)_n$]

4.2. Microsized PS beads as support, the supported catalyst and the ethylene polymerization

Microsized polystyrene beads have been used for immobilizing metallocene catalysts in heterogeneous olefin polymerization [11]. These beads were prepared by suspension polymerization with styrene, divinylbenzene as crosslinker and styrene functionalized any anchor group [12]. The polystyrene beads have good morphology, well-defined spherical shape and an average particle size of 100 μm in diameter. The microsized polystyrene support used in heterogeneous olefin polymerization is crosslinked only by a very small amount of divinylbenzene (less than 1 mol % - 2 mol %) to enhance fragmentation of catalyst particles in heterogeneous olefin polymerization. These microsized PS beads are primary particles that are different from nanosized PS beads and silica supports. In the case of the catalyst supported on the nanosized PS beads and silica support, the primary particles have nearly 50 - 100 nm in diameter and the secondary particles (the supported catalysts) are about 100 micrometer in diameter formed by the aggregation of nanosized primary particles. By using these different supports having different primary particle sizes, one can study the influence of the primary particle size on the catalyst behavior and the distribution of the supported catalyst within the PE product.

4.2.1. Preparation of the catalyst supported on the microsized PS beads functionalized with hydroxyl groups

Microsized polystyrene (PS) beads functionalized with hydroxyl groups were used. These are commercial products with well-defined spherical structure (Figure 4-2). The microsized PS beads are crosslinked with 1 mol % divinylbenzene.

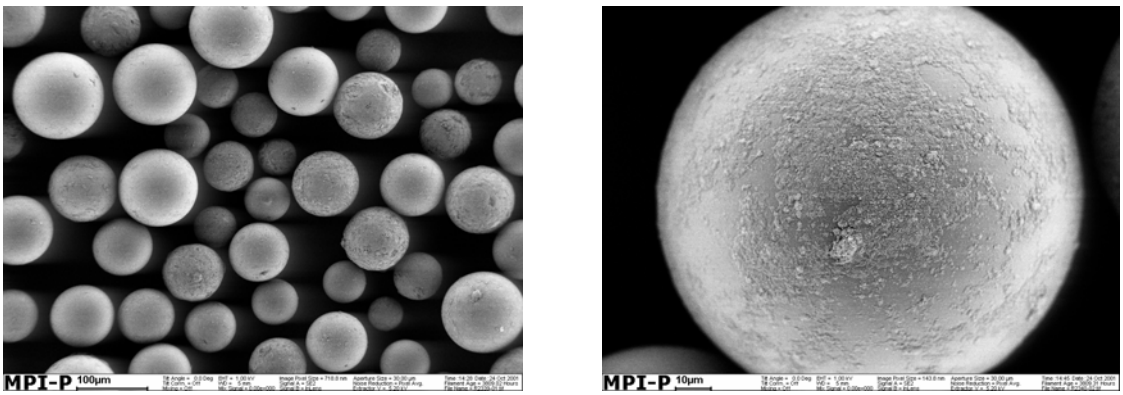

(A) (B)

Figure 4-2. SEM images of microsized polystyrene (PS) beads as support: scale bar – (A) 100 μm and (B) 10 μm

The hydroxyl groups on the PS beads are loaded with about 0.6 – 1.6 mmol OH / g and these hydroxyl groups react with MAO like in silica case to immobilize the metallocene (Scheme 4-1).

To immobilize the metallocene catalyst on the microsized PS beads functionalized with hydroxyl groups, the microsized PS beads were mixed with a solution of MAO in toluene to remove traces of water. The zirconocene and MAO were mixed in toluene and stirred until the catalyst was completely dissolved. A calculated amount of the preactivated zirconocene / MAO complex was added to the PS beads. After 1 hour of stirring the PS beads together with the zirconocene / MAO complex, the supported catalyst was washed with a toluene / hexane mixture several times and dried under vacuum.

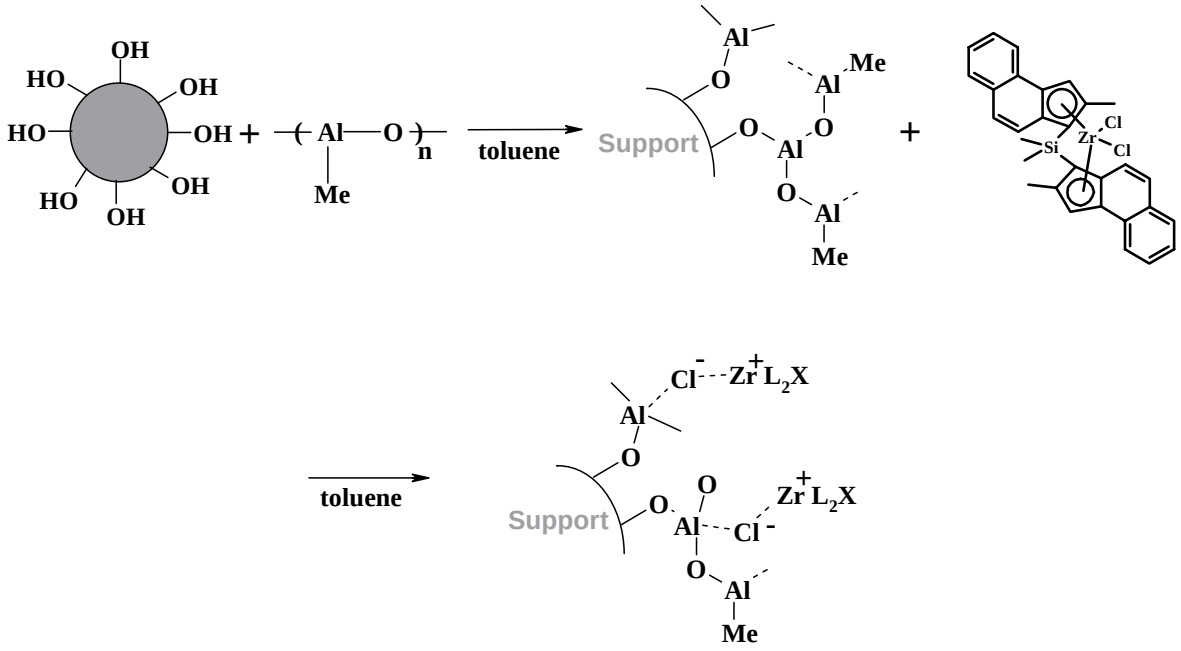

Scheme 4-1. Immobilization of methylalumoxane (MAO) as a cocatalyst and metallocene catalyst on the PS beads functionalized with hydroxyl groups

The supporting system of the metallocene catalyst on this PS beads functionalized with hydroxyl groups is different from the system of nanosized PS beads functionalized with PEO or PPO chains. In the case of PS beads functionalized with PEO or PPO, the immobilization occurs through a reversible non-covalent bonding of the metallocene / MAO complex with the nucleophilic ether groups. However, in the case of PS beads functionalized with hydroxyl groups, the immobilization proceeds a covalent bonding between the hydroxyl groups and MAO followed by the immobilization of metallocene catalyst.

4.2.2. Preparation of nanosized PS beads functionalized with hydroxyl groups as support and the supported catalyst

Nanosized PS beads functionalized with hydroxyl groups were used to compare the results of ethylene polymerization by the catalyst supported on the microsized PS beads. The nanosized PS beads were prepared by miniemulsion polymerization (Scheme 4-2). The used monomers were styrene, divinylbenzene as crosslinker and hydroxylmethyl styrene. The procedure to synthesize nanosized PS beads functionalized with hydroxyl groups was as follows in chapter 3.3.1.1. The resulting polystyrene beads as shown in Figure 4-3 exhibit a spherical shape and about 60 nm particle in diameter.

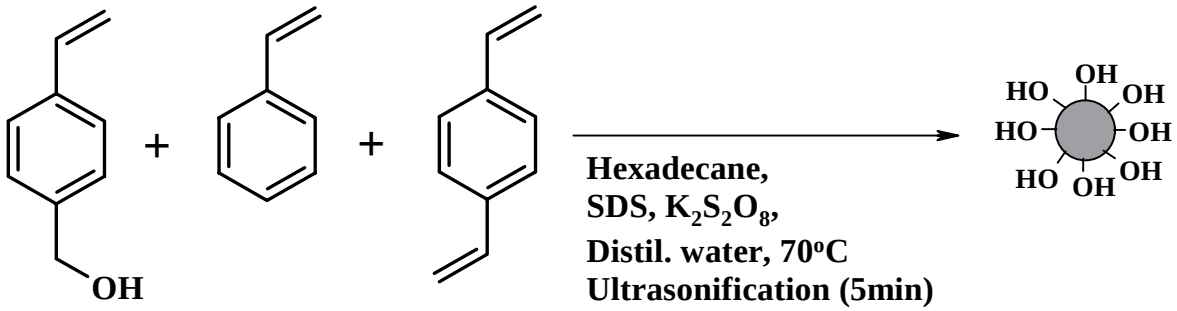

Scheme 4-2. Preparation of nanosized PS beads functionalized with hydroxyl group

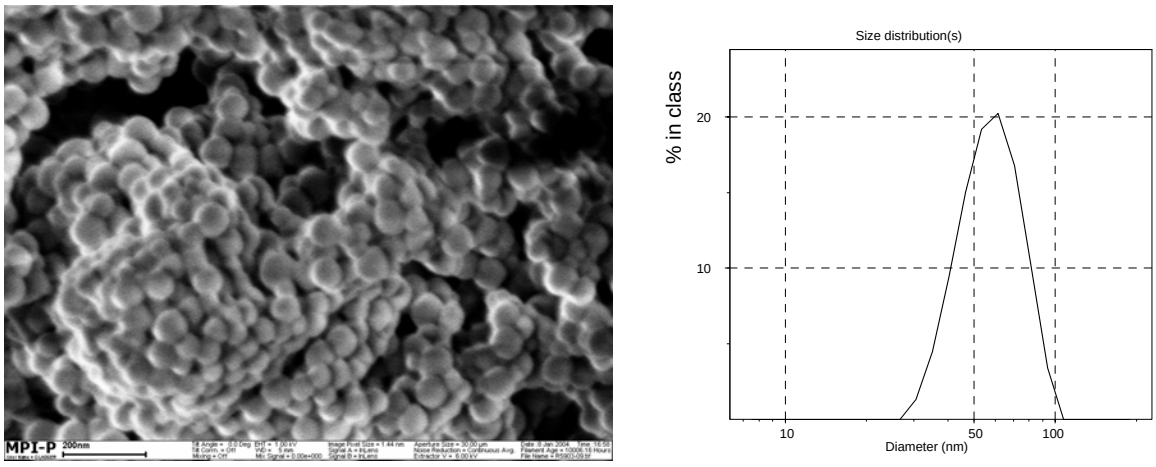

(A) (B)

Figure 4-3. (A) SEM image (scale bar – 200 nm) and (B) particle size distribution of nanosized PS beads

Table 4-1 presents the results of elemental analysis of the microsized PS beads functionalized with hydroxyl groups and nanosized PS beads functionalized with hydroxyl

groups (10 mol %). The hydroxyl group concentration of microsized PS beads is similar to that in the nanosized PS beads. As shown in chapters 3, the concentration of functional groups on the support surface is a very important factor in influencing the catalyst behavior in heterogeneous ethylene polymerization. In the silica-supported catalyst system, the concentration of hydroxyl groups on the silica surface must be controlled by calcination because the concentration of functional groups on the silica surface (hydroxyl group) influences the catalyst activity and the stereoregularity of the polypropylene obtained [13]. Furthermore, the hydroxyl group on the silica can deactivate the metallocene and affect the way of immobilization of the metallocene catalyst on the catalyst carrier [14, 15 and 16].

Table 4-1. Elemental analysis of the microsized PS beads functionalized with hydroxyl groups and nanosized PS beads functionalized with hydroxyl groups

Support	C	H	O	Amount of sample [a]
Microsized PS beads	86.4 %	7.5 %	5.9 %	2.101 mg
Nanosized PS beads	87.6 %	7.6 %	4.7 %	2.704 mg

[a] amount of sample for measurement of elemental analysis.

With the same procedure in the case of the microsized PS beads, the catalyst supported on the nanosized PS beads functionalized with hydroxyl groups was prepared. The shape and size of the supported catalyst are non-uniform like with the catalyst supported on nanosized PS beads functionalized with PEO or PPO group (Figure 4-4, A).

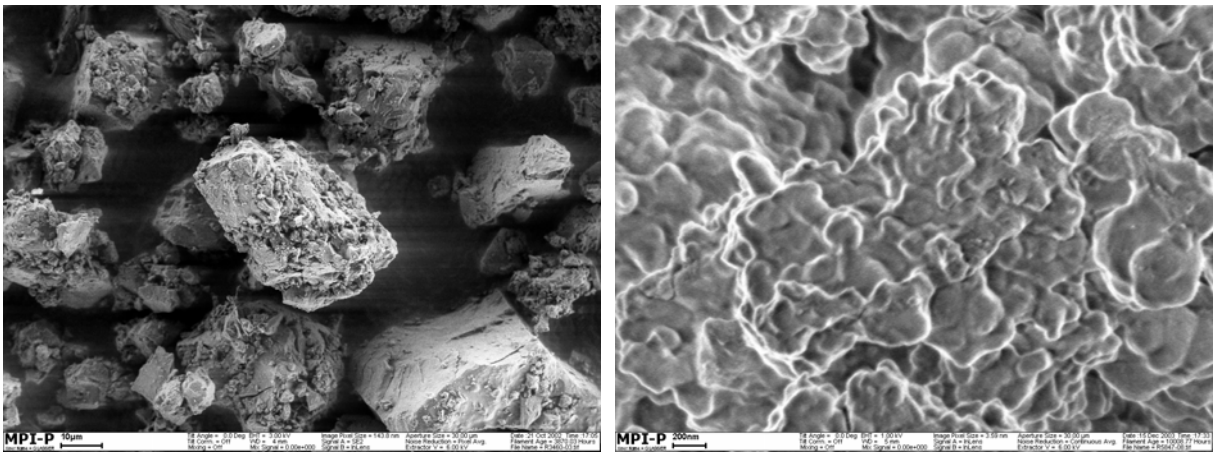

(A) (B)

Figure 4-4. SEM images of the catalyst supported on the nanosized PS beads: scale bar – (A) 10 μm and (B) 200 nm

Figure 4-4 (B) shows SEM pictures of the surface microstructure on the supported catalyst particle. Nanosized PS beads can well be seen on the surface of the supported catalyst. Small distorted spheres conglomerate due to the interaction of nanosized PS beads with metallocene / MAO. This surface microstructure is different from that of the catalyst supported on the microsized PS beads. In the microsized PS beads, one PS bead is itself a primary particle which differs from the supported catalyst particles formed by aggregation of primary (nanosized) PS beads.

4.2.3. Ethylene polymerization by the catalyst supported on the microsized and nanosized PS beads and the characterization of PE products

At 70 ^{o}C polymerization temperature and 40 bar ethylene monomer pressure, ethylene polymerization was carried out by using the catalyst supported on the microsized PS beads and compared to the results of the catalyst supported on the nanosized PS functionalized with hydroxyl groups. In this heterogeneous ethylene polymerization, 40 μmol / g metallocence activation and 350 MAO / Zr mol ratio were used. Table 4-2 shows the results of ethylene polymerizations.

Table 4-2. Ethylene polymerization [a] (catalyst: $Me_2Si(2MeBenzInd)_2ZrCl_2$ / MAO supported on microsized or nanosized PS beads)

Run	support	Zr/cat (μmol/g)	MAO/Zr	Activity [c]	Productivity [c]	BD [d]
PE-35	microsized PS	40	350	320	440	340
PE-36	microsized PS	40	350	310	425	340
PE-38	nanosized PS (10 mol% OH)	40	350	1000	1950	380
PE-39	nanosized PS (10 mol% OH)	40	350	1010	2075	380

[a] Reaction condition: 1 L autoclave, isobutane 400 ml, ethylene pressure 40 bar, 70 °C, 1 hr, amount of catalyst: 20 - 24mg. [b] BD: bulk density(g/l). [c] kg PE / mol Zr hr bar. [d] g PE / g cat hr.

The catalyst supported on the microsized PS beads exhibits an activity of about 300 (kg PE

/ mol Zr hr bar) and the bulk density of PE products is 340 (g / l) in Run PE 35 and PE-36. On the other hand, the catalyst supported on the nanosized PS beads has an activity of about 1000 (kg PE / mol Zr hr bar) and a bulk density of PE of 380 (g / l) in Run PE-38 and PE-39. At the same polymerization condition, the activity of the catalyst supported on the nanosized PS is higher than the activity of the supported catalyst on the microsized PS beads. This result is not unexpected that the primary particle size of the support influences the catalyst behavior in ethylene polymerization. The catalyst activities of the catalyst supported on the nanosized PS beads functionalized with hydroxyl groups have lower than that in the case of the nanosized PS functionalized with PPO. In the case of 10 mol % PPO functionalized PS beads, the catalyst activity is 1250 (kg PE / mol Zr hr bar) [Run PE-23]. On the other hand, the catalyst activity is about 1000 (kg PE / mol Zr hr bar) in the case of 10 mol % hydroxyl group functionalized PS beads in Run PE-38. At the same amount of functional group (10 mol %) on the support, the activities of the catalyst supported on the PS beads functionalized with hydroxyl groups and the PS beads functionalized with PPO are different, which means that the different supporting systems have an influence on the catalyst behavior in heterogeneous polymerization.

The melting point of the PE produced by the catalyst supported on the PS beads is about 134 ^{o}C and the molecular weight of the PE is about 1,100,000 – 1,200,000 (Table 4-3). These melting point and molecular weight of the PE are similar to those of the polyethylene produced by the catalyst supported on the PS functionalized with PPO or PEO groups.

Table 4-3. Characteristics of polyethylene (PE) [a]: melting point, molecular number, molecular weight and polydispersity index

Run	Tm [b] (^{o}C)	Mn [c] (g / mol)	Mw [c] (g / mol)	PDI
PE-35	134.6	472,000	1,158,000	2.45
PE-36	134.5	507,000	1,197,000	2.36
PE-38	134.4	453,000	1,120,000	2.47
PE-39	134.6	495,000	1,106,000	2.23

[a] Reaction condition: in a 1 L autoclave, isobutane 400 ml, ethylene pressure 40 bar, 70 °C, 1 hr, catalyst activation: 40 Zr / cat (μmol / g), 350 MAO / Zr molar ratio. amount of catalyst 20 - 24 mg. [b] by differential scanning calorimetry (DSC). [c] by gel permeation chromatography (GPC).

Figure 4-6 shows SEM images of PE produced by the catalyst supported on the microsized PS beads (A and B) and by the catalyst supported on the nanosized PS beads (C and D). In image (A) of Figure 4-6, the particle shape of PE product (PE-36) replicates that of the microsized PS beads. The surface morphology of the polyethylene product generated by the catalyst supported on the microsized PS beads is as smooth as that of the supported catalyst shown in Figure 4-3 (B). On the other hand, the particle size distribution of PE produced by the catalyst supported on the nanosized PS shown in image (C) of Figure 4-5 is wide. The surface of the PE particle contains many aggregated particles (~ 20 μm) formed from the nanosized PS beads (primary particles ~ 80 nm) shown in Figure 4-4 (B). The surface morphology of the supported catalyst has a direct influence on the surface morphology of polyethylene product.

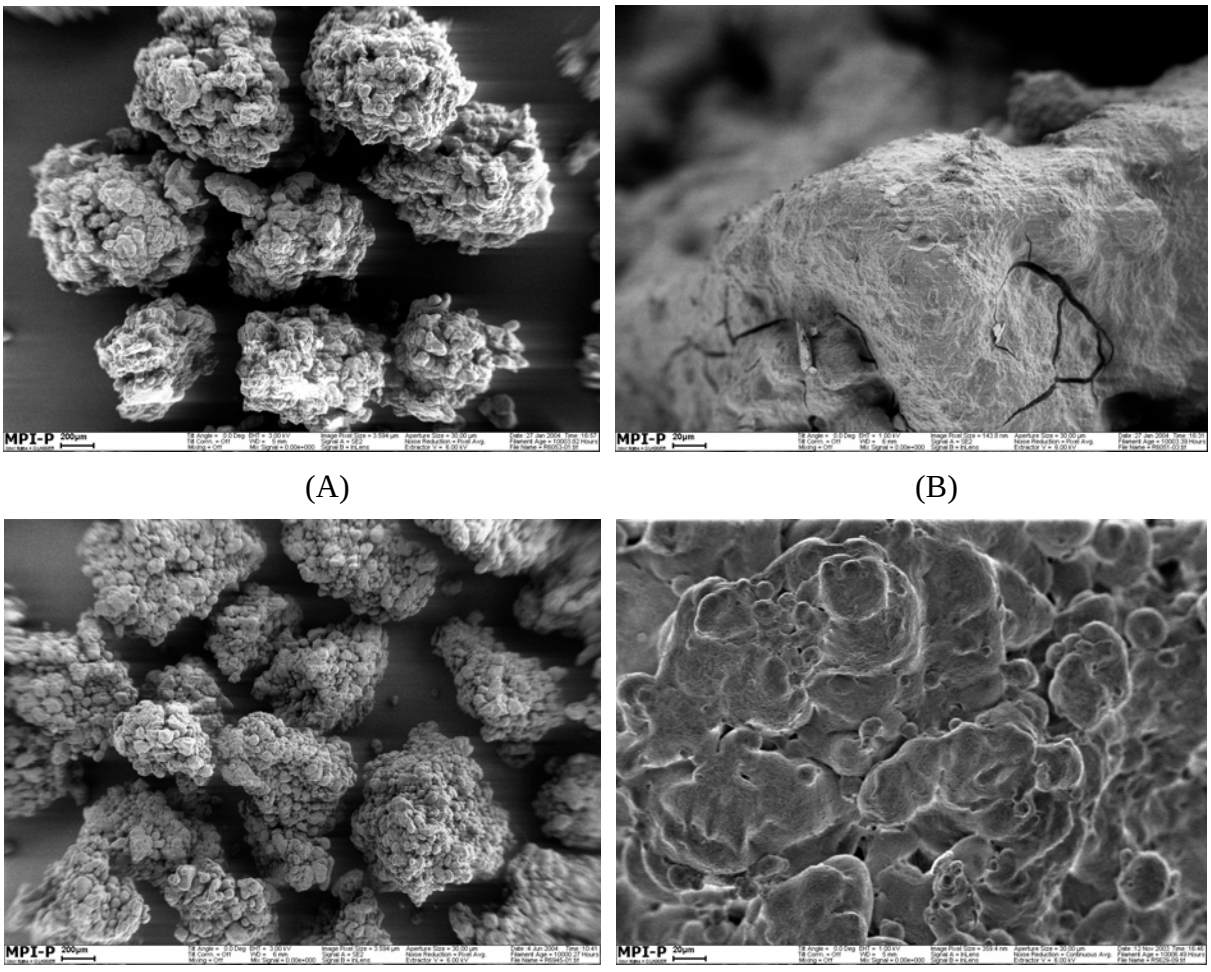

(A) (B)

(C) (D)

Figure 4-5. SEM images of PE-36 produced by the catalyst supported on the microsized PS beads (A and B) and PE-39 produced by the catalyst supported on the nanosized PS beads (C and D): scale bar – (A) 200 μm, (B) 20 μm, (C) 200 μm and (D) 20 μm

4.3. Silica as support, the supported catalyst and the ethylene polymerization

4.3.1 Preparation of silica supported catalyst

As silica support, Davison 952 was used for this experiment. Davison 952 is a commercial silica gel which has been used for heterogeneous polymerizations using different procedures for preparing the supported catalyst [17, 18 and 19]. Figure 4-6 shows the SEM images of Davison 952 silica gel at different magnifications. The particle size of the silica gel is about 100 μm with a quasi-spherical shape. The surface of the silica looks smooth on the macroscale but consists of rounded nodular clusters that have different sizes.

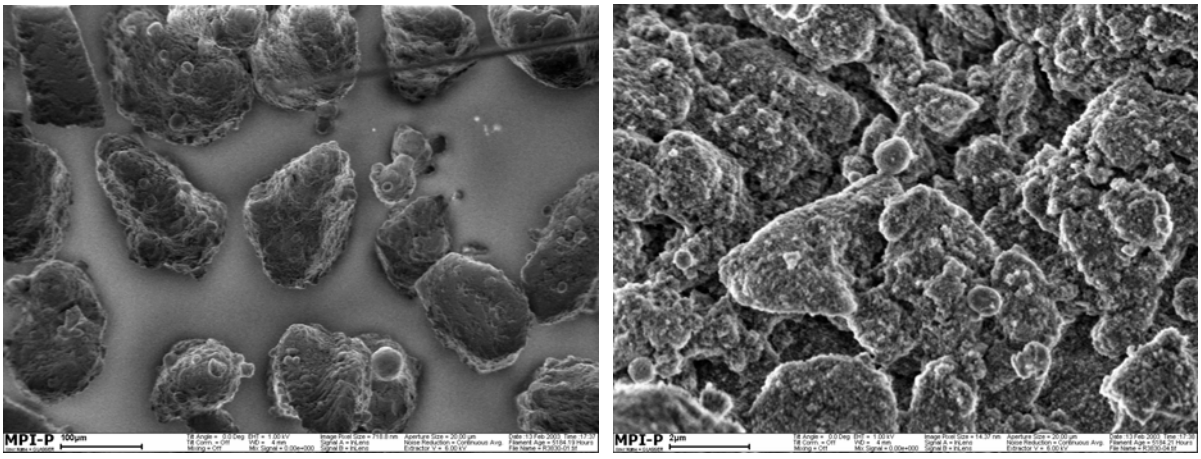

(A) (B)

Figure 4-6. SEM images of silica gel (Davison 952) as catalyst carrier in different magnification: scale bar – (A) 100 μm and (B) 2 μm

This silica is a white powder consisting of synthetic and amorphous silica with the following properties; pore volume: 1.5 – 1.9 ml / g, surface area: 280 – 355 m^2 / g, average pore diameter: 20 nm, distribution of small and large pores, cylindrical pore shape, about 100 μm particle size. The primary building blocks of the silica support are 10 – 50 nm diameter spheroids formed during polymerization in solution of silicic acid and subsequent aggregation of colloidal silica [20]. They are loosely cemented into larger aggregates that, in turn, are packed into even larger clusters. There are pores between the primary particles as well as between the clusters. Specific structural properties of the support such as particle size, surface area, pore size and pore-size distribution depend on the preparation procedures [11].

Before using silica as support in the heterogeneous polymerization, the silica gel was

calcinated at 200 ^{o}C under flowing argon gas to control the amount of silanol groups (Scheme 4-3). After 3 hours of calcination, the silica was cooled down to room temperature and MAO solution in toluene was added to the silica. After stirring for 12 hours at room temperature, a metallocene / MAO solution in toluene was reacted with the silica / MAO suspension for 1 hour. The suspended silica in metallocene and MAO solution was then washed several times with a dry hexane / toluene mixture. The remaining silica-supported catalyst was dried under vacuum for 24 hours. This method of preparing the supported catalyst is called indirect impregnation [21].

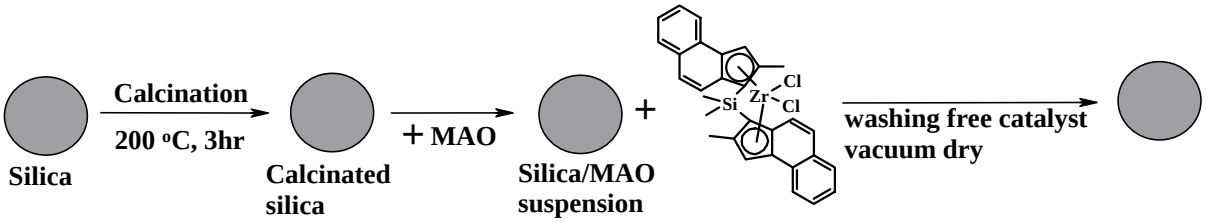

Scheme 4-3. Preparation of the calcinated silica and the silica-supported catalyst

As mentioned for the microsized PS beads as supporting system, MAO is bound chemically to the silica surface by its reaction with the hydroxyl groups (Scheme 4-4). As a second stage, the metallocene reacts with MAO fixed on silica to form the supported metallocene and then the supported catalyst is activated by further MAO co-catalysts [22].

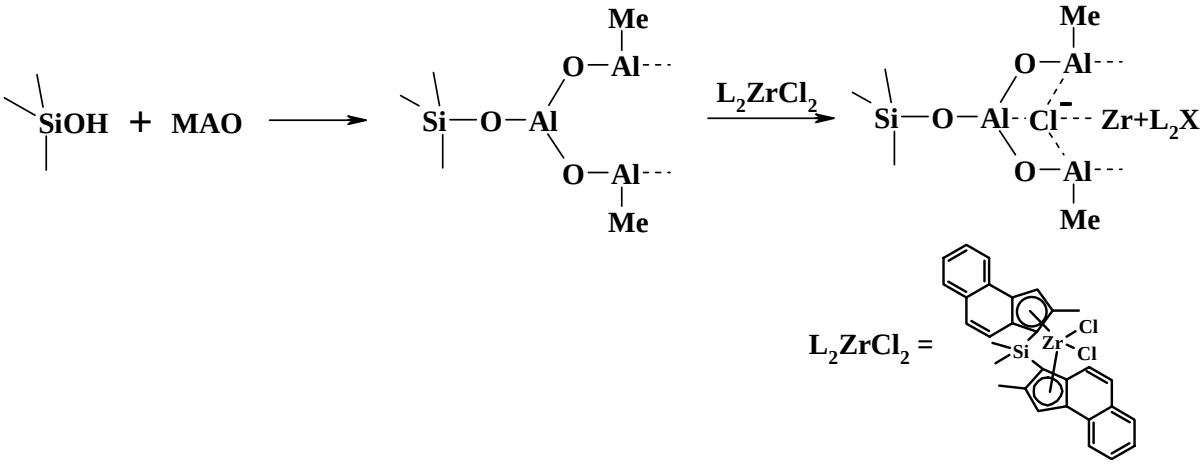

Scheme 4-4. The formation mechanism of zirconocenium species for MAO-mediated catalyst

For preparing the supported catalyst, the silica-supported catalyst required a different procedure in comparison with the support catalyst on the nanosized PS beads (Scheme 4-5).

In the case of the silica-supported catalyst (Scheme 4-5, A), at first silicic acid is polymerized to form the nanosized silica beads (primary particles) and then these aggregates form particles of about 50 - 100 μm size. On the other hand, the nanosized PS beads (primary particles of about 50 - 100 nm size) functionalized with anchor group for immobilizing metallocene are first prepared using styrene monomers and then these beads aggregate with MAO / metallocene by reversible non-covalent bonding to form particles of about 50-100 μm size (Scheme 4-5, B).

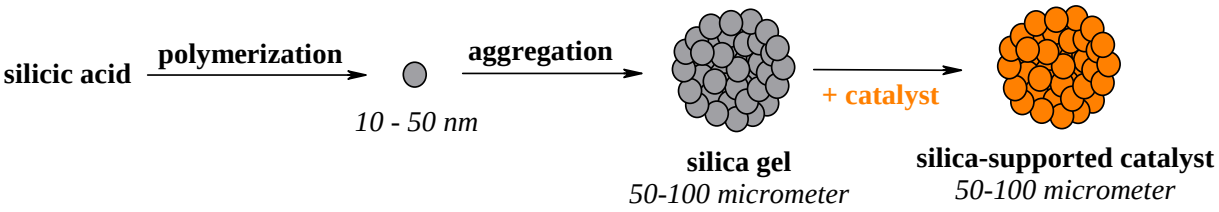

(A) Silica and silica-supported catalyst

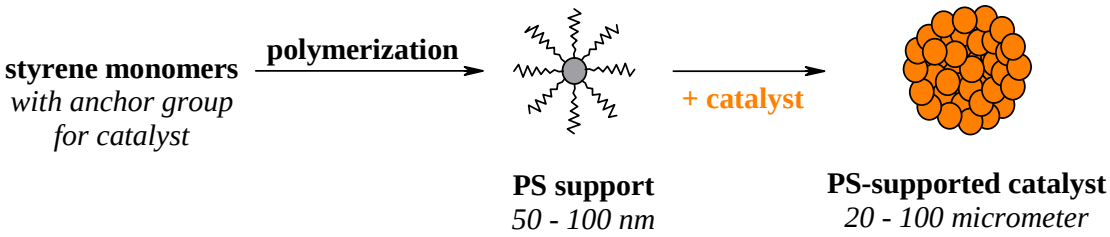

(B) Nanosized polystyrene (PS) beads and PS-supported catalyst

Scheme 4-5. The different procedures for preparation of silica gel (A) and nanosized PS beads (B) as a support and the supported catalyst

4.3.2. Ethylene polymerization with the silica supported catalyst and the characterization of PE products

Under the conditions of 70 ^{o}C polymerization temperature and 40 bar ethylene pressure in 400 ml isobutane as solvent, the silica supported catalyst was used for heterogeneous ethylene polymerization (Table 4-4). In this heterogeneous ethylene polymerization, 40 μmol / g metallocence activation and 350 MAO / Zr mol ratio was used. In the Run PE-40 and PE-41, a catalyst supported on the non-calcinated silica was used. The catalyst supported on the non-calcinated silica exhibits an activity of 600 (kg PE / mol Zr hr bar) which is lower than the activity for the supported catalyst on the calcinated silica gel of about 700 (kg PE / mol Zr hr bar) in Run PE-42 and PE-43. The bulk densities of the PE produced by both silica-

supported catalysts have similar values of about 360 (g / l).

Table 4-4. Ethylene polymerization[a] (catalyst: $Me_2Si(2MeBenzInd)_2ZrCl_2$ /MAO/ silica)

Run	Support	Zr/cat (μmol/g)	MAO/Zr	Activity [b]	Productivity [c]	BD [d]
PE-40	Noncalcinated silica	40	350	610	840	360
PE-41	Noncalcinated silica	40	350	620	850	350
PE-42 [e]	Calcinated silica	40	350	735	1000	360
PE-43	Calcinated silica	40	350	705	960	370

[a] Reaction condition: 1 L autoclave, isobutene 400 ml, ethylene pressure 40 bar, 70 °C, 1 hr, amount of catalyst 22 - 24 mg. [b] kg PE / mol Zr hr bar. [c] g PE / g cat hr. [d] BD: bulk density (g / l). [e] polymerized by the supported catalyst on the calcinated silica under the 200 °C and 3 hr.

The activities of the silica supported catalyst are higher than those obtained by the catalyst supported on the microsized PS beads functionalized with hydroxyl group. On the other hand, the activities of the silica supported catalyst are lower than those for the supported catalyst on the nanosized PS beads. These different results could be related to the catalyst fragmentation and the distribution of the catalyst within the PE products. However, just based on catalyst activity and bulk density of the PE product, it is not possible to confirm a different fragmentation behavior of the different supported catalysts.

Polyethylene (PE-42) obtained by the silica supported catalyst shows a spherical shape in Figure 4-7 (A). This replication of the silica support by the product is a representative example of polyolefin products obtained from a silica-supported catalyst [2]. Further, the particle size distribution of PE produced by this silica supported catalyst is also narrower than that of PE produced by the catalyst supported on nanosized PS beads. The SEM pictures shown in (B) of Figure 4-7 clearly indicate that the original surface microstructure on the silica supported catalyst is maintained in the resulting polyethylene product with the spherical shape of small particle having a diameter of about 20 μm. The result is similar with

the surface morphology of the catalyst supported on the nanosized PS beads and the polyethylene product in that the surface morphology of polyethylene product is replicated from the supported catalyst constituting the primary particle.

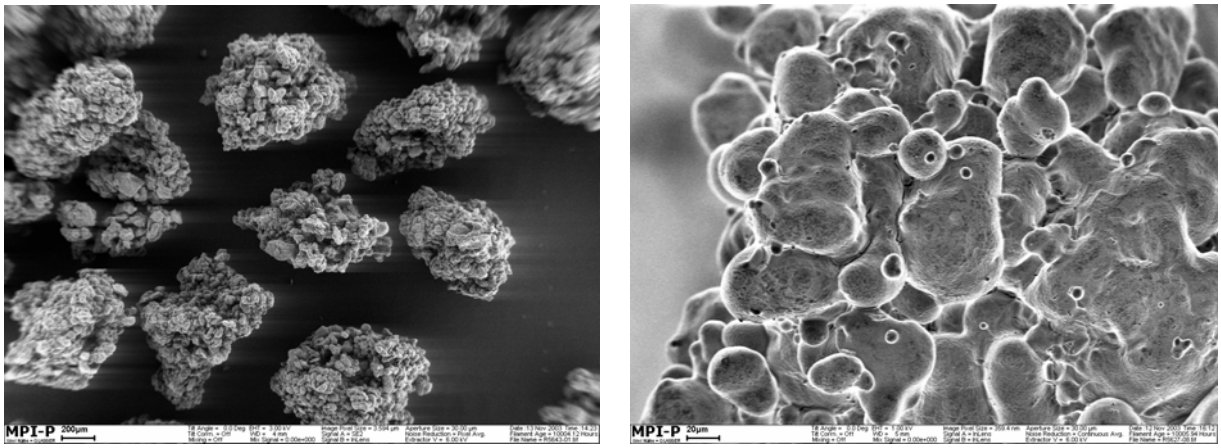

(A) (B)

Figure 4-7. SEM images of polyethylene (PE-42) produced by the silica-supported catalyst (A and B): scale bar – (A) 200 μm and (B) 20 μm

The characteristics of the polyethylene (PE) products are presented in Table 4-5. The molecular weight is about 1.110,000 – 1.200,000 and the melting point is about 134 ^{o}C. The molecular weight, polydispersity and melting point of PE obtained are similar to the results of polyethylene produced by the catalyst supported on the microsized or nanosized PS beads functionalized with hydroxyl groups.

Table 4-5. Characteristics of polyethylene produced by the silica supported catalyst [a]: melting point and molecular weight of polyethylene

Run	Tm [b] (^{o}C)	Mn [c] (g / mol)	Mw [c] (g / mol)	PDI
PE-40	134.1	457,000	1,213,000	2.65
PE-41	134.2	507,000	1,286,000	2.53
PE-42	133.7	429,000	1,117,000	2.60
PE-43	133.9	516,000	1,239,000	2.39

[a] Reaction condition: in a 1 L autoclave, isobutane 400 ml, ethylene pressure 40 bar, 70 °C, 1 hr, catalyst activation: 40 Zr / cat (μmol/g), 350 MAO / Zr molar ratio, amount of catalyst 24 mg. [b] by differential scanning calorimetry (DSC). [c] by gel permeation chromatography (GPC).

4.4. A dendritic perylenediimide core functionalized with polyethyleneoxide groups [$PDIG_2(PEO)_n$] as support, the supported catalyst and ethylene polymerization

4.4.1 Preparation of dendrimer- supported catalyst

In this chapter, a dendritic perylenediimide core functionalized with polyethyleneoxide groups [$PDIG_2(PEO)_n$] is introduced as catalyst carrier. Dendrimer as support is expected to be fragmented homogeneously within polyolefin products due to the well defined nanostructure. The dendritic perylenediimide core functionalized with polyethyleneoxide groups [$PDIG_2(PEO)_n$] has been prepared by two Ph. D students - Roland Bauer and Vladimir Atanasov in our group at the Max-Planck Institute for Polymer Research.

The starting dendrimer $PDIG_2(CH_2OH)_n$ was converted to a macromolecular initiator $PDIG_2(CH_2O^-)_n$ by deprotonation with naphthalene potassium using procedure for deprotonation of hydroxy-functionalized dendrimers [23] and the dendritic perylenediimide core functionalized with polyethyleneoxide groups [$PDIG_2\,(PEO)_n$] was prepared by using naphthalene potassium initiator with ethyleneoxide monomer in an anionic polymerization (Scheme 4-6).

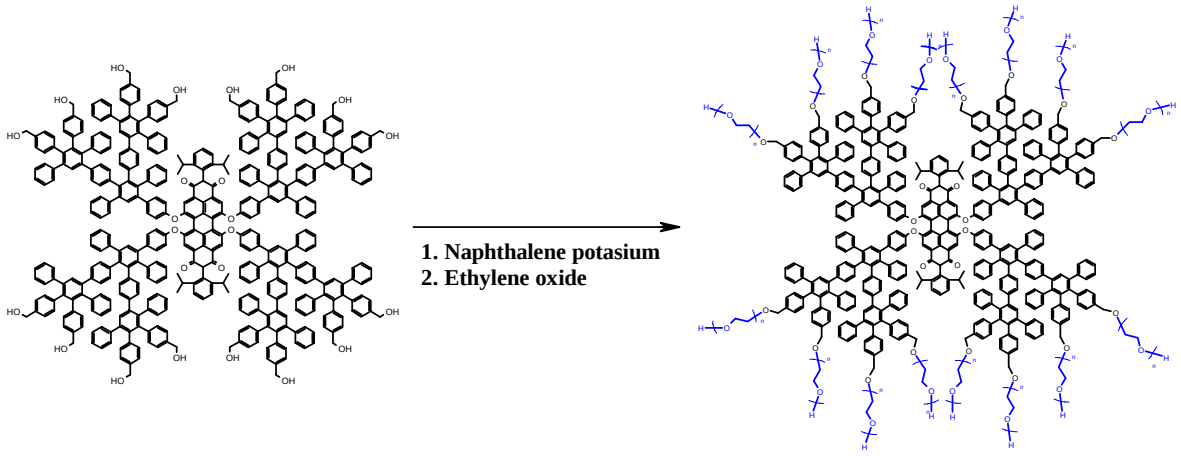

Scheme 4-6. Preparation of polyethyleneoxide functionalized dendrimer with dye.

Depending on the ratio of initiator and monomer, the polyethyleneoxide (PEO) chain length was controlled from 133 repeat units to 730 repeat units (Table 4-6). The dendrimers had about 10 to 30 nm size dispersed in water depending on the repeat units of PEO which is

smaller than the nanosized polystyrene (PS) beads prepared in miniemulsion polymerization.

Table 4-6. Polyethyleneoxide repeat units and particle size of dendritic perylenediimide core functionalized with polyethyleneoxide groups [$PDIG_2(PEO)_n$]

Support	PEO (repeat units of ethyleneoxide) [a]	Particle size (nm) [b]
DEN 1	750	28.3
DEN 2	166	16.8
DEN 3	133	10.9

[a] measured by ^{1}H-NMR. [b] measured by dynamic laser scattering in water.

For supporting the metallocene / MAO on the polyethyleneoxide (PEO) functionalized dendrimer (Scheme 4-7), the dry dendrimer was mixed with a solution of MAO in toluene to remove traces of water. After stirring for 12 hr, a solution of metallocene and MAO as cocatalyst was added to the MAO / support suspension. After stirring the mixture for 1 hour, the supported catalyst was washed with dry toluene / hexane mixture and the extra metallocene / MAO solution was removed from the supported catalyst via a cannula. In all experiments performed, $Me_2Si(2MeBenzInd)_2\ ZrCl_2$ was used as metallocene.

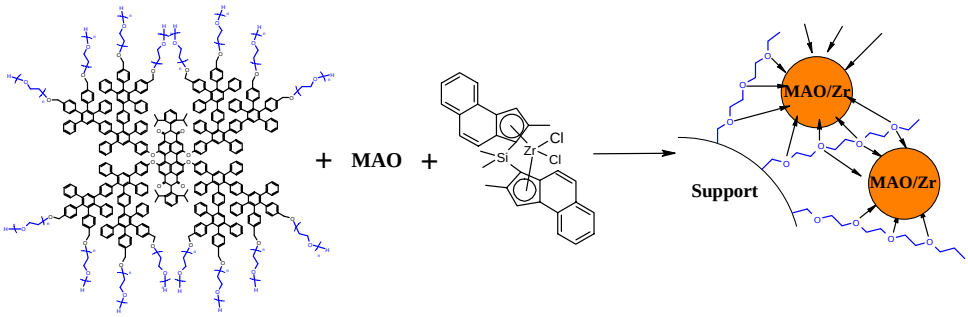

Scheme 4-7. Preparation of the supported catalyst on a dendritic perylenediimide core functionalized with polyethyleneoxide groups [$PDIG_2(PEO)_n$]

The dendrimer supported catalysts in Figure 4-8 show a different surface morphology in comparison with that in the catalyst supported on the nanosized PS beads (Figure 4-4). The catalyst supported on the nanosized PS beads has a rough surface structure due to the conglomerates of nanosized PS beads (Figure 4-4). On the other hand, even if the dendrimer supported catalyst constitutes the nanosized primary particles, the surface is much smoother. This result of the surface morphology may be due to the very small core size of less than 10

nm of the dendrimer. This small particle is different from the size of the nanosized PS beads having a crosslinked polystyrene core of about 60 nm in diameter.

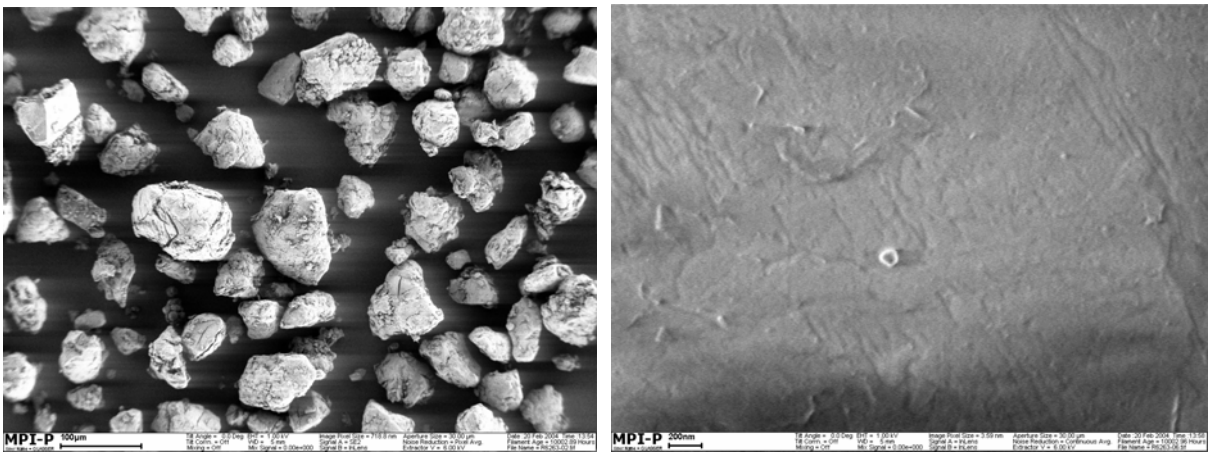

(A) (B)

Figure 4-8. SEM images of the catalyst supported on the dendrimer (DEN 2): scale bar – (A) 100 µm and (B) 200 nm

4.4.2. Ethylene polymerization by the dendrimer supported catalyst and the characterization of PE products

At 70 ^{o}C polymerization temperature and 40 bar ethylene monomer pressure, ethylene polymerization was carried out in 400 ml isobutane as solvent by using the catalyst supported on the dendrimer. In this heterogeneous ethylene polymerization, 40 µmol / g metallocence activation and 350 MAO / Zr mol ratio was used. Table 4-7 presents the results of the ethylene polymerization performed with dendrimer supported $Me_2Si(2MeBenzInd)_2ZrCl_2$ activated with methylalumoxane (MAO) as co-catalyst. In the case of the supported catalyst on dendrimer DEN 1 (730 repeat units of PEO), the catalyst has an activity of 1070 (kg PE / mol Zr hr bar) in Run PE-44. On the other hand, in the case of the supported catalyst on the dendrimer DEN 3 (133 repeat units of PEO), the catalyst exhibits an activity of 940 (kg PE / mol Zr hr bar) in Run PE-48. These catalyst activities are higher than the activity of the catalyst supported on the microsized PS beads in Run PE-35 to PE-36. On the other hand, the dendrimer supported catalyst activities are slightly higher than the catalyst activity in the case of 10 mol% hydroxyl group functionalized PS beads (Run PE-38) which is dependent on the concentration of PEO on the dendrimer. This result shows that the supported catalyst constituted of the nanosized primary particles exhibits a higher activity than that having one

big primary particle like the microsized PS beads. As for increasing the length of PEO chains on the dendrimer, the activity of the dendrimer-supported catalyst in ethylene polymerization decreases slightly. The bulk densities of polyethylene (PE) produced by the catalyst supported on the dendrimer with different chain lengths are about 260 (g / l) which is similar to that in all PE products. Even after 90 min polymerization in Run PE-45, Run PE-47 and Run PE-49, the bulk density is improved but it is still not high (~ 300 g / l). The polyethylene particles obtained are not uniform which is similar to the results from the nanosized PS support and the particle size distribution is wide as seen for the nanosized PS support case in heterogeneous polymerization (Figure 4-9, A and B). The surface morphology of the polyethylene product is different from the results of the nanosized PS supported catalyst and the silica supported catalyst (Figure 4-9, C). The PE produced by the dendrimer-supported catalysts have a smooth surface structure like the surface structure of the dendrimer-supported catalyst due to the very small core size less than 10 nm of the dendrimer.

Table 4-7. Ethylene polymerization[a] (catalyst: $Me_2Si(2Me\ BenzInd)_2ZrCl_2$ / MAO supported on the dendritic perylenediimide core functionalized with polyethyleneoxide groups)

Run	Support	Zr/cat (μmol/g)	MAO/Zr	Time (min)	Activity [b]	Productivity [c]	BD [d]
PE-44	DEN 1	40	350	60	1073	1460	260
PE-45	DEN 1	40	350	90	917	1247	310
PE-46	DEN 2	40	350	60	980	1340	260
PE-47	DEN 2	40	350	90	650	890	290
PE-48	DEN 3	40	350	60	940	1278	270
PE-49	DEN 3	40	350	90	620	850	300

[a] Reaction condition: 1 L autoclave, isobutane 400 ml, ethylene pressure 40 bar, 70 °C, 60 – 90 min, amount of catalyst: 22 – 24 mg. [b] kg PE / mol Zr hr bar. [c] g PE / g cat hr. [d] BD: bulk density (g / l).

The melting point is about 134 ^oC and the molecular weight and molecular weight distribution are about 1,300,000 and 2.5 respectively (Table 4-8). In spite of changing the catalyst carrier to the dendrimer, the polyethylene properties are similar to the previously reported ones in chapter 3. The different supports have little influence on the characteristics of the PE product.

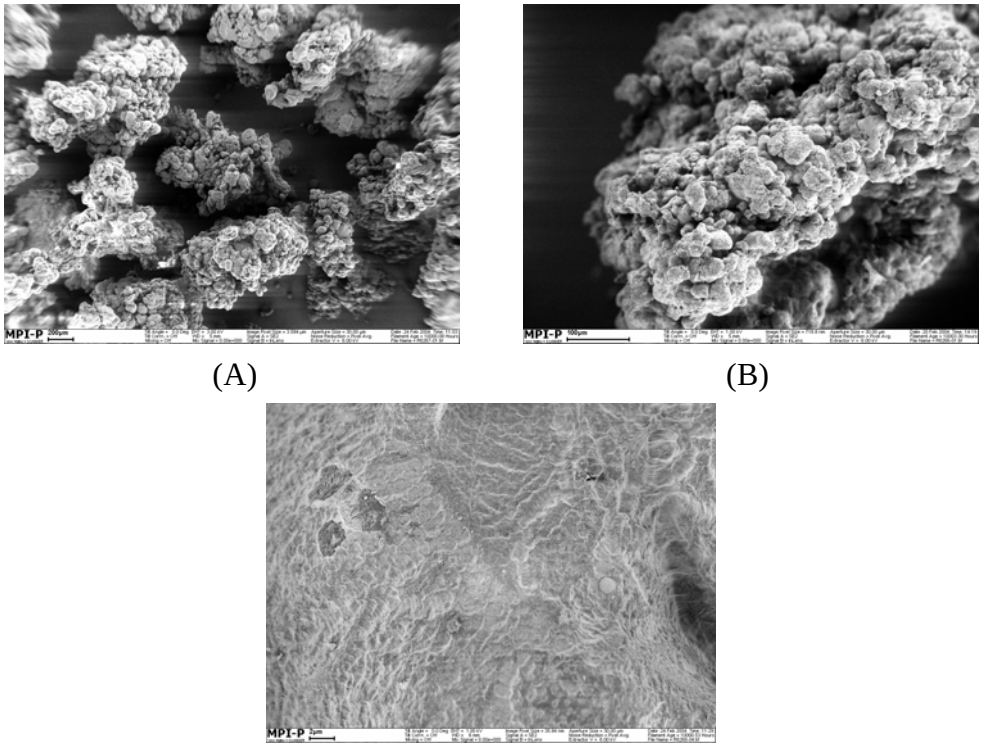

(A) (B)

(C)

Figure 4-9. SEM images of polyethylene (PE-46) produced by the dendrimer-supported catalyst: scale bar – (A) 200 μm, (B) 100 μm and (C) 2 μm

Table 4-8. PE characterization produced by the dendrimer-supported catalyst [a]: melting point, molecular weight and molecular weight distribution of PE

Run	Tm [b] (^{o}C)	Mn [c] (g / mol)	Mw [c] (g / mol)	PDI
PE-44	134.7	495,000	1,333,000	2.68
PE-45	134.2	482,000	1,273,000	2.63
PE-46	134.4	518,000	1,423,000	2.74
PE-47	134.9	469,000	1,244,000	2.64
PE-48	134.3	476,000	1,375,000	2.84
PE-49	134.4	511,000	1,270,000	2.48

[a] Reaction condition: in a 1 L autoclave, isobutane 400 ml, ethylene pressure 40 bar, 70 °C, 1 hr, catalyst activation: 40 Zr / cat (μmol / g), 350 MAO / Zr molar ratio, amount of catalyst: 22-24 mg. [b] by differential scanning calorimetry (DSC). [c] by gel permeation chromatography (GPC).

4.5. Summary

In this chapter, the influence of the different supports on the catalyst behavior in ethylene polymerization and the resulting polyethylene properties were studied. Four kinds of supports were used for these investigations: microsized PS beads functionalized with hydroxyl groups, nanosized PS beads functionalized with hydroxyl groups, silica gel and dendritic perylenediimide core functionalized with polyethyleneoxide groups [$PDIG_2(PEO)_n$]. The size of the primary particles of these supports varied from 10 nm to 100 μm.

The different sizes of these supports influenced the catalyst behavior in heterogeneous ethylene polymerization and the surface microstructure of the polyethylene products. The activities of the dendrimer-supported catalyst were dependant on the amount of polyethyleneoxide groups on the shell of the dendrimer which is higher than for the catalyst supported on the nanosized PS beads, microsized PS beads or silica. The catalyst activity of the catalyst supported on the nanosized PS beads functionalized with hydroxyl groups was higher than that of the catalyst supported on the microsized PS beads under the same polymerization conditions. This result confirmed that the primary particle size of the support influences the catalyst behavior such as the catalyst activity and fragmentation in ethylene polymerization. Even when nanosized primary particles constituted the supported catalyst such as the nanosized PS beads, silica and dendrimer, the catalyst activity was different depending on the property of each support. The activities of the silica-supported catalyst were lower than those on the nanosized PS beads and on the dendrimer because the catalyst supported on the nanosized PS beads and dendrimer is more fragile than the silica supported catalyst.

The different morphology of the supported catalysts strongly influenced the surface microstructure of the resulting polyethylene product. The surface microstructure of the polyethylene product generated by the catalyst supported on the microsized PS beads was smoother than that of the catalyst supported on the nanosized PS beads and silica due to the size of the primary particles. On the other hand, even if the dendrimer supported catalyst is constituted of nanosized primary particles, the surface is much smoother. This result of the surface morphology may be due to the very small core size (less than 10 nm) of the dendrimer in comparison with the catalyst supported on nanosized PS beads and silica.

1. F. Ciardelli, A. Altomare and M. Michelotti, *Catal. Today*, **1998**, 41, 149.

2. J.C.W. Chien and D. He. *J. Polym. Sci. Part A: Polym. Chem*., **1991**, 29, 1603.

3. K. Soga and M. Kaminaka, *Makromol. Chem*., **1993**, 194, 1745.

4. R. Quijada, R. Rojas, L. Alzamora, and F.M. Rabagliati, *Catal. Lett*., **1997**, 46, 107.

5. F.C. Franceschini, T.T.daR. Tavares, P.P. Greco, D. Bianchini, F.C. Stedile, G.B. Galland, J.H.Z. dos Santos and J.B.P. Soares, *J. Mol. Catal*., **2003**, 202, 127.

6. M. de Fátima, V. Marques and S.C. Moreira, *J. Mol. Catal.*, **2003**, 192, 93.

7. H. Nishida, T. Uozumi, T. Arai and K. Soga, *Macromol. Rapid Commun*., **1995**, 16, 821.

8. K. Soga and M. Kaminaka, *Makromol. Chem. Rapid Commun*., **1992**, 13, 221.

9. G. Fink, B. Steinmetz, J. Zechlin, C. Przybyla, and B. Tesche, *Chem. Rev*., **2000**, 100, 1377.

10. G. Fink, B. Tesche, F. Korber, S. Knoke, *Macromol. Symp*., 2001, 173, 77.

11. A. G. M. Barrett and Y. R. de Miguel, *Chem. Commun*., **1998**, 2079.

12. T. Kitagawa, T. Uozumi and K. Soga and T. Takata, *Polymer*, **1997**, 38, 615.

13. J.L. Atwood, W.E. Hunter, D.C. Hrncir, E. Samuel, H. Alt and M. Rausch, *Inorg. Chem*., **1975**, 14, 1757.

14. F. Wochner, L. Zsolnai and H.H. Brintzinger, *J. Organomet. Chem*., **1985**, 288, 69.

15. C. Liu, T. Tang and B. Huang, *J. Catal*., **2004**, 221, 162.

16. F.R.W.P. Wild, M. Wasiucionek, G. Huttner and H.H. Brintzinger. *J. Organomet. Chem*., **1985**, 288, 63.

17. N. V. Semikolenova, V. A. Zakharov, E. P. Talsi, D. E. Babushkin, A. P. Sobolev, L. G. Echevskaya and M. M. Khysniyarov, *J Mol. Catal. A: Chem*., **2002**, 182, 283.

18. V. N. Panchenko, N. V. Semikolenova, I. G. Danilova, E. A. Paukshtis and V. A. Zakharov, *J. Mol. Catal. A: Chem*., **1999**, 142, 27.

19. J. H. Yim, K. J. Chu, K. W. Choi and S. K. Ihm, *Eur. Polym. J*., **1996**, 32, 1381.

20. W. D. Niegisch, S. T. Crisafulli, T. S. Nagel, B. E. Wagner, *Macromolecules*, **1995**, 25, 3910.

21. M.R. Ribeiro, A.D. Deffieux and M.F. Portela, *Ind. Eng. Chem. Res.*, **1997**, 1224. 36.

22. Y. X. Chen, M. D. Rausch and J. C. W. Chien, *J. Polym. Sci. Part A: Polym. Chem*., **1995**, 33, 2093.

23. I. Gitsov, P. I. Ivanova, J. M. J. Fréchet, *Macromol. Rapid Commun*., **1994**, 15, 384.

Chapter 5. Fragmentation of the supported catalyst in ethylene polymerization

5.1 Introduction

The fragmentation of a supported catalyst is of fundamental importance for performing a successful polymerization [1, 2 and 3]. By catalyst fragmentation in a proper and controlled way, high activity of catalyst and high yield of polymer with good morphology of product can be obtained in olefin polymerizations [4, 5 and 6]. However, if the fragmentation of the catalyst particle is not controlled properly, intact large particles of the catalyst supports remain within the polyolefin product or a considerable amount of non-spherically shaped and fluffy particles of polymer may be produced leading to serious operation problems in an industrial plant.

As mentioned in chapter 1, many research groups have tried to visualize the catalyst fragmentation within polyolefin particles or during olefin polymerization [7, 8, 9, 10 and 11]. To visualize the supported catalyst fragmentation, scanning electron microscopy (SEM), transmission electron microscopy (TEM), X-ray tomography and atomic force microscopy (AFM) have been used [12 and 13]. In particular electron microscopy (SEM and TEM) is a good tool for the investigation of the catalyst fragmentation within the polyolefin. Recently, Fink et al. investigated the polymerization kinetics, polymer particle growth, polymer morphology and particle fragmentation process by using electron microscopy [14, 15, and 16]. This work contributed greatly to the understanding of the polymerization behavior of the silica-supported metallocene catalysts. However, for the investigation of catalyst fragmentation by using SEM and TEM, additional techniques such as sectioning the particle and staining the slice of polyolefin product are necessary.

Laser scanning confocal fluorescence microscopy has therefore been introduced in order to study the fragmentation of supported catalysts in heterogeneous polymerization in our group. Confocal fluorescence microscope is able to observe selected thin layers of a thick specimen placed under a microscope. The confocal fluorescence images have significantly less fluorescent blur and out-of-focus light than conventional fluorescence microscopy. Further resolution as well as contrast is better than in conventional fluorescence microscopy [17]. The first attempt to use the confocal fluorescence microscope for catalyst fragmentation study was carried out by Martin Stork at MPIP [18]. Also Matthias Koch in MPIP used this

technique to investigate the distribution of fluorescent dyes in a PE film (Figure 5-1) [19].

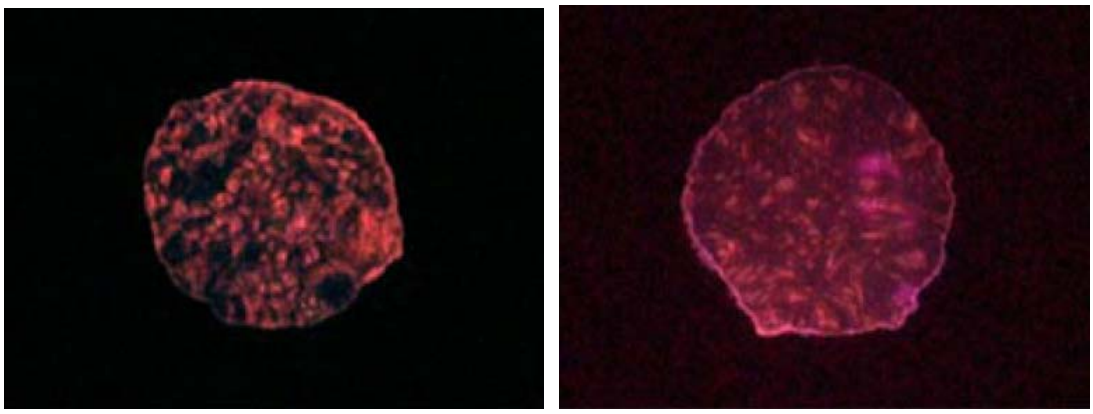

(A) (B)

Figure 5-1. Fluorescence images polyethylene films obtained from catalysts tagged with fluorescent dyes; (A) 15 min and (B) 45 min [18].

In the current work, the fragmentation of catalyst particles within the polyethylene product was directly characterized and visualized by laser scanning confocal fluorescence microscopy - a convenient and nondestructive method. For this work, different types of supports stained or tagged with dyes were prepared and the fragmentation of the supported catalyst particle within the polyethylene product was studied with confocal fluorescence images. Nanosized PS beads, silica gel, microsized PS beads and a dendrimer containing dyes at the core were used as dye-stained supports in heterogeneous ethylene polymerization.

5.2. Fragmentation of the catalyst supported on the nanosized PS beads in ethylene polymerization

5.2.1. Preparation of nanosized PS beads tagged with dye and functionalized with polyethyleneoxide (PEO) and of the supported catalyst

Nanosized PS beads copolymerized with N-(2,6-diisopropylphenyl)-9-(4-ethenylphenyl) perylene-3,4-dicarboximide and functionalized with polyethyleneoxide (PEO) were prepared for investigating the fragmentation behavior of the supported catalyst within the polyethylene product. The monomers used were styrene, divinylbenzene as crosslinker, polyethyleneoxide-block-polystyrene (PEO-b-PS) co-polymer and N-(2,6-diisopropyl

phenyl)-9-(4-ethenylphenyl)perylene-3,4-dicarboximide (Scheme 5-1). This low concentration of dye does not influence the catalyst activity in heterogeneous ethylene polymerization [18]. The procedure used was as follows: styrene, divinylbenzene as crosslinker, N-(2,6-diisopropylphenyl)-9-(4-ethenylphenyl)perylene-3,4-dicarboximide (0.3 mol %) and hexadecane were stirred for 5 min. The PEO-PS block copolymer (10 mol %) was dispersed in water homogeneously at 80 ^{o}C and then cooled down to room temperature. The homogeneous block copolymer dispersed in water was mixed with the oil phase of styrene derivatives (styrene, divinylbenzene and N-(2,6-Diisopropylphenyl)-9-(4-Ethenylphenyl)perylene-3,4-dicarboximide) and stirred for 1 hr to form a microemulsion. The microemulsion was sonificated for 5 min under ice cooling to form a miniemulsion. The miniemulsion was heated in an oil bath at 72 °C and then the initiator $K_2S_2O_8$ was dissolved in a small quantity of distilled water and added to the miniemulsion reactor. The PS product was filtered with polyethersulfone membrane and dried in vacuum.

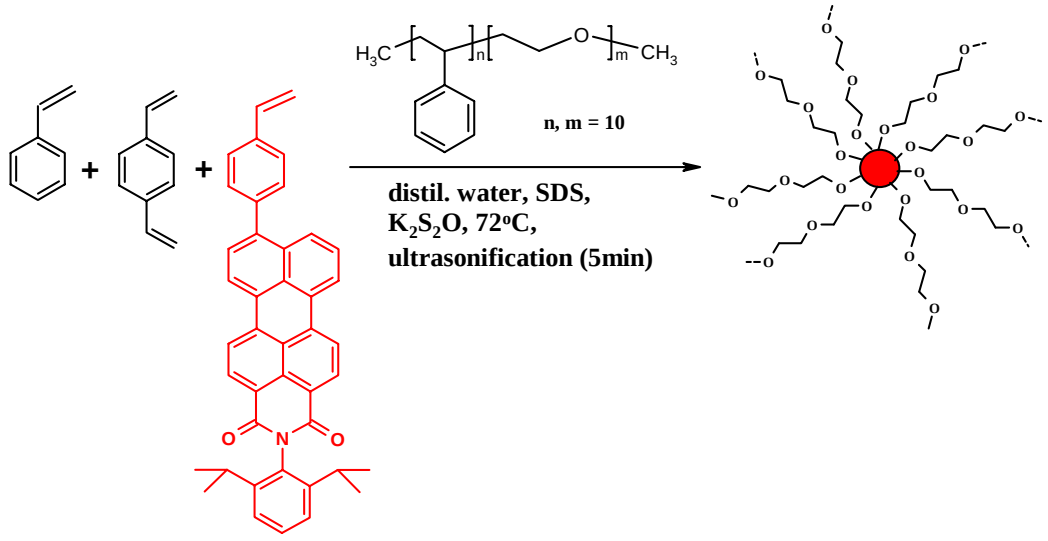

Scheme 5-1. Preparation of nanosized PS beads tagged with N-(2,6-diisopropylphenyl)-9-(4-ethenylphenyl)perylene-3,4-dicarboximide and functionalized with polyethyleneoxide (PEO)

The procedure for immobilizing the metallocene catalyst on the nanosized PS beads tagged with N-(2,6-diisopropylphenyl)-9-(4-ethenylphenyl)perylene-3,4-dicarboximide and functionalized with PEO was identical to the procedure in given chapter 3.2.

5.2.2. Ethylene polymerization and fragmentation of the supported catalyst within PE particle

Using the catalyst supported on the nanosized PS beads tagged with the dye, ethylene polymerizations were carried out at different polymerization times of 2, 5, 10, 15, 30 and 60 min at the 70 ^{o}C and 40 bar (Table 5-1). In this heterogeneous ethylene polymerization, 40 μmol / g metallocene activation and 350 MAO / Zr mol ratio were used. The catalyst activity after 60 min polymerization are similar to that of the catalyst supported on the PS beads without tagging dye which means that the dye does not have any noticeable influence on catalyst activity and productivity in ethylene polymerization. Upon increasing polymerization time, the catalyst activity is decreased steadily.

Table 5-1. Ethylene Polymerization [a] (catalyst: PEO functionalized PE beads tagged dye / $Me_2Si(2MeBenzInd)_2ZrCl_2$ / MAO)

Run	Zr/cat (μmol/g)	MAO/Zr	Time (min)	Activity [kgPE/molZrhrbar]	Productivity [gPE/gcathr]	BD[b]
PE-50	40	350	2	2750	3750	-[c]
PE-51	40	350	5	2450	2780	-
PE-52	40	350	10	1970	2670	-
PE-53	40	350	15	1830	2500	320
PE-54	40	350	30	1400	1960	350
PE-55	40	350	60	1220	1660	400

[a] Reaction condition: 1 L autoclave, isobutene 400 ml, ethylene pressure 40 bar, 70 °C, amount of catalyst: 24 mg. [b] BD: bulk density (g / l). [c] not enough material for measurement

Polyethylene particles produced after various reaction times were isolated using a sieve with pores of 100 - 500 μm and then examined by laser scanning confocal fluorescence microscopy. In the imaging by confocal fluorescence microscopy, PE samples were placed in the plane perpendicular to the optical axis of the microscope objective. Figure 5-2 shows 58 fluorescence images of a single PE particle cross-sectioned optically at different depths of the focus into the particle. Figure 5-3 shows an SEM image (A) and a confocal fluorescence image (B) of polyethylene particles produced after 5 min polymerization. Figure 5-3 (B) is one of the middle slice images from Figure 5-2. Upon close examination of the confocal fluorescence images, three types of image regions are identified as bright red colored particles, white / gray colored areas and black colored parts.

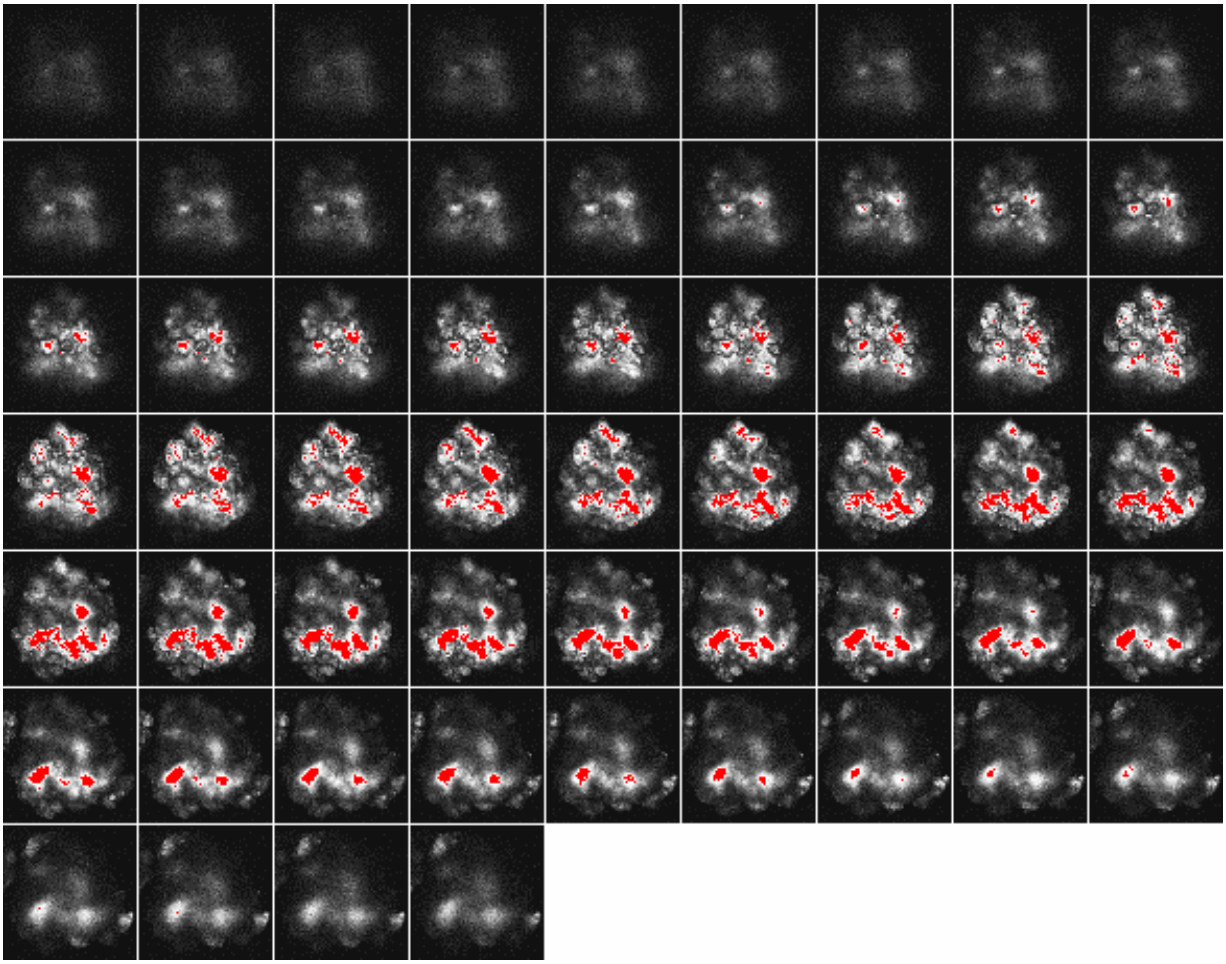

Figure 5-2. Confocal fluorescence images (58 slices) of PE (PE-51) particle sectioned at different depths of focus into single PE particle (C) obtained after 5 min polymerization

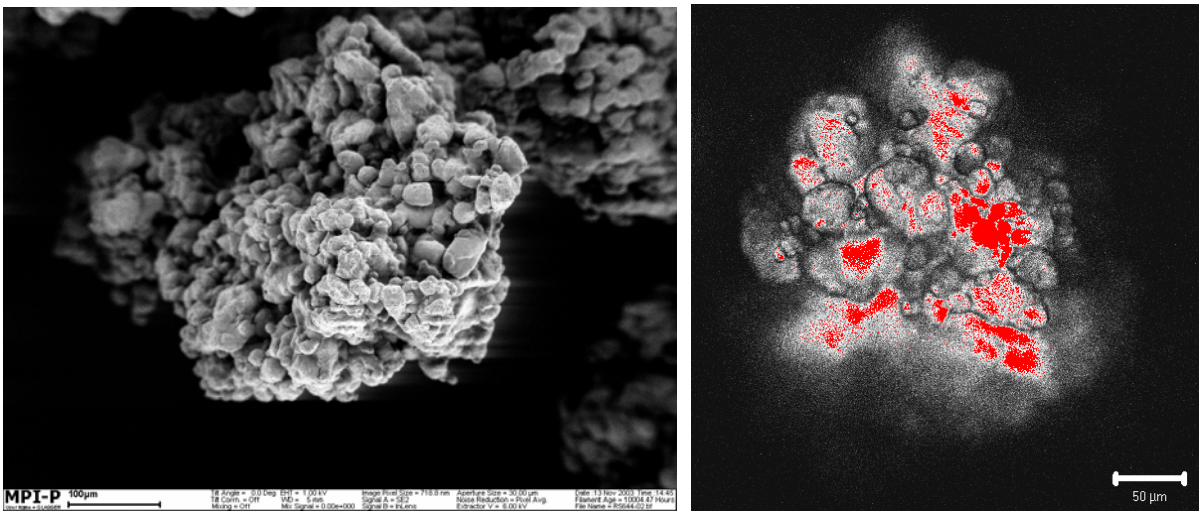

(A) (B)

Figure 5-3. SEM image of PE (PE-51) particle (A) and confocal fluorescence middle slice image of single PE particle (B) obtained after 5 min polymerization: scale bar – 100 µm (A) and 50 µm (B)

The bright red-colored particles in the image represent the fragmented catalyst particle and the white / gray areas in each PE sample thus represent the mixture of catalyst fragments and polyethylene formed. The black areas in the PE sample indicate just polyethylene. Based on these confocal fluorescence images, one can see that the catalyst particle is fragmented and dispersed within the PE particle. The distribution of the fragmented catalyst particles in each PE is not homogeneous at early polymerization times. One can see that there are small sub-particles inside the PE particle because the supported catalyst particle has broken down. The spherical sub-particles are about 20 – 30 μm in size within the confocal fluorescence image of the PE particle. The shape and size of these sub-particles is similar to those of the aggregated particles on the surface of the PE in Figure 5-3 (A). The distribution of the supported catalyst particle is not uniform within the PE particle; that means the breaking direction of the catalyst particle within the PE product during polymerization is not uniform (Figure 5-3, B). After 15 min of polymerization, the supported catalyst particles within the PE particle are dispersed more homogeneously than after 5 min of polymerization with an increase in the PE particle size as shown in Figure 5-4. The number of dense-red particles within the PE particle (Figure 5-4, B) is reduced and the white / dark areas have increased in comparison with that of the PE produced after 5 min of polymerization. One can see that only a few small red spots are dispersed in the fluorescence image of the single PE particle which means that the supported catalyst particles are almost totally fragmented and dispersed homogeneously within the PE particle after 15 min of polymerization under 70 ^{o}C and 40 bar (Figure 5-5). This fragmentation behavior of the catalyst supported on the nanosized PS beads is different from that of the silica-supported catalyst described by Fink and coworkers [13]. They described three particle growth steps; at first polymerization occurs at the outer surface of the catalyst carrier, then polymer growth is accompanied by the fragmentation of the supported catalyst and finally the polymer particle is expanded.

The fragmentation behavior of the catalyst supported on the nanosized PS beads is similar to that of a Ziegler–Natta catalyst supported on $MgCl_2$ and follows the multigrain model (MGM). In the multigrain model for a Ziegler-Natta catalyst supported on $MgCl_2$, monomer diffuses through the pores of the supported catalysts (secondary particles) and the resulting polymer layer surrounds the fragments of the $MgCl_2$ supported catalyst [20]. Through the polymer layer, monomer diffuses to the active sites on the surface of the fragments where polymerization occurs inside and outside simultaneously within the fragile catalyst particle. The newly formed polymers push the previously formed polymer layer, thus increasing the

radius of the polymer sub-particles and consequently the size of the polymer particles.

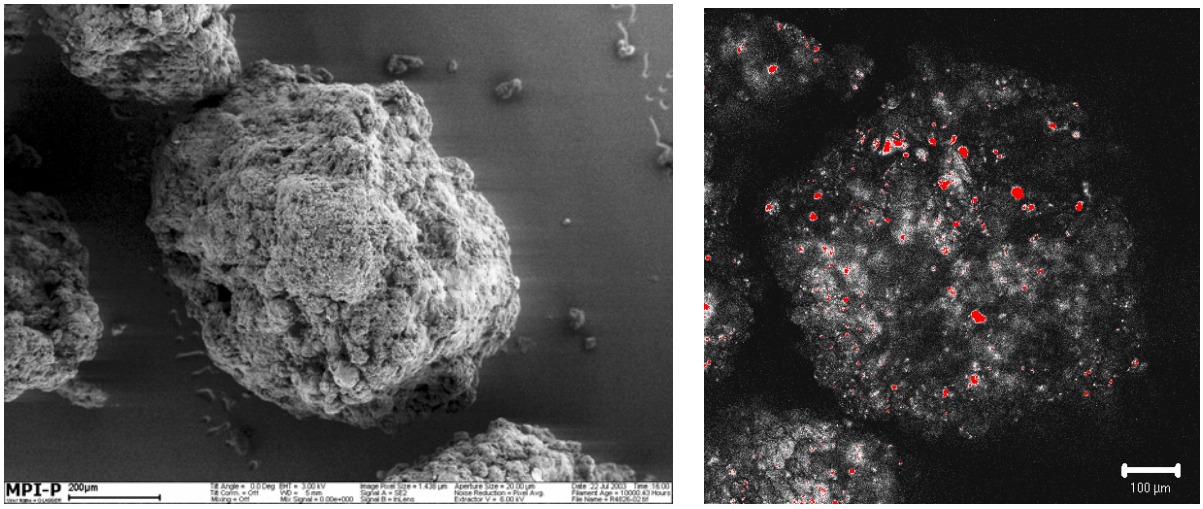

(A) (B)

Figure 5-4. SEM image of PE (PE-53) particle (A) and confocal fluorescence image of the middle slice image of single PE particle (B) obtained after 15 min polymerization; scale bar – 200 µm (A) and 100 µm (B)

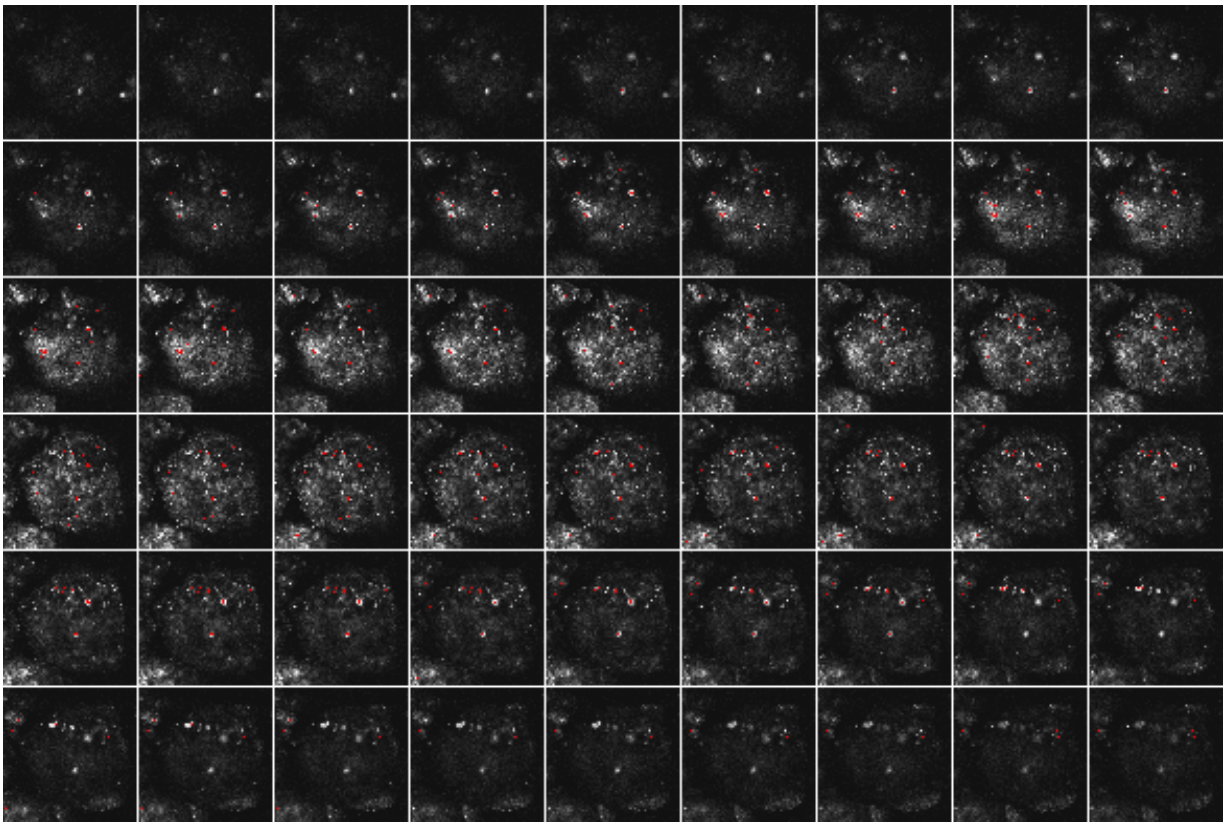

Figure 5-5. Confocal fluorescence image (53 slices) sectioned at different depths of focus into single PE (PE-54) particle obtained after 15 min polymerization

5.2.3. Internal structure and surface morphology of PE single particle produced by the catalyst supported on the nanosized PS beads

To study the internal structure of polyethylene for proving the mechanism of the particle growth and the catalyst fragmentation, a considerable amount of research has been carried out using transmission electron microscopy (TEM) [21]. However, as mentioned previously TEM needs additional processes such as cutting and staining of single particles for sampling. On the other hand, the laser scanning confocal fluorescence microscopy provides a convenient and non-destructive way to visualize the sub-particle in the PE particle as well as to explain the catalyst fragmentation behavior. Figure 5-6 shows the fluorescence images of the internal structure of a single PE particle obtained by the catalyst supported on the nanosized PS beads after 5 min polymerization. One is an original fluorescence image (A) and the other is a fluorescence image modified by changing the colour (B). There are small sub-particles on the confocal fluorescence image of the PE middle slice and black lines between the sub-particles. The red-colored particles represent fragmented catalyst sub-particles and the black lines are supposed to be the access of monomer gas. The sub-particles have 5 - 20 μm diameter and the channels between the sub-particles have 2 - 3 μm.

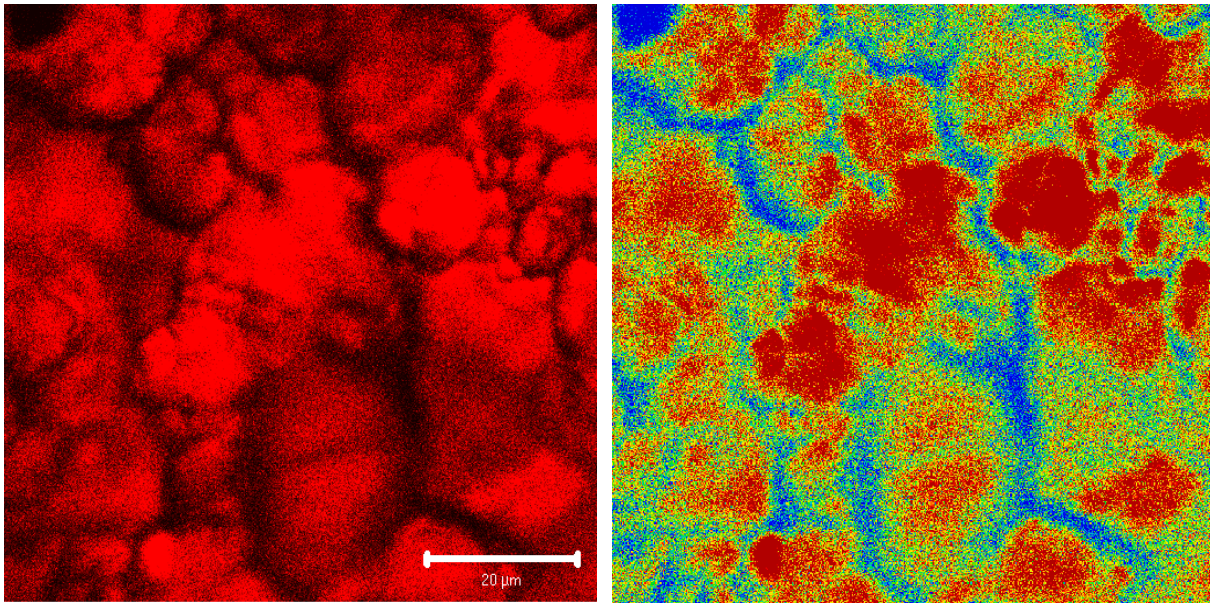

(A) (B)

Figure 5-6. Confocal fluorescence images of the internal structure of single polyethylene (PE-51) particle obtained by the catalyst supported on the nanosized PS beads; (A) original fluorescence image and (B) colour-modified fluorescence image (scale bar – 20 μm)

The surface structures of PE particles produced by the supported catalyst after different polymerization times are shown in Figure 5-7. In the case of PE produced after 2 min polymerization, there are many cracks of about 5 μm on the surface of PE (Figure 5-7, A). It is presumed that ethylene monomer diffuses inside the polyethylene particle through these cracks during ethylene polymerization and reaches the active metal sites for polymerization. After 5 min polymerization, the number of cracks on the surface of PE is reduced and the cracks are partially closed due to the formed polyethylene (Figure 5-7, B). The image exhibits sub-particles on the surface of polyethylene with a similar shape and size to the internal particles within the PE product shown in Figure 5-6.

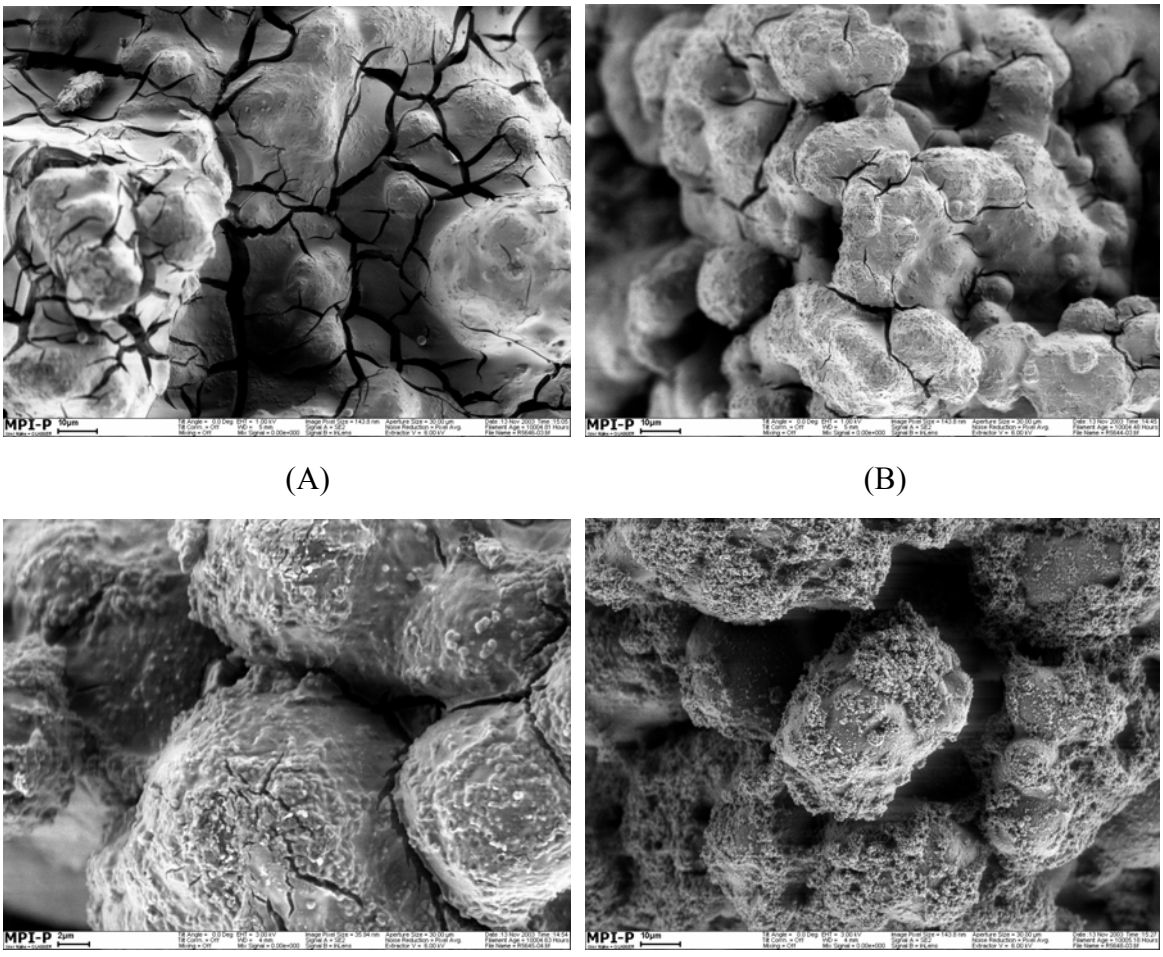

(A) (B)

(C) (D)

Figure 5-7. SEM images of the surface structure of the PE produced by the catalyst supported on the nanosized PS after reaction times: (A) PE-50 (2 min), (B) PE-51 (5 min), (C) PE-53 (15 min) and (D) PE-54 (30 min): scale bar – (A) 10 μm, (B) 10 μm, (C) 2 μm and 10 μm (D)

After 15 min polymerization, the size of small sub-particles on the PE surface increases due to the accumulation of polyethylene product as shown in Figure 5-7 (C). After 30 min polymerization, there are no cracks any more and many particles are agglomerated strongly on the surface of PE as seen in Figure 5-7 (D). The polymer globules become more round and are apparently much larger than the previous particles.

5.2.4. Study of the dependence of the catalyst behavior on the concentration of functional groups of the nanosized PS beads

In chapter 3, the influence of the different concentrations of functional groups on the ethylene polymerization and the bulk density of the obtained polyethylene was studied for ethylene polymerizations at 40 bar and 70 ^{o}C. These results were confirmed by the kinetics of the ethylene polymerization at 2 bar and 70 ^{o}C. In this chapter, the dependence of the catalyst performances on the concentration of the functional group is studied again in the aspect with regards to the catalyst fragmentation, by using confocal fluorescence images.

5.2.4.1. Preparation of nanosized PS beads tagged with dye [N-(2,6-diisopropylphenyl)-9-(4-ethenylphenyl)perylene-3,4-dicarboximide] and functionalized with polypropylene-oxide (PPO)

The nanosized polystyrene (PS) beads copolymerized with N-(2,6-diisopropylphenyl)-9-(4-ethenylphenyl)perylene-3,4-dicarboximide and functionalized with polypropyleneoxide (PPO) as a support for heterogeneous olefin polymerization were prepared by miniemulsion polymerization (Scheme 5-2). PS beads with different concentrations of PPO functionalized styrene (0.5 mol % and 10 mol %) were used to study the different fragmentation behavior of each supported catalyst. The PS beads were stained with N-(2,6-diisopropylphenyl)-9-(4-ethenylphenyl)perylene-3,4-dicarboximide in the core by its covalent bonding with styrene and divinylstyrene. The procedure for immobilizing the metallocene catalyst on the nanosized PS beads tagged with dye and functionalized with PPO followed the procedure given in chapter 3.2. In this heterogeneous ethylene polymerization, 40 μmol / g metallocene activation and 350 MAO / Zr mol ratio were used.

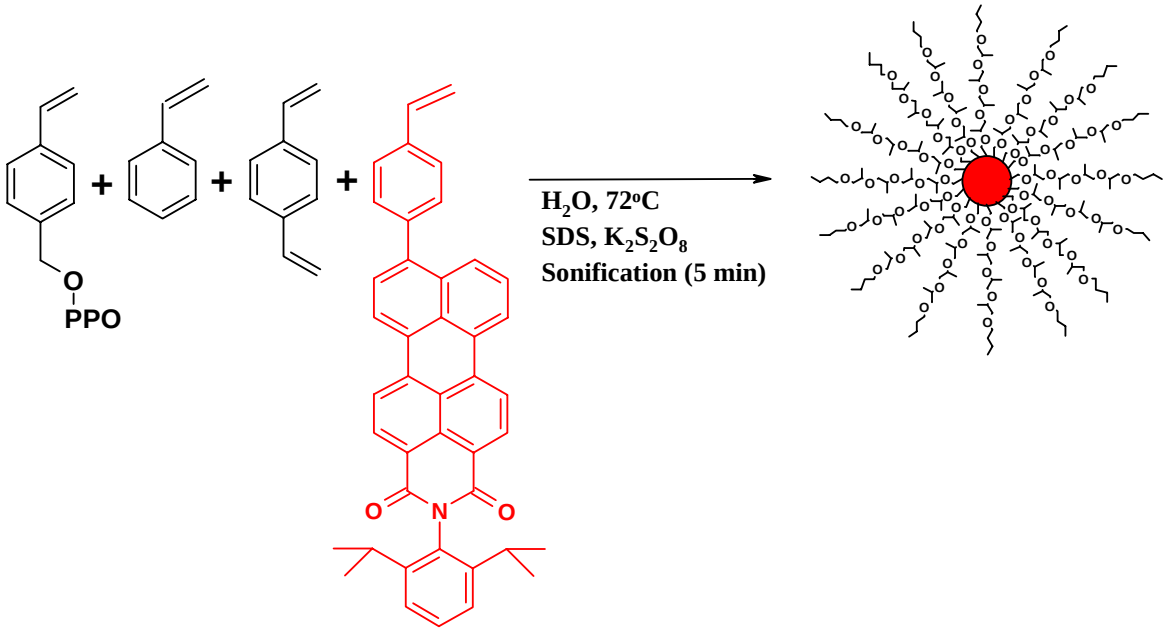

Scheme 5-2. The preparation of nanosized PS beads tagged with N-(2,6-diisopropylphenyl)-9-(4-ethenylphenyl)perylene-3,4-dicarboximide and functionalized with polypropylene-oxide (PPO)

5.2.4.2. Ethylene polymerization and fragmentation study of the supported catalyst in PE single particle

In chapter 3.4.2, the dependence of the catalyst activity on the concentration of polypropyleneoxide (PPO) on the PS beads was investigated. Several PS beads with the concentration of PPO functionalized styrene varying from 0.5 to 20 mol % were prepared. Upon decreasing the concentration of PPO chains on the PS beads, the activity of the catalyst supported on the nanosized PS beads increased, however, the bulk density of polyethylene particle decreased. This was interpreted as indicating that the interaction of PPO and MAO / metallocene as well as the coordination of catalyst between them was weak as seen at low PPO concentrations on the support. This caused the supported catalyst to induce more homogeneous polymerization and therefore show higher activities with a low bulk density of PE. Furthermore, we considered the interaction of the PS beads functionalized with PPO that are reversibly crosslinked via the interaction of the MAO / metallocene and PPO nucleophilic groups. This interaction could be strengthened drastically by increasing the amount of PPO on the PS particles resulting in a more stable network. Such a denser network could limit the diffusion of the monomer gas into the active sites of the catalyst as well as the fragmentation

of the catalyst.

To support these interpretations of the results in chapter 3.4.2, ethylene polymerization was carried out again using the catalyst supported on nanosized PS beads with incorporated florescent dye and functionalized with PPO under the same polymerization conditions. The ethylene polymerization was stopped at several reaction times from 5 min to 60 min (Table 5-2 and 5-3). As in the results of the supported catalyst in chapter 3.4.2, each supported catalyst prepared by nanosized PS beads with different concentrations of polypropyleneoxide (PPO) in the same polymerization time shows different activities. The catalyst supported on the PS beads with 0.5 mol % of PPO (Catalyst 85) is more active than the catalyst supported on the PS beads with 10 mol % of PPO (Catalyst 86).

Table 5-2. Ethylene polymerization [a] (Catalyst 85: PPO functionalized PE beads tagged dye / $Me_2Si(2MeBenzInd)_2ZrCl_2$ / MAO)

Run	Amount of PPO (mol%)	Time (min)	Activity (kg PE / mol Zr hr bar)	Productivity (g PE/g cat hr)
PE-56	0.5	5	3400	4550
PE-57	0.5	15	3350	4450
PE-58	0.5	40	3200	4300
PE-59	0.5	60	2920	4100

[a] Reaction condition: in a 1L autoclave, isobutene 400 ml, ethylene pressure 40 bar, 70 °C, 40 Zr / cat (μmol / g) & 350 MAO / Zr, amount of catalyst: 15 - 17 mg.

Table 5-2. Ethylene polymerization [a] (Catalyst 86: PPO functionalized PE beads tagged dye / $Me_2Si(2MeBenzInd)_2ZrCl_2$ / MAO)

Run	Amount of PPO (mol%)	Time (min)	Activity (kg PE / mol Zr hr bar)	Productivity (g PE/g cat hr)
PE-60	10	5	2010	3100
PE-61	10	15	1870	2780
PE-62	10	40	1500	2150
PE-63	10	60	1220	1750

PE particles were separated after different polymerization times of 5, 15, 40 and 60 min

and isolated by using sieves with the pore of 100 - 500 μm. Single PE particles were examined by laser confocal fluorescence microscopy and the distribution of the catalyst particle within each single PE particle was investigated by using the confocal fluorescence images. The dye concentration in the supported catalysts prepared with metallocene and MAO is just than 10^{-5} wt % which is not enough to influence the confocal fluorescence image of polyethylene produced by catalysts supported on the PS beads with different concentration of PPO (0.5 mol % and 10 mol %) as well as the catalyst activity.

The fluorescence image of polyethylene particles produced by the catalyst 85 (0.5 mol %) (Figure 5-8, A) shows that a single polyethylene (PE-56) particle has a few bright red-colored spots dispersed throughout the particle. The fluorescence image of the polyethylene (PE-57) product after 15 min of polymerization (Figure 5-8, B) indicates that the catalyst particle was more homogeneously dispersed than that after 5 min polymerization shown in Figure 5-8 (A). That means that at the beginning of polymerization (5 min) the supported catalyst is already broken down and that intensive fluorescent spots are almost absent from the polyethylene. After 15 min polymerization, the catalyst particle has fragmented completely within the PE product.

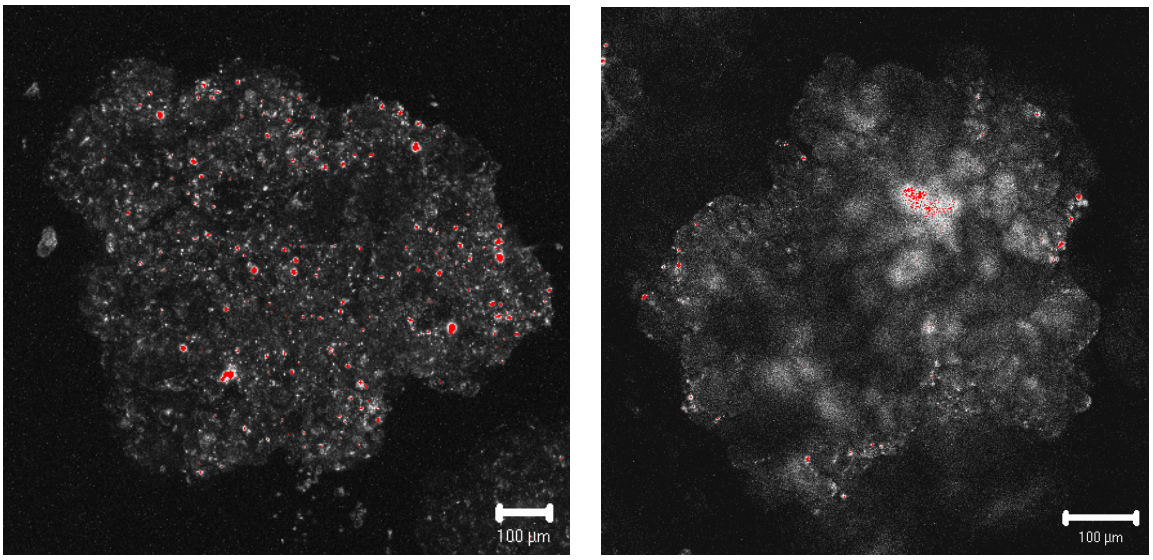

(A) (B)

Figure 5-8. Confocal fluorescence image of polyethylene produced by the catalyst 85; (A) single PE particle (PE-56, 5 min) and (B) single PE particle (PE-57, 15 min); scale bar: 100 μm

On the other hand, in the case of polyethylene produced by the catalyst 86 (10 mol %), the

fluorescence image in Figure 5-9 (A) shows that there are many concentrated and bright red-colored particles within the polyethylene (PE-60) particle after 5 min polymerization. When one compares the fluorescence image of a PE particle produced by the different catalysts after 5 min polymerization, the fragmentation rate of the catalyst 86 is slower than that of the catalyst 85. After 15 min polymerization, the bright red-colored particles are more fragmented within the whole polyethylene (PE-61) particle than after 5 min polymerization (Figure 5-9, B). By comparing these fluorescence results in Figure 5-8 (B) and 5-9 (B), one can conclude that the concentration of functional groups on the carrier does influence the fragmentation of the supported catalyst and the catalyst activity at the same polymerization condition. To be precise, the supported catalysts on the PS beads with the lower concentration of PPO are fragmented more quickly than the supported catalysts on the PS beads with the higher concentration of PPO.

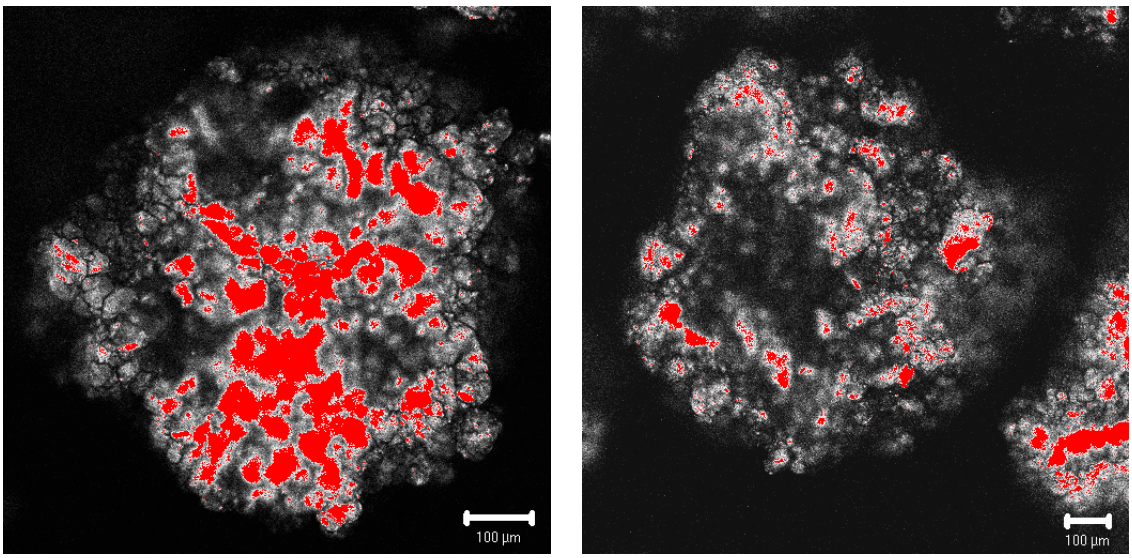

(A) (B)

Figure 5-9. Confocal fluorescence image of polyethylene produced by the catalyst 86; (A) single PE particle (PE-60, 5 min) and (B) single PE particle (PE-61, 15 min); scale bar: 100 µm

So far, the fluorescence images of single PE particle produced at the same polymerization time have been compared. To confirm the fragmentation behavior of the catalyst supported on the nanosized PS beads having different concentration of functional groups, fluorescence images of single PE particles with the same yield must be compared. For this work, five polymerizations were carried out using the catalyst 86 at polymerization times from 4 to 20

min (Table 5-3).

Table 5-4. Polymerization of ethylene [a] (catalyst 85: 0.5 mol % PPO functionalized PE beads tagged dye / $Me_2Si(2MeBenzInd)_2ZrCl_2$ / MAO).

Run	Amount of PPO (mol %)	Amount of catalyst (mg)	Yield (g)	Time (min)
PE 64	0.5	30	4.7	1
PE 65	0.5	29	6	2
PE 66	0.5	26	9 g	5
PE 67	0.5	33	11 g	5
PE 68	0.5	22	11g	9

[a] Reaction condition: in a 1L autoclave, isobutene 400 ml, ethylene pressure 40 bar, 70 °C, 40 Zr / cat (μmol / g) & 350 MAO / Zr, amount of catalyst: 15 - 17 mg.

Table 5-3. Polymerization of ethylene [a] (catalyst 86: 10 mol % PPO functionalized PE beads tagged dye / $Me_2Si(2MeBenzInd)_2ZrCl_2$ / MAO).

Run	Amount of PPO (mol %)	Amount of catalyst 85 (mg)	Yield (g)	Time (min)
PE 69	10	30	4.6	4
PE 70	10	39	6.5	10
PE 71	10	28	6	10
PE 72	10	34	11	17
PE 73	10	38	8	20

[a] Reaction condition: in a 1L autoclave, isobutene 400 ml, ethylene pressure 40 bar, 70 °C, 40 Zr / cat (μmol / g) & 350 MAO / Zr, amount of catalyst: 15 - 17 mg.

Based on the yield obtained for the catalyst 85 (0.5 mol % PPO), ethylene polymerizations were carried out using the catalyst 86 (10 mol % PPO). The same yield of PE produced by using the same amount of the catalyst 85 and 86 was produced in each catalyst system. 29 mg of the catalyst 85 produced 6 g yield of PE in 2 min polymerization (Run PE-65). In the case of the catalyst 86 (Table 5-4), 28 mg of the supported catalyst produced 6 g yield of PE in 10 min polymerization (Run PE-71) (Table 5-3). Single PE particles of the same particle size

obtained from each supported catalyst were isolated and then examined by laser scanning confocal fluorescence microscopy to investigate the catalyst fragmentation. The fluorescence images of each PE particle obtained from the catalyst 85 and 86 are compared in Figure 5-10 and 5-11 respectively. The fluorescence images within a single polyethylene particle (PE-65) in Figure 5-10 (A) show that the supported catalyst particles are more fragmented and dispersed than the catalyst particle within single polyethylene particle (PE-71) in Figure 5-11 (A) obtained by the same amount of catalyst and with the same yield.

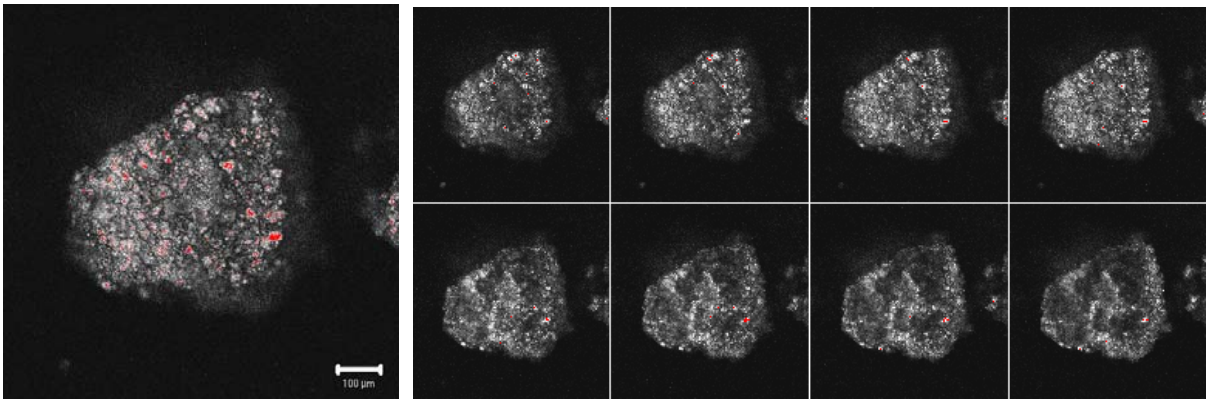

(A) (B)

Figure 5-10. Confocal fluorescence image in middle slice (A) and 8 slices image (B) of the single PE (PE-70) particle produced (2 min) produced by the catalyst 85; scale bar: 100µm

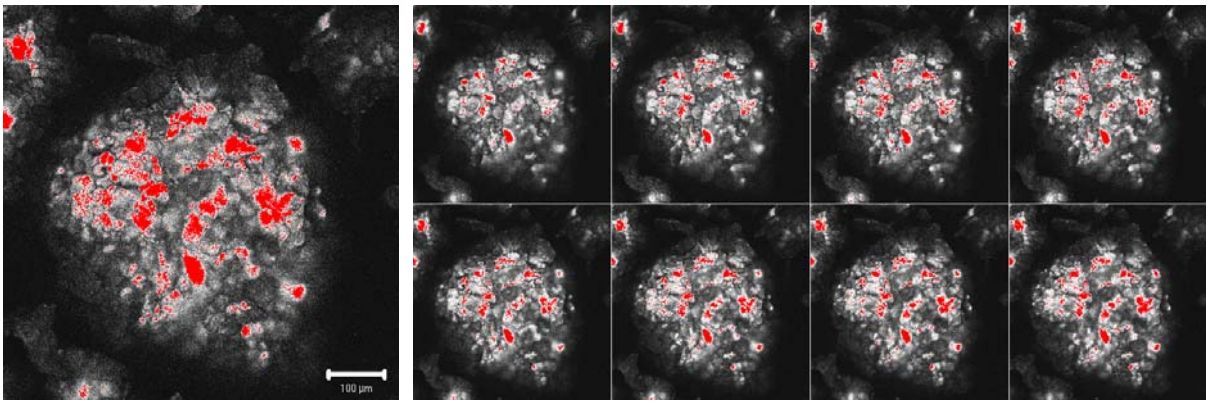

(A) (B)

Figure 5-11. Confocal fluorescence image in middle slice (A) and 8 slices image (B) of the single PE (PE-66) particle produced (10 min) produced by the catalyst 86 (scale bar - 100µm)

Also, 8 confocal fluorescence slice images of Figure 5-10 (B) show that the fluorescent dye-tagged PS support particles are dispersed homogeneously within the PE particle (PE-65). On the other hand, 8 confocal fluorescence slice images of single PE particle (PE-71) in

Figure 5-11 (B) show that the fluorescent dye-tagged PS support particles are non-homogeneously fragmented within the PE single particle. These results of Figure 5-10 and 5-11 confirm the conclusions from the above results in Figure 5-8 and 5-9.

5.2.5. Summary

In this chapter, the catalyst fragmentation within the polyethylene single particle was investigated by comparing fluorescence images. For this work, a dye was used as probe for the distribution of the catalyst within the PE particle. The dye-tagged PS beads and the supported catalyst were prepared and ethylene polymerizations were carried out at 40 bar and 70 ^{o}C. Single PE particles were examined by laser scanning confocal fluorescence microscopy. Confocal fluorescence microscopy provided a convenient and nondestructive way to study the three-dimensional structure of single PE particles. The fluorescence image of single PE particles showed the fragmentation of the supported catalyst within the PE particle at increasing polymerization times. Early in the polymerization, the supported catalyst particles become fragmented and simultaneously dispersed inside and outside the PE particle. After longer polymerization times, the catalyst particle are dispersed homogeneously within the PE particle. The fragmentation behavior of the catalyst supported on the nanosized PS beads is different from that of the silica-supported catalyst described by Fink and coworker. However, this behavior is similar to that of a Zieler-Natta catalyst supported on $MgCl_2$ in heterogeneous olefin polymerization. In the next chapter, the different fragmentation behavior of catalysts supported on different carriers will be compared.

By using laser scanning confocal fluorescence microscopy, the internal structure of individual PE particles was visualized. There were small sub-particles on the confocal fluorescence image of the PE middle slice and there were black lines between the sub-particles. The sub-particles represented the fragmented catalyst and the black lines were supposed to be channels for the pathway of monomer gas. The sub-particles were about 5 - 20 μm in size and the channel between the sub-particles were about 2-3 μm in width.

The influence of the different concentrations of functional groups on the ethylene polymerization was investigated again by using confocal fluorescence images. The dependence of the activity on the concentration of functional group on the PS beads was investigated in chapter 3. The fluorescence image showed the catalyst fragmentation of the catalyst supported on the nanosized PS beads with 0.5 mol % PPO was faster than that of the

catalyst supported on the nanosized PS beads with 10 mol % PPO because of the different interaction between the concentration of functional group on the support and metallocene complex and thus the monomer diffusion within the supported catalyst.

5.3. Fragmentation of the silica supported catalyst in ethylene polymerization

In chapter 4.3, the silica-supported catalyst's activity and the surface microstructure of the PE product were compared with those of various other supported catalyst systems such as microsized PS beads, nanosized PS beads, silica gel and dendrimer. The catalyst activity and the surface morphology were strongly dependent on the catalyst support. However, it was not possible to explain and compare the different fragmentation behavior of each supported catalyst by using just the catalyst activity and the morphology of the products. In this chapter, the catalyst fragmentation of the silica-supported catalyst is distinguished by using confocal fluorescence images.

5.3.1. Preparation of silica stained with dye and the silica-supported catalyst

Silica gel was stained with N,N′-bis(2,6-diisopropylphenyl)-1,6,7,12-tetra(4-sulfonyl phenoxy)perylene-3,4:9,10-tetracarboxdiimide and the silica-supported catalyst was prepared to compare the fragmentation behavior of the different supported catalysts in ethylene polymerization. For this work, this water-soluble dye (N,N′-Bis(2,6-diisopropyl phenyl)-1,6,7,12-tetra(4-sulfonylphenoxy)perylene-3,4:9,10-tetracarboxdiimide) was used that had been prepared by Dr Christopher Kohl at the MPIP [22]. The procedure to prepare the dye-stained silica and the silica-supported catalyst was as follows (Scheme 5-3); silica gel (Grace Davison Silopol 952) was dried for 48 hr to remove air and water from the pores of the silica gel. A saturated solution of the dye in methanol was mixed with the dried silica and stirred slowly at 50 ^{o}C for 5 hr. The silica gel was removed from the solution by filtration and the dye-stained silica filtrated was mixed with chloroform before drying in air. The chloroform was removed by decantation and this process was repeated several times. Initially the chloroform was slightly red due to some remaining methanol / dye solution on the silica gel.

Using the same procedure as elsewhere in this work, the silica-supported catalyst was prepared. At first, the dye-stained silica support was mixed with methylalumoxane (MAO) and stirred for 12hr. The metallocene / MAO solution was mixed and stirred for 1 hr. The silica-supported catalyst was washed with dry hexane / toluene mixture several times and then dried under vacuum. To test the leaching of the dye from the silica supported catalyst, the dye-stained silica and the dye-stained silica supported catalyst were mixed in methanol and the results were compared.

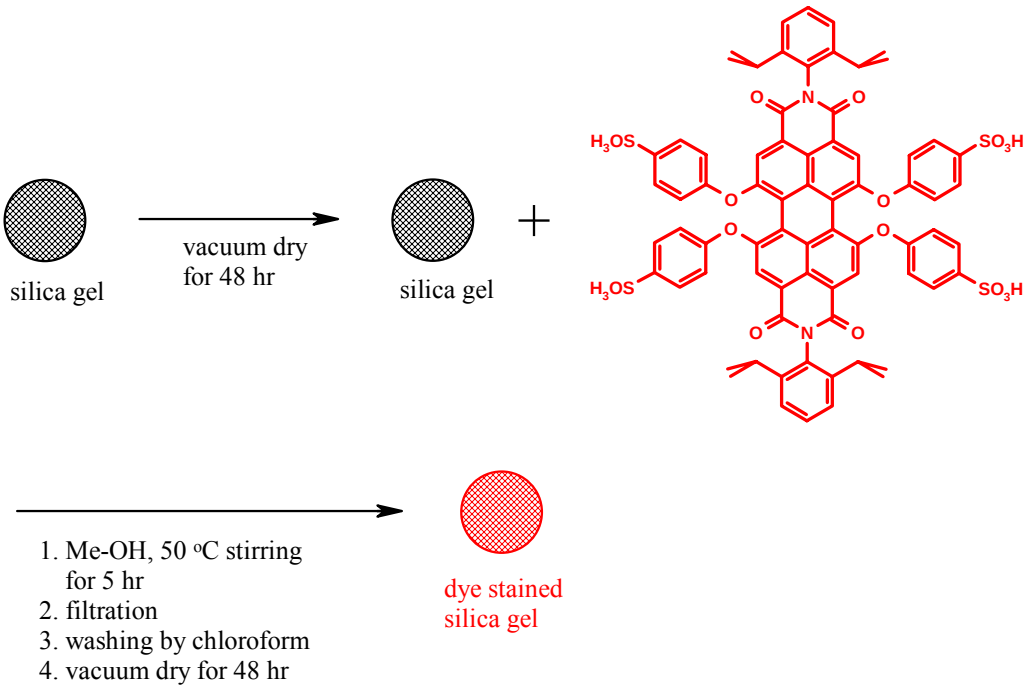

Scheme 5-3. Preparation of silica stained with dye (N,N′-bis(2,6-diisopropylphenyl)-1,6,7,12-tetra(4-sulfonylphenoxy)perylene-3,4:9,10- tetracarboxdiimide)

Figure 5-12 shows the picture of the two tubes containing the dye-stained silica gel (A) and the dye-stained silica supported catalyst (B) in methanol. One can see that leaching of dye is observed from the dye-stained silica in methanol (Figure 5-12, A), but that there is no leaching of dye from the dye-stained silica supported catalyst in methanol (Figure 5-12, B).

Figure 5-12. The leaching test of dye in methanol from the dye-stained silica (A) and the dye-stained silica supported catalyst with MAO / metallocene (B)

This result suggests that the 4 sulfonic acid groups of N,N′-bis(2,6-diisopropyl phenyl)-1,6,7,12-tetra(4-sulfonylphenoxy)perylene-3,4:9,10-tetracarboxdiimide react with the MAO and the dye is bound covalently by the hydroxy groups of silica gel as is the MAO (Scheme 5-4) and the MAO on the surface of the PS then immobilizes the metallocene catalyst.

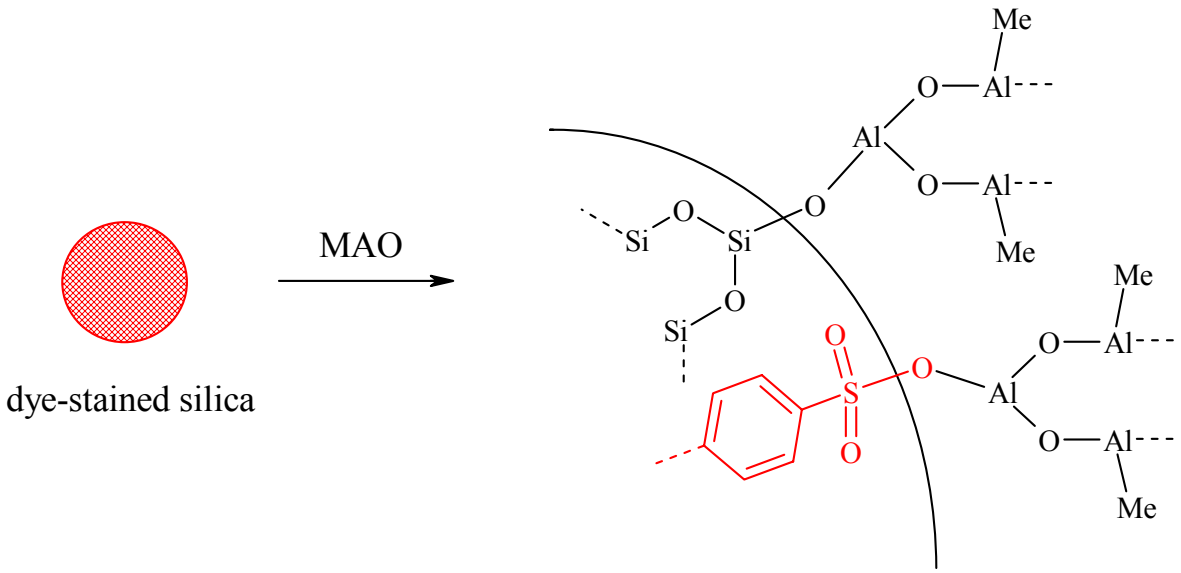

Scheme 5-4. The reaction of the dye-stained silica and MAO as cocatalyst

5.3.2. Ethylene polymerization and fragmentation study of the silica-supported catalyst in PE single particle

Ethylene polymerizations were carried out at 70 ^{o}C and 40 bar using the dye-stained silica supported catalyst. In this heterogeneous ethylene polymerization, 40 μmol / g metallocene activation and 350 MAO / Zr mol ratio were used. The polymerization was stopped at different reaction times (1 to 60 min) and the particles separated by 100 - 500 μm pore-size sieves. In the case of Run 74 and Run 75, the polyethylene (PE) obtained is not enough to evaluate the catalyst activity and the bulk density of polyethylene after 1 or 3 min polymerization (Table 5-5). The catalyst activities calculated after 60 min polymerization are similar to those of the catalyst supported on silica gel without staining dye which means that the dye does not have any noticeable influence on catalyst activity and productivity in ethylene polymerization.

Table 5-5. Ethylene polymerization [a] (catalyst: $Me_2Si(2MeBenzInd)_2ZrCl_2$ / MAO / the dye-stained silica support)

Run	Zr/cat (μmol/g)	MAO/Zr	Polym. Time (min)	Activity[b]	Productivity[c]	BD[d]
PE-74	40	350	1	-	-	-
PE-75	40	350	3	-	-	-
PE-76	40	350	5	1410	1920	-
PE-77	40	350	15	1160	1640	-
PE-78	40	350	20	880	1200	350
PE-79	40	350	30	800	1050	360
PE-80	40	350	60	700	945	380

[a] Reaction condition: 1 L autoclave, isobutene 400 ml, ethylene pressure 40 bar, 70 °C, amount of catalyst: 24 mg. [b] kg PE / mol Zr hr bar. [c] g PE / g cat hr. [d] BD: bulk density (g / l).

A single polyethylene particle separated after different polymerization times was examined by laser scanning confocal fluorescence microscopy. Figure 5-13 shows SEM image and confocal fluorescence image of polyethylene particle (PE-76) produced after 5 min polymerization.

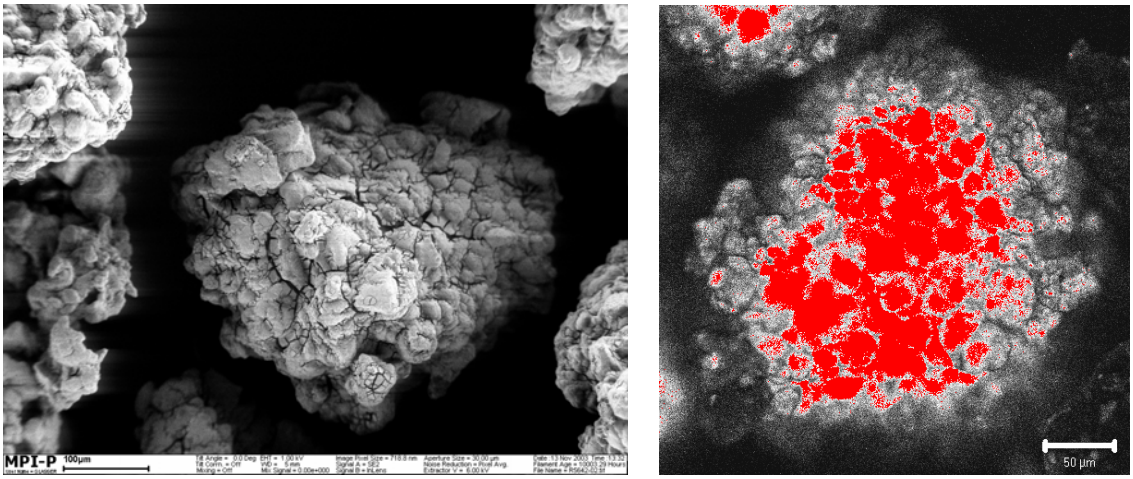

(A) (B)

Figure 5-13. SEM image of PE particles (A) and confocal fluorescence image of the middle slice image of single polyethylene (PE-76) particle (B) obtained after 5 min polymerization; scale bar – 100 μm (A) and 50 μm (B)

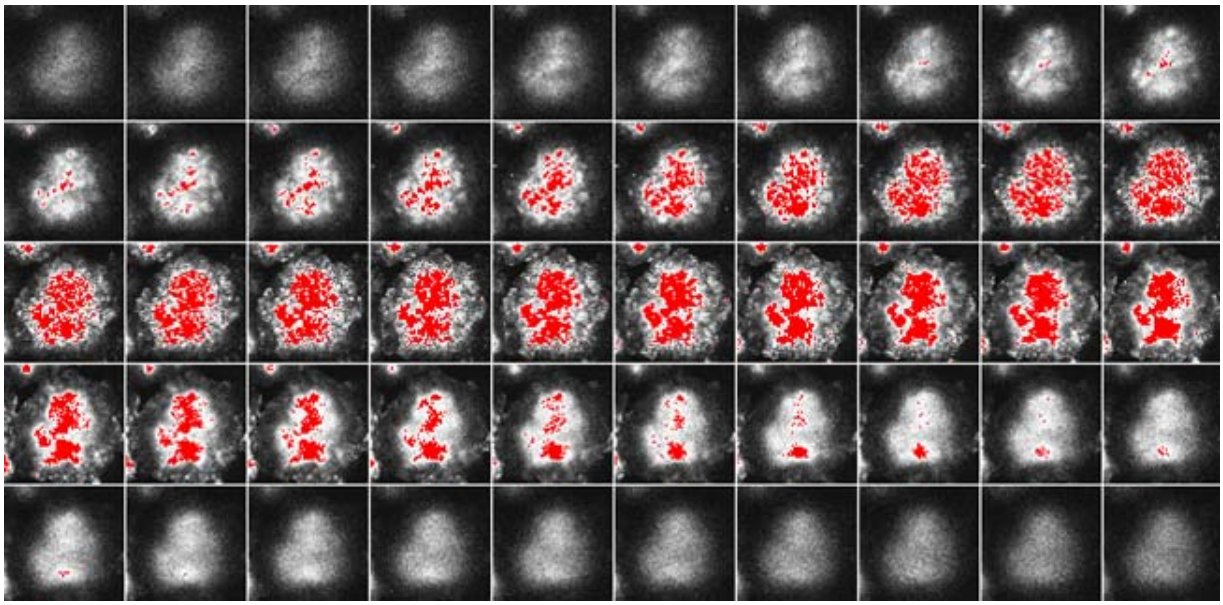

Figure 5-14. Confocal fluorescence images (50 slices) sectioned at different depths of focus into single polyethylene (PE-76) particle obtained after 5 min polymerization

The SEM image in Figure 5-13 (A) shows that the PE particle has a spherical shape and that there are many cracks on its surface. As small particles are aggregated on the surface of the PE shown in SEM images of Figure 5-13 (A), there are sub-particles within the confocal fluorescence image of polyethylene (PE-76) in Figure 5-13 (B). Figure 5-14 shows confocal fluorescence images of a single PE particle sectioned optically at different depths of focus. In the fluorescence image of single PE particles produced by the silica-supported catalyst, the silica supported catalyst particles (dense-red particles) are concentrated in the core of the polyethylene particle and the fragmented catalyst particles filled with polyethylene (white-colored spots) are on the outside of each PE particle. This means that the fragmentation of the supported catalyst initially occurred from the outside of the silica supported particle. This fragmentation behavior of the silica supported catalyst is similar to the results of Fink and co-workers, i.e. that a thin polyolefin film is formed around the particle during the pre-polymerization time [13]. However, the fragmentation behavior of the silica supported catalyst is different from the fragmentation behavior of the catalyst supported on the nanosized PS beads which showed the supported catalyst initially fragmented inside and outside of PE particle. Figure 5-15 exhibits SEM and confocal fluorescence image of single polyethylene (PE-77) particle obtained after 15 min polymerization. Figure 5-16 shows 32 fluorescence images of the single PE particle cross-sectioned optically at different depths of focus into a single PE particle.

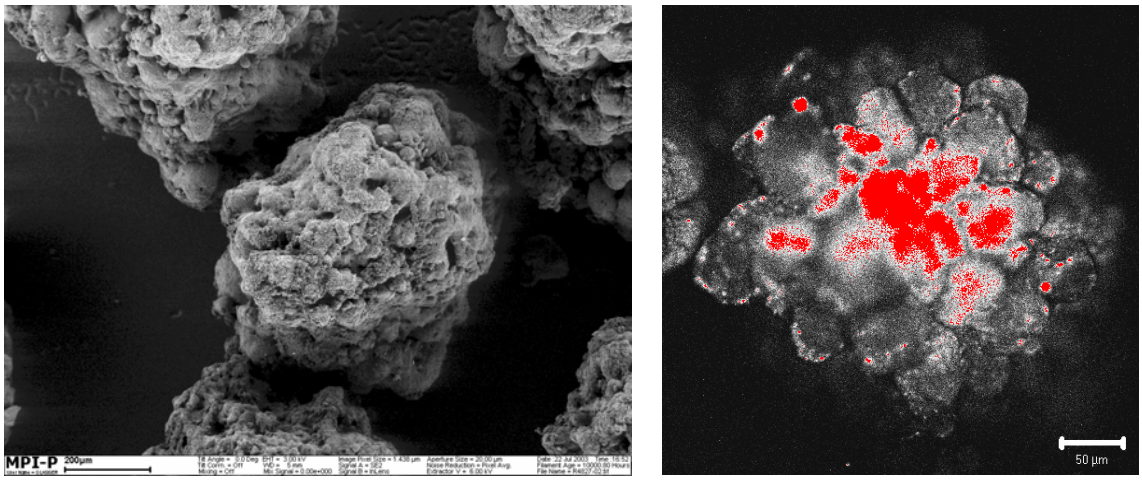

(A) (B)

Figure 5-15. SEM image of polyethylene (PE-77) particles (A) and confocal fluorescence image of the middle slice image of single polyethylene (PE-77) particle (B) obtained after 15 min polymerization; scale bar – 200 µm (A) and 50 µm (B)

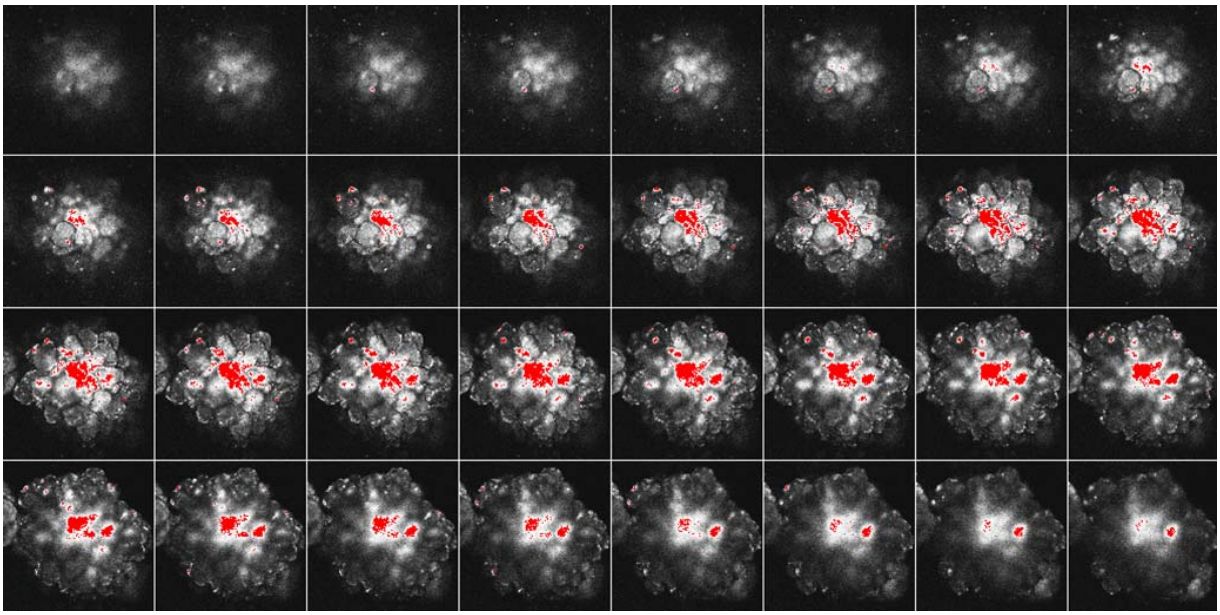

Figure 5-16. Confocal fluorescence images (32 slices) sectioned at different depths of focus into single polyethylene (PE-77) particle obtained after 15 min polymerization

The fluorescence images of the polyethylene particle show that the supported catalyst breaks down from outside to inside after 15 min polymerization. The less-fragmented support within the core of the polyethylene particle produced after 5 min reaction is fragmented more from the outside of the support and the red-colored core becomes smaller. With increasing polymerization time, the growth of the polymer layer continues from the outside to the inside

of the silica-supported catalyst particle. The particle fragmentation allows the ethylene monomer to reach the active centers. After 30 min polymerization, the catalyst particle is fragmented homogeneously within the whole PE particle as shown in Figure 5-17 and Figure 5-18.

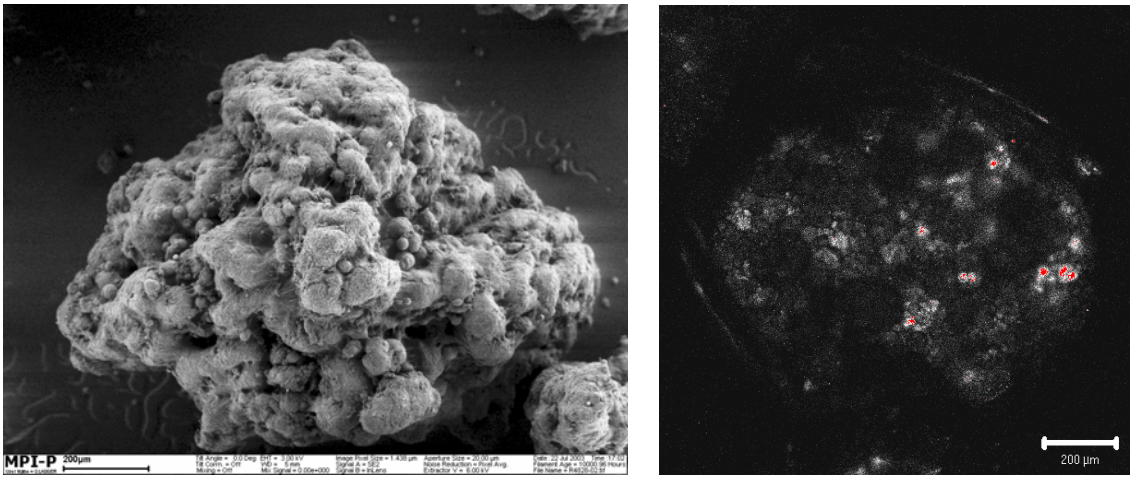

(A) (B)

Figure 5-17. SEM image of polyethylene (PE-79) particles (A) and confocal fluorescence image of the middle slice image of polyethylene (PE-79) particle (B) obtained after 30 min polymerization; scale bar – 200 µm (A) and 200 µm (B)

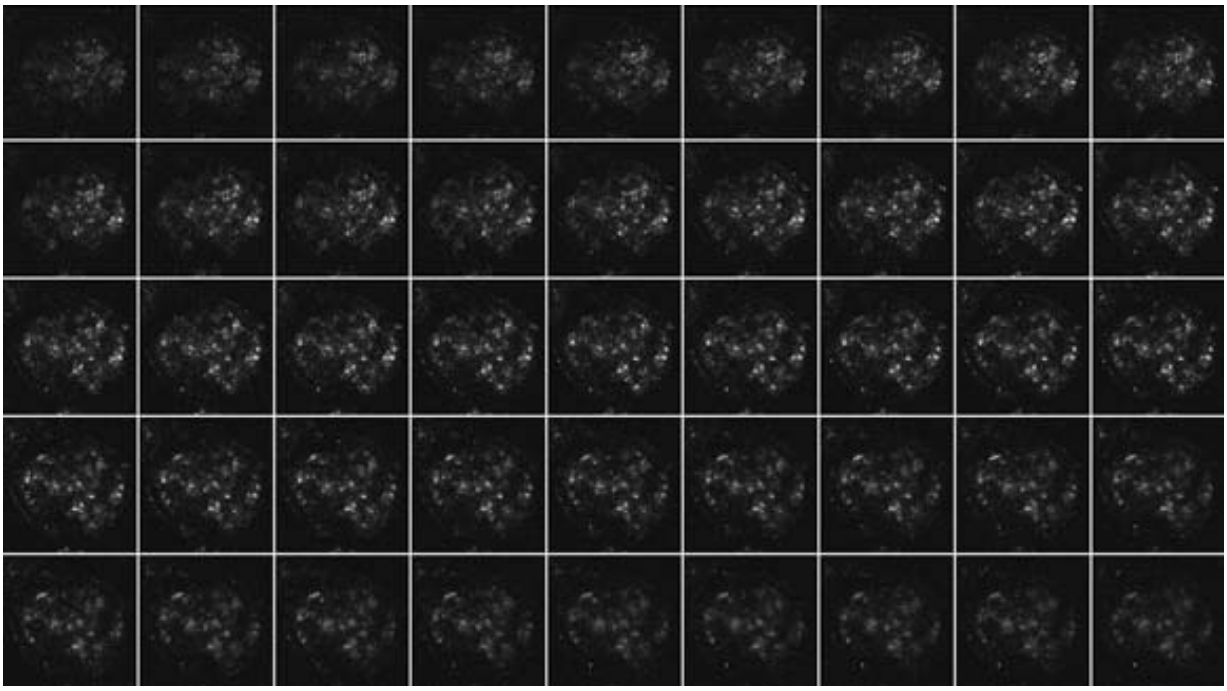

Figure 5-18. Confocal fluorescence (45 slices) images sectioned at different depths of focus into single polyethylene (PE-79) particle obtained after 30 min polymerization

There are almost no red-colored particles in this image which means that the catalyst supported on the silica stained dye is dispersed more homogeneously than in the images of the PE single particle measured after 5 and 15 min polymerization.

These fluorescence results are similar to the TEM results of Fink and coworkers (Figure 5-19 and 5-20) [23 and 24]. Figure 5-19 shows polyethylene particles from a silica supported catalyst after 5 min (A) and after 45 min (B) of ethylene polymerization which were embedded and sectioned by microtome. These PE products were generated at 2 bar ethylene pressure and 20 ^{o}C polymerization temperature. After 5 min polymerization, the catalyst particle was already covered with polyethylene, during the following 40 min polymerization the polyethylene layer increased significantly. Each silica-supported catalyst particle fragmented from the outside.

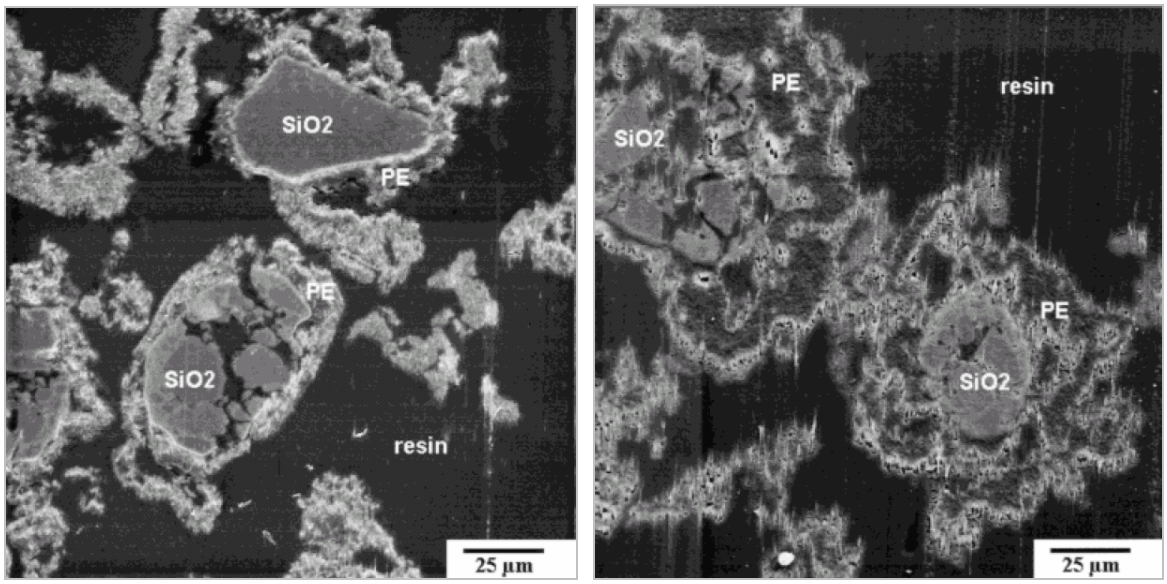

(A) (B)

Figure 5-19. Microtome section of embedded particles generated by silica supported catalyst after 5 min (A) and after 45 min (B) of ethylene polymerization (2 bar and 20 ^{o}C); scale bar – 25 (A and B) [23]

Another image in Figure 5-20 shows particle growth of polypropylene produced at 2 bar ethylene pressure and 40 ^{o}C polymerization temperature by the silica supported metallocene / MAO catalyst. The break-up of the silica supported catalyst during polymer formation was divided into three phases according to Fink and coworkers. The first stage is an induction period, where the olefin monomer is polymerized at the outer surface of the carrier (Figure 5-

20, A). The second is a polymer growth accompanied by the fragmentation of the supported catalyst (Figure 5-20, B). In the third stage, the polymer particle is expanded (Figure 5-20, C). Initially, an external polypropylene film generated through the polymerization starts at the surface and covers the silica-supported catalyst particle. With the ongoing polymerization, a shell-by-shell fragmentation process of the silica particle from the surface to the center occurs which is driven by the hydraulic forces of new polymer continuously produced at the accessible polymerization active centers. This fragmentation releases more and more active sites and the final situation is a completely fragmented particle.

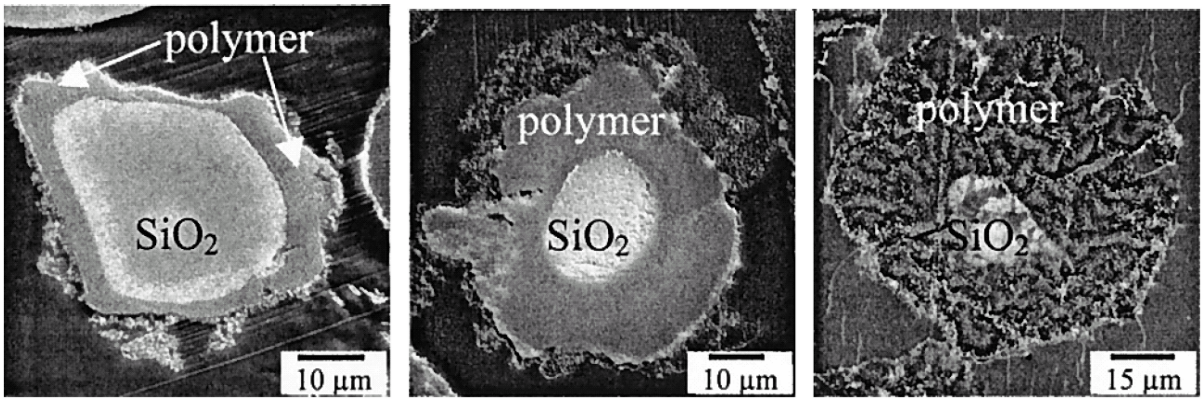

(A) (B) (C)

Figure 5-20. Stages of particle growth in the system of the silica supported catalyst: (A) in the induction period (~ 5 min), (B) in polymer growth (~30 min) and (C) in expansion (~50 min); scale bar – 10 µm (A and B) and 15 µm (C) [24]

5.3.3. Internal structure and surface morphology of PE single particles produced by the silica-supported catalyst

The internal structure of PE produced by the silica supported catalyst is investigated to compare the result from the catalyst supported on the nanosized PS beads. Figure 5-21 shows the internal structure in the PE single particle produced by the silica-supported catalyst. There are many sub-particles inside the PE particle and channels between each sub-particle. The dense red-colored and spherical particles are the fragmented catalyst and the black line is supposed to be a channel for monomer gas passing through. The sub-particles are 10 - 20 µm in size and have almost spherical shape. These channels having widths of 2 - 3 µm are considered to be originated from cracks on the PE surface. The sub-particle size and size distribution within the PE produced from the silica supported catalyst are different from

those of PE produced from the catalyst supported on the nanosized PS beads shown in Figure 5-16. In the case of the catalyst supported on the catalyst supported on the nanosized PS beads, the sub-particle size distribution is wide and the shape is non-uniform. On the other hand, the sub-particle size distribution is narrow and the shape is more uniform. To visualize the internal structure of polymer product by using TEM (transmission electron microscopy), many procedures are necessary such as the embedding of samples in an epoxy resin, curing the resin containing sample, cutting it with a diamond knife (Ultracut microtome) and then coating the cross-sectioned specimens with gold layer [25]. On the other hand, by laser scanning confocal fluorescence microscopy (LSCFM) it is simple to view the internal structure without destruction of the sample.

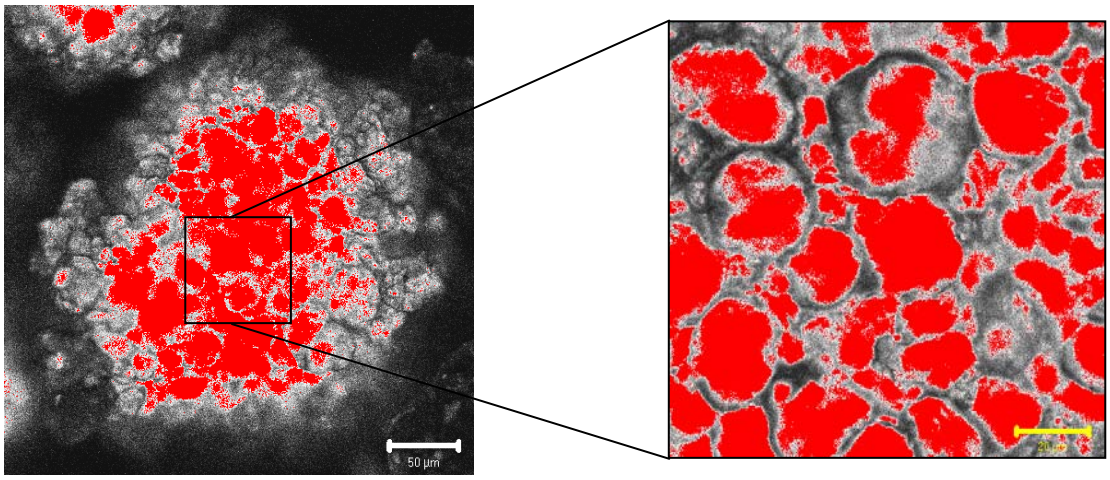

(A)

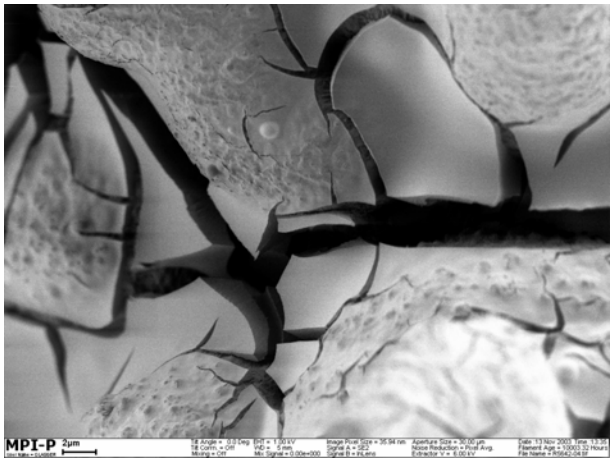

(B)

Figure 5-21. Confocal fluorescence image of internal structure (A) and SEM image of the surface structure (B) of single polyethylene (PE-76) particles produced by the silica-supported catalyst (scale bar – 2 µm)

Using SEM images of PE single particle, the morphology of the polyethylene product generated by the silica supported catalyst at different polymerization times is investigated in Figure 5-22. These images show surfaces of PE single particles obtained after 3, 5, 15 and 30 min polymerization. In the case of the first SEM image (A) of Figure 5-22, there are many small cracks and nodules on the surface of polyethylene (PE-75) produced after 3 min polymerization. After 5 min polymerization, there are also many cracks on the polyethylene (PE-76) surface in Figure 5-22 (B) however the surface is smoother than the polyethylene (PE-75) surface after 3 min polymerization. The size of the crack is about 1 – 2 μm and these cracks play the role of a channel through which monomer gas can go inside and meet the active metallocene catalyst. After 15 min polymerization, the cracks on the polyethylene (PE-77) are narrower than the previous one (Figure 5-22, C). There are small spheres but almost no cracks on the polyethylene (PE-79) surface after 30 min polymerization (Figure 5-22, D).

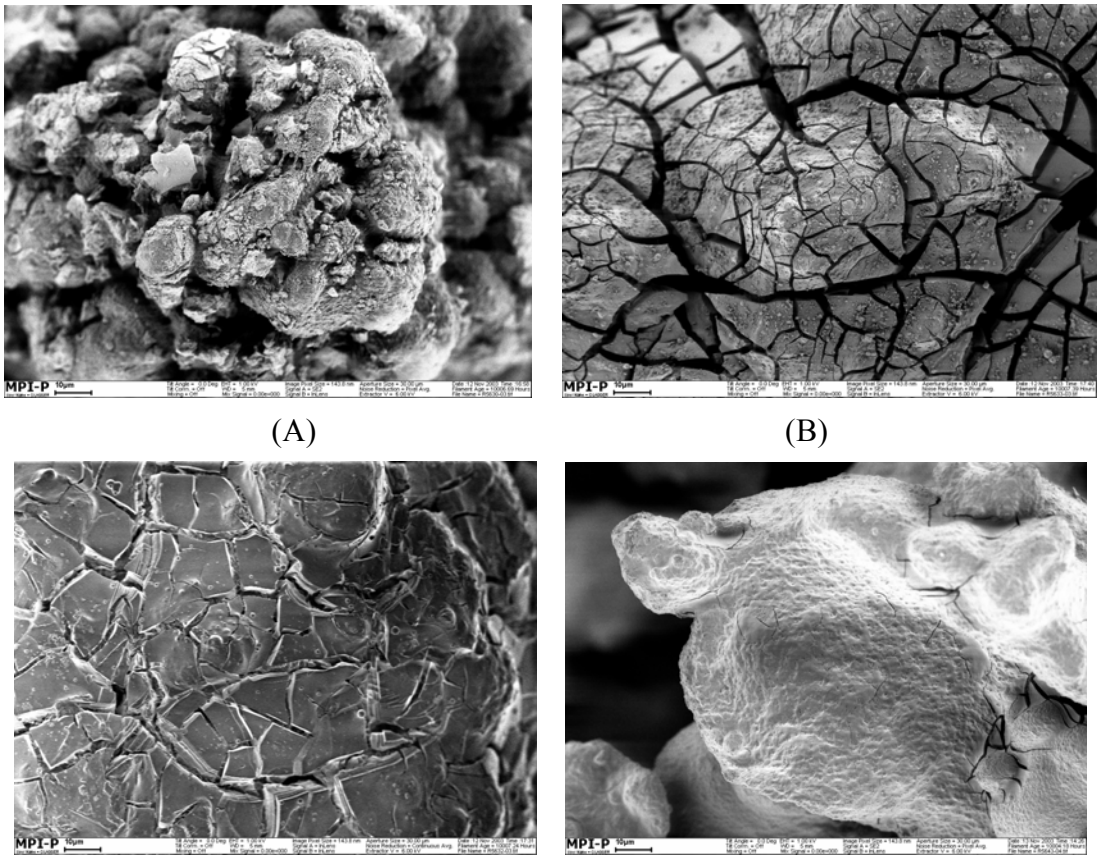

Figure 5-22. SEM micrographs of the surface structure of PE produced by the silica-supported catalyst after different reaction times; (A) PE-75 (3 min), (B) PE-76 (5 min), (C) PE-77 (15 min) and (D) PE-79 (30 min); scale bar – 10 μm

5.3.4. Summary

In the previous chapter, we used laser scanning confocal fluorescence microscopy to study the catalyst fragmentation and to visualize the internal structure of the PE single particles produced by the catalyst supported on the nanosized PS beads.

In this chapter, the silica-supported catalyst was stained with N,N′-bis(2,6-diisopropyl phenyl)-1,6,7,12-tetra(4-sulfonylphenoxy)perylene-3,4:9,10-tetracarboxdiimide to study the fragmentation behavior of the silica-supported catalyst and compare with the catalyst supported on the nanosized PS beads in ethylene polymerization. The silica-supported catalyst had a different fragmentation behavior in comparison with the catalyst supported on the nanosized PS beads. The catalysts supported on the nanosized PS beads fragmented inside and outside simultaneously. On the other hand, the silica-supported catalysts fragmented from the outside to the inside (layer-by-layer) of the PE particle (Figure 5-23).

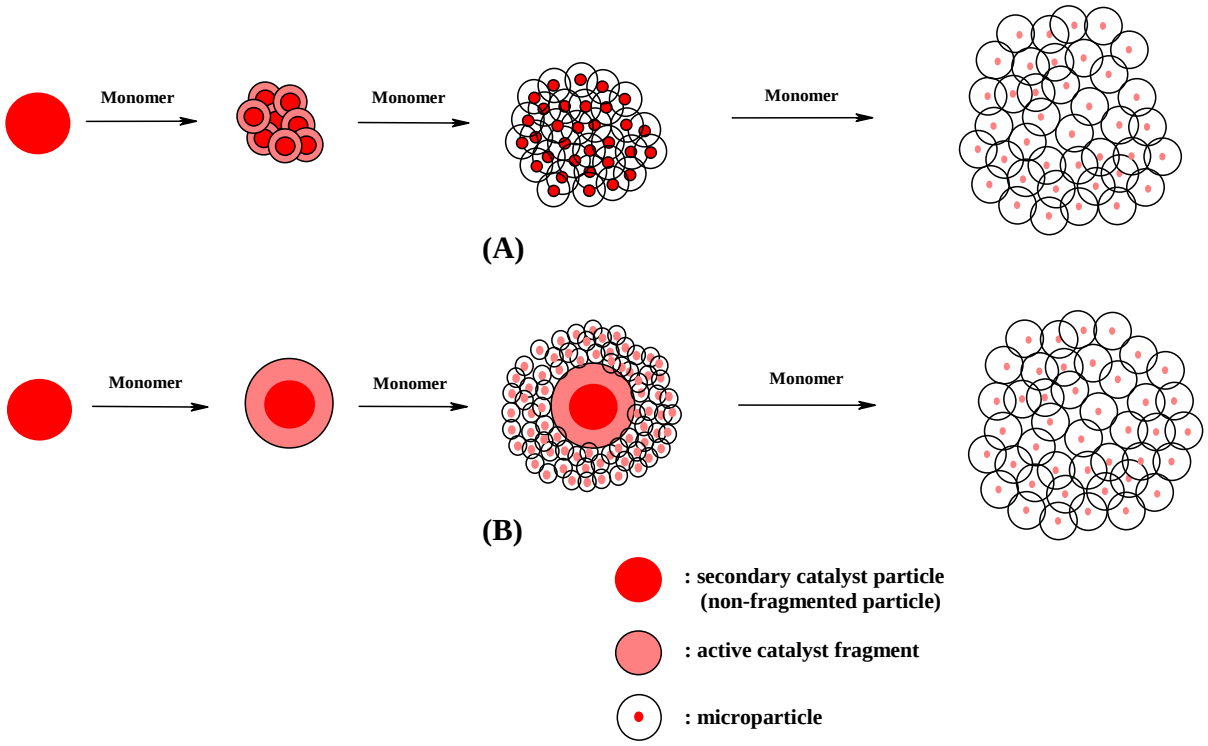

Figure 5-23. Particle growing progress of the different supported catalysts in ethylene polymerization; (A) the catalysts supported on the nanosized PS beads and (B) the catalysts supported on the silica

The sub-particle size and size distribution within the PE produced from the silica supported

catalyst were different from those of PE produced from the catalyst supported on the nanosized PS beads. These different fragmentation behaviors of the catalysts supported on the nanosized PS beads and silica reflect the different properties of the supported catalysts, i.e. the catalysts supported on the nanosized PS beads are more fragile than the silica supported catalyst.

5.4. Fragmentation of the catalyst supported on microsized polystyrene (PS) beads in ethylene polymerization

In chapter 4.2, the influence of the microsized PS beads on the ethylene polymerization and the morphology of the polyethylene product was studied. Each supported catalyst showed a different activity under the same reaction condition. Especially, the catalyst supported on the microsized PS beads showed lower activity than the other supported catalysts. In this chapter, the fragmentation of the catalyst supported on the microsized PS beads is investigated and compared with the fragmentation behavior of the other supported catalyst particles.

5.4.1. Preparation of microsized PS beads stained with dye and the catalyst supported on the dye-stained PS beads

Microsized PS beads stained with N,N′-bis(2,6-diisopropylphenyl)-1,6,7,12-tetra(4-sulfonyl phenoxy)perylene-3,4:9,10-tetracarboxdiimide were prepared to study the catalyst fragmentation in ethylene polymerization to compare with the results from the other supported catalysts. For this work, N,N′-bis(2,6-diisopropylphenyl)-1,6,7,12-tetra(4-sulfonyl phenoxy)perylene-3,4:9,10-tetracarboxdiimide prepared by Dr Christopher Kohl at the MPIP, previously used to stain the silica gel in the previous chapter, was used [26]. The swelling and shrinking properties of the polystyrene beads were used for staining the microsized PS beads (Scheme 5-5).

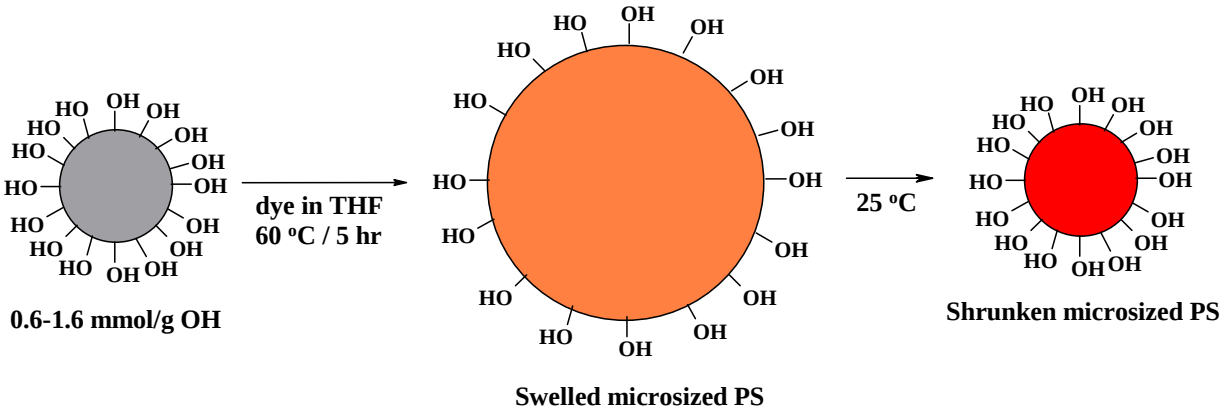

Scheme 5-5. The procedure of preparing the PS beads stained dye by swelling and shrinking process

The procedure for staining the microsized PS with dye was as follows: microsized PS functionalized with hydroxy groups was washed with methanol several times and dried for 48 hr. A saturated solution of the dye in THF was mixed with the polystyrene beads and stirred slowly at 50 ^{o}C for 5 hr to swell the PS and allow the dye to stain the inside of the PS beads. Then, the swollen PS beads were cooled down to room temperature and separated from the THF solution of the dye by filtration and the filtered beads were washed with chloroform. The chloroform solution was removed by decantation and this process was repeated several times. Initially the chloroform became slightly red due to mixing of the chloroform with the remaining THF / dye solution on the surface of the PS beads but after 5 washings with chloroform, the solvent remained colorless. The dye stained PS beads were then dried under vacuum. The microsized PS beads stained with dye were mixed with methylalumoxane (MAO) and stirred for 12 hr (Scheme 5-6). As the hydroxy groups of silica gel reacted with MAO, the dye was bound covalently. The metallocene / MAO solution was added and stirred slowly. The supported catalyst was washed with dry hexane / toluene mixture (50 / 50 Vol %) several times and dried under vacuum.

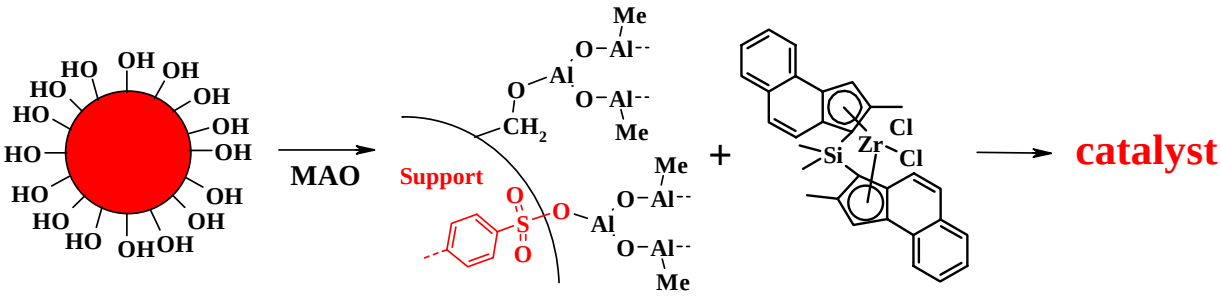

Scheme 5-6. The procedure of preparing the catalyst supported on the PS beads stained with dye [N,N′-bis(2,6-diisopropylphenyl)-1,6,7,12-tetra(4-sulfonylphenoxy)perylene-3,4:9,10-tetracarboxdiimide]

To compare the fragmentation result of the supported catalyst on the microsized PS beads functionalized with hydroxyl groups, nanosized PS beads tagged with N-(2,6-diisopropylphenyl)-9-(4-ethenylphenyl)perylene-3,4-dicarboximide and functionalized with the hydroxyl groups were prepared by miniemulsion polymerization (Scheme 5-7). The procedure of supporting the metallocene / MAO on the PS beads was the same as that in chapter 4.2.

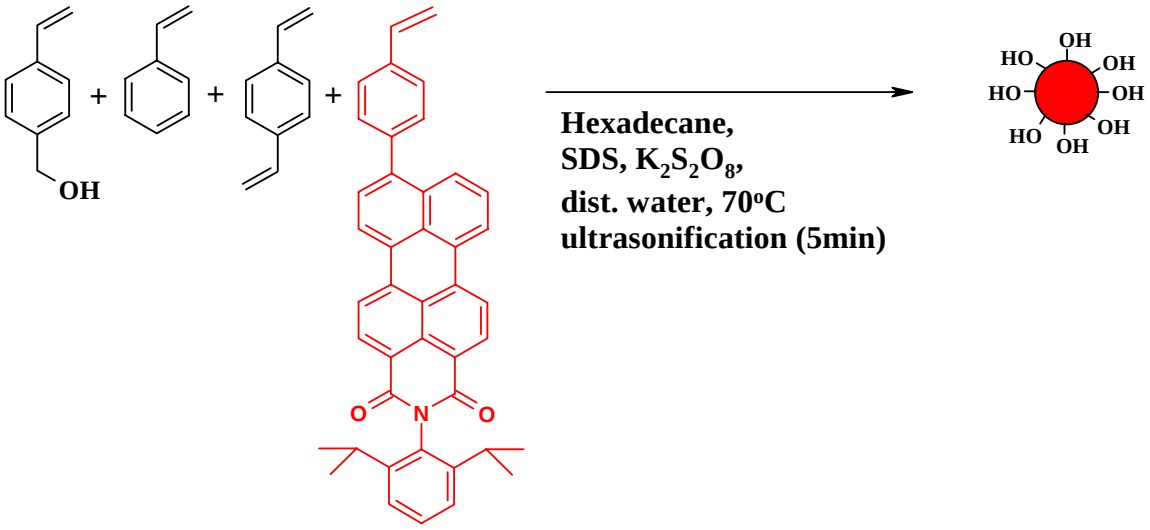

Scheme 5-7. The preparation of nanosized PS tagged with the dye [N-(2,6-diisopropylphenyl)-9-(4-ethenylphenyl)perylene-3,4-dicarboximide] and functionalized with hydroxyl groups

5.4.2. Ethylene polymerization and fragmentation of the catalyst supported on the nanosized PS beads within polyethylene particle

Ethylene polymerizations were carried out by using the catalyst supported on the microsized PS beads stained with dye at different polymerization times of 1, 2, 5, 10, 15 and 30 min at 70 °C and 40 bar (Table 5-6).

Table 5-6. Ethylene Polymerization [a] by the catalyst supported on the microsized PS stained with dye and functionalized hydroxyl groups depending on the polymerization time

Run	Zr/cat (μmol/g)	MAO/Zr	Time (min)	Activity (kg PE/mol Zr hr bar)	Productivity (g PE/g cat hr)
PE-81	40	350	1	- [b]	- [b]
PE-82	40	350	2	-	-
PE-83	40	350	5	840	1140
PE-84	40	350	10	530	720
PE-85	40	350	15	410	560
PE-86	40	350	30	350	480

[a] Reaction condition: 1 L autoclave, isobutane 400 ml, ethylene pressure 40 bar, 70 °C, amount of catalyst: 20 – 24 mg. [b] not enough material for measurement.

In this heterogeneous ethylene polymerization, 40 μmol / g metallocene activation and 350 MAO / Zr mol ratio were used. The polyethylene yields obtained after 1 and 2 min ethylene polymerization were so low that the catalyst activity could not be calculated. The activity and productivity of the catalyst supported on the microsized PS stained with dye is much lower than that of the catalyst supported on the nanosized PS tagged with dye (Table 5-7) - the same result as seen in the chapter 4.

Table 5-7. Ethylene Polymerization [a] by the catalyst supported on the nanosized PS tagged with dye and functionalized hydroxyl groups depending on the polymerization time

Run	Zr/cat (μmol/g)	MAO/Zr	Time (min)	Activity (kg PE/mol Zr hr bar)	Productivity (g PE/g cat hr)
PE-87	40	350	1	- [b]	- [b]
PE-88	40	350	2	-	-
PE-89	40	350	5	2590	3519
PE-90	40	350	10	2205	3000
PE-91	40	350	15	2040	2770
PE-92	40	350	30	1580	2200

[a] Reaction condition: 1 L autoclave, isobutane 400 ml, ethylene pressure 40 bar, 70 °C, amount of catalyst: 20 – 24 mg. [b] not enough material for measurement.

Polyethylene particles obtained from each polymerization were isolated using a 100 or 500 μm sieve and the distribution of the fluorescent dye within the PE particle was investigated with laser scanning confocal fluorescence microscopy.

Figure 5-24 shows fluorescence images of PE particles produced after the first minute of polymerization by using the catalysts supported on the microsized PS beads (A of Figure 5-24) and nanosized PS beads (B of Figure 5-24). In both pictures, there are red-colored particles and dispersed white / gray-colored areas. The red part represents less-fragmented catalyst particles and the white / gray part represents the fragmented catalyst within the polyethylene formed. In the case of the catalyst supported on the microsized PS beads (Figure 5-24, A), there is a dense red-colored part in the core of the PE particle and white / gray-colored part outside of each PE particle meaning that the fragmentation of the supported catalyst has started from the outside of the catalyst particles. In this image, the fragmentation

of the catalyst supported on the microsized PS beads is very similar to that of the silica-supported catalyst shown in Figure 5-13. On the other hand, in the case of the catalyst supported on the nanosized PS beads (Figure 5-24, B), the red-colored part is dispersed inside and outside of each PE particle. This differs from the results with the catalyst supported on the microsized PS beads and is similar to the result of the nanosized PS beads functionalized with PEO discussed in chapter 5.2.

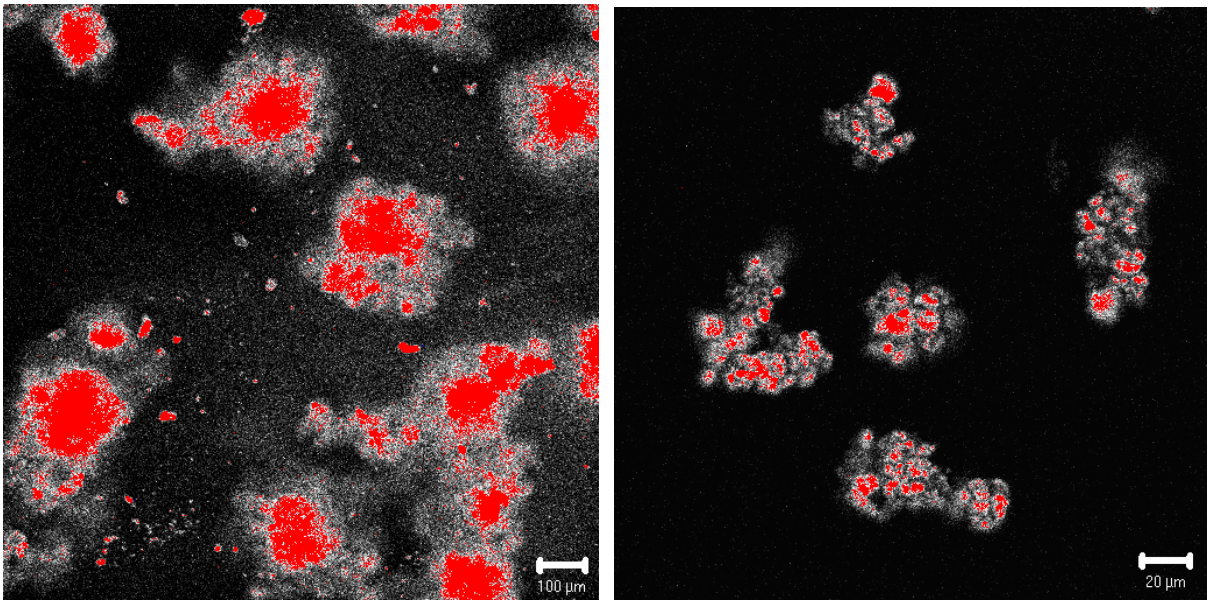

(A) (B)

Figure 5-24. Confocal fluorescence images of polyethylene particles obtained after 1 min polymerization; (A) polyethylene (PE-81) by the catalyst supported on the microsized PS beads and (B) polyethylene (PE-87) by the catalyst supported on the nanosized PS beads; scale bar – 100 µm (A) and 20 µm (B)

We also obtained more detailed fluorescence images of each single PE particle. Figure 5-25 shows the SEM image of PE particles and confocal fluorescence image of single PE particle produced by the catalyst supported on the microsized PS beads. After 5 min polymerization, the particle size of PE is about 200 µm which is bigger than the catalyst supported on the microsized PS having about 100 µm in size. The polyethylene particle is spherical as is the supported catalyst on the microszied PS beads (Figure 5-25, A). Figure 5-26 shows 40 confocal fluorescence images cross-sectioned optically at different depths of focus into single PE particle produced after 5 min polymerization. The outside of the supported catalyst particle is fragmented as shown by the white color between the broken

catalyst particles. However at the inside of the PE particle, the supported catalyst is not yet fragmented and shows a red color.

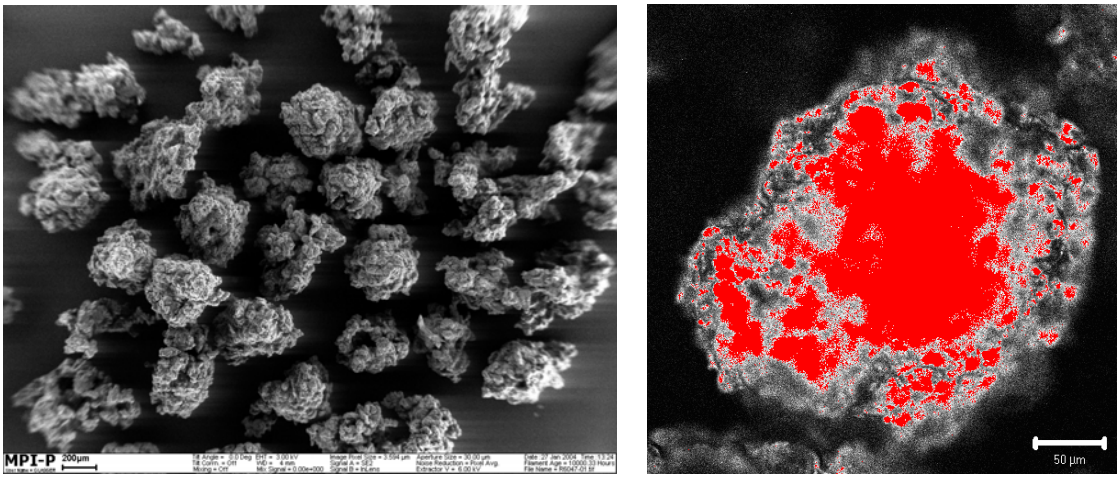

(A) (B)

Figure 5-25. SEM image of polyethylene (PE-89) particles (A) and confocal fluorescence image of the middle slice image of single polyethylene (PE-83) particle (B) obtained after 5 min polymerization; scale bar – 200 µm (A) and 50 µm (B)

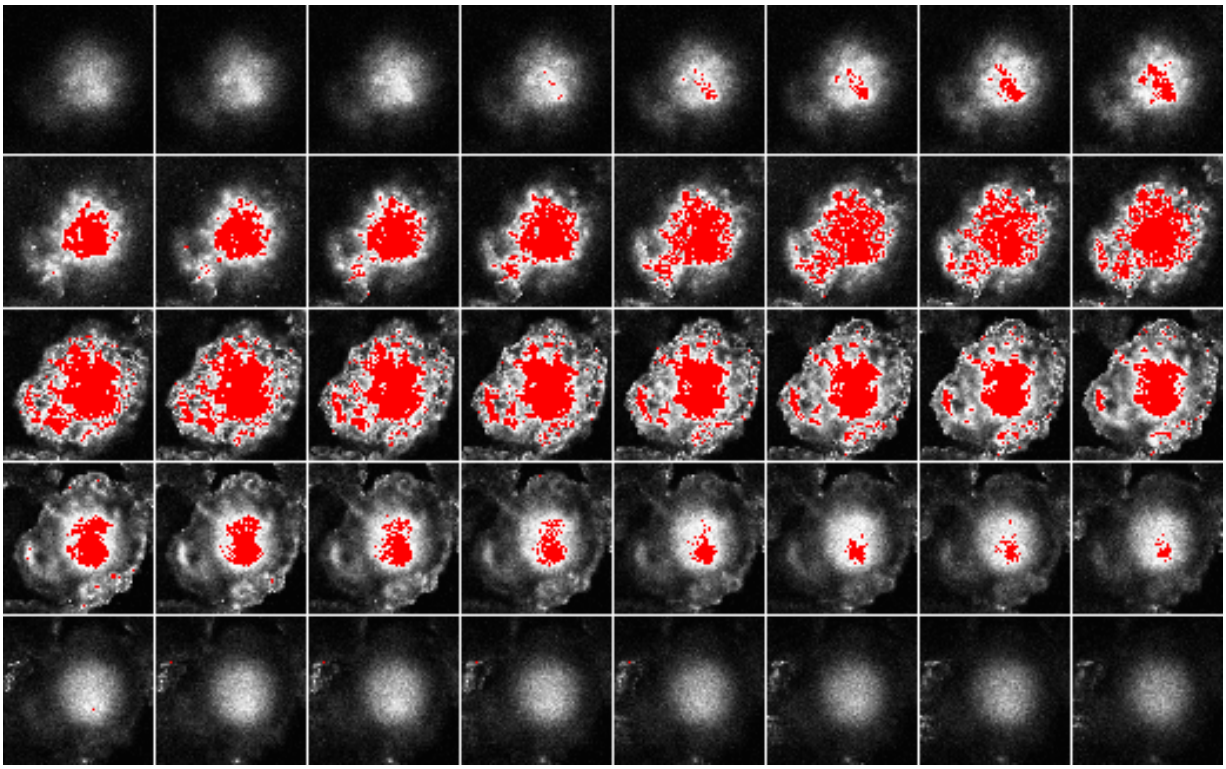

Figure 5-26. Confocal fluorescence image (40 slices) sectioned at different depths of focus into single polyethylene (PE-83) particle obtained after 5 min polymerization

After 10 min polymerization, the particle size increases and the supported catalyst particle is more fragmented from outside of PE particle than that produced after 5 min polymerization (Figure 5-27 ad 5-28).

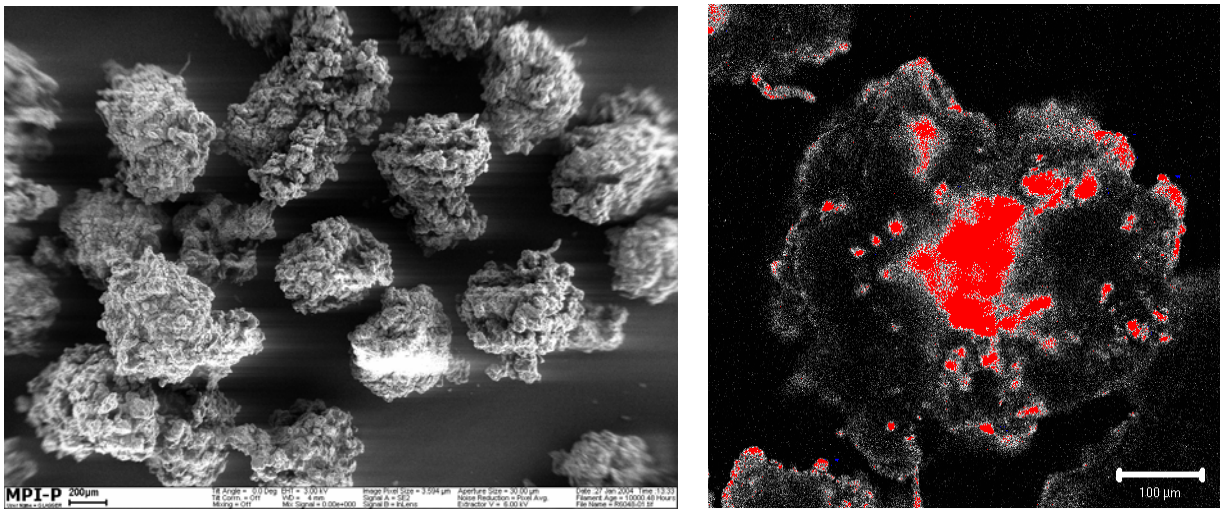

(A) (B)

Figure 5-27. SEM image of polyethylene (PE-84) particles (A) and confocal fluorescence image of the middle slice image of single polyethylene (PE-84) particles (B) obtained after 10 min polymerization; scale bar – 200 µm (A) and 100 µm (B)

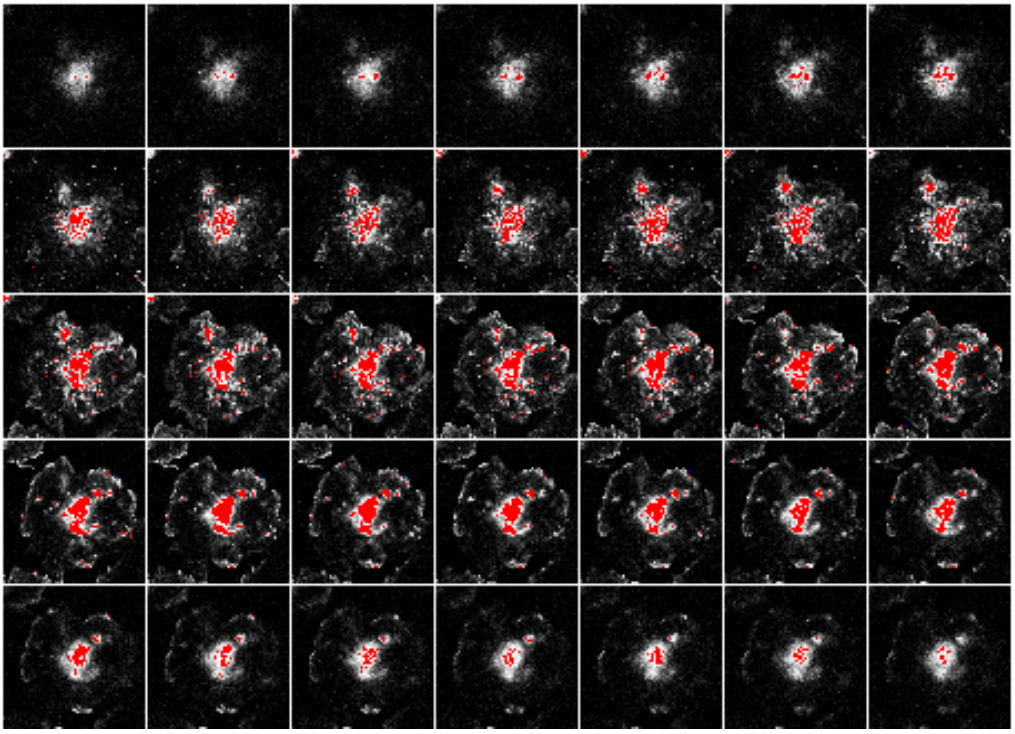

Figure 5-28. Confocal fluorescence image (35 slices) sectioned at different depths of focus into single polyethylene (PE-84) particle obtained after 10 min polymerization

In this fluorescence image of a single PE particle produced by this supported catalyst, the catalyst particle (dense-red particle) is unbroken in the core of polyethylene particle and the fragmented catalyst particles filled with polyethylene (white-colored spots) are on the outside of each PE particle. The catalyst supported on the microsized PS beads fragments within the PE particle gradually and the fragmentation process occurs in a layer-by-layer fashion. This fragmentation behavior of the catalyst supported on the microsized PS beads is similar to that of the silica-supported catalyst described in chapter 5.3.

In the case of the catalyst supported on the nanosized PS, the fragmentation behavior is different from the result of the catalyst supported on the microsized PS. Figure 5-29 shows SEM image and confocal fluorescence image of single PE particle produced by the catalyst supported on the nanosized PS beads produced after 2 min polymerization. In comparison with the shape of PE particle generated by the catalyst supported on the microsized PS, the PE particle shape shown in SEM image (A) of Figure 5-29 is non-uniform. In confocal fluorescence images of Figure 5-29 and 5-30, one can see that the supported catalyst is fragmented outside and inside evenly within the PE particle after just 2 min polymerization. At the inside and outside of a single PE particle, the supported catalyst (red color) is fragmented non-homogeneously and polyethylene (white and gray color) is visible between the supported catalysts. After 10 min polymerization (Figure 5-31 and 5-32), the supported catalyst is fragmented more homogeneously than after 5 min polymerization.

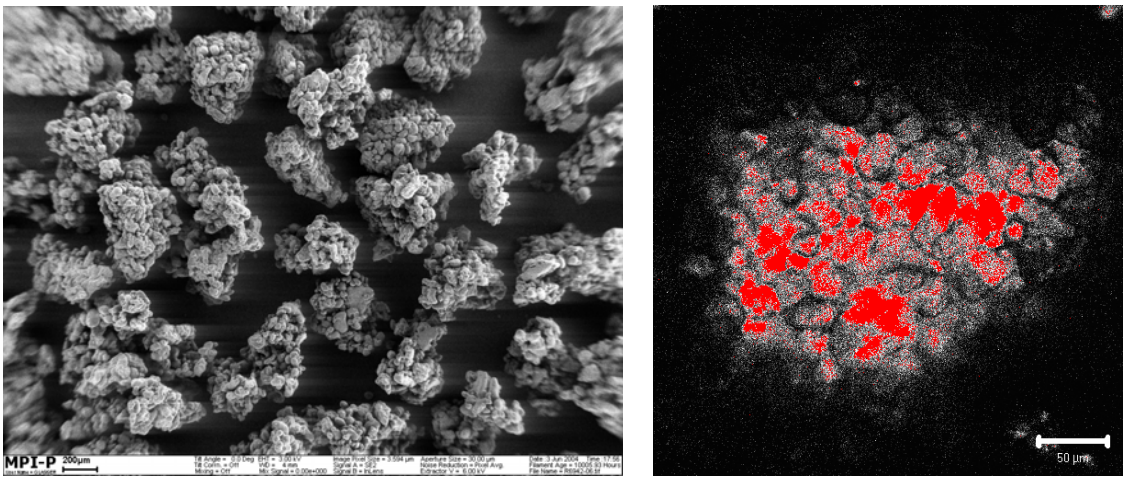

(A) (B)

Figure 5-29. SEM image of PE particle (A) and confocal fluorescence image of the middle slice image of single polyethylene (PE-88) particles (B) obtained after 2 min polymerization; scale bar – 200 µm (A) and 50 µm (B)

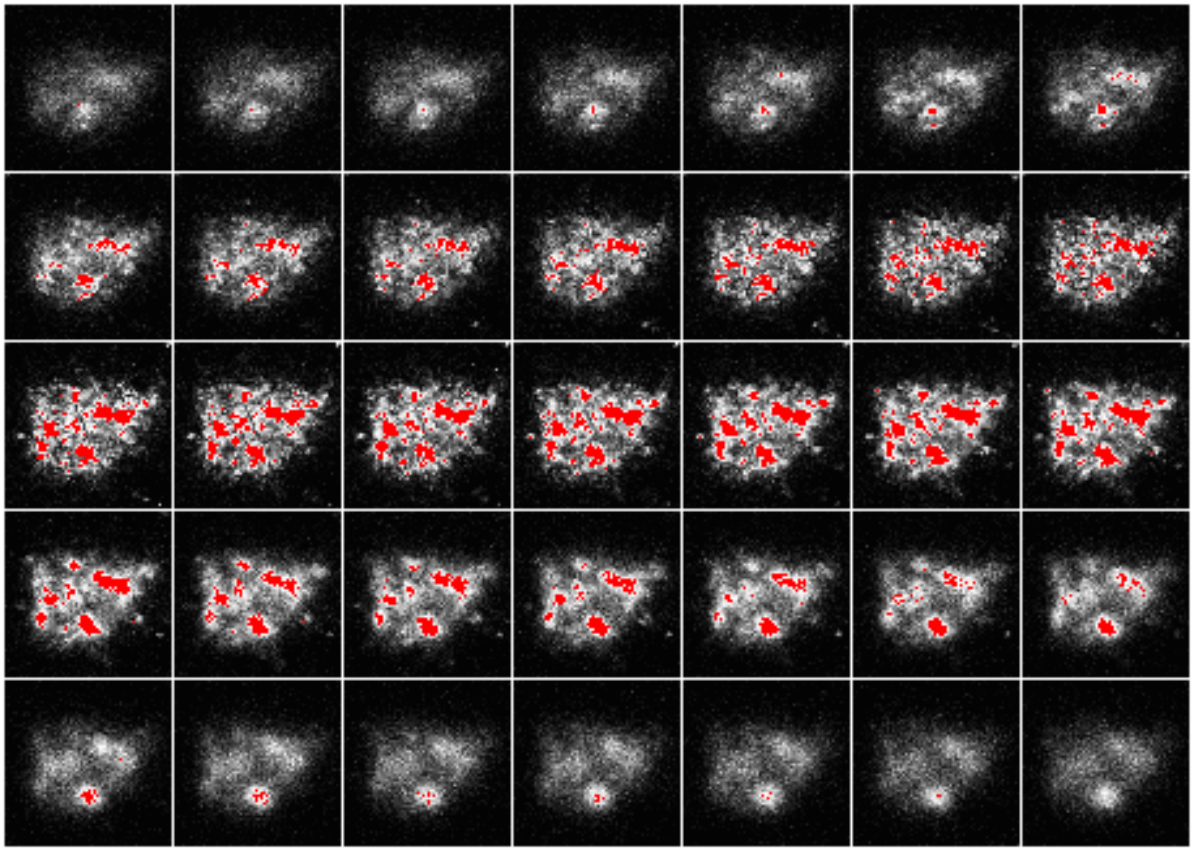

Figure 5-30. Confocal fluorescence image (35 slices) sectioned at different depths of focus into single polyethylene (PE-88) PE particle obtained after 2 min polymerization

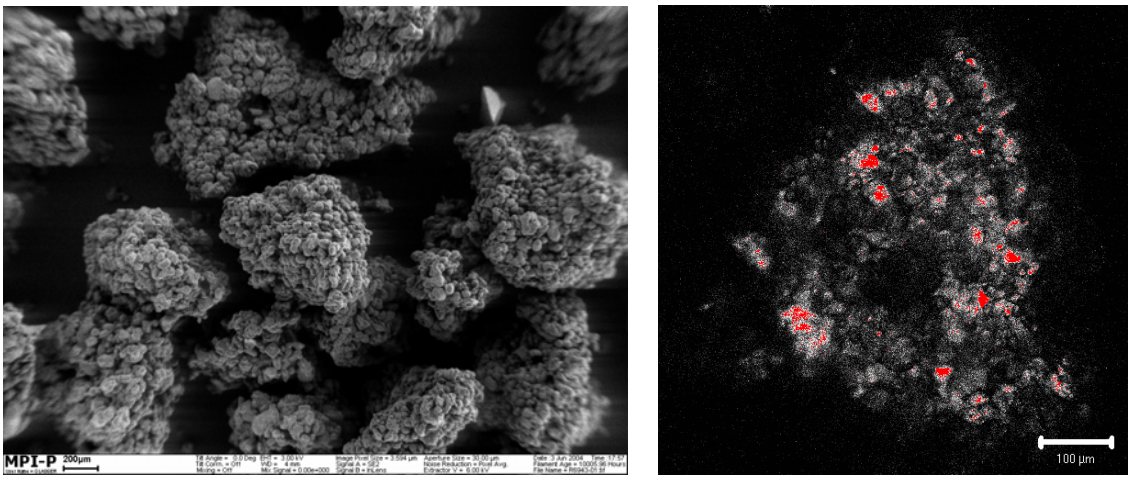

(A) (B)

Figure 5-31. SEM image of PE particle (A) and confocal fluorescence image of the middle slice image of single polyethylene (PE-90) particles (B) obtained after 10 min polymerization; scale bar – 200 µm (A) and 100 µm (B)

The number of dense-red particles within PE is reduced and the white / dark areas are

increased in comparison with the PE produced after 5 min polymerization. One can see few small red spots in the fluorescence image of PE single particle which means that the supported catalyst is almost totally fragmented and spread homogeneously within the PE particle after 10 min polymerization under 70 ^{o}C and 40 bar. These detailed fluorescence images show that the fragmentation behavior of the catalyst supported on the nanosized PS is different from that of the catalyst supported on the microsized PS beads and similar to that of the other nanosized PS beads.

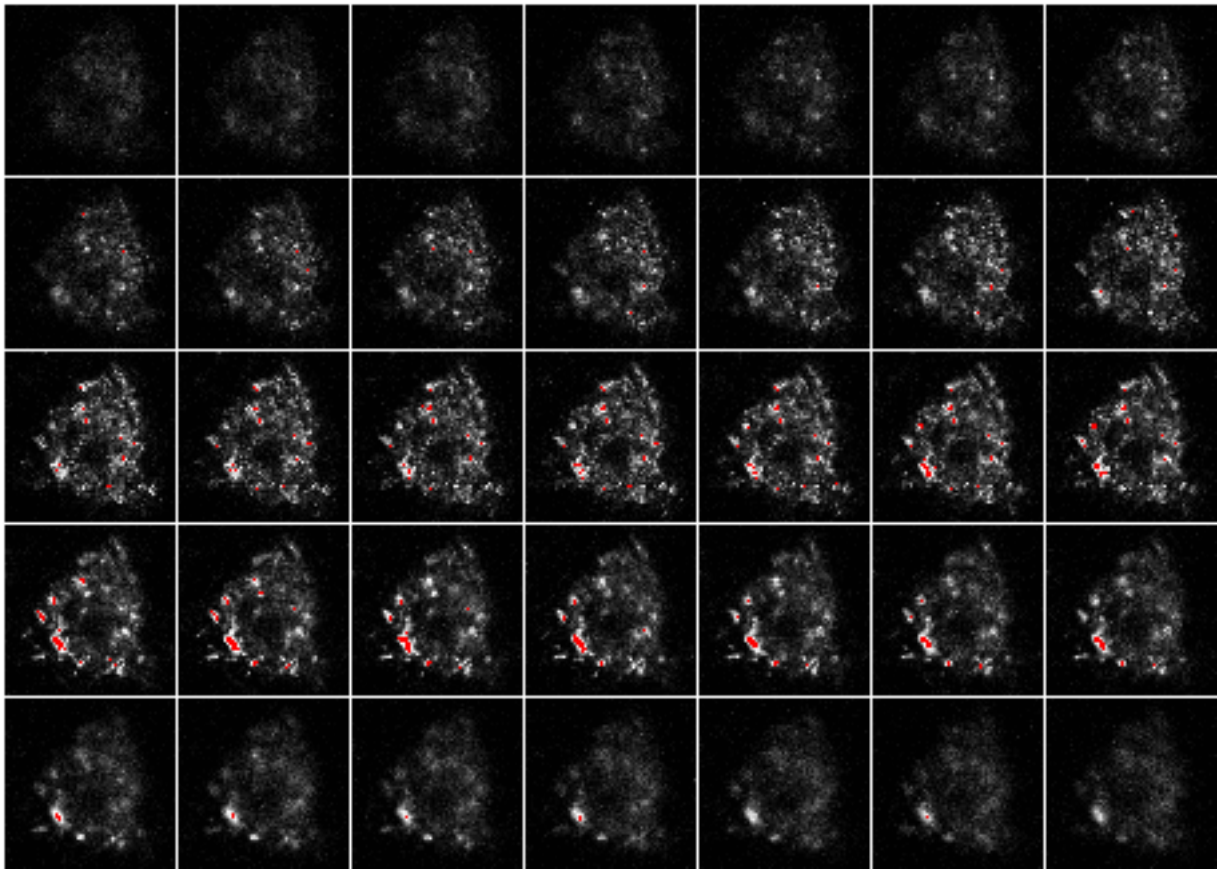

Figure 5-32. Confocal fluorescence image (35 slices) sectioned at different depths of focus into single polyethylene (PE-90) particle obtained after 10 min polymerization

Based on these results, the fragmentation behavior of the catalyst supported on the nanosized PS appears to be similar to the fragmentation behavior of the magnesium chloride supported Ziegler-Natta catalyst [26]. We compared more details of the internal structure of PE produced by the two catalysts supported on the microsized PS and nanosized PS beads. Figure 5-33 and 5-34 displays confocal fluorescence images of the internal structure of polyethylene single particles obtained by the catalyst supported on the nanosized PS and the

microsized PS supported catalyst after 5 min polymerization. In the image of Figure 5-33, there are narrow lines having 2 - 3 μm in width between the red-colored catalyst particles. The lines supposed to be channels for monomer gas are similar to those shown for the silica supported catalyst and the catalyst supported on the nanosized PS beads. On the other hand, there are no lines and no sub-particles within the PE produced by the catalyst supported on the microsized PS beads shown in Figure 5-34 because the microsized PS beads are one big primary particle without constituent nanosized particles.

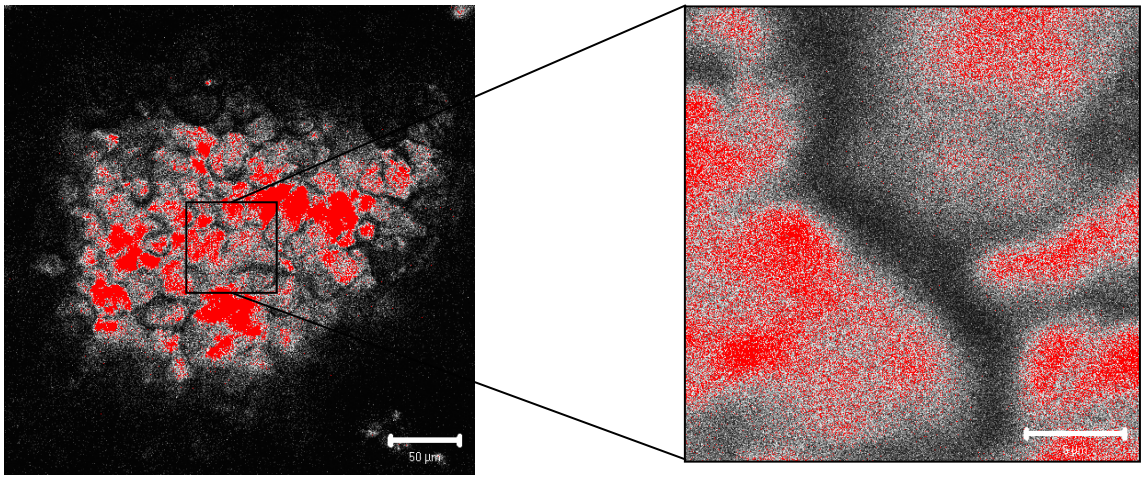

Figure 5-33. Confocal fluorescence image of the internal structure of single polyethylene (PE-88) particle obtained by the catalyst supported on the nanosized PS in 2 min polymerization

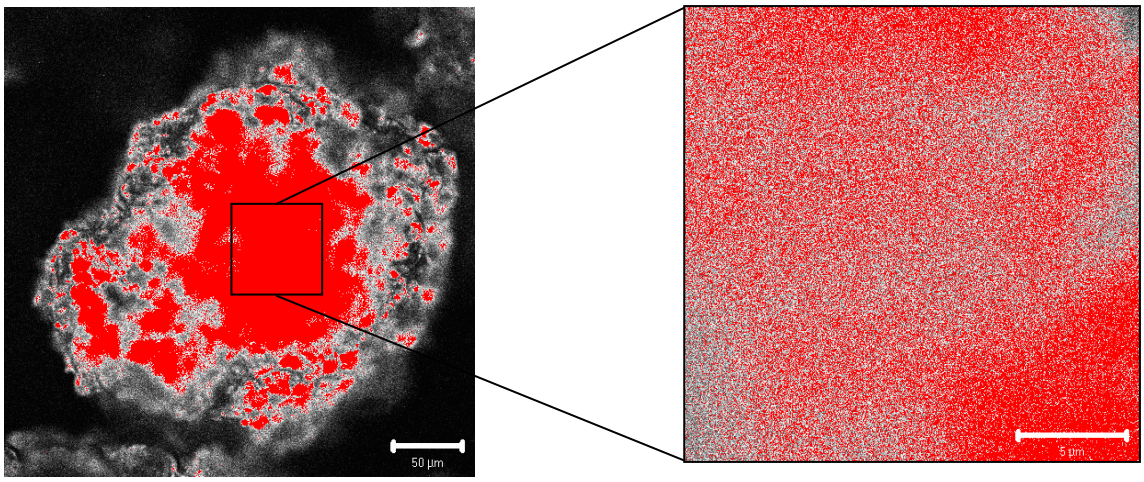

Figure 5-34. Confocal fluorescence image of the internal structure of polyethylene (PE-83) single particle obtained by the catalyst supported on the microsized PS beads in 5 min polymerization

SEM images in Figure 5-35 and Figure 5-36 show the surface morphology of a PE particle produced by the catalyst supported on the nanosized PS beads and the microsized PS beads in different polymerization time. In the case of the PE particle generated by the catalyst supported on the nanosized PS beads, many cracks are shown on the surface of PE obtained after 5 min polymerization in Figure 5-35 (A). After 10 min polymerization, the cracks in (B) of Figure 5-35 become smaller than the previous one in (A) of Figure 5-35. The morphology in this image shows that there are spherical particles on the PE surface between cracks which is different from Figure 5-35 (C) exhibiting a very smooth surface. Each spherical sub-particle is connected with the polyethylene strings produced after 15 min polymerization and the cracks on the surface of PE particle are filled with polyethylene product.

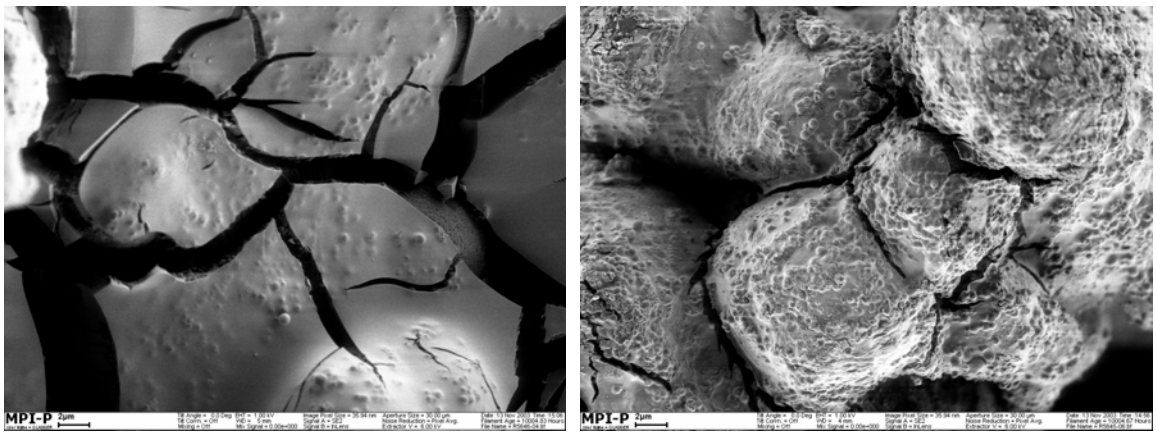

(A) (B)

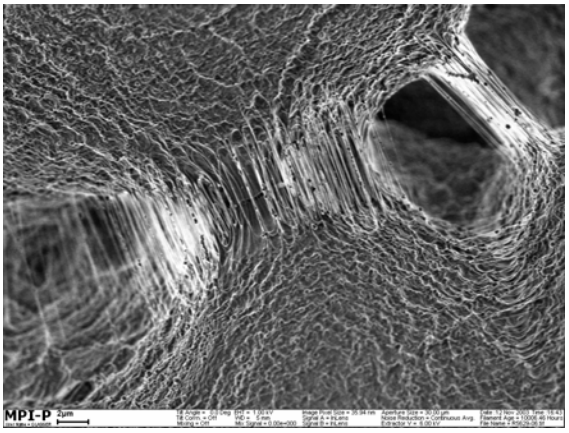

(C)

Figure 5-35. SEM micrographs of the surface structure of PE produced by the catalyst supported on the nanosized PS beads depending on the polymerization time; (A) PE-89 (5 min), (B) PE-90 (10 min) and (C) PE-91 (15 min); scale bar – 2 μm

On the other hand, on the surface of PE produced by the catalyst supported on the microsized PS beads after 5 min and 10 min polymerization, there are many cracks of about 0.5 to 3 μm width (Figure 5-36, A and B). There are no spherical sub-particles on the surface of the PE product unlike that from the catalyst supported on the nanosized PS. After 15 min polymerization, the cracks on the surface of PE particle are covered on the surface of the particle and filled with polyethylene product (Figure 5-36, C).

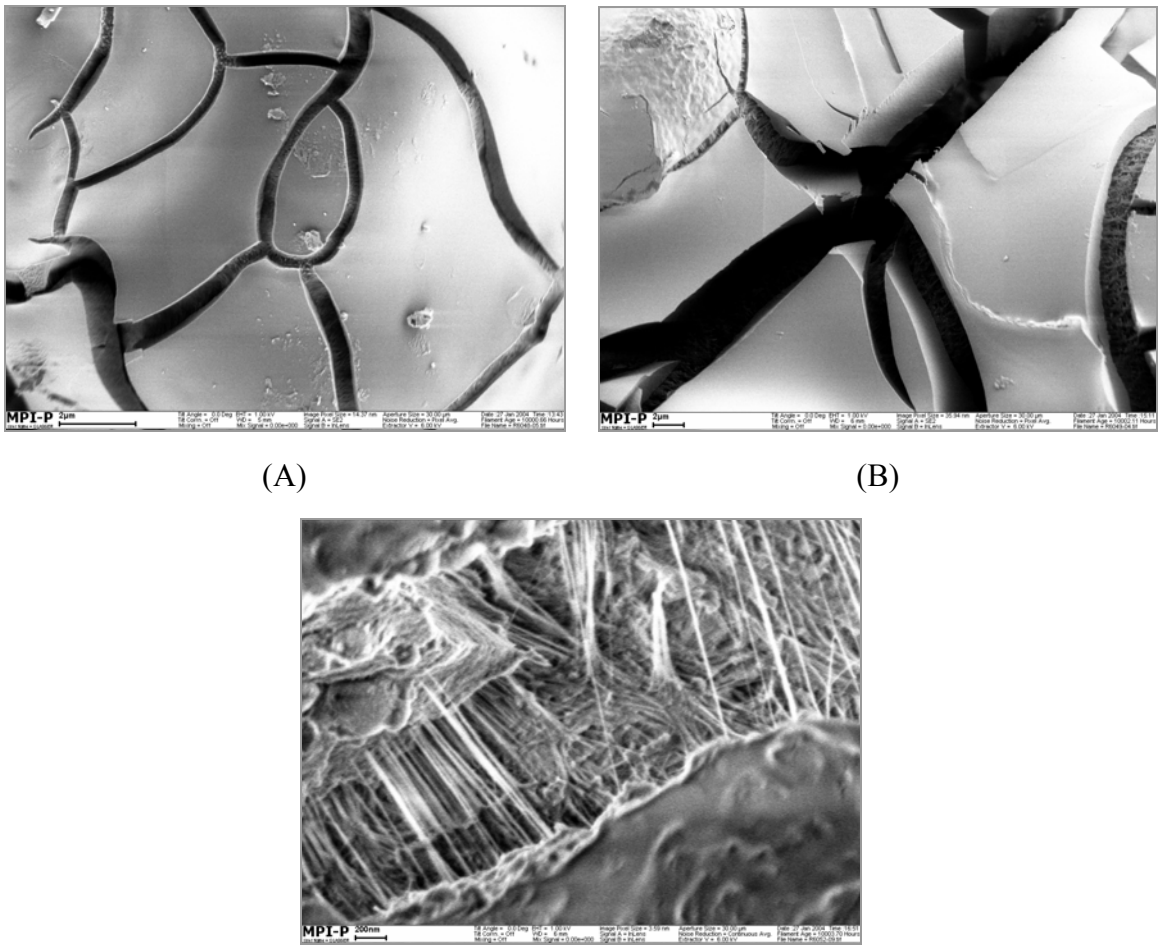

(A) (B)

(C)

Figure 5-36. SEM micrographs of the surface structure of PE produced by the catalyst supported on the microsized PS beads depending on the polymerization time; (A) PE-83 (5 min), (B) PE-84 (10 min) and (C) PE-85 (15 min); scale bar – 2 μm (A), 2 μm (B) and 200nm (C)

5.4.3. Summary

In this chapter, microsized PS beads stained with dye [N,N′-bis(2,6-diisopropylphenyl)-

1,6,7,12-tetra(4-sulfonylphenoxy)perylene-3,4:9,10-tetracarboxdiimide] were prepared to study their catalyst fragmentation in ethylene polymerization and to compare this with the results from the other supported catalysts. For staining the microsized PS beads, the swelling and shrinking property of the polystyrene beads were used. Also the nanosized PS beads tagged with dye [N-(2,6-diisopropylphenyl)-9-(4-ethenylphenyl)perylene-3,4-dicarboximide] and functionalized with the same groups (hydroxyl group) were prepared by miniemulsion polymerization to compare the fragmentation results of the catalyst supported on the microsized PS beads functionalized with hydroxyl groups.

The fragmentation behavior of the catalyst supported on the microsized PS beads was similar to that of the silica-supported catalyst, i.e. the supported catalyst fragmented from the outside to the inside (layer-by-layer) of the PE particle. However, the structure of sub-particles within PE produced from the catalyst supported on the microsized PS beads was different from that produced by the silica supported catalyst due to the different primary particle size of these supports. The fragmentation behavior of the catalyst supported on the microsized PS was different from that of the catalyst supported on the nanosized PS beads which fragmented inside and outside simultaneously at the initial polymerization time. Even if the support had the same chemical structure, the primary particle size influenced the catalyst fragmentation behavior in ethylene polymerization.

5.5. Fragmentation of dendrimer-supported catalyst in ethylene polymerization

In this chapter, dendritic perylenediimide core functionalized with polyethyleneoxide groups [$PDIG_2(PEO)_n$] is used as support in heterogeneous ethylene polymerization to study the fragmentation behavior of the dendrimer-supported catalyst. In the previous chapter 5.1 – 5.4, the process of loading a dye on the supports was necessary, but one can avoid this process mentioned above by using a dye-containing dendrimer. The dendrimer containing dye and functionalized with PEO was prepared by two Ph. D students - Roland Bauer and Vladimir Atanasov in our group at the Max-Planck Institute for Polymer Research.

5.5.1. Preparation of the dendrimer-supported catalyst

A polyphenylene dendrimer with a chemically bonded perylenediimide molecule in a focal point possessing 16 hydroxymethyl groups on its surface synthesized by Roland Bauer used as a multifunctional macroinitiator in anionic polymerization of ethylene oxide, which gives access to core-shell systems synthesized by a 'grafting-from' procedure from Vladimir Atanasov (Scheme 5-8). The procedure of supporting the metallocene / MAO on dendrimer containing dye and functionalized with PEO (Scheme 5-9) was the same as that given in chapter 4.4.

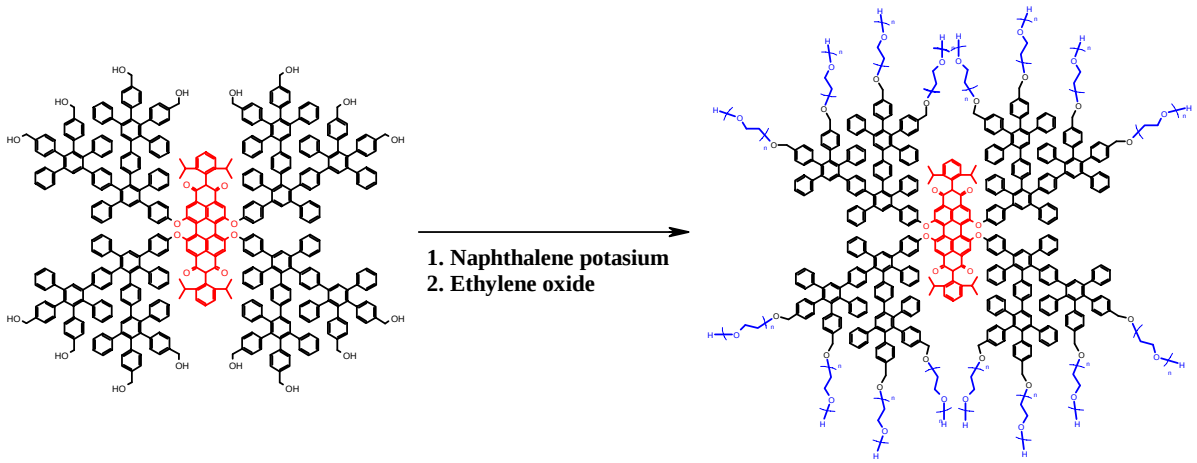

Scheme 5-8. Preparation of dendritic perylenediimide core functionalized with polyethyleneoxide groups [$PDIG_2(PEO)_n$].

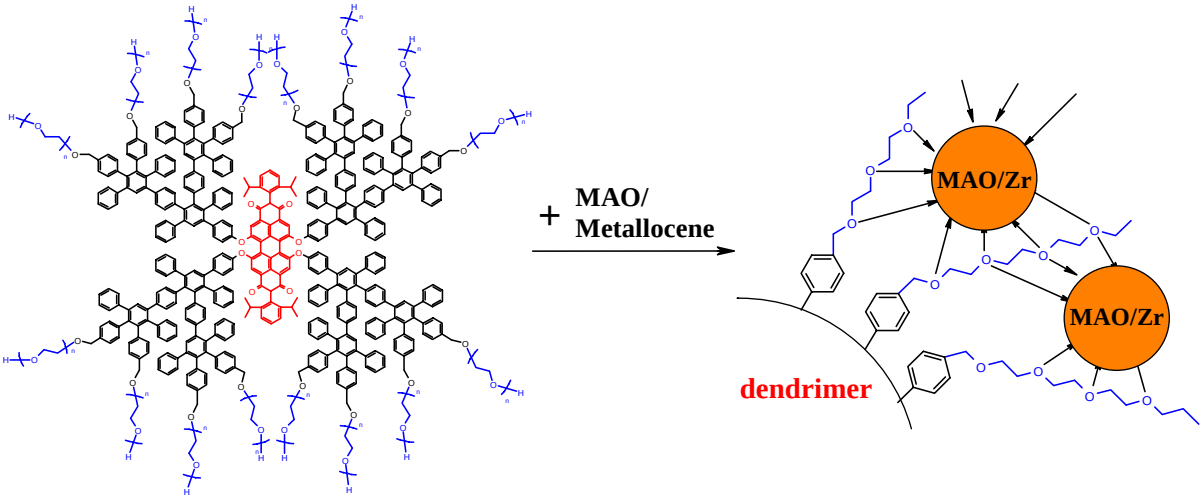

Scheme 5-9. Preparation of the catalyst supported on the dendritic perylenediimide core functionalized with polyethyleneoxide groups [$PDIG_2(PEO)_n$]

5.5.2. Ethylene polymerization and fragmentation study of the supported catalyst in PE single particle

Ethylene polymerization was also carried out at 70 ^oC polymerization temperature and 40 bar monomer gas pressure with the heterogeneous catalyst system ($Me_2Si(2MeBenzInd)_2$ $ZrCl_2$ / MAO supported on dendrimer with dye (Table 5-8). In this heterogeneous ethylene polymerization, 40 µmol / g metallocene activation and 350 MAO / Zr mol ratio were used.

Table 5-8. Ethylene Polymerization [a] by the catalyst supported on the dendritic perylenediimide core functionalized with polyethyleneoxide groups [$PDIG_2(PEO)_n$]

Run	Zr/cat (µmol/g)	MAO/Zr	Time (min)	Activity (kg PE/mol Zr hr bar)	Productivity (g PE/g cat hr)
PE-93	40	350	1	- [b]	-
PE-94	40	350	2	-	-
PE-95	40	350	5	-	-
PE-96	40	350	10	2110	2810
PE-97	40	350	15	1950	2620

[a] Reaction condition: 1 L autoclave, isobutane 400 ml, ethylene pressure 40 bar, 70 °C, amount of catalyst 20 mg. [b] not enough material for measurement.

The activity of the dendrimer supported catalyst is higher than that of the catalyst supported on the miscosized PS beads but lower than that of the catalyst supported on the nanosized PS beads. Polyethylene particles obtained by each polymerization were isolated using 100 or 500 μm sieves and the distribution of the fluorescent dye within the PE particles was investigated with laser scanning confocal fluorescence microscopy.

The fragmentation behavior of the dendrimer-supported catalyst (Figure 5-37 to 5-38) is similar to that of the catalyst supported on nanosized PS beads shown in from Figure 5-2 to 5-5. The catalyst fragmentation occurs inside and outside of the polymer particle (Figure 5-37, A and B). There are sub-particles within the confocal fluorescence image having about 5 – 10 μm size. After 10 min polymerization, the dendrimer-supported catalyst is fragmented and dispersed homogeneously within the PE particle (Figure 5-38, A and B). Though the laser scanning confocal fluorescence microscopy is useful for studying the internal structure of the PE single particle and the fragmentation of the supported catalyst within the PE particle, the difference of the fragmentation behavior between the dendrimer-supported catalyst and the catalyst supported on the nanosized PS beads could not be detected in these images. However, the florescence images emphasize the difference of the catalyst fragmentation between the nanosized supports (nanosized PS beads and dendrimer) and the microsized supports (silica and microsized PS beads).

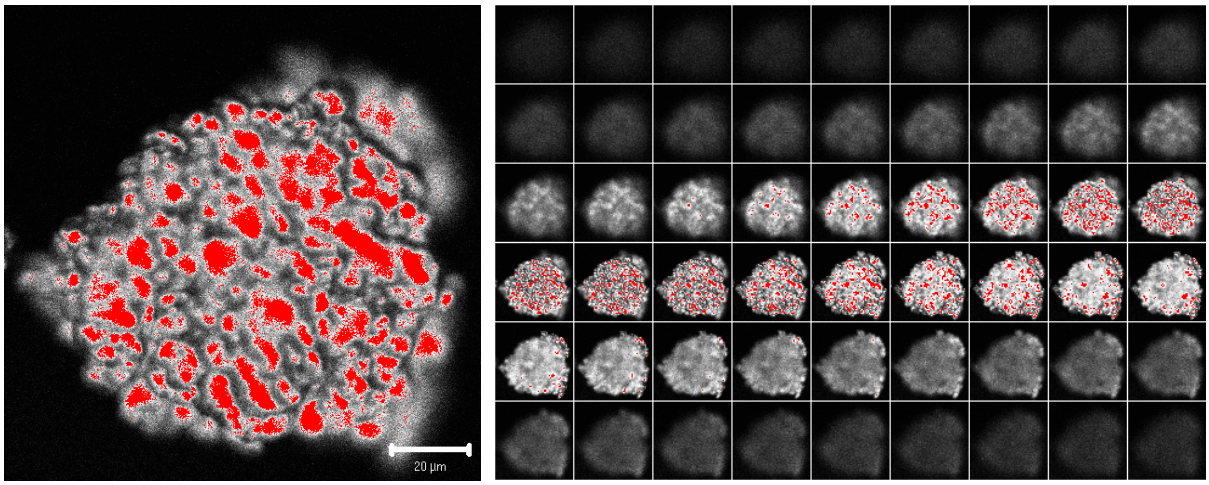

(A) (B)

Figure 5-37. Confocal fluorescence image of single PE particles (A) middle slice image and (B) 54 slice images sectioned at different depths of focus into single polyethylene (PE-94) particle obtained after 2 min polymerization (scale bar – 20 μm)

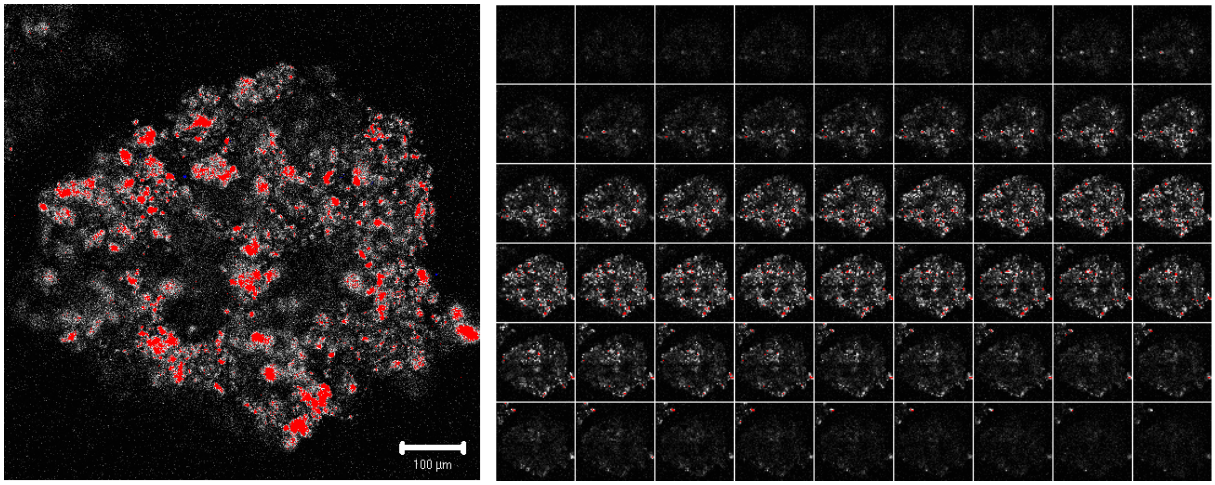

(A) (B)

Figure 5-38. Confocal fluorescence image of single PE particles (A) middle slice image and (B) 54 slice images sectioned at different depths of focus into single polyethylene (PE-96) particle obtained after 10 min polymerization (scale bar – 100 µm)

Figure 5-39 exhibits confocal fluorescence images of the internal structure of single polyethylene (PE-95) particles obtained by the dendrimer supported catalyst in 5 min polymerization.

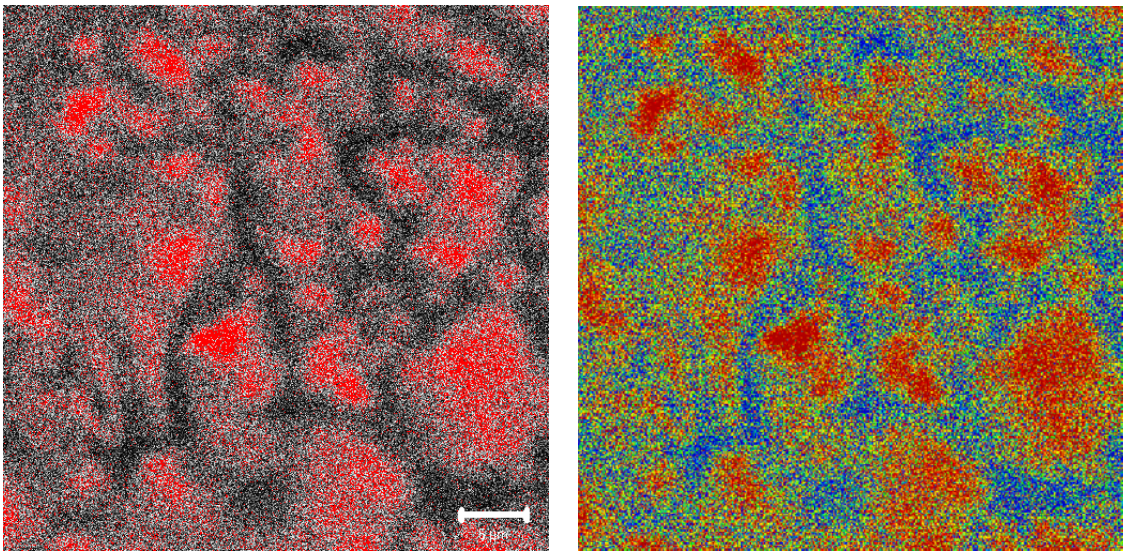

(A) (B)

Figure 5-39. Laser scanning confocal fluorescence image of the internal structure of polyethylene (PE-95) single particle obtained by the dendrimer supported catalyst in 5 min polymerization; (A) original fluorescence image and (B) color-modified fluorescence image (scale bar – 5 µm)

There are narrow lines having 2 - 3 μm between the red-colored catalyst particles which is similar to those in the products from the catalysts supported on the nanosized PS beads. The sub-particle shape of the dendrimer supported catalyst in the fluorescence image is not globular which is different from the sub-particle shape of the catalyst supported on the nanosized PS beads shown in Figure 5-6 and Figure 5-39.

5.5.3. Summary

In this chapter, the fragmentation of the dendrimer-supported catalyst was introduced. The dendritic perylenediimide core functionalized with polyethyleneoxide groups [$PDIG_2(PEO)_n$] as a probe was useful to study the catalyst fragmentation within PE single particle in fluorescence image because the procedure of staining support was avoided. The fragmentation behavior of the dendrimer-supported catalyst was similar to that of the catalyst supported on nanosized PS beads. The catalyst fragmentation occurred inside and outside of the polymer particle. It can be concluded that the fragmentation process of the nanosized PS beads and dendrimer supported catalyst are similar to that of Ziegler-Natta catalyst supported on $MgCl_2$ because these supported catalyst particles are friable in olefin polymerization.

1. P. Galli and G. Vecellio, *Prog. Polym. Sci*., **2001**, 26, 1287.

2. J. H. Z. dos Santos, H. T. Ban, T. Teranishi, T. Uozumi, T. Sano and K. Soga, *J Mol. Catal. A: Chem.*, **2000**, 158, 541.

3. G. G. Hlatky, Coord. *Chem. Rev*., **2000**, 199, 235.

4. B. Steinmetz, B. Tesche, C. Przybyla, J. Zechlin and G. Fink. *Acta Polym*., **1997**, 48, 392.

5. G. B. Galland, M. Seferin, R. Guimarães, J. A. Rohrmann, F. C. Stedile and J. H. Z. dos Santos; *J Mol. Catal. A: Chem*., **2002**, 189, 233.

6. J. H. Z. dos Santos, H. T. Ban, T. Teranishi, T. Uozumi, T. Sano and K. Soga, *Appl. Catal. A*, **2001**, 220, 287.

7. P. Blais, R. St. John Manley, *J. Polym. Sci., Polym. Chem Ed.,* **1971**, 196, 64.

8. J. Y. Guttman and J. E. Guillet, *Macromolecules*, **1968**, 1, 461.

9. A. Keller, F. M. Willmouth, *Makromol. Chem*., **1969**, 121, 42.

10. H. D. Chanzy, R. H. Marchessault, *Macromolecules*, **1969**, 2, 108.

11. R. T. K. Baker, P. S. Harris, R. J. Waite and A. N. Roper, J. *Polym. Sci. Polym. Lett. Ed.,* **1973**, 11, 45.

12. Z. Ye, H. Alsyouri, S. Zhu and Y. S. Lin; *Polymer*, **2003**, 44, 969.

13. G. Fink, B. Steinmetz, J. Zechlin, C. Przybyla and B. Tesche *Chem. Rev*., **2000**, 100, 1377.

14. A. Alexiadis, C. Andes, D. Ferrari, F. Korber, K. Hauschild, M. Bochmann, G. Fink, *Macromol. Mat. Eng*., **2004**, 289, 457.

15. S. Knoke, F. Korber, G. Fink, B. Tesche, *Macromol. Chem. Phy*., **2003**, 204, 607.

16. F. Bonini, V. Fraaije, G. Fink, *J. Polym. Sci. Part A*, **1995**, 33, 2393.

17 Zeno Földes-Papp, Ulrike Demel and Gernot P. Tilz, International Immunopharmacology, 2003, 13, 1715.

18. Martin Stork, Dissertation, Johannes Gutenberg Universitat, Mainz, **2000**.

19. M. Koch, A. Falcou, N. Nenov, M. Klapper and K. Müllen, *Macromol. Rapid. Commun*., **2001**, 22, 1455.

20 C. Martin and T. F. McKenna, *Chem. Eng. J.,* **2002**, 87, 89-

21. M. A. Katz, *Microvascular Research*, **1978**, 16, 316.

22. Christopher Kohl, Dessertation, Johanes Gutenberg universität, Mainz, **2003**.

23. R. Goretzki, G. Fink, B. Tesche, B. Steinmetz, R. Rieger, W. Uzick, *J. Polym. Sci. A: Polym. Chem*., **1999**, 677, 37.

24. G. Fink, B. Tesche, F. Korber, S. Knoke, *Macromol. Symp.*, **2001**,173, 77.

25. R. Goretzki, G. Fink, B. Tesche, B. Steinmetz, R. Rieger, W. Uzick, *J. Polym. Sci. Part A*, **1999**, 37, 677.

26. T. F. McKenna, D. Cokljat, R. Spitz and D. Schweich, *Catalysis Today*, **1999**, 48, 101.

Chapter 6. Summary and conclusions

The aim of the current work was the synthesis of well-defined, spherical and nanosized polymer beads as supports for the immobilization of metallocene catalysts. These demands required a homogeneous distribution of metallocene catalysts on the carrier and the homogeneous fragmentation of the supported catalyst within the polyolefin products. For this objective, several nanosized PS beads were introduced. The nanosized PS beads had several functional groups on the surface such as polyethyleneoxide (PEO), polypropyleneoxide (PPO) and hydroxyl groups for immobilizing the metallocene catalyst and MAO (Scheme 6-1). The influence of nanosized PS beads as a catalyst carrier on the catalyst activity and the characteristics of the produced polyolefin such as molecular weight and morphology were investigated. To compare the results of the nanosized PS beads in heterogeneous olefin polymerization, microsized PS beads, silica and dendrimers were also used as catalyst carriers. The fragmentation behavior of the different supports was studied by laser scanning confocal fluorescence microscopy.

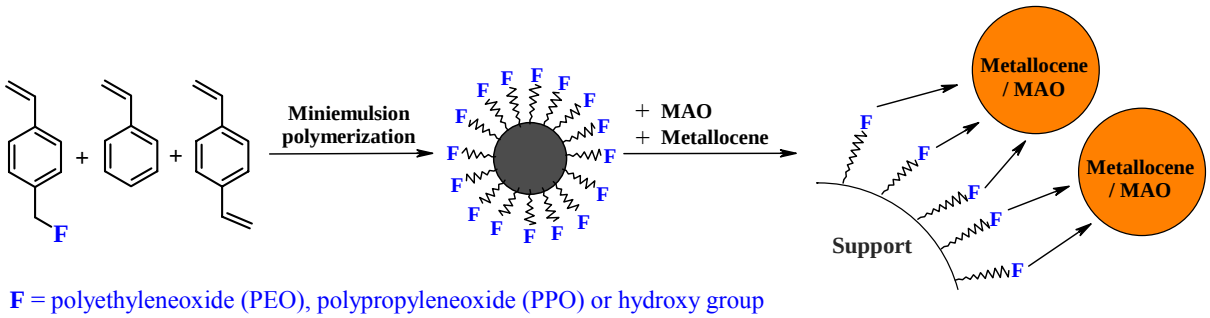

F = polyethyleneoxide (PEO), polypropyleneoxide (PPO) or hydroxy group

Scheme 6-1. Preparation of the nanosized PS beads functionalized with PEO or PPO and the immobilization process with MAO and metallocene

As a first catalyst carrier, nanosized polystyrene (PS) beads functionalized with polyethyleneoxide (PEO) were prepared by miniemulsion polymerization. As the PEO shell of the nanosized particles consisted of nucleophilic ether groups, immobilization via a non-covalent bonding of the MAO / metallocene complexes was achieved. Figure 6-1 shows the SEM images of nanosized PS beads and the supported catalyst particle. Several nanosized PS beads functionalized with varying concentrations of PS-co-PEO were prepared to study the influence of PEO concentration of the nanosized PS beads on the catalyst behavior. As the concentration of polyethyleneoxide (PEO) on the surface of PS beads was increased, the

catalyst activity decreased but the bulk density of the polyethylene increased.

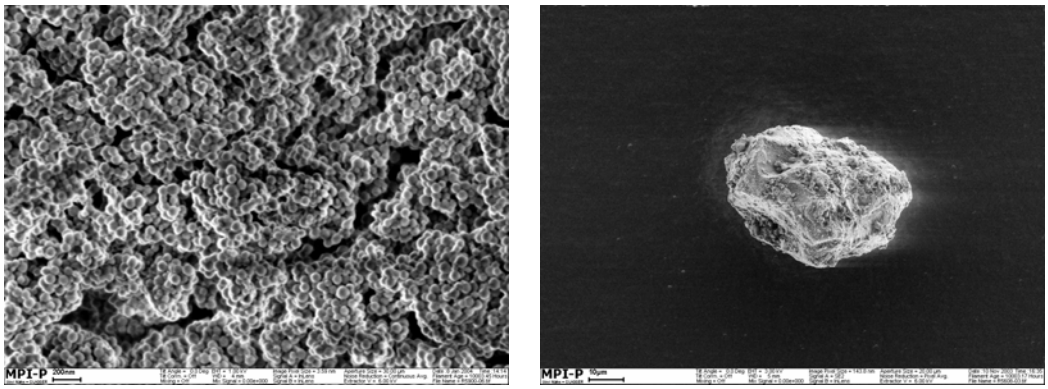

(A) (B)

Figure 6-1. SEM images of nanosized PS beads functionalized with polyethyleneoxide (PEO) (A) and the catalyst supported on the nanosized PS beads

To confirm the behavior of the catalyst supported on the nanosized PS beads, nanosized PS beads functionalized with polypropyleneoxide were prepared and the influence of the concentration of polypropyleneoxide (PPO) on the nanosized polystyrene (PS) on ethylene polymerizations was investigated. Polypropyleneoxide (PPO) on the nanosized PS beads is less hydrophilic than polyethyleneoxide (PEO) but still possesses the nucleophilic ether groups for the immobilization of the metallocene complexes. The immobilization of metallocene catalyst on the nanosized polystyrene beads functionalized with polypropyleneoxide was sufficient for use in heterogeneous ethylene polymerization. Several PS beads with varying concentrations of polypropyleneoxide (PPO) chain on the PS beads were prepared. As the concentration of polypropyleneoxide (PPO) chains on the PS beads was increased, the catalyst activity in ethylene polymerization decreased. However, the bulk density of the polyethylene obtained was greatly improved. These results were explained by the interaction between functional groups on the support and the metallocene complex and the different fragmentation behavior of the catalysts supported on the PS beads. Upon increasing the concentration of functional groups on the support, the interaction between functional groups and the metallocene complex is strongly increased which makes monomer diffusion into the supported catalyst particle more difficult and hinders the fragmentation of the catalyst particles.

To investigate the applicability of the catalyst supported on the nanosized PS beads in heterogeneous olefin polymerization, copolymerizations of ethylene with several

comonomers (1-hexene, 1-octene, 1-decene or norbornene) and propylene polymerizations were carried out. As the comonomer content increased, there was a decrease in the degree of crystallinity and the melting temperature for the ethylene / α-olefin copolymers. The copolymers from copolymerization of ethylene with aliphatic monomer (1-hexene, 1-octene and 1-decene) were obtained as spherical beads and the morphology of copolymers was good. On the other hand, the copolymers from copolymerization of ethylene with norbornene monomer were rubber-like materials even if using supported catalysts. In the case of the propylene polymerization, two different metallocene catalysts were used in homogeneous and heterogeneous polymerization.

$Ph_2C(2,7\text{-}Bu_2Flu)(Cp)ZrCl_2$ catalyst system in homogeneous and heterogeneous polymerization produced high syndiotactic polypropylenes. The supported catalyst system influenced slightly the stereoregularity of PP obtained. The morphology of polypropylene particles produced from heterogeneous polymerization was good and well defined. In the case of the bis[η^5-1-(5-methyl-2-furyl)indenyl]$ZrCl_2$ catalyst system, the different catalyst systems in homogeneous and heterogeneous polymerization influenced also the stereoregularity of the obtained elastomeric PPs. These two elastomeric polypropylenes produced by homogeneous and heterogeneous polymerization showed different hysteresis property. The more highly isotactic polypropylenes obtained from the heterogeneous catalyst system had lower elastomeric properties compared to those made by the homogeneous catalyst system.

The influence of different supports on the catalyst behavior in ethylene polymerization and the properties of the polyethylene such as morphology were investigated. Four kinds of supports were used for this investigation; microsized PS beads functionalized with hydroxyl groups, nanosized PS beads functionalized with hydroxyl groups, silica gel and dendrimer [$PDIG_2(PEO)_n$] (Figure 6-2). The primary particle size of these supports ranged from 10 nm to 100 μm. These different particle sizes and the surface morphology of the supported catalyst strongly influenced the surface microstructure of polyethylene product and the catalyst behavior in heterogeneous ethylene polymerization. The surface morphology of the polyethylene product generated by the catalyst supported on the microsized PS beads was as smooth as the supported catalyst. On the other hand, the surface microstructure on the silica supported catalyst was retained in the resulting polyethylene product which maintained a spherical particle shape having a diameter of about 20 μm. The dendrimer supported catalysts had a different surface morphology in comparison with that of the supported catalyst on the

nanosized PS beads, namely a smoother surface structure than that of the catalyst supported on the nanosized PS. Even if the dendrimer supported catalyst was constituted of nanosized primary particles, the surface was much smoother due to a very small core size (less than 10 nm) of the dendrimer.

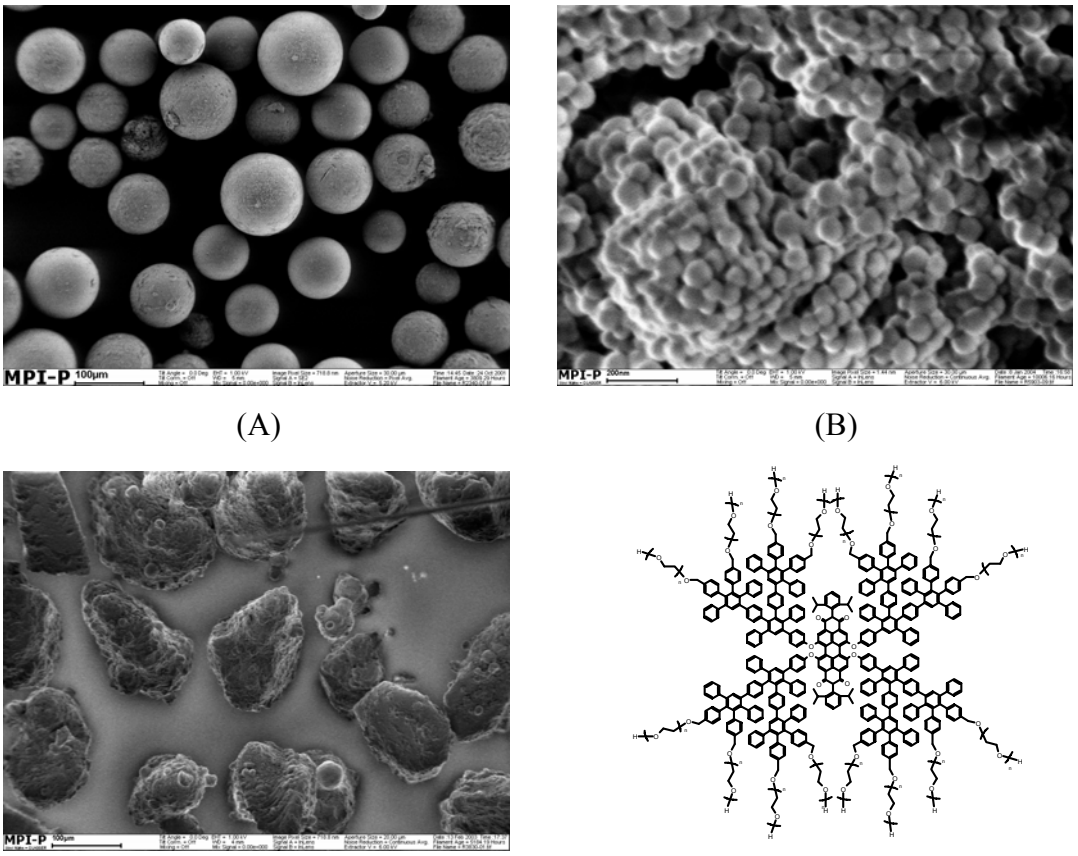

(A) (B)

(C) (D)

Figure 6-2. Four different supports; (A) microsized PS beads, (B) nanosized PS beads, (C) silica gel and (D) dendrimer [$PDIG_2(PEO)_n$]

At the same polymerization condition, the catalyst supported on different carriers showed different catalyst activity. These different activities were interpreted by the fragmentation behavior of the different supports in heterogeneous ethylene polymerization. To compare the catalyst fragmentation behavior within the PE product by the different supported catalysts, laser scanning confocal fluorescence microscopy was utilized for the investigation of catalyst fragmentation within polyethylene particles. The confocal fluorescence images have significantly less fluorescence blur and out-of-focus light than conventional fluorescence microscopy. Using the confocal fluorescence microscope, it was possible to observe the selected thin layers of a thick specimen placed under a microscope. The distribution of the

catalyst particle within single PE particle was directly characterized in a nondestructive way for the PE sample. Figure 6-3 shows the example of a polyethylene single particle that was produced by the catalyst supported on the nanosized PS beads copolymerized with N-(2,6-diisopropylphenyl)-9-(4-ethenylphenyl)perylene-3.4-dicarboximide and three fluorescent images of PE single particle cross-sectioned optically by laser scanning confocal fluorescence microscopy. Depending on the depth of polyethylene single article, one can see three different images (A, B and C). In these images, the bright red-colored particles in the image represent the fragmented catalyst particle and the white / gray areas in each PE sample thus represent the mixture of catalyst fragments and polyethylene formed. The black areas in the PE sample exhibit just polyethylene.

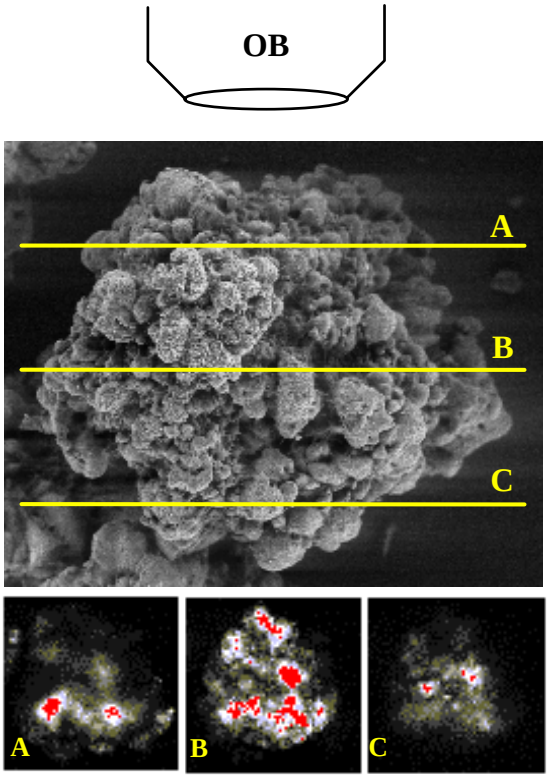

Figure 6-3. The optical section of polyethylene (PE) single particle by confocal fluorescence microscopy and confocal fluorescence images depending on the slice position

Nanosized PS beads copolymerized with N-(2,6-diisopropylphenyl)-9-(4-ethenylphenyl) perylene-3,4-dicarboximide and functionalized with polyethyleneoxide (PEO) were prepared for the investigation of supported catalyst fragmentation. By using the supported catalyst on the nanosized PS beads tagged with the dye, ethylene polymerizations were carried out at different polymerization times and the isolated PE particles were measured by laser scanning

confocal fluorescence microscopy. At the beginning of the polymerization, the catalyst supported on nanosized PS beads was fragmented inside and outside simultaneously (Figure 6-4). This fragmentation behavior of the catalyst supported on the nanosized PS was similar to that of the Ziegler-Natta catalysts supported on $MgCl_2$ in heterogeneous olefin polymerization. After a longer polymerization time, the catalyst particle was dispersed more homogeneously within the PE particle with an increase in PE particle size.

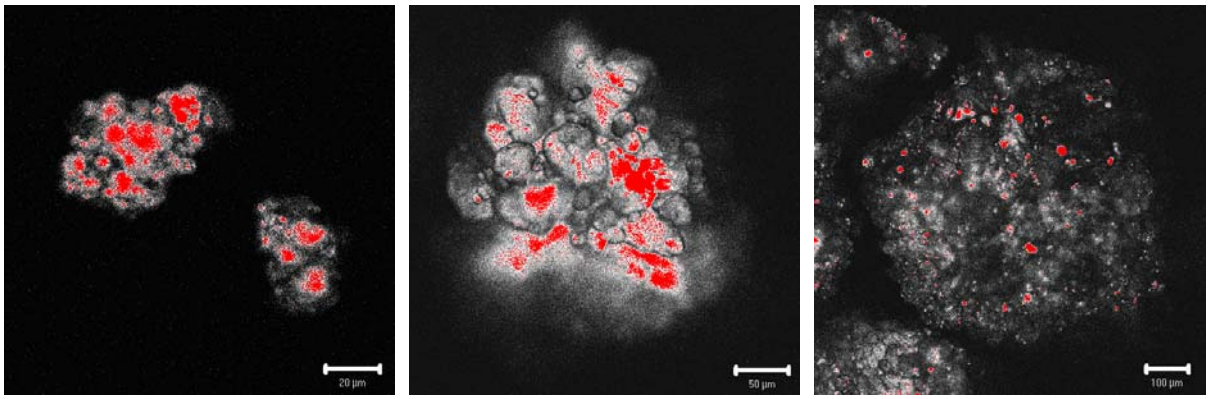

(A) (B) (C)

Figure 6-4. Confocal fluorescence image of single PE particle produced by the catalyst supported on the nanosized PS; (A) 2 min, (B) 5min and (C) 15 min polymerization

To compare the fragmentation behavior of the different supported catalysts, silica gel was stained with N,N′-bis(2,6-diisopropylphenyl)-1,6,7,12-tetra(4-sulfonylphenoxy)perylene-3,4:9,10-tetracarboxdiimide and silica-supported catalyst was prepared. Ethylene polymerizations using the silica-supported catalyst were carried out at different reaction times and the separated PE particles were measured by laser scanning confocal fluorescence microscopy. Confocal fluorescence images of single PE particles showed that the silica supported catalyst particles within the single PE particles had a different fragmentation behavior in comparison to the fragmentation results of the catalyst supported on the nanosized PS beads within single PE particles. The fragmentation of the supported catalyst occurred from outside of the silica supported particle (Figure 6-5). With increasing polymerization time, a fluorescence image of a polyethylene particle showed that the supported catalyst particle broke down from outside to inside gradually. This result was similar to the results of Fink and co-workers who showed the polymerization started at the surface of the silica-supported catalyst particle and then the fragmentation was progressed from outside to inside of the support.

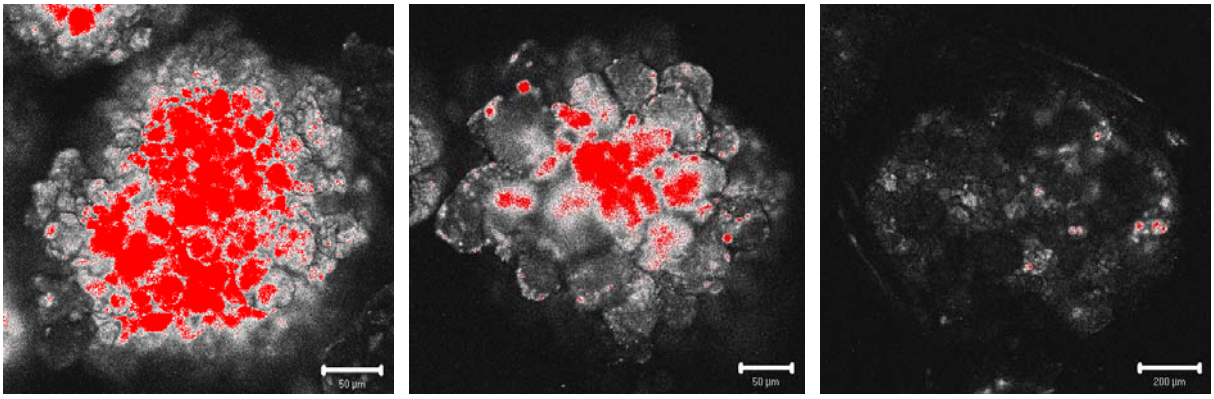

(A) (B) (C)

Figure 6-5. Confocal fluorescence image of single PE particle produced by the silica supported catalyst; (A) 2 min, (B) 5min and (C) 15 min polymerization

Microsized PS beads stained with dye [N,N′-bis(2,6-diisopropylphenyl)-1,6,7,12-tetra(4-sulfonylphenoxy)perylene-3,4:9,10-tetracarboxdiimide] were prepared to study the catalyst fragmentation in ethylene polymerization and to compare with other results from the different supported catalysts. For staining the microsized PS beads with the dye, the properties of the swelling and shrinking process of the polystyrene beads were used. Confocal fluorescence image of the catalyst supported on the microsized PS stained dye showed that the dye was dispersed homogeneously in the PS beads through the swelling and shrinking process. To compare the fragmentation result of the supported catalyst on the microsized PS beads functionalized with hydroxyl groups, the nanosized PS beads tagged with dye and functionalized with the hydroxyl groups were prepared by miniemulsion polymerization. Confocal fluorescence images of a single PE particle showed that the catalyst supported on the microsized PS beads was fragmented within the PE particle gradually and the fragmentation progress occurred in a layer-by-layer fashion. This fragmentation behavior of the catalyst supported on the microsized PS beads was similar to that of the silica-supported catalyst but different from the result of the catalyst supported on the nanosized PS beads. The catalyst supported on the nanosized PS was fragmented evenly throughout the PE particle during the polymerization. Upon prolonged polymerization, the supported catalyst was almost fragmented and spread homogeneously within the PE particle. Confocal fluorescence images of single PE particles obtained by the catalyst supported on the nanosized PS beads and the catalyst supported on the microsized PS beads displayed different internal structures of the PE. The catalyst supported on the nanosized PS displayed narrow lines between the catalyst particles attributed to channels for monomer gas which

were similar to those seen for silica supported catalyst and the catalyst supported on the nanosized PS. However, there were sub-particles within the PE produced by the catalyst supported on the microsized PS beads. This is because the microsized PS beads have microsized primary particles without constituent nanosized primary particles. The fragmentation behavior of the dendrimer-supported catalyst was similar to that of the catalyst supported on nanosized PS beads. The catalyst fragmentation occurred inside and outside of the polymer particle. Even with laser scanning confocal fluorescence microscopy, the difference of the fragmentation behavior between the dendrimer-supported catalyst and the catalyst supported on the nanosized PS beads could not be detected.

Summarizing all the results obtained, it can be concluded that these polystyrene beads are new and powerful supports for heterogeneous polymerization systems were developed. These polystyrene supports were composed of well-defined, spherical and nanosized particle beads which had a homogeneous distribution of metallocene catalyst on the carrier and allowed a complete fragmentation of the supported catalyst within the polyolefin products. Catalyst systems of nanosized PS beads and metallocene catalyst were tested in different polymerizations such as ethylene polymerization, copolymerization of ethylene with α-olefin monomers and propylene polymerization. Nanosized PS beads functionalized with nucleophilic ether groups immobilized metallocene catalyst without leaching of the catalyst from carrier and the polyolefin products showed good morphologies. To investigate the catalyst fragmentation and the internal structure within polyethylene products, laser scanning confocal fluorescence microscopy was used. This method was very useful to visualize the distribution of the supported catalyst particle within polyolefin particles and characterize the fragmentation behavior of the different supported catalyst. The fragmentation behavior of the nanosized PS or dendrimer supported catalyst was similar to that of the Ziegler-Natta catalysts supported on $MgCl_2$ in heterogeneous olefin polymerization. However, the fragmentation behavior of the silica or microsized PS supported catalyst occurred in the layer-by-layer fashion described by Fink and coworkers.

Chapter 7. Experimental part

7.1. General remarks and analytical instruments

All experiments were carried out under argon atmosphere with dried solvents using standard Schlenk techniques. The argon was passed through a deoxygenation coloumn (BASF R3-11) with two connected drying columns filled with 4Å molecular sieve. Hexane, THF and toluene were dried by distillation over sodium/potassium alloy. MAO solution in toluene was donated from Crompton GmbH. Metallocenes were donated by BASF AG, Basell Polyolefins, Max Planck Institute für Kohlenforschung in Mülheim, Hamburg University and Münster University. Triisobutylaluminium (TIBA) (1.0 M in hexane, Aldrich) was used without further purification. All other chemicals were purchased from Aldrich and used without further purification. Deionized water (Millipore water) was used for the miniemulsion polymerization.

The analytical measurements were performed using the following instruments:
Particle Size Analizer: Malvern-Zetasizer 3000 HAS
SEM: LEO 1530 Gemini
DSC: Mettler Digital Scanning Calorimeter 300, at a heating rate of 10 K/min - Polymer melting points (Tm) and crystallinities (Xc) were determined on a differential scanning calorimeter (DSC) using a heating rate of 10 °C/ min in the temperature range 20 – 200 °C. The heating cycle was performed twice, but only the results of the second scan were reported. Crystallinity was represented as the ratio of melting enthalpy of the DSC thermogram to that of a perfect polyethylene crystal (290 J / g).
Laser Scanning Confocal Fluorescence Microscopy: ZEISS Axiovert 200M / LSM 500
GPC: The molecular weight distribution of the polystyrenes was measured using Waters equipment at room temperature in THF. The polyolefins were analyzed in Waters GPC 2000 high temperature equipment in trichlorobenzene or o-dichlorobenzene at 135 ºC. For both types of analysis, polystyrene standard was used for calibration
TGA: Mettler 300 Thermogravimetric analyser
IR: Nicolet 320 FT-IR
NMR: Bruker DXP 250, AMX 500 or 750 MHz

7.2. Preparation of monomer and polymerization of latex particle as support

7.2.1. Synthesis of the nanosized polystyrene beads functionalized with polyethyleneoxide via miniemulsion

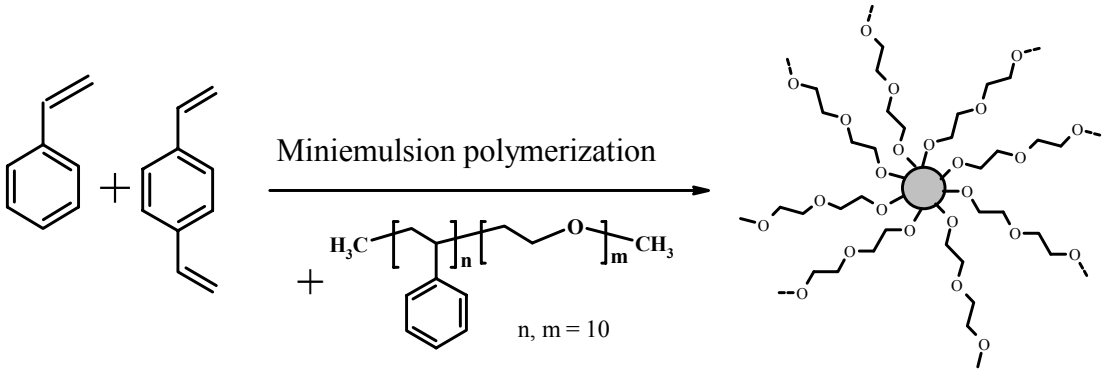

Material: Polyethyleneoxide-co-polystyrene: 0.51 g (0.36 mmol, 10 mol %)

Styrene: 0.3 g (2.9 mmol, 80 mol %)

Divinylbenzene: 0.047 g (0.36 mmol, 10 mol %)

Hexandecane: 250 ml

$K_2S_2O_8$: 100 mg

Distillated water: 24 g

Styrene (0.3 g), divinylbenzene (0.047 g) and hexadecane (250 ml) were stirred for 5 min. PEO-co-PS block copolymer (0.54 g) was dissolved in distilled water, mixed with oil phases and then stirred at the highest power (1200 rpm) of the magnetic stirrer for 1 hour to form a microemulsion. The microemulsion was ultrasonicated for 5 min with a Branson Sonifier 450W 70% power under ice cooling to form a miniemulsion. The miniemulsion was heated in an oil bath at 72 °C. Initiator $K_2S_2O_8$ (100 mg) was dissolved in a small quantity of distilled water and added to the miniemulsion reactor. The product was then filtered by a stirred Ultrafiltration Millipore model 8050 with polyethersulfone membrane and dried in vacuum.

IR (KBr) [cm^{-1}]: 541, 698, 758, 829, 906, 1028, 1112, 1244, 1370, 1452, 1492, 1601, 2852,

2923, 3025

Elemental analysis:

Support	Calculated		Obtained	
	C [%]	H [%]	C [%]	H [%]
NPS1-1	85.35	7.85	86.44	7.63
NPS1-2	82.27	8.12	83.04	9.09
NPS1-3	80.55	9.34	81.32	10.61
NPS1-4	75.32	9.05	76.46	10.34
NPS1-5	73.83	10.37	75.41	11.59

Particle size of PS beads varying the different concentration of PEO:

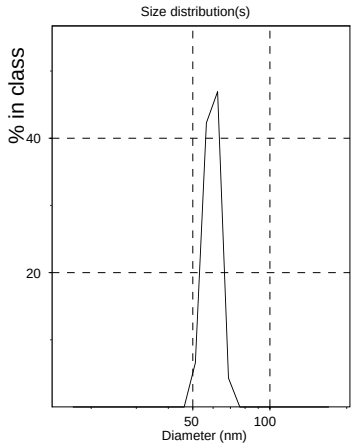

(A) NPS1-1

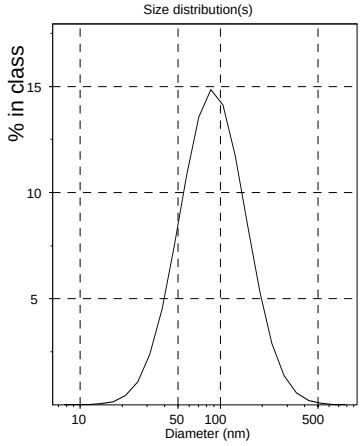

(B) NPS1-2

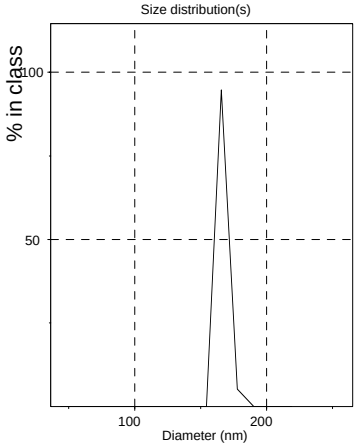

(C) NPS1-3

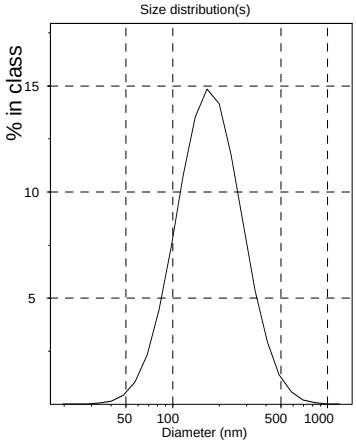

(D) NPS1-4

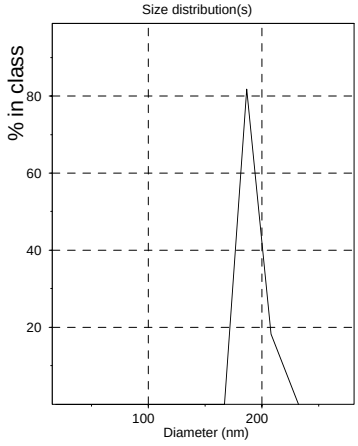

(E) NPS1-5

7.2.2. Synthesis of the nanosized polystyrene beads functionalized with polyethyleneoxide via miniemulsion

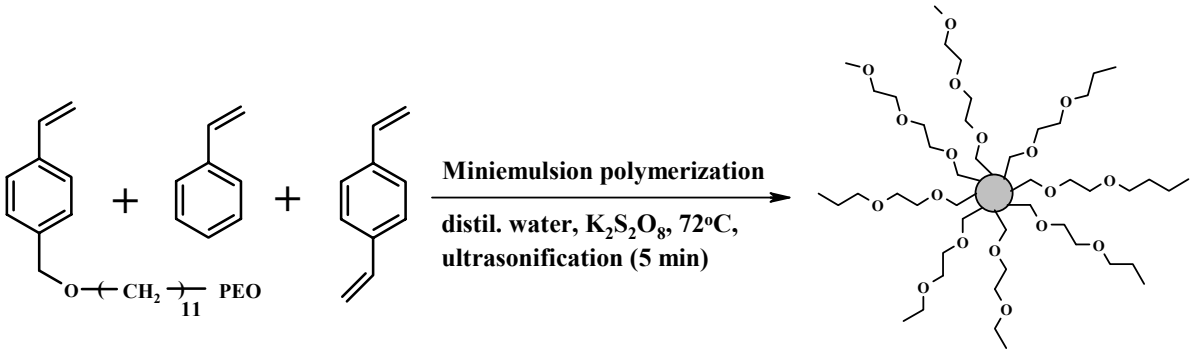

Material: 4-Vinylphenyloxyundecanyl-oligo(ethylene oxide): 0.6 g (0.26 mmol)

Styrene: 0.21 g (20 mmol)

Divinylbenzene: 0.25 g (1.95 mmol)

Hexandecane: 250 ml

$K_2S_2O_8$: 100 mg

Distillated water: 24 g

The emulsifier (0.6 g) was dissolved in dimethylformamide (5 ml) and then distilled water (20 ml) was added to the solution of emulsifier in DMF. The mixture was evaporated until the DMF was completely removed as its azeotropic mixture with water. To basify the reaction medium (necessary condition for the emulsion polymerization), 1N KOH (1.5 ml per 50 ml residual distilled water) was added. Styrene, divinylbenzene as crosslinker and hexadecane were stirred for 5 min and mixed with the solution of emulsifier / KOH. The mixture was stirred at the highest power of the magnetic stirrer for 1 hr to form a microemulsion. The microemulsion was ultrasonicated for 5 min with a Branson Sonifier 450 W AND 70 % power under ice cooling to form a miniemulsion. The miniemulsion was heated in oil bath at 72 °C and then the initiator $K_2S_2O_8$ was dissolved in a small quantity of distilled water and added to the miniemulsion reactor. After 12 hr, the PS product was then filtered by a stirred Ultrafiltration Millipore model 8050 with polyethersulfone membrane and dried in vacuum.

IR (KBr) [cm^{-1}]: 541, 698, 758, 829, 906, 1028, 1112, 1244, 1370, 1452, 1492, 1601, 2852, 2923, 3025

Elemental analysis:

Support	Calculated		Obtained	
	C [%]	H [%]	C [%]	H [%]
NPS2-1	85.75	7.34	86.83	8.51
NPS2-2	83.27	10.05	84.94	11.34

7.2.3. Synthesis of 4-Vinylphenyloxy-polypropyleneoxide

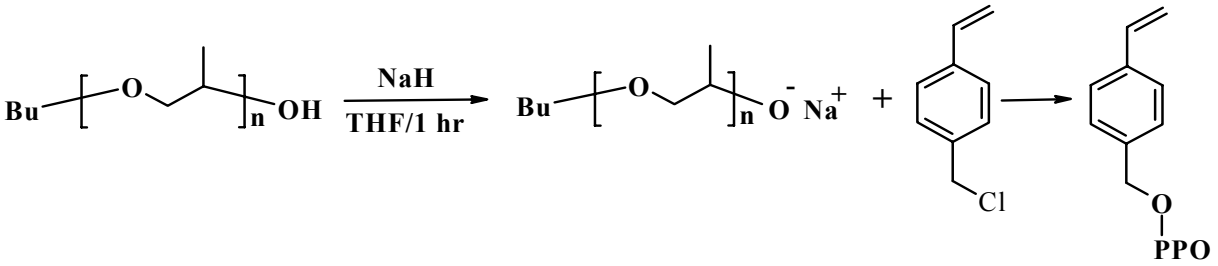

Material: 4-Vinylphenyloxy-polypropyleneoxide: 19.79 ml (19 mmol)

NaH: 0.55 g (23 mmol)

Chloromethylstyrene: 3.27 ml (23 mmol)

THF: 100 ml

NaH was suspended in THF (40 ml) and hydroxy terminated polypropyleneoxide-monobutylether (Mn = 1000) solution in THF (50 ml) was added dropwise. The mixture was stirred for 1hr at room temperature. p-Chloromethylstyrene in THF (10 ml) was added at 0 °C and the resultant mixture was stirred for 24 hr at room temperature. The solvent was evaporated and the residue was purified by column chromatography on silica gel with dichloromethane to give yellow oil (yield: 12.77 g, 60 %).

^{1}H NMR (250 MHz, $CDCl_3$): 0.85-0.91 (3H, t), 1.22- 1.76 (49H, m), 3.34- 3.55(47H, m), 4.57 (2H, s), 5.19 (1H, d), 5.69 (1H, d), 6.73 (1H, dd), 7.26-7.36 (4H, m).

Elemental analysis:

Measured: C: 65.03%, H: 9.95%

Calculated: C: 64.65%, H: 10.10%, O: 25.24%

7.2.4. Synthesis of the nanosized polystyrene beads functionalized with polypropyleneoxide via miniemulsion

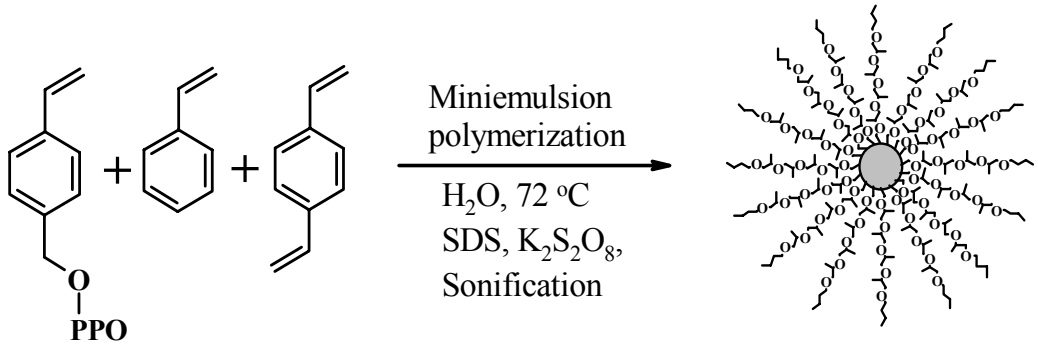

Material: 4-Vinylphenyloxy-polypropyleneoxide: 0.51 g (0.45 mmol, 10 mol %)

Styrene: 0.37 g (3.6 mmol, 80 mol %)

Divinylbenzene: 0.058 g (0.45 mmol, 10 mol %)

Hexadecane: 250 ml

Sodium dodecylsulfate (SDS): 72 mg

$K_2S_2O_8$: 100 mg

Distillated water: 24 g

Styrene, divinylbenzene, and hexadecane were stirred for 5 min. Styrylpolypropyleneoxide was mixed with sodium dodecylsulfate dissolved in distilled water and then mixed with oil phases and stirred at the highest power (1200 rpm) of the magnetic stirrer for 1 hour to form a microemulsion. The microemulsion was ultrasonicated for 5 min with a Branson Sonifier 450W 70% power under ice cooling to form a miniemulsion. The miniemulsion was heated in an oil bath at 72 °C. Initiator $K_2S_2O_8$ (100 mg) was dissolved in a small quantity of distilled water and added to the miniemulsion reactor. The obtained product was filtered by a stirred Ultrafiltration Millipore model 8050 with polyethersulfone membrane and dried in vacuum.

IR (KBr) [cm^{-1}]: 540, 698, 757, 839, 906, 1028, 1107, 1372, 1452, 1492, 1601, 1941, 2851, 2923, 3025

Elemental analysis:

Support	Calculated		Obtained	
	C [%]	H [%]	C [%]	H [%]
NPS3-1	86.34	8.12	88.67	8.26
NPS3-2	83.73	9.13	85.22	10.47
NPS3-3	81.05	9.48	81.85	10.05
NPS3-4	76.13	8.48	76.50	9.13
NPS3-5	74.23	8.27	74.64	9.48

Particle size distribution of PS beads:

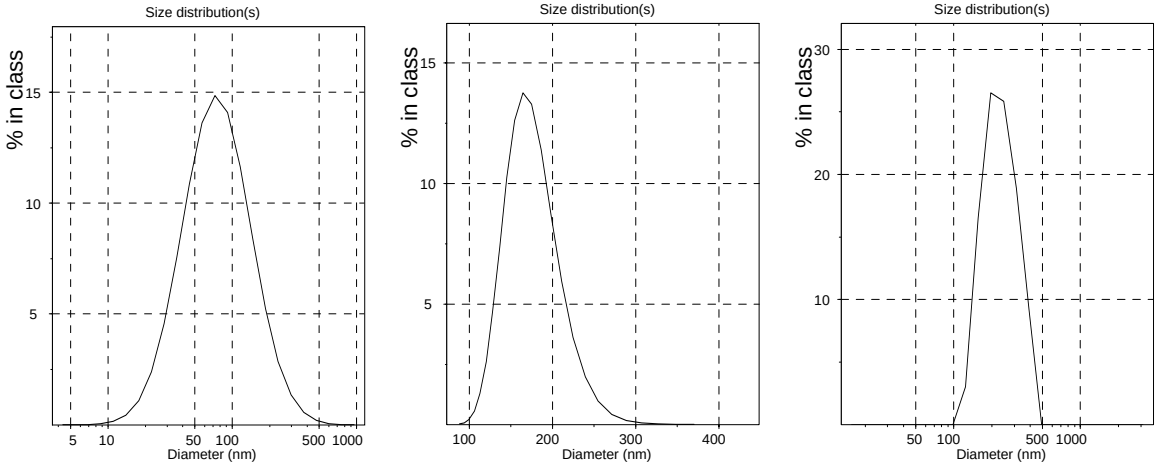

(A) NPS3-1 (B) NPS3- 2 (C) NPS3-3

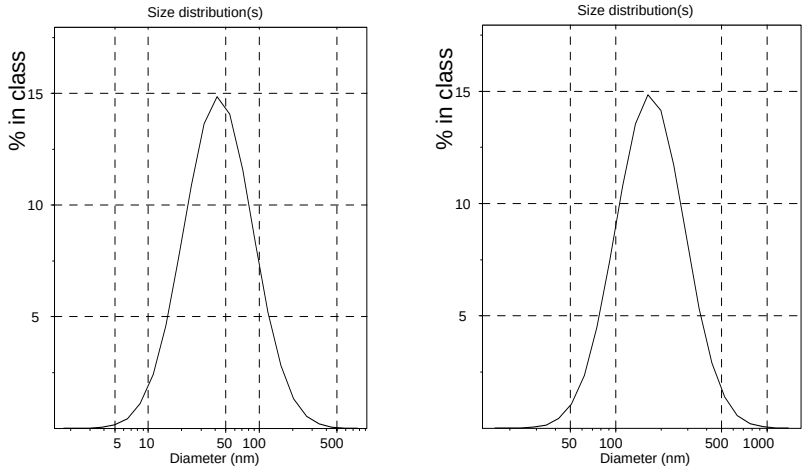

(D) NPS3-4 (E) NPS3-5

7.2.5. Synthesis of the nanosized polystyrene beads functionalized with hydroxymethyl via miniemulsion

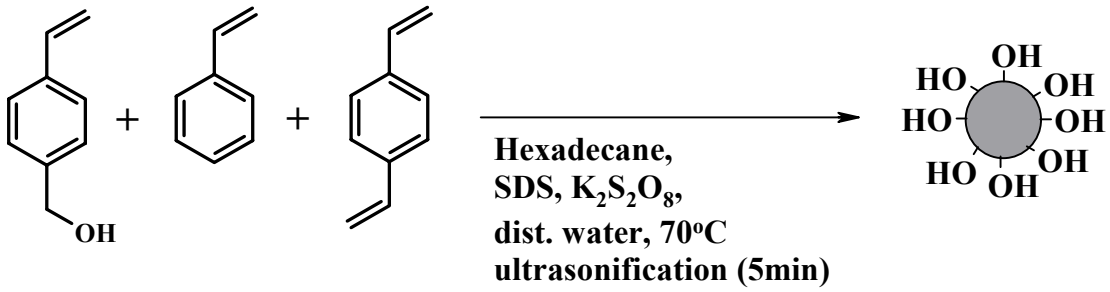

Material: Hydroxymethylstyrene: 0.16 g (1.20 mmol, 10 mol %)

Styrene: 1 g (9.60 mmol, 80 mol %)

Divinylbenzene: 0.15 g (1.20 mmol, 10 mol %)

Hexadecane: 250 ml

Sodium dodecylsulfate (SDS): 72 mg

$K_2S_2O_8$: 100 mg

Distillated water: 24 g

Styrene (1 g), divinylbenzene (0.15 g), and hexadecane were stirred for 5 min. Hydroxymethyl functionalized styrene (0.16 g) was mixed with sodium dodecylsulfate (72 mg) dissolved in distilled water and then mixed with oil phases and stirred at the highest power (1200 rpm) of the magnetic stirrer for 1 hour to form a microemulsion. The microemulsion was ultrasonicated for 5 min with a Branson Sonifier 450W 70% power under ice cooling to form a miniemulsion. The miniemulsion was heated in an oil bath at 72 °C. Initiator $K_2S_2O_8$ (100 mg) was dissolved in a small quantity of distilled water and added to the miniemulsion reactor. The product was then filtered by a stirred Ultrafiltration Millipore model 8050 with polyethersulfone membrane and dried in vacuum.

IR (KBr) [cm^{-1}]: 540, 698, 758, 795, 905, 1066, 1181, 1370, 1451, 1492, 1601, 1801, 2851, 2922, 3024, 3445

Elemental analysis:

Support	Calculated		Obtained	
	C [%]	H [%]	C [%]	H [%]
NPS4-1	87.23	7.43	87.6 %	7.6 %

Particle size distribution of PS beads:

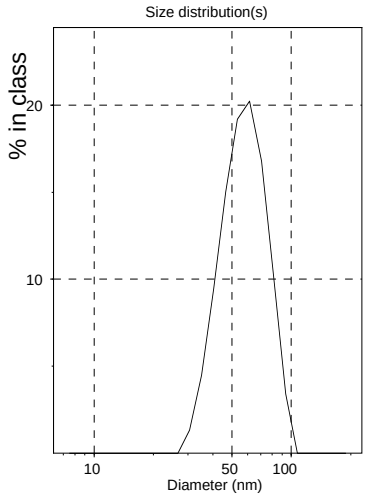

NPS4-1

7.2.6. Synthesis of the nanosized polystyrene beads tagged with dye and functionalized with polyethyleneoxide via miniemulsion

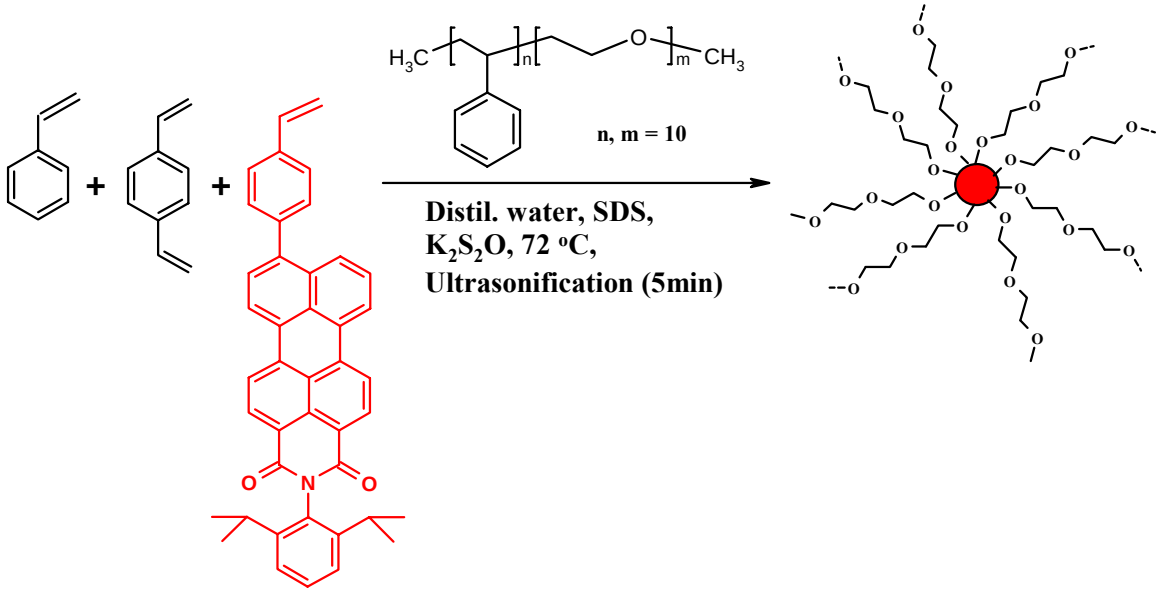

Material: Polystyrene-co-polyethyleneoxide: 1.02g (0.72 mmol, 10 mol %)

Styrene: 0.6 g (5.80 mmol, 79.7 mol %)

Divinylbenzene: 0.094g (0.72 mmol, 10 mol %)

N-(2,6-diisopropylphenyl)-9-(4-ethenylphenyl)perylene-3,4-dicarboximide:

0.013g (0.022 mmol, 0.3 mol %)

Hexadecane: 250 ml

$K_2S_2O_8$: 100 mg

Distillated water: 24 g

Styrene (0.6 g), divinylbenzene (0.094 g), N-(2,6-diisopropylphenyl)-9-(4-ethenylphenyl) perylene-3,4-dicarboximide (0.013 g) and hexadecane (250 ml) were stirred for 5 min. PEO-co-PS block copolymer (1.1 g) was dissolved in distilled water, mixed with oil phases and then stirred at the highest power (1200 rpm) of the magnetic stirrer for 1 hour to form a microemulsion. The microemulsion was ultrasonicated for 5 min with a Branson Sonifier 450W 70% power under ice cooling to form a miniemulsion. The miniemulsion was heated in an oil bath at 72 °C. Initiator $K_2S_2O_8$ (100 mg) was dissolved in a small quantity of distilled water and added to the miniemulsion reactor. The product was then filtered by a stirred Ultrafiltration Millipore model 8050 with polyethersulfone membrane and dried in vacuum.

IR (KBr) [cm^{-1}]: 541, 698, 757, 1028, 1112, 1251, 1357, 1451, 1600, 1798, 1866, 1938, 2848, 2922, 3024

Elemental analysis:

Support	Calculated		Obtained	
	C [%]	H [%]	C [%]	H [%]
NPS5-1	75.75	9.95	76.63	10.28

Particle size distribution of PS beads:

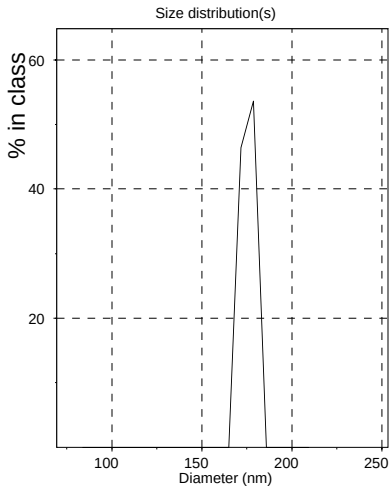

NPS5-1

7.2.7. Synthesis of the nanosized polystyrene beads tagged with dye and functionalized with

polypropyleneoxide via miniemulsion

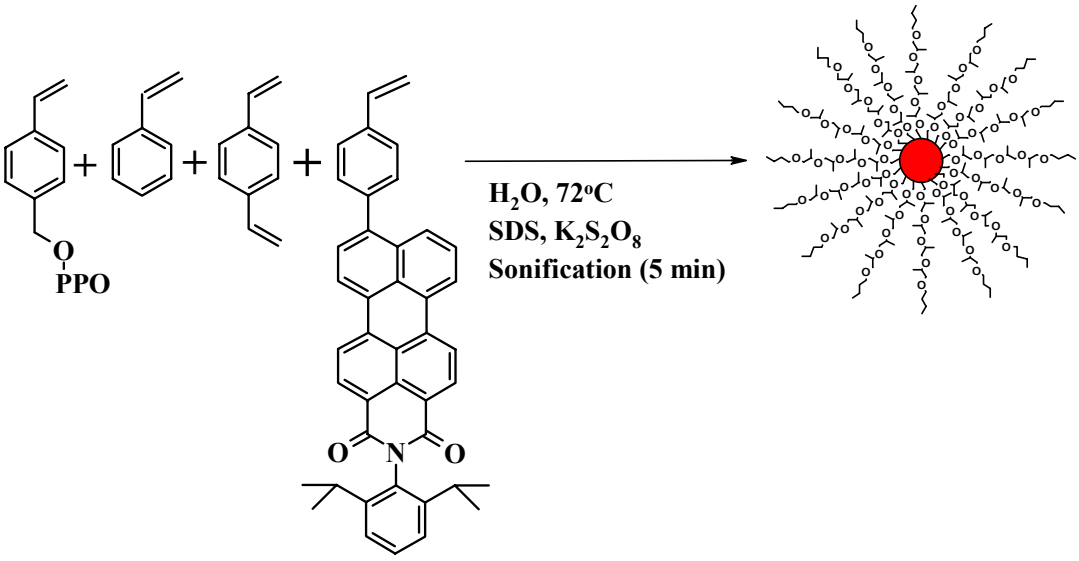

Material: Styrylpolypropyleneoxide: 0.68 g (0.60 mmol, 10 mol %)

Styrene: 0.5 g (4.8 mmol, 79.7 mol %)

Divinylbenzene: 0.078 g (0.60 mmol, 10 mol %)

N-(2,6-diisopropylphenyl)-9-(4-ethenylphenyl)perylene-3,4-dicarboximide:

: 0.01 g (0.018 mmol, 0.3 mol %)

Hexandecane: 250 ml

Sodium dodecylsulfate (SDS): 72 mg

$K_2S_2O_8$: 100 mg

Distillated water: 24 g

Styrene (0.5 g), divinylbenzene (0.078 g), N-(2,6-diisopropylphenyl)-9-(4-ethenylphenyl) perylene-3,4-dicarboximide (0.01 g) and hexadecane (250 ml) were stirred for 5 min. PPO functionalized styrene (0.68 g) was mixed with sodium dodecylsulfate (72 mg) dissolved in distilled water (24 g) and mixed with oil phases and then stirred at the highest power (1200 rpm) of the magnetic stirrer for 1 hour to form a microemulsion. The microemulsion was ultrasonicated for 5 min with a Branson Sonifier 450W 70% power under ice cooling to form a miniemulsion. The miniemulsion was heated in an oil bath at 72 °C. Initiator $K_2S_2O_8$ (100 mg) was dissolved in a small quantity of distilled water and added to the miniemulsion reactor. The product was then filtered by a stirred Ultrafiltration Millipore model 8050 with polyethersulfone membrane and dried in vacuum.

IR (KBr) [cm^{-1}]: 541, 698, 758, 839, 907, 1028, 1107, 1236, 1376, 1452, 1492, 1600, 1693, 2848, 2923, 3022

Elemental analysis:

Support	Calculated		Obtained	
	C [%]	H [%]	C [%]	H [%]
NPS5-2 (0.5 mol% PPO)	86.48	8.78	87.16	9.24
NPS5-3 (10 mol% PPO)	73.22	8.47	75.22	9.88

Particle size distribution of PS beads:

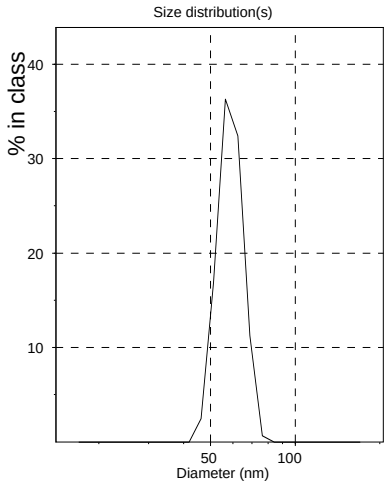

NPS5-2

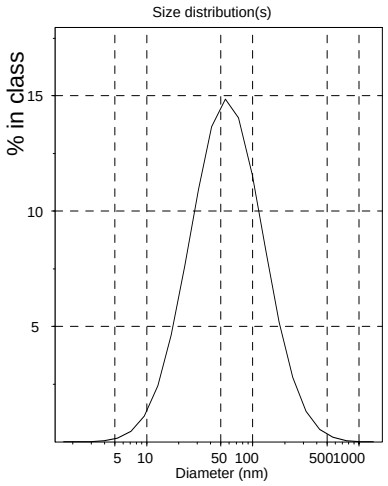

NPS5-3

7.2.8. Synthesis of the nanosized polystyrene beads tagged with dye and functionalized with hydroxyl via miniemulsion

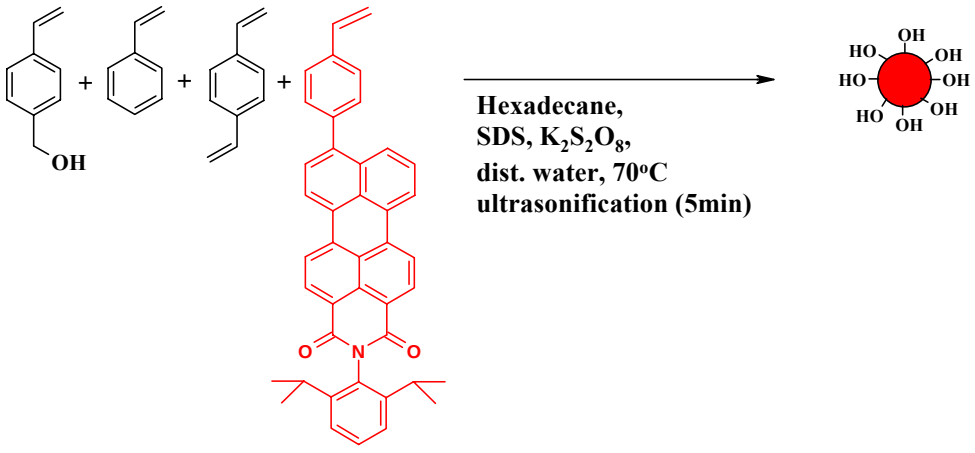

Material: Styrene functionalized with hydroxymethyl : 0.08 g (0.60 mmol, 10 mol %)

Styrene: 0.5 g (4.8 mmol, 79.7 mol %)

Divinylbenzene: 0.078 g (0.60 mmol, 10 mol %)

N-(2,6-diisopropylphenyl)-9-(4-ethenylphenyl)perylene-3,4-dicarboximide:

: 0.01 g (0.018 mmol, 0.3 mol %)

Hexandecane: 250 ml

Sodium dodecylsulfate (SDS): 72 mg

$K_2S_2O_8$: 100 mg

Distillated water: 24 g

Styrene (0.5 g), divinylbenzene (0.078 g), N-(2,6-diisopropylphenyl)-9-(4-ethenylphenyl) perylene-3,4-dicarboximide (0.01 g) and hexadecane (250 ml) were stirred for 5 min. Styrene functionalized with hydroxymethyl (0.08 g) was mixed with sodium dodecylsulfate (72 mg) dissolved in distilled water (24 g) and mixed with oil phases and then stirred at the highest power (1200 rpm) of the magnetic stirrer for 1 hour to form a microemulsion. The microemulsion was ultrasonicated for 5 min with a Branson Sonifier 450W 70% power under ice cooling to form a miniemulsion. The miniemulsion was heated in an oil bath at 72 °C. Initiator $K_2S_2O_8$ (100 mg) was dissolved in a small quantity of distilled water and added to the miniemulsion reactor. The product was then filtered by a stirred Ultrafiltration Millipore model 8050 with polyethersulfone membrane and dried in vacuum.

IR (KBr) [cm^{-1}]: 583, 698, 758, 847, 903, 1017, 1221, 1357, 1451, 1492, 1700, 1863, 1938, 2852, 3024, 3439

Elemental analysis:

Support	Calculated		Obtained	
	C [%]	H [%]	C [%]	H [%]
NPS5-4	86.89	8.23	87.20	8..42

Particle size distribution of PS beads:

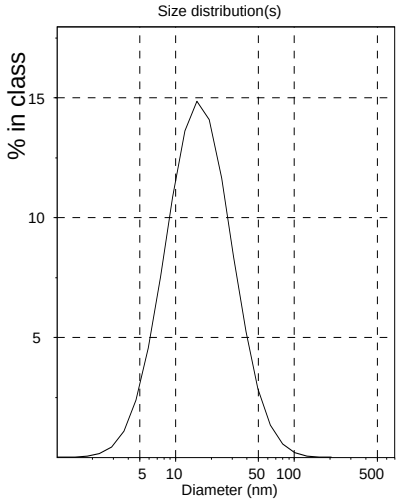

NPS5-4

7.2.9. Staining silica gel with dye

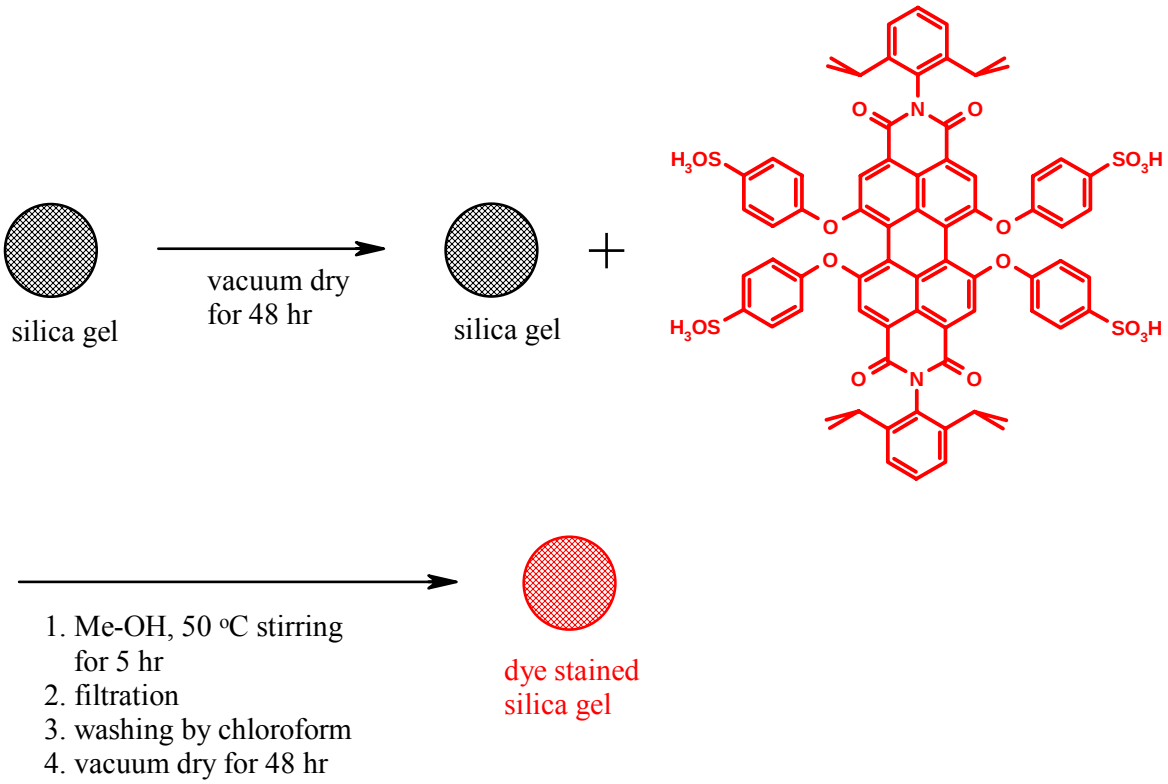

Material: Silica gel (Grace Davison Silopol 952): 0.5 g

N,N′-bis(2,6-diisopropylphenyl)-1,6,7,12-tetra(4-sulfonylphenoxy)perylene-3,4:9,10-tetracarboxdiimide: 0.05 g

Methanol: 2 ml

Chloroform: 100 ml

Silica gel (0.5 g) was dried for 48 hr to remove air and water from the pores of the silica gel. A saturated solution of N,N′-bis(2,6-diisopropylphenyl)-1,6,7,12-tetra(4-sulfonylphenoxy) perylene-3,4:9,10-tetracarboxdiimide (0.015 g) in methanol (2 ml) was mixed with the dried silica (0.3 g) and stirred slowly at 50 ^{o}C for 5 hr. The silica gel was removed from the solution by filtration and the dye-stained silica filtrated was mixed with chloroform before drying in air. The chloroform was removed by decantation and this process was repeated several times. Initially the chloroform was slightly red due to some remaining methanol / dye solution on the silica gel. However, after 5 washings with chloroform, the solvent remained colorless. The dye-stained silica was then dried for 48 hr under vacuum (60 ^{o}C).

7.2.10. Staining mircosized PS beads with dye

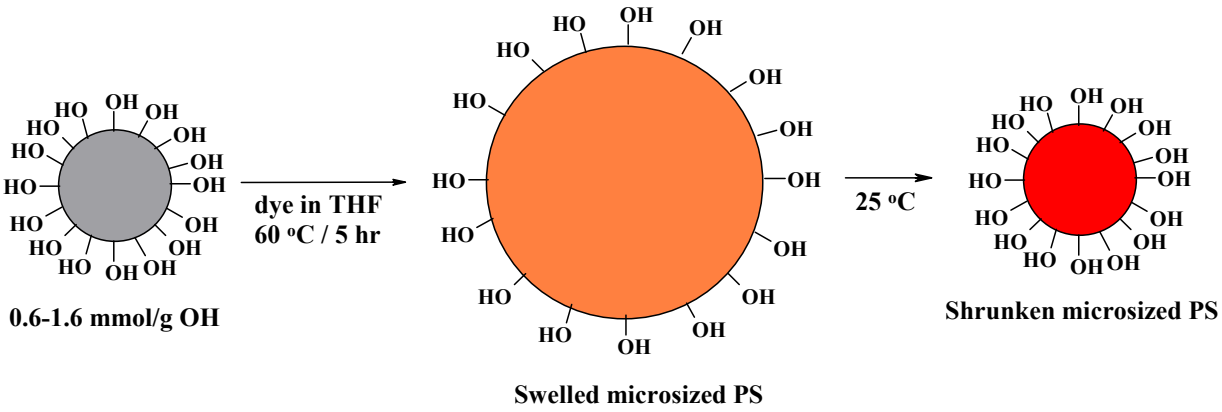

Material: Microsized PS beads functionalized with hydroxyl group: 1 g

N,N′-bis(2,6-diisopropylphenyl)-1,6,7,12-tetra(4-sulfonylphenoxy)perylene-3,4:9,10-tetracarboxdiimide: 0.08 g

THF: 10 ml

Chloroform: 100 ml

Microsized PS functionalized hydroxy group was washed with methanol several times and dried for 48 hr. A saturated solution of N,N′-bis(2,6-diisopropylphenyl)-1,6,7,12-tetra(4-sulfonylphenoxy)perylene-3,4:9,10-tetracarboxdiimide (0.08 g) in THF (10 ml) was mixed with the polystyrene beads (1 g) and stirred slowly at 50 ^{o}C for 5 hr to swell the PS and allow the dye to stain the inside of the PS bead. Then, the swelled PS beads were cooled down to

room temperature and separated from THF solution of the dye by filtration and the filtered PS beads stained with dye were washed with chloroform. The upper chloroform solution was removed by decantation and this process was repeated several times before drying it. Initially the chloroform became slightly red due to mixing of the chloroform with the remaining THF / dye solution on the surface of the PS beads but after 5 washings with chloroform, the solvent remained colorless. The microsized PS beads stained with dye were then dried under vacuum.

7.3. Supporting of metallocene on the nanosized PS beads, microsized PS, silica and dendrimer support for ethylene polymerization

Each support (80 mg) was mixed with a solution of MAO (2 ml) in toluene and stirred overnight to remove traces of water. The amount of MAO depended on the desired activation. After 30 min, a solution of metallocene and MAO (1.5 ml) was added to the MAO/polymer support mixture and dried hexane (20 ml) was added. Then after stirring for another 30 min, the catalyst was precipitated. The supernatant colorless hexane solution was removed, the procedure was repeated 3 times and the remaining solid was dried under vacuum to give the catalyst ready for use.

7.4. Polymerization of ethylene, propylene and ethylene with α-olefins

7.4.1. Homo-polymerization of ethylene

A stainless steel autoclave (Figure 7-1) with maximal pressure of 60 bars was used for all ethylene polymerizations. The monomer was introduced as a gas and the pressure set to 40 bars. The argon used was purified through oxisorb and hydrosorb elements supplied by Messer Griesheim. The ethylene was purchased from BASF as polymerization quality and was used without further purification. Isobutane was used as solvent for all polymerizations. For a typical polymerization, the reactor was heated to 80 °C and nitrogen was flown through it and through the pressure gate in order to remove all possible traces of air or moisture. After 1 h the temperature was decreased to 40 °C, the nitrogen flow was stopped and argon was flown through the autoclave and the pressure gate. When the temperature reached 40°C, triisobuthylaluminium (TIBA) used as scavenger and in copolymerizations the co-monomers,

were introduced. As the same time, a special pressure was filled with isobutene in 'gas pressure tube'. 400ml of isobutane were introduced into the autoclave, while another 10 ml were placed in a 'metal pressure tube' connected to the reactor for washing catalyst residues into the reactor.

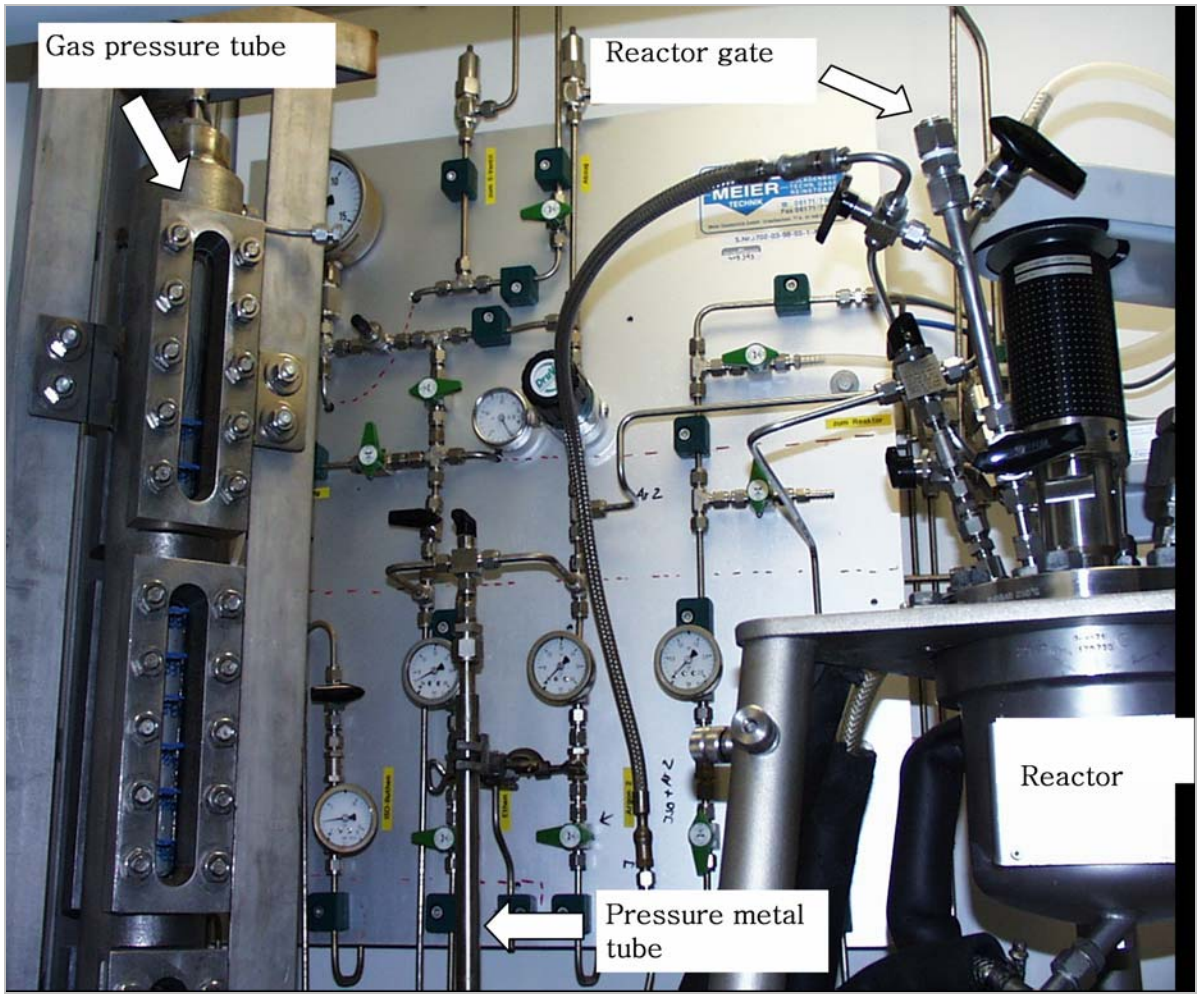

Figure 7-1. Reactor for ethylene polymerization

The argon was stopped, the stirrer was switched on and the autoclave was saturated with ethylene to a pressure of 37 bars and heated to 70 °C. The catalyst was then introduced into the pressure gate using a steady reverse stream of argon. The gate was closed, the argon stream was stopped and the catalyst was inserted into the reactor together with the 10ml isobutane from the 'pressure metal' using argon overpressure. The polymerization was stopped by closing the valve of the monomer flow and decreasing the pressure. As isobutene at normal conditions (room temperature and 1atm) is a gas, the product was obtained directly dried.

7.4.2. Co-polymerization of ethylene with α-olefin (1-hexene, 1-octene, 1-decene, 1-norbornene)

The reactor (1 L Büchi stainless steel, equipped with stirrer) was purged with argon and charged with isobutane 400 ml, comonomer (1-hexene, 1-octene, 1-decene or norbornene) and TIBA (triisobutyl aluminium) 5 ml. An ethylene pressure of 40 bar was applied and the reactor heated to 70 °C. The catalyst was injected into the reactor under argon through the pressure lock without further activation with MAO.

7.4.2.1. Preparation of the co-monomers

1-Hexene, 1-octene, 1-decene were purchased from Fluka and dried for several days over 4Å molecular sieve. The corresponding amount of the co-monomer was introduced in the reactor using argon reverse stream.
Norbornene was purchased from Aldrich and dissolved in dry (distilled over Na/K alloy) hexane. A calculated amount of a solution of 500g norbornene in 200ml hexane was introduced into the reactor using an argon reverse stream.

7.4.3. Polymerization of propylene

A glass autoclave (Figure 7-2) with maximal pressure of 12 bars was used for all propylene polymerizations. The propylene was purchased from BASF as polymerization quality and used without further purification. Toluene was used as solvent for all polymerizations, and was distilled over Na/K alloy directly before the reaction. For a typical polymerization, the reactor was heated to 80 °C and nitrogen was flown through it and through the pressure gate in order to remove traces of air or moisture.

Homogeneous polymerization: all homogeneous polymerizations were carried out in a 1 L glass autoclave charged with 400 ml toluene and 20 ml MAO (10 weight % solution in toluene). The stirred (100 rpm) mixture was saturated for 1hr with propylene gas at 2.5 bar. The catalyst solution in toluene (5 ml) was injected by using argon gas pressure to reactor and the propylene gas charged up to 4 bar. After polymerization at a permanent propylene pressure of 4 bar, the reaction mixture was terminated with 5 ml MeOH, treated with HCl / MeOH solution for overnight and then the PP product was washed by MeOH, filtrated and

dried in vacuum.

Heterogeneous polymerization: All heterogeneous polymerizations were carried out in a 1 L glass autoclave charged with 400 ml toluene and 10 ml MAO (10 weight % solution in toluene). The stirred (100 rpm) mixture was saturated for 1hr with propylene gas at 2.5 bar. The supported catalyst (100 – 120 mg) suspended in TIBA 5 ml (in hexane) was injected by using argon gas pressure to reactor and the propylene gas charged up to 4 bar. After polymerization at a permanent propylene pressure of 4 bar, the reaction mixture was terminated with 5 ml MeOH, treated HCl / MeOH solution for overnight and the filtrated PP product dried in vacuum oven.

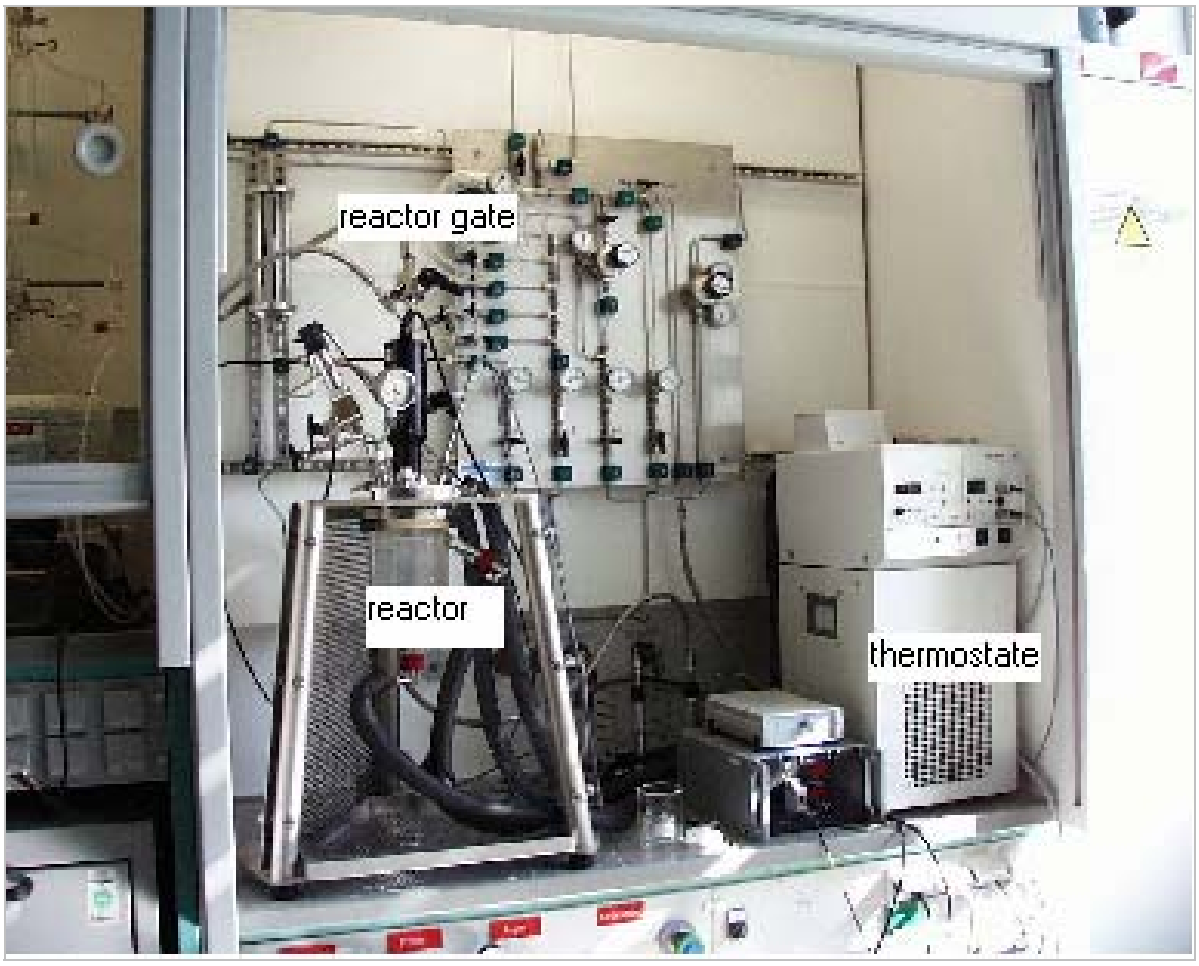

Figure 7-2. Reactor for propylene polymerization

7.4.4. Kinetic studies of the catalyst systems on polymerization of ethylene

All kinetic investigation of the prepared catalyst systems were carried out in the Max-Planck Institute for Carbon research at Mülheim (Prof. G. Fink). All catalyst systems were

prepared in MPI-P Mainz and used directly without further processing. The polymerization experiments were carried out in Büchi glass autoclave at constant monomer pressure. The monomer consumption was measured by a flow-meter – 5850 TRC 126 ZBD 41, Brooks Instrument (Holland), supplied with channels measuring the monomer flow with a speed of 0-100 ml / min, 0-1000 ml / min and 0-5000 ml / min. As solvent, toluene was used. They were dried first by distilling over Na/K alloy and then additionally distilled directly before use over $NaAlEt_4$. In a typical polymerization, the reactor was dried under vacuum at 80ºC for 1 h, then the temperature was decreased to 50 ºC and the solvent and TIBA were added to the reactor. The stirring was switched on and the reactor was saturated with the monomer to the desired pressure. The catalyst was mixed with a small amount of the solvent used and introduced as a suspension into the pressure gate. An additional amount of the solvent was added to the gate to remove all residual catalyst and this suspension was injected into the reactor using an argon overpressure. The reaction was stopped by introducing methanol into the reactor and releasing the monomer pressure. The product was collected by filtration, washed with a mixture of methanol and HCl and dried under high vacuum.

Acknowledgements

First of all, I would like to thank God for blessing me.

Professor Dr. K. Müllen for giving me the opportunity to do Ph.D work in his group at the Max-Planck-Institute for Polymer Research and making me a real scientist.

Dr. Markus Klapper for supporting my whole Ph.D work and helping me all of my life in Germany.

Dr. Nikolay Nenov, Kirsten Bieber, Corrina Naundorf, Tanja Nemnich, Dr. Victor Khrenov, Dr. Maria Doycheva, Dirk Fischer, and Svetlin Nenov for discussing about scientific field in nanosized polymer latex and heterogeneous olefin polymerization and helping a science problem each other.

Dr. Christopher Kohl, Bassem El Hamaoui, Fabian Nolde for enjoying every lunch times and discussing deep life as a scientist. **Dr. Andrew Grimsdale and Dr. Neil G. Pschirer** for correcting the English in this thesis.

Christopher Clark, Vladimir Atanassov, Vesko Synigerski, Petko Petkov, Roland Bauer, Guido Vandermuellen, Kundu Nihar Ranjan, Nigel Lucas, Gueorgui Mihov, Christophe Ego, Dirk Marsitzki, Josemon Jacob, Jeljko Tomovic, Weicheng Wu, Jishan Wu, Karl Wang, Jianqiang Qu, Jiaoli Li, Meryem Safak, Kevin Müller, Junji Sakamoto, Fikri Emrah Alemdaroglu, Eva Sebold, Josemon Jacob, Hans-Joachim Räder, Petra Rapp, Florian Schwager, Eva Sebold, Manfred Wagner, Andreas Best, and Luke Oldridge for enjoying with me in Germany and talking about personal life.

Korean colleagues in MPIP – **이상영, 이우상, 장원석, 이남경, 임찬, 고한봉, 안택, 김동하, 김병석, 박혜영, 김주연, 이맹은, 전현표, 양창덕, 정성현, 이옥주, 박진, 박미경, 문철순, 김연환, 이영주, 최경선**. 지루하고 힘든 유학 생활을 함께 한 나의 동지들에게 진심으로 감사합니다.

항상 기도로 후원해 주신 **박의석**, **전용근 목사님 가정**과 **마인츠 교회** 식구들에게도 감사의 마음을 전합니다.

Finally, my wife (Young-Sil, Yang) and family in Korea for their endless encouragement, support and love!

Publications:

1. **Jang, Y.J.**; Nenov, N.; Klapper, M.; Müllen, K.; 'Organic Nanoparticles with Polypropyleneoxide Chains as Support for Metallocene Catalysts: Ethylene Homopolymerization and Ethylene/α-olefin Copolymerization' *Polymer Bulletin*, **2003**, 50, 343.
2. **Jang, Y.J.**; Nenov, N.; Klapper, M.; Müllen, K.; 'Organic Nanoparticles with Polypropyleneoxide Chains as Support for Metallocene Catalysts: Influence of the Concentration of PPO chains on the Surface of NAnoparticles on the Catalyst Activity in Ethylene Polymerization', *Polymer Bulletin*, **2003**, 50, 351.
3. Klapper, M.; **Jang, Y.J.**; Nenov, N.; Bieber, K.; Nemnich, T.; Müllen, K.; 'Nanosized Latexes as support for Metallocene Catalysts in Ethylene Polymerization', *Macromolecular Symposia*, **2004**, 213, 131.
4. M. Klapper, D. Fischer, **Y.J. Jang**, C. Naundorf , K. Müllen, "Organic Supports for Heterogeneous Metallocene Catalyzed Olefin Polymerization" in Dechema Monographien, 138, 275-, ISBN 3-527-102332-9
5. **Jang, Y.J.**; Klapper, M.; Müllen, K.; Fink, G.; 'Fragmentation Study of Metallocene Catalyst Supported on Nanosized Organic Particles in Ethylene Polymerization', *e-Polymers*, **2005**, 13, 1.
6. **Jang, Y.J.**; Klapper, M.; Müllen, K.; 'Ethylene Polymerization with Supported Metallocenes As Studied by Laser Scanning Confocal Fluorescence Microscopy', in Macromolecular Chemistry and Physics.
7. Atanassov, V.; **Jang, Y.J.**; Nenov, N.; Bauer, R.; Sinigersky, V.; Klapper, M.; Muellen, K.; 'Core-Shell Macromolecules with Dendritic Polyphenylene Core and Poly(ethyleneoxide) Shell - Applications as Metallocene Supports in Heterogeneous Olefin Polymerization', in preparation.
8. **Jang, Y.J.**; Klapper, M.; Müllen, K.; Schultz, S.; Erker, G.; 'Metallocene Catalysts Supported Nanosize Polystyrene Beads for Elastomeric Propylene Polymerization', in preparation.

Presentations:

1. **Jang, Y.J.**; Naundorf, C.; Klapper, M.; Müllen, K.; 'Optical Method for

the Study of Catalyst Fragmentation in Olefin Polymerization', MOSPOL 2004, International Olefin Polymerization Conference in Moscow, Russia, June 22-25, 2004.

2. Naundorf, C.; **Jang, Y.J.**; Klapper, M.; Müllen, K.; 'Surface Functionalized Latex Particles as Polymeric Supports for Metallocenes in Olefin Polymerization', MACRO 2004, 40th IUPAC World Polymer Congress, in Paris, France, July 4-9, 2004.
3. Klapper, M.; **Jang, Y.J.**; Naundorf, C.; Müllen, K.; 'Optical methods for the study of the catalyst fragmentation during the olefin polymerization', 2nd Blue Sky Conference on Catalytic Olefin Polymerization, in Sorrento, Italy, June 26-29, 2005.
4. Klapper, M.; **Jang, Y.J.**; Müllen, K.; Schultz, S.; Erker, G.; 'Metallocene catalysts supported on nanosize polystyrene beads for elastomeric polypropylenes', 2nd Blue Sky Conference on Catalytic Olefin Polymerization, in Sorrento, Italy, June 26-29, 2005.